

DRAFT

Coastal Morphology

&

Coastal Protection

CT5309

January 2009



# Preface

The objective of the lecture notes on ‘Coastal Morphology and Coastal Protection’ is not to provide all the details required to understand coastal morphology and to define coastal protection measures. It is to help the students who are interested in this topic to understand the basic principles so they are able to find their way in the background information more effectively.

The project to make new lecture notes is a co-operation between Delft University of Technology and Alkyon Hydraulic Consultancy & Research BV.

The cover of this book reflects the interwoven relation between coastal morphology and coastal protection. The background illustration<sup>\*)</sup> shows some impact of a long dam constructed at the north-western part of the Dutch island Texel on the local morphology.

The lecture notes are still ‘under construction’. That means for the course 2008-2009 that students who follow CT5309 will find the text at Blackboard.

Some of the figures are still in a sketch phase; the references are not yet complete.

Comments of the users are welcomed.

Delft, January 2009

Jan van de Graaff

Room 3.77 Building Civil Engineering

Tel.: 015 2784846

e-mail: [j.vandegraaff@tudelft.nl](mailto:j.vandegraaff@tudelft.nl)

---

<sup>\*)</sup> *Obtained from regular photo flight in 1999. Courtesy of RWS.*





Contents

**Preface.....iii**

**List of Figures ..... ix**

**List of Tables ..... xii**

**List of Examples ..... xii**

**1 Introduction..... 1**

1.1 Position of Coastal Morphology and Coastal Protection 1

1.2 Interrelationships 1

1.3 Objective of lecture notes 2

1.4 ‘Players’ in coastal engineering in The Netherlands 2

1.5 ‘Players’ in coastal engineering in the world 4

1.6 Overview of contents 4

**2 Tides, Currents and Waves ..... 7**

2.1 Introduction 7

2.2 Tides 8

2.3 Currents 10

2.4 Wave characteristics 12

2.5 Wave deformation 24

2.6 Software 33

2.7 Wave measurements 33

**3 Coastal Problems ..... 35**

3.1 Introduction 35

3.2 Cross-shore profile 35

3.3 Morphological development in vicinity of a port 38

3.4 Pipeline at the sea bed 40

3.5 Delta near river mouth 41

3.6 Tidal inlets 42

3.7 Dune erosion during a severe storm surge 43

3.8 Large artificial island in open sea 46

3.9 Conclusions of Chapter 3 47

---

<b>4</b>	<b>Sediment Transport Processes.....</b>	<b>49</b>
4.1	Introduction	49
4.2	Sediment properties	50
4.3	Initiation of motion	55
4.4	Bottom shear stress	61
4.5	Sediment transport modes	78
4.6	Sediment transport by currents	88
4.7	Sediment transport by waves	94
4.8	Transport by waves and currents combined	94
<b>5</b>	<b>Coastal Transport Modes.....</b>	<b>105</b>
5.1	Introduction	105
5.2	Discussion on scales	106
5.3	Coastal transport modes	109
<b>6</b>	<b>Longshore transport.....</b>	<b>115</b>
6.1	Introduction	115
6.2	Longshore current	115
6.3	Longshore sediment transport	139
6.4	Shoreline dynamics	150
<b>7</b>	<b>Cross-shore transport.....</b>	<b>169</b>
7.1	Introduction	169
7.2	Cross-shore morphology of beaches	170
7.3	Cross-shore sediment transport	179
7.4	Dune Erosion	182
<b>8</b>	<b>Combination of Long- and Cross-shore Transport .....</b>	<b>191</b>
<b>9</b>	<b>Fundamentals of Mud .....</b>	<b>209</b>
9.1	Introduction	209
9.2	Examples of Coastal Systems with Mud	209
9.3	Characteristics of Mud	211
9.4	Sediment Transport	213
9.5	Bed level change	215
9.6	Environmental Issues	216

---

<b>10</b>	<b>Channels and Trenches.....</b>	<b>219</b>
10.1	Introduction	219
10.2	Examples	219
10.3	Current pattern	220
10.4	Wave pattern	224
10.5	Current-wave interaction	225
10.6	Transport processes	226
10.7	Sedimentation computation	228
<b>11</b>	<b>Coastal Protection.....</b>	<b>233</b>
11.1	Introduction	233
11.2	Coastal erosion	234
11.3	Protection measures	243
11.4	Coastal Zone Management	248
<b>12</b>	<b>Application of Structures.....</b>	<b>251</b>
12.1	Introduction	233
12.2	Seawalls	233
12.3	Revetments	256
12.4	Jetties / (port) breakwaters	258
12.5	(Series) of groynes	260
12.6	Detached shore parallel offshore breakwaters	263
12.7	Piers and trestles	270
12.8	Sea-dikes	271
12.9	Miscellaneous	272
<b>13</b>	<b>Application of Nourishments.....</b>	<b>275</b>
13.1	Introduction	275
13.2	Problems to be resolved with artificial nourishments	275
13.3	Various aspects	283

<b>14</b>	<b>Background Information.....</b>	<b>287</b>
14.1	General handbooks	287
14.2	Interesting journals	288
14.3	Conference proceedings	288
14.4	Interesting internet sites	290
<b>15</b>	<b>References .....</b>	<b>291</b>

## List of Figures

- 1.1 The Netherlands below Mean Sea Level
- 2.1 Wave energy spectrum
- 2.2 Tidal variations (spring and neap tide)
- 2.3 Tidal current pattern
- 2.4 Water surface measurements
- 2.5 Definition sketch of progressive, sinusoidal wave (horizontal and vertical scale quite different)
- 2.6 Regions of validity for various wave theories
- 2.7 Simplified hyperbolic functions
- 2.8 Orbital motion under a shallow water wave and a deep water wave
- 2.9 Local fluid velocities and accelerations at certain phases in the wave period
- 2.10 Uniform probability distribution
- 2.11 Zero-down crossing periods and wave heights
- 2.12 Energy spectrum with peak-period
- 2.13 Maximum crest angle
- 2.14 Breaker types as a function of  $\xi$  [Eq.(2.54)]
- 2.15 Wave refraction over straight parallel depth contours
- 2.16 Wave refraction diagram
- 2.17 Diffraction of an incident wave train
- 2.18 Wave measuring locations
- 3.1 Plan view of a coastal area
- 3.2 Cross-shore profile (measured at Egmond aan Zee)
- 3.3 Wave height distribution over cross-shore profile
- 3.4 Maximum horizontal velocity components near the bed over cross-shore profile
- 3.5 Plan view of a uniform sandy coast
- 3.6 Plan view of a uniform sandy coast with port breakwaters
- 3.7 Unprotected pipeline at seabed
- 3.8 Cross-section of unprotected pipeline at seabed
- 3.9 Plan view of a sandy coast with a river outfall in initial situation (a) and with a developing delta (b)
- 3.10 Tidal inlets in the Waddenzee (The Netherlands)
- 3.11 Schematic plan view of a tidal inlet
- 3.12 Cross-shore profile under normal conditions
- 3.13 Funnel shaped North Sea
- 3.14 Measured and predicted water levels at Vlissingen (The Netherlands)
- 3.15 Cross-shore profile directly after storm conditions
- 4.1 Forces on a “sphere” in clear water
- 4.2 Drag coefficient as a function of Reynolds Number (Vanoni 1975)
- 4.3 Fall velocities of sediment for fresh water with a temperature of 18 degrees Celsius (after Siermans, 2002)
- 4.4 Forces on an individual grain: drag force, lift force and gravity force
- 4.5 Resulting forces and moments on a grain
- 4.6 Shields curve
- 4.7 Force balance
- 4.8 Velocity distribution for a uniform stationary current
- 4.9 Water particle movement in waves
- 4.10 Boundary layer thickness
- 4.11 Velocity field near a rippled bed in oscillatory flow (Du Toit, 1982)
- 4.12 Wave friction parameter
- 4.13 Velocity distribution in stationary current and under waves
- 4.14 Plan view and specific velocity components at an elevation  $z_i$  above the bottom
- 4.15 Plan view and bottom shear stress components
- 4.16 Components of mean shear stress
- 4.17 Principle of (suspended) sediment transport computation

- 
- 4.18 Sediment concentrations as a function of time (99 individual records); Bosman (1986)
  - 4.19 Overview of  $\varepsilon_s$  distributions [after Sistermans (2002)]
  - 4.20 Sediment concentration distribution over water depth (constant mixing coefficient)
  - 4.21 Sediment concentration distribution over water depth (parabolic mixing coefficient)
  - 4.22 Computation of the mean velocity in the bottom layer
  - 4.23 Suspended sediment transport parameters
  
  - 5.1 Different scales
  - 5.2 Distinction between longshore and cross-shore transport
  - 5.3 Measured velocities under a propagating wave (undertow)
  
  - 6.1 Wave-induced changes in pressures compared to hydrostatic pressure under still water
  - 6.2 Principal radiation stresses
  - 6.3 Effect of changes in the radiation stress component  $S_{xx}$
  - 6.4 Equilibrium of forces in the entire breaker zone
  - 6.5 Radiation shear stresses
  - 6.6 Radiation stresses for oblique approaching waves
  - 6.7 Computed radiation shear stresses
  - 6.8 Tidal current along the shore
  - 6.9 Typical velocity distribution for wind-driven current
  - 6.10 Forces acting on water columns
  - 6.11 Longshore velocity distribution (regular wave field)
  - 6.12 Effect of turbulence on the velocity profile
  - 6.13 Examples of velocity profiles
  - 6.14 Wave driven velocity computed with UNIBEST-LT
  - 6.15 Inclusion of tidal currents
  - 6.16 Results of Example 6.4
  - 6.17 Examples of transport distributions
  - 6.18 Sensitivity analysis with UNIBEST-LT
  - 6.19 Typical cases of possible drastic coastline change
  - 6.20 Sediment balance (*not to scale*)
  - 6.21 Single line theory
  - 6.22 Definition sketch for single line theory
  - 6.23 Accretion of the shore near a breakwater. The wave conditions given in the sketch refer to the conditions at the assumed horizontal part in the coastal area.
  - 6.24 Shoreline development at the lee side of a breakwater (simplified)
  - 6.25 PonTos layer schematisation
  - 6.26 Coastline development with breakwater
  - 6.27  $(S, \varphi)$ -curves for various cross-sections of Fig.6.26
  - 6.28 Prolonged coastline development with breakwater
  
  - 7.1 Profile schematisation and indication of different zones
  - 7.2 3D image of the coast of Holland
  - 7.3 Summer and winter profile
  - 7.4 Dune erosion during severe storm
  - 7.5 Erosion in front of an almost vertical wall
  - 7.6 Redistribution of material due to cross-shore transport
  - 7.7 Sea level rise: Bruun rule
  - 7.8 Dune erosion during a severe storm surge
  - 7.9 Rate of erosion as function of frequency of exceedance
  - 7.10 DUROSTA versus Delta Flume results [Steetzel (1993)]
  
  - 8.1 Basic set-up of complex morphological computation model
  
  - 9.1 Mangroves
  - 9.2 Satellite image of the Wadden Sea
  - 9.3 Wentworth classification
  - 9.4 Structure of clay particles
  - 9.5 Definition sketch of suspended sediment transport
  - 9.6 Critical velocities as a function of silt content
-

- 
- 9.7 The Slufter (Rotterdam, The Netherlands)
  
  - 10.1 Dredging in the Euro-Channel, Rotterdam, The Netherlands
  - 10.2 Current pattern across a channel
  - 10.3 Relationship  $v_2/v_1$
  - 10.4 Sketch of a tidal channel
  - 10.5 Sedimentation mechanism
  - 10.6 Sedimentation rate in a wide channel
  - 10.7 Continuity equation
  
  
  - 11.1 Control volume
  - 11.2 Dune erosion due to storm
  - 11.3 Structural erosion
  - 11.4 Volume loss out of control volume due to structural erosion
  - 11.5 Developments of coastline near port
  - 11.6 Spit and river mouth
  - 11.7 Stabilized river mouth
  - 11.8 Developments of coastline near river outflow
  - 11.9 Scour in front of seawall
  - 11.10 Graphical representation of the “5 I-approach”
  
  
  - 12.1 Seawall
  - 12.2 Seawall and boulevard
  - 12.3 Seawall with measures to reduce overtopping
  - 12.4 Seawall and gradient in longshore sediment transport
  - 12.5 Revetment
  - 12.6 Scour in front of revetment
  - 12.7 Port breakwaters
  - 12.8 Long dam Texel
  - 12.9 Groynes
  - 12.10 Row of piles
  - 12.11 Sketch of rate of interruption of sediment transport by a groyne
  - 12.12 Detached shore parallel offshore breakwaters
  - 12.13 Emerging breakwaters
  - 12.14 Processes near emerging breakwater
  - 12.15 Tombolo and salient
  - 12.16 Tombolo behind island
  - 12.17 Submerged breakwater
  - 12.18 Processes near submerged breakwater
  - 12.19 Application of structures to confine sand
  - 12.20 Real life example
  - 12.21 Expected cross-shore profiles large scale land reclamation
  - 12.22 Recreation pier
  - 12.23 Sea-dike
  - 12.24 Hondsbossche and Pettemer sea defence
  - 12.25 Additional sheet piling
  
  
  - 13.1 Development with time of volume of cross-shore profile with nourishment
  - 13.2 Beach nourishment and shoreface nourishment
  - 13.3 Reinforcement of dunes
  - 13.4 Losses in longshore direction
  - 13.5 Land reclamation: cross-shore profile entirely shifted
  - 13.6 Land reclamation: shifted profile with transition slope
  - 13.7 Land reclamation: shifted profile with 'supporting' breakwater
  - 13.8 Profile adaptations and sea level rise

---

## List of Tables

- 2.1 Formulae for shallow, transitional and deep water wave computations
- 2.2 Criteria for deep and shallow water waves
  
- 4.1 Values of  $Q$  for different  $r/h$ -values
- 4.2 Values for  $Q$  and  $S_s/S_b$  for different  $r/h$ -values
  
- 5.1 Examples of morphological time scales
- 5.2 Order of magnitude of time spans, during which sedimentary features are active [from Oost (1995)]

## List of Examples

- 2.1 Wave height in case of a current
  
- 4.1 Critical velocity
- 4.2 Bottom shear stress under current
- 4.3 Bottom shear stress under waves
- 4.4 Bottom shear stress under current and waves combined
- 4.5 Bottom shear stress under longshore current
- 4.6 Sediment transport by current and by current and waves
  
- 6.1 Maximum wave set-up relative to the still water level
- 6.2 Radiation shear stresses and gradients in  $S_{yx}$  for various positions
- 6.3 Distribution of the depth-averaged longshore current
- 6.4 Sediment transport rate  $S_x$  for different values of  $\phi_0$
- 6.5 Sediment transport using the Bijker formulation
- 6.6 Application of single line theory to a breakwater
- 6.7  $(S, \phi)$ -curve
- 6.8  $(S, \phi)$ -curve (partial blocking of waves)
  
- 7.1 Unibest-TC calculation
  
- 11.1 Rate of recession versus volume rate of erosion
- 11.2 Convex coast
- 11.3 Chances, consequences and risks
- 11.4 Basic notions 'hard' solution of structural erosion



# 1 Introduction

## 1.1 Position of Coastal Morphology and Coastal Protection

‘Coastal Engineering’ concerns engineering topics in coastal areas. Because Coastal Engineering is so extensive, often a sub-division is made in three main areas:

- Port Engineering
- Coastal Morphology and Coastal Protection
- Offshore Engineering

### Port Engineering

Port Engineering covers topics like port layout, breakwater design and wave penetration in harbour areas. These topics, while quite interesting, are not dealt with in these lecture notes. Special courses at Delft University of Technology (DUT) are devoted to these topics (e.g. CT5306 and CT5308).

### Coastal Morphology and Coastal Protection

Coastal Morphology and Coastal Protection is the subject of the present lecture notes. A topic like ‘Dynamics of Estuaries and Tidal Inlets’ belongs for sure to coastal morphology. Because of the importance of ‘Dynamics of Estuaries and Tidal Inlets’ at DUT a special course is devoted to that topic (CT5303).

Coastal Zone Management (CZM) has strong links with Coastal Morphology and Coastal Protection. At DUT, CT5307 is devoted to Integrated Coastal Zone Management topics.

### Offshore Engineering

There are many links between Offshore Engineering and Coastal Morphology, e.g. scour around offshore structures and scour underneath pipelines at the sea floor. These topics are not dealt with in the present lecture notes. See courses on Offshore Engineering.

## 1.2 Interrelationships

Coastal Morphology means the physical shape and structure of the coast. If a sandy coast is considered, tides, currents and waves may cause sediment transports. Gradients in the sediment transport rates, cause changes in coastal morphology. So to understand coastal morphology, it is necessary to understand the process of sediment transport due to waves and currents. Fluid mechanics and wave theories are indispensable topics in coastal morphology. (E.g. courses CT4320, CT4340 and

CT5316 at DUT.) Within the curriculum of DUT Coastal Morphology and Coastal Protection builds on ‘Introduction to Coastal Engineering’ (CT4300).

### 1.3 Objective of lecture notes

Lecture notes are meant to be a guide for students while studying a particular subject. That means that it is attempted to stick to the basics of the subject. Related to each topic to be discussed, an overwhelming amount of literature does exist. Often references are made. It is of course recommended to consult literature. In Chapter 15, an overview is given of general books, journals and proceedings of related conferences.

In this book often specific literature references are given; they are noted in the text by author(s) and year of publication. At the end all relevant details of the references as mentioned, are given.

### 1.4 ‘Players’ in coastal engineering in The Netherlands

In The Netherlands coastal engineering is a very important topic. The bottom level of large parts of The Netherlands is below Mean Sea Level (MSL); see Fig.1.1. Without dikes and dunes people would not be able to live in these parts of the country.

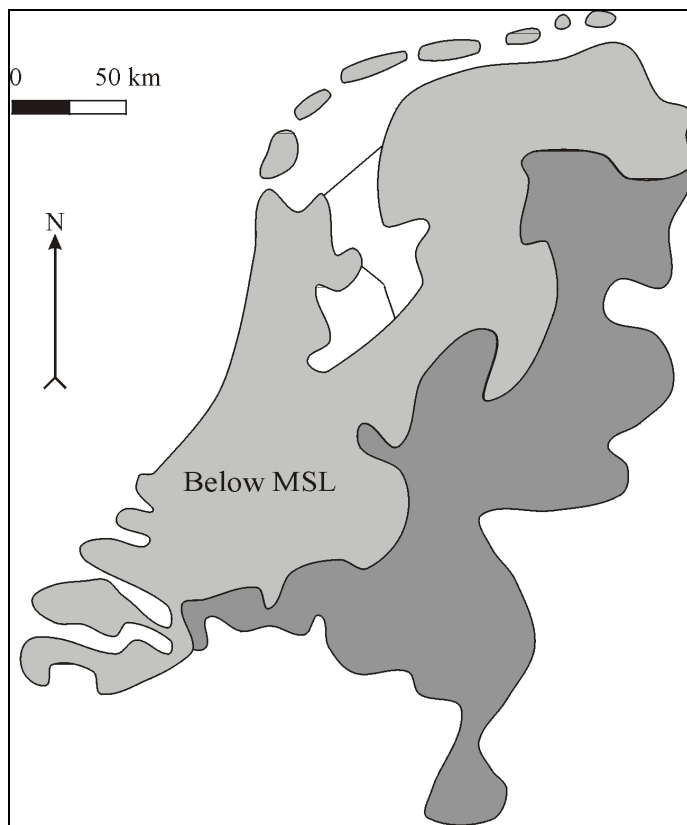


**Figure 1.1 The Netherlands below Mean Sea Level**

In The Netherlands many governmental organisations, consultants, contractors, research institutes and universities, are active in the field of coastal engineering.

## Government

Various parts of the Directorate-General of Rijkswaterstaat (RWS) and the Directorate-General Water, which are parts of the Ministry of Transport, Public Works and Water Management, are active in the field of coastal engineering.

- Waterdienst Lelystad;
- Directorate North sea;
- Regional Directorates of RWS.

The various Provinces bordering the North Sea, are, at a mainly co-ordination level, also involved in coastal matters, e.g. coastal zone management. Also Water Boards play an important role in coastal zone management in The Netherlands.

## Consulting companies/contractors

Many Dutch consulting companies and contractors are active in the field of coastal engineering; either in the design phase or in the execution of specific works.

A certainly not complete list of companies involves (in alphabetical order):

- Alkyon / Arcadis;
- DHV;
- Hydronamic (Boskalis);
- Royal Boskalis Westminster;
- Royal Haskoning;
- Van Oord;
- Witteveen + Bos.

## Research institutes

Research institutes are in The Netherlands often positioned in between consulting activities and academic, more fundamental research. Institutes active in the field of coastal engineering and coastal morphology are amongst others:

- NIOZ - The Netherlands Institute for Sea Research (Nederlands Instituut voor Onderzoek der Zee);
- Deltares (Delft Hydraulics, GeoDelft, the Subsurface and Groundwater unit of TNO and parts of Rijkswaterstaat have joined forces since 2008 to become an independent institute for delta technology; Deltares).

## Universities

In The Netherlands three universities are in particular involved in education and research related to coastal engineering and coastal morphology:

- DUT - Delft University of Technology;
- UU - Utrecht University;
- UT - Twente University.

Besides these, the UNESCO-IHE (Institute for Water Education) focuses on the education of people from developing countries.

## Research co-operation in The Netherlands

- Delft Cluster - a co-operation between UNESCO-IHE, DUT, Deltares;
- NCK - Netherlands Centre for Coastal Research, a co-operation between DUT, UU, UT, Waterdienst, Deltares, NIOZ and NIOO-CEMO (The Netherlands Institute for Ecology-Centre for Estuarine and Marine Ecology);
- ENW - Expertise Network Water Safety (Expertise Netwerk Waterveiligheid).

## 1.5 ‘Players’ in coastal engineering in the world

All over the world, many organisations, institutes, universities, consultants and contractors are active in the field of coastal engineering.

More or less 'leading' countries in the world, where coastal engineering and coastal morphology are important subjects, are amongst others:

- Australia;
- Denmark;
- Germany;
- Japan;
- South Africa;
- Spain;
- The Netherlands;
- UK;
- USA.

## 1.6 Overview of contents

Because sediment transport is often directly related to tides, currents and wave characteristics, these topics are briefly discussed in **Chapter 2**. Also the general descriptions of water motion and wave formulae, which are used in these lecture notes, are presented in this chapter.

**Chapter 3** contains a few example problems in coastal engineering practice. From these examples the relevance of the subject will become clear.

**Chapter 4** is devoted to general aspects of sediment transport; the additional effect of waves is discussed. An overview of relevant formulae is given.

For many applications it is still useful to make a distinction between longshore transport (i.e. parallel to the coast) and cross-shore transport (i.e. perpendicular to the coast). **Chapter 5** deals with these two modes of sediment transport.

In **Chapter 6** some typical longshore transport applications in coastal engineering practice are discussed.

**Chapter 7** deals with cross-shore transport applications. Amongst others the problem of dune erosion during a severe storm surge is discussed. The latter problem is especially important in The Netherlands.

Not all problems can be schematised as being either longshore or cross-shore related. These more complex processes and the role of so-called 2DH-morphological models are discussed in **Chapter 8**.

The main emphasis in these lecture notes is on sandy coasts. But even in sand at the bottom of the sea silt and clay particles often occur. **Chapter 9** deals with some fundamentals of mud in coastal areas.

**Chapter 10** considers the problems of channels and trenches in coastal areas. The problems of siltation and sedimentation of these channels and trenches are discussed.

Adequate coastal protection is a wide spread problem all over the world. **Chapter 11** deals with related coastal management issues and introduces two basic approaches to coastal protection.

One of the approaches concerns the application of structures and is elaborated in **Chapter 12**, whereas the application of artificial nourishments is discussed in **Chapter 13**.

**Chapter 14** gives an overview of relevant background information, including general handbooks, interesting journals and conference proceedings.

Finally, all **References** as cited in the main text are summarised.



## 2 Tides, Currents and Waves

### 2.1 Introduction

If the seas were always quiet and smooth, coastal engineering would not be very interesting. But this is not the case. Fluctuations in the sea level, at long (e.g. astronomical tide) and short term (e.g. wind waves) and often very irregular, make the sea so powerful and coastal engineering so important and interesting.

For many years, people were afraid of the sea because they knew almost nothing about these fluctuations which were unpredictable and often came completely by surprise. Today we know a lot more, but not all, about these fluctuations, where they originate and what their consequences are. Though no longer 'afraid' we still must exercise great caution in our dealings with the sea.

The purpose of this chapter is not to give a 'textbook' on tide, current and wave theories but to give a short overview of the theories involved, which is necessary to complete these lecture notes. Knowledge of some basic notions facilitates the use of these lecture notes. Furthermore the notation as is used for these basic notions, is used throughout the lecture notes.

Since waves or wave movements are used in the remainder of the lecture notes for amongst others describing and calculating sediment transport, it is useful to first briefly discuss the subject of waves and give the basic formulae and parameters. We assume that the reader is familiar with common parameters like  $H$ ,  $c$ ,  $k$ ,  $\omega$  and  $T$  in wave theory. A list of symbols is enclosed in the last pages of these lecture notes. A more extensive description of wave theories is given in the lecture notes CT4320.

There are many different types of water level/surface fluctuations; for example:

- astronomical tides;
- wind waves / surface waves (capillary waves, ship waves);
- tsunamis;
- seiches;
- wave set-up;
- storm surges / wind set-up;
- water level fluctuations caused by specific mechanisms (e.g. coastal upwelling);
- climatological variations.

Most of these fluctuations occur periodically, their periods varying from seconds to months. Fig.2.1 (next page) shows a wave energy spectrum. In the figure periodic fluctuations are given with their range of periods (horizontally) and the relative quantity of energy (vertically). The figure also indicates the forces initiating the wave, the forces reducing the wave, and the way in which we classify the wave.

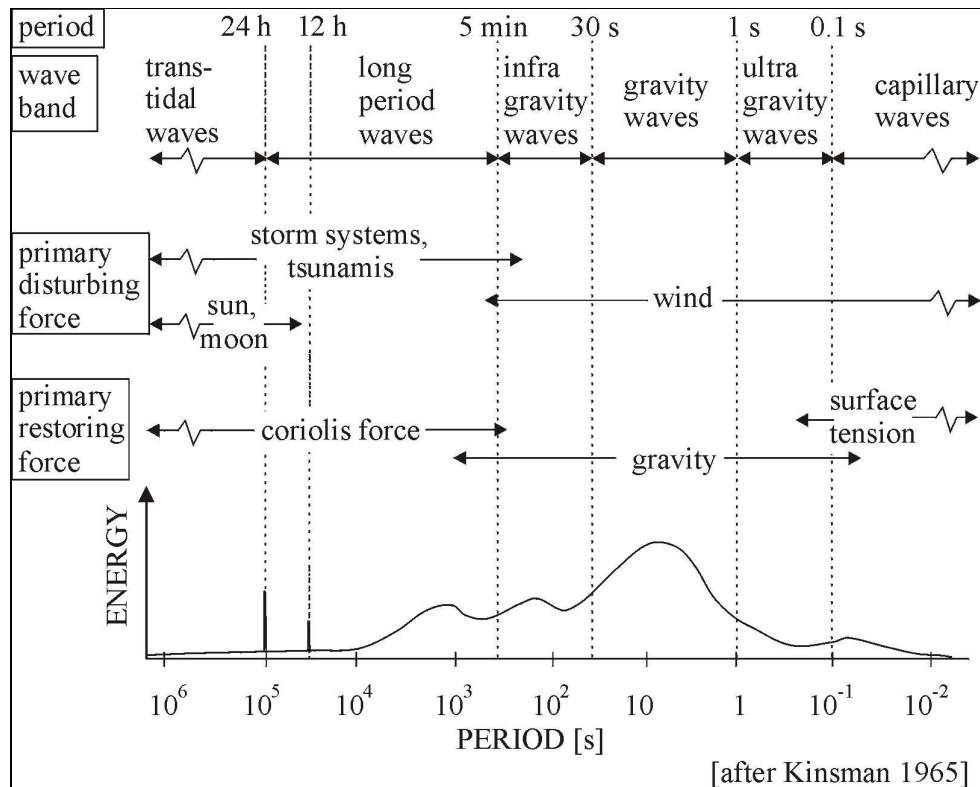


**Figure 2.1** Wave energy spectrum

Of greatest interest in coastal engineering in our region [in Europe (in the North Sea) there are no tsunamis] are the water level fluctuations due to astronomical tide and wind-generated waves and wind-generated storm surges.

In Section 2.2 a few remarks concerning astronomical tides are made whereas in Section 2.3 some remarks with respect to currents in the coastal zone are dealt with. Section 2.4 discusses how wind-generated waves can be analysed and can be described. Also the combination of waves and currents is discussed.

What happens if waves reach the coast is described in Section 2.5.

Finally, some attention is paid to the available software and wave measurements (Section 2.6 and 2.7 respectively).

Chapter 3 discusses the consequences of wind-generated waves, or more generally currents and surface waves for sediment transport along the coastline.

## 2.2 Tides

### 2.2.1 Vertical tide

Gravitational attraction of the moon and the sun to the rotating earth, causes the water level to fluctuate with time. The effect of the moon (small mass, but short distance to earth) on the tidal variations is much larger than the effect of the sun (large mass, but large distance).



The ratio of the effects of sun and moon is approximately 1 in 4 along the Dutch coast (ratio  $S_2/M_2 \approx 1/4$ ). Both near the times of new moon and full moon, sun, moon and earth are more or less in one line. The effects of moon and sun on the tide work together; so-called spring tides are to be expected. At the first and the last quarter position of the moon, the effects of moon and sun on the tide are opposite; neap tides occur. Fig.2.2 shows an example of these tidal variations.

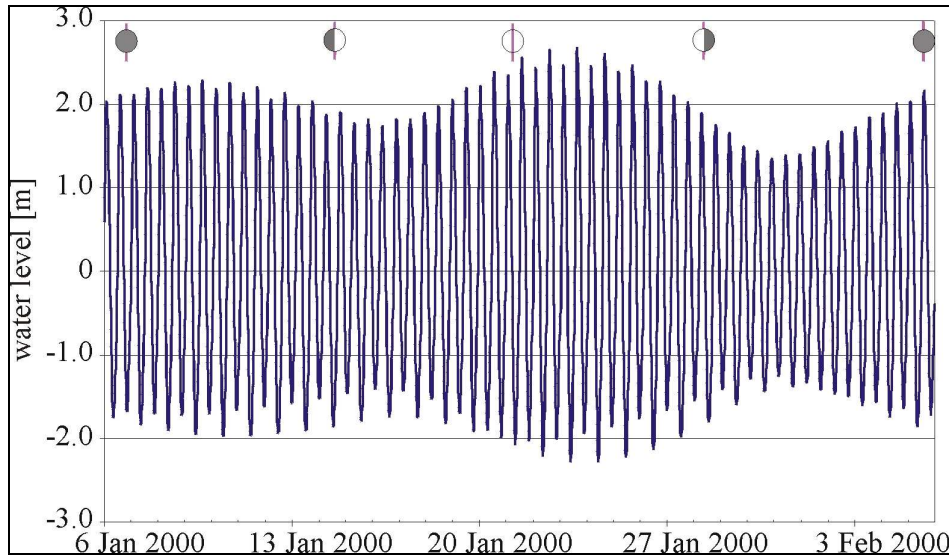


**Figure 2.2 Tidal variations (spring and neap tide)**

The difference between high water and low water is the tidal range.

The period of the water level fluctuation due to the tide is site-specific. In many cases the so-called  $M_2$ -component dominates; semi-diurnal tides (period: 12 hr. 25 min.) occur. This means that two high waters per tidal day (lunar day; 24 hr. 50 min.) do occur. In some areas diurnal tides occur; one high water per tidal day.

The lecture notes CT5317 contain much more information concerning topics like tide generation and tide prediction.

### 2.2.2 Horizontal tide

Periodic water level fluctuations are coupled with periodic tidal currents. During spring tide the currents are stronger than during neap tide.

Of course depending on the specific conditions, maximum current velocities in the order of magnitude of 1 m/s do occur. In Section 2.3 the mathematical description of currents is discussed.

Fig.2.3 (next page) shows examples of tidal current patterns.

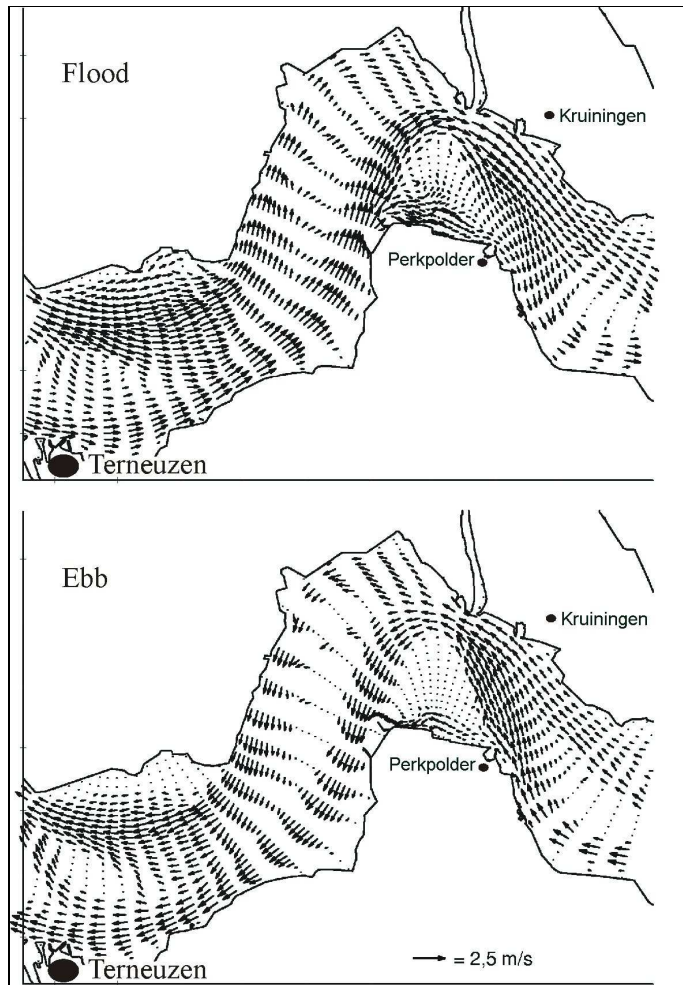


**Figure 2.3** Tidal current pattern

## 2.3 Currents

Currents generated by many different processes occur in the sea bordering coasts (e.g. tidal currents, wind-driven currents and currents induced by differences in density). For many practical applications a description of the flow field with depth-averaged currents is sufficient. For other applications knowledge of the vertical distribution of the currents is necessary.

In two horizontal dimensions (depth averaging), the fluid dynamics in open sea can be described by a continuity and a momentum equation.

The continuity or mass balance equation reads:

$$\frac{\partial \zeta}{\partial t} + \frac{\partial}{\partial x} ((h + \zeta)u) + \frac{\partial}{\partial y} ((h + \zeta)v) + source = 0 \quad (2.1)$$

where:

$u, v$	components of depth averaged velocities	[m/s]
$\zeta$	water elevation above the reference plane	[m]

$h$	water depth below the reference plane	[m]
$x, y$	horizontal co-ordinates	[m]
$t$	time	[s]

For the *source* term, any discharge can be included e.g. evaporation, precipitation, river discharges etc.

The momentum or impulse equations are also called the equations of motion. The equation of motion for the x-direction is given in Eq.(2.2), for the y-direction in Eq.(2.3).

$$\begin{aligned} \frac{\partial u}{\partial t} + u \frac{\partial u}{\partial x} + v \frac{\partial u}{\partial y} - f_c v + g \frac{\partial \zeta}{\partial x} + g u \frac{\sqrt{u^2 + v^2}}{C^2(h + \zeta)} = \\ = \frac{\rho_a C_d W_x \sqrt{W_x^2 + W_y^2}}{\rho(h + \zeta)} + v \left( \frac{\partial^2 u}{\partial x^2} + \frac{\partial^2 u}{\partial y^2} \right) + Forces \end{aligned} \quad (2.2)$$

$$\begin{aligned} \frac{\partial v}{\partial t} + u \frac{\partial v}{\partial x} + v \frac{\partial v}{\partial y} - f_c u + g \frac{\partial \zeta}{\partial y} + g v \frac{\sqrt{u^2 + v^2}}{C^2(h + \zeta)} = \\ = \frac{\rho_a C_d W_y \sqrt{W_x^2 + W_y^2}}{\rho(h + \zeta)} + v \left( \frac{\partial^2 v}{\partial x^2} + \frac{\partial^2 v}{\partial y^2} \right) + Forces \end{aligned} \quad (2.3)$$

where:

$f_c$	Coriolis parameter	[-]
$g$	acceleration due to gravity	[m/s <sup>2</sup> ]
$C$	coefficient of Chézy, representing bottom roughness	[m <sup>1/2</sup> /s]
$W_x, W_y$	components of surface wind velocity	[m/s]
$\rho_a, \rho$	air density, water density	[kg/m <sup>3</sup> ]
$C_d$	wind drag coefficient	[-]
$\nu$	eddy-viscosity coefficient	[m <sup>2</sup> /s]

At the left hand side, the normal physical behaviour of open water in shallow areas is described. At the right hand side, wind and internal fluid friction are shown. Additional terms can be added at the right hand side to represent additional physical phenomena, which are able to drive or slow down a fluid. Examples are a series of terms, which represent the short wave effects on the flow. The wave energy dissipation (important when waves break in the nearshore zone), the enhanced bottom friction due to waves and the additional mass flux caused by the Stokes drift of short waves, are examples of wave effects.

Another example is the effect of atmospheric pressure differences or density differences. These terms are in the depth-averaged equations represented by a local pressure correction.

In a further simplification, e.g. a uniform beach (having straight and parallel depth contours) with the x-axis parallel to the shoreline, the equation reads as a balance between driving forces and friction forces:

$$\frac{\partial u}{\partial t} + u \frac{\partial u}{\partial x} + g \frac{\partial \zeta}{\partial x} + g \frac{u|u|}{C^2 h} = \frac{\rho_a C_d W_x^2}{\rho(h + \zeta)} \quad (2.4)$$

The first three terms represent the tidal force, the fourth term the bottom friction and the right hand term the wind effect. Assuming steady state flow conditions in the absence of wind, we can make a further simplification. In that case the simple Chézy relation results:

$$g \frac{\partial \zeta}{\partial x} + g \frac{u|u|}{C^2 h} = 0 \quad (2.5)$$

$$\text{with } i = -\frac{\partial \zeta}{\partial x} \text{ follows: } i = \frac{u|u|}{C^2 h} \quad (2.6)$$

$$\text{and: } u = C\sqrt{hi} \quad (2.7)$$

The equation shows the balance between bottom friction due to currents and the local nearshore water level slope in a certain tidal phase.

Multiplying both terms of Eq.(2.6) with  $\rho gh$  yields the well-known equation for the bottom shear stress in case of a current,  $\tau_c$ :

$$\tau_c = \frac{\rho g u^2}{C^2} \quad [\text{N/m}^2] \quad (2.8)$$

In Section 4.4 we will see that in the combination of currents and waves, the wave effect increases the bottom friction, but also that wave effects may contribute to current generating forces. In that case Eq.(2.7) cannot be applied anymore.

## 2.4 Wave characteristics

### 2.4.1 General

If we put a buoy in the sea and keep it in one (horizontal) position, we can record its level. Measuring the level of the water surface as a function of time we get a graph similar to that shown in Fig.2.4. That figure presents an irregular picture. In order to get a better idea about wave movements, wave fields are often schematised into regular waves or even a sinusoidal wave form.

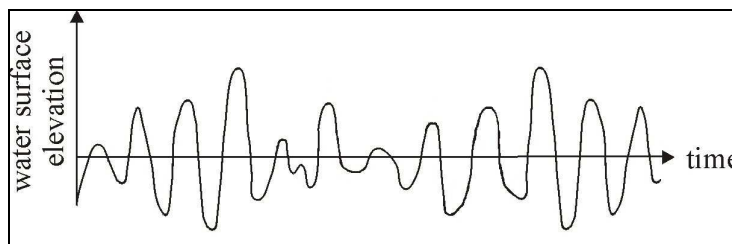


**Figure 2.4 Water surface measurements**

Fig.2.5 gives a definition sketch for the most elementary properties of such a sinusoidal progressive wave. It should be noted that in these lecture notes the axis-system starts at the sea bottom. [In most wave theories the axis-system starts at mean sea level (and then mean sea level  $z = 0$ )]. However, because this course is amongst

others about sediment transport and in sediment transport discussions it is handy to choose the  $x$ -axis ( $z = 0$ ) on the sea bottom, we will treat the wave theories with the  $x$ -axis ( $z = 0$ ) on the sea bottom as well. One has to bear in mind therefore that some formulae will possibly be different from wave formulae as found in wave related literature.

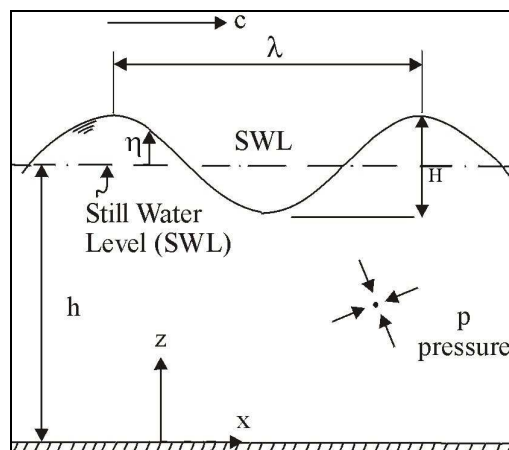


**Figure 2.5 Definition sketch of progressive, sinusoidal wave (horizontal and vertical scale quite different)**

In reality waves are not regular and are certainly not sinusoidal. However, it is often useful to work with the regular monochromatic (and in theoretical problems also sinusoidal) waves because the results give a good first impression of what happens, and give yet a reasonable similarity to reality. A lot of research has already been done on regular waves and on the consequences of regular waves (e.g. water velocity profiles, wave penetration in harbours, sand concentrations).

Nowadays, theories and computer programs have been extended to handle irregular waves. In many cases equipment is available to generate pre-described irregular wave fields (physical model research) or to calculate the consequences of irregular wave fields (computers). When using irregular waves it is first necessary to analyse and characterise wave records such as that shown in Fig.2.4. This can be done probabilistically. The approach used for analysing and characterising an irregular wave record is discussed in Section 2.4.4 after a short discussion on regular waves in Sections 2.4.2 and 2.4.3.

## 2.4.2 Regular waves

Even truly monochromatic regular waves are difficult to describe because of their non-sinusoidal profile. There are several theories, varying both in complexity and in accuracy, for describing these waves.

The simplest and generally most useful theory is the Airy theory. Airy presented this wave theory in which he simplified the wave profile to a linear sinusoidal wave form [Airy (1845)]. His theory provides equations for the most important properties of

surface gravity waves, and predicts these properties within useful limits in a number of practical conditions, even though real water waves are not sinusoidal.

As non-linear theories for periodic, regular waves we can mention:

- Shallow water theories ( $\lambda/h \gg 1$ ,  $H/h < 1$ ). In this category we find the cnoidal wave and the solitary wave theory [Boussinesq (1872)];
- Rotational wave theories in which the distribution of vorticity is taken into account. An example of this theory is the Gerstner or trochoidal wave theory [Gerstner (1802)];
- Edge waves that develop on a sloping bottom and propagate along the shore with the wave crests perpendicular to the shore line;
- Numerical theories which give the most accurate solutions (also for near-breaking waves). We can also mention the stream-function wave theory of Dean (1965), who gives tabulated results (often used in offshore technology), Cokelet (1965) for an exact solution in the case of a steady wave train in water of constant depth, and the vocoidal theory of Swart and Loubser (1978). The latter suggest that their theory is available for a wider range of conditions than Dean's theory.

Fig.2.6 indicates the regions to which the various wave theories apply. The figure is based on similar plots provided by Le Mehaute and Dean [see Le Mehaute (1976) and (Dean 1970)].

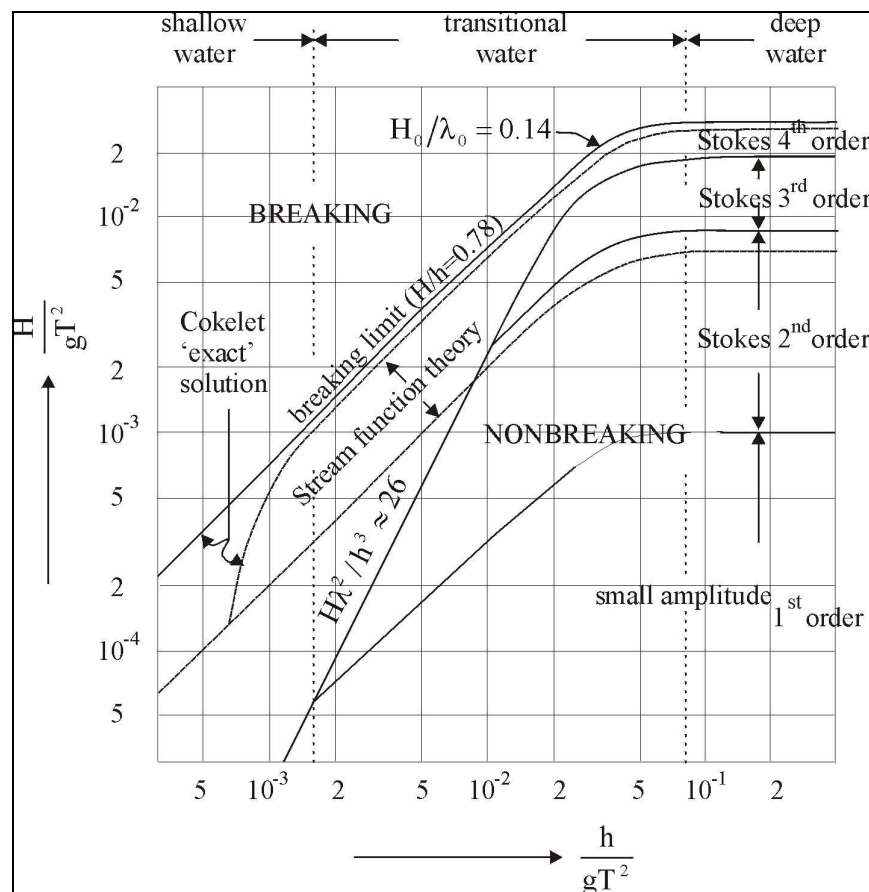


**Figure 2.6 Regions of validity for various wave theories**

More information on the linear sinusoidal wave theory is provided in the following.

### 2.4.3 Linear sinusoidal waves

In the theory for linear waves, equations are given for properties like:

- the particle velocity ( $u, w$ ) at any height in the water column [m/s]
- the particle acceleration ( $a_x, a_z$ ) at any height in the water column [m/s<sup>2</sup>]
- the particle displacement ( $\xi, \zeta$ ) at any height in the water column [m]
- the pressure ( $p$ ) at any height in the water column [N/m<sup>2</sup>]
- the wave speed ( $c$ ) [m/s]
- the wave group speed ( $c_g$ ) [m/s]
- the wavelength ( $\lambda$ ) [m]
- the wave profile ( $\eta(x)$ ) [m]
- the wave energy per wavelength per unit crest length ( $E_l$ ) [J/m]
- the energy per unit water surface area ( $E$ ) [J/m<sup>2</sup>]
- the wave power ( $U$ ) [J/ms]

The general equations for these properties can be found in Table 2.1 (next page) in the 'Transitional Water Depth' column. The equations for transitional water depth are not easy to solve because simplifications can not be made.

However, the equations can be simplified both for deep and shallow water (see Table 2.2 for the limits). The simplifications are made in the hyperbolic function terms (Fig.2.7).

	shallow water			deep water		
	$h/\lambda_0$	$h/\lambda$	$kh$	$h/\lambda_0$	$h/\lambda$	$kh$
Mathematicians	<1/25	<1/12	<1/2	>1/2	>1/2	> $\pi$
Engineers	<1/20	<1/11	<1/1.7	>1/4	>1/4	> $\pi/2$

**Table 2.2 Criteria for deep and shallow water waves**

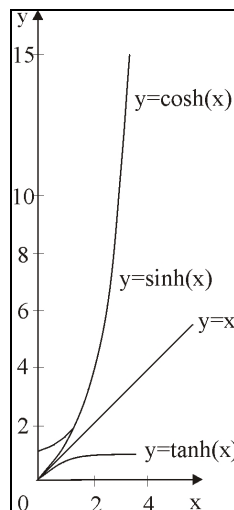


**Figure 2.7 Simplified hyperbolic functions**

PARAMETER	DIMENSIONS	SHALLOW WATER	TRANSITIONAL WATER DEPTH	DEEP WATER
wave profile	m	→	$\eta = \frac{H}{2} \cos(kx - \omega t)$	←
wave celerity	m/s	$c = \frac{\omega}{k} = \sqrt{gh}$	$c = \frac{\omega}{k} = \frac{\sqrt{g \tanh kh}}{k} = \frac{gT}{2\pi} \tanh kh$	$c = c_0 = \frac{\lambda_0}{T} = \frac{gT}{2\pi} \approx \frac{g}{\omega} (\approx 1.56T)$
wave group celerity	m/s	$c_g = c = \sqrt{gh}$	$c_g = nc = \frac{1}{2} \left[ 1 + \frac{2kh}{\sinh 2kh} \right] c$	$c_{g0} = \frac{1}{2} c_0 = \frac{gT}{4\pi}$
wavelength	m	$\lambda = cT = \sqrt{gh}T$	$\lambda = cT = \frac{gT^2}{2\pi} \tanh kh$	$\lambda = \lambda_0 = c_0 T = \frac{gT^2}{2\pi} (\approx 1.56T^2)$
wave particle velocity horizontal	m/s	$u = \frac{\omega H}{2kh} \cos(kx - \omega t)$	$u = \frac{\omega H \cosh kz}{2 \sinh kh} \cos(kx - \omega t)$	$u = \frac{\omega H_0}{2} e^{k_0(z-h)} \cos(k_0 x - \omega t)$
vertical	m/s	$w = \frac{\omega Hz}{2h} \sin(kx - \omega t)$	$w = \frac{\omega H \sinh kz}{2 \sinh kh} \sin(kx - \omega t)$	$w = \frac{\omega H_0}{2} e^{k_0(z-h)} \sin(k_0 x - \omega t)$
wave particle acceleration horizontal	m/s <sup>2</sup>	$a_x = \frac{\omega^2 H}{2kh} \sin(kx - \omega t)$	$a_x = \frac{\omega^2 H \cosh kz}{2 \sinh kh} \sin(kx - \omega t)$	$a_x = \frac{\omega^2 H_0}{2} e^{k_0(z-h)} \sin(k_0 x - \omega t)$
vertical	m/s <sup>2</sup>	$a_z = \frac{-\omega^2 Hz}{2h} \cos(kx - \omega t)$	$a_z = \frac{-\omega^2 H \sinh kz}{2 \sinh kh} \cos(kx - \omega t)$	$a_z = \frac{-\omega^2 H_0}{2} e^{k_0(z-h)} \cos(k_0 x - \omega t)$
wave particle displacement horizontal	m	$\xi = \frac{H}{2kh} \sin(kx - \omega t)$	$\xi = \frac{-H \cosh kz}{2 \sinh kh} \sin(kx - \omega t)$	$\xi = \frac{-H_0}{2} e^{k_0(z-h)} \sin(k_0 x - \omega t)$
vertical	m	$\zeta = \frac{Hz}{2h} \cos(kx - \omega t)$	$\zeta = \frac{H \sinh kz}{2 \sinh kh} \cos(kx - \omega t)$	$\zeta = \frac{H_0}{2} e^{k_0(z-h)} \cos(k_0 x - \omega t)$
subsurface pressure	N/m <sup>2</sup>	$p = \rho g(h-z) + \frac{\rho g H}{2} \cos(kx - \omega t)$	$p = \rho g(h-z) + \frac{\rho g H}{2} \frac{\cosh kz}{\cosh kh} \cos(kx - \omega t)$	$p = \rho g(h-z) + \frac{\rho g H_0}{2} e^{k_0(z-h)} \cos(k_0 x - \omega t)$
wave energy per wavelength per unit crest length	J/m	$E_t = \frac{1}{8} \rho g H^2 \lambda$	$E_t = \frac{1}{8} \rho g H^2 \lambda$	$E_{t0} = \frac{1}{8} \rho g H_0^2 \lambda_0$
specific wave energy	J/m <sup>2</sup>	$E_t = \frac{1}{8} \rho g H^2$	$E_t = \frac{1}{8} \rho g H^2$	$E_{t0} = \frac{1}{8} \rho g H_0^2$
wave power	J/ms	$U = E c_g = E c = Ec$	$U = E c_g = E n c$	$U_0 = E_0 n_0 c_0 = \frac{1}{2} E_0 c_0$

Table 2.1 Formulae for shallow, transitional and deep water wave computations



For relatively deep water ( $h > \lambda_0/2$  so  $kh > \pi$  where  $k = 2\pi/\lambda$  is the wave number):

$$\sinh kh = \frac{1}{2}(e^{kh} - e^{-kh}) = \frac{1}{2}e^{kh} \quad \text{for } kh \rightarrow \infty \quad (2.9)$$

$$\cosh kh = \frac{1}{2}(e^{kh} + e^{-kh}) = \frac{1}{2}e^{kh} \quad \text{for } kh \rightarrow \infty \quad (2.10)$$

$$\tanh kh = 1 \quad \text{for } kh \rightarrow \infty \quad (2.11)$$

For relatively shallow water ( $h < \lambda_0/25$  so  $kh < 1/2$ ):

$$\sinh kh = kh \quad \text{for } kh \rightarrow 0 \quad (2.12)$$

$$\cosh kh = 1 \quad \text{for } kh \rightarrow 0 \quad (2.13)$$

$$\tanh kh = kh \quad \text{for } kh \rightarrow 0 \quad (2.14)$$

There are different views about the criteria for deep and shallow water waves, but the limits of Table 2.2 can be 'safely' used.

Some useful relationships to remember are:

$$\omega^2 = \left(\frac{2\pi}{T}\right)^2 = gk \tanh kh \quad \text{dispersion relation [1/s}^2\text{]} \quad (2.15)$$

$$k = \frac{2\pi}{\lambda} \quad \text{wave number [1/m]} \quad (2.16)$$

$$k_0 = \frac{2\pi}{\lambda_0} \quad \text{wave number deep water [1/m]} \quad (2.17)$$

$$n = \frac{c_g}{c} = 0.5 \left(1 + \frac{2kh}{\sinh 2kh}\right) \quad \text{[-]} \quad (2.18)$$

The water particle displacement is shown in Fig.2.8 for a wave in shallow water and for a wave in deep water. In deep water the effect of the waves does not extend down to the bed; in shallow water the water makes an oscillating movement over the entire depth. Near the surface the water particles describe an elliptical path; near the bottom the water particles make a horizontal oscillating movement.

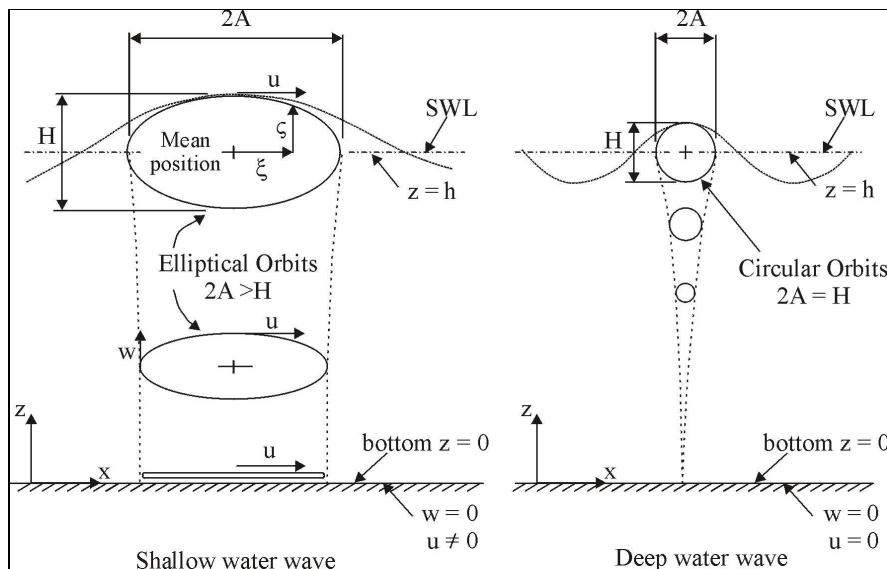


**Figure 2.8 Orbital motion under a shallow water wave and a deep water wave**

Fig.2.9 shows the relation between the direction of the velocity and the acceleration of water particles at certain phases in the wave period.

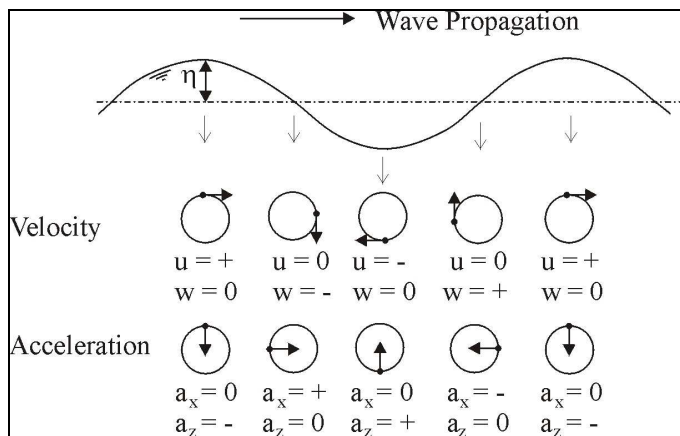


**Figure 2.9 Local fluid velocities and accelerations at certain phases in the wave period**

### 2.4.4 Irregular waves

It is not possible to use the regular wave theories described in Section 2.4.2 to analyse and describe wave records of the type shown in Fig.2.4 measured at sea or near the shore. The waves shown in Fig.2.4 have been caused by the wind and form together a very irregular water surface profile.

It has been found to be a useful method to consider wind waves as a superposition of a lot of sinusoidal waves with different amplitudes, frequencies, phases and directions, referred to as spectral components [see Battjes (2001)].

Describing the variation of the water level in time as the sum of a lot of sinusoidal terms we get:

$$\eta(t) = \sum a_i \cos(2\pi f_i t + \alpha_i) \quad (2.19)$$

where:

$\eta(t)$	the instantaneous surface elevation	[m]
$a_i$	the amplitude of the $i^{\text{th}}$ cosine component	[m]
$f_i$	the frequency of the $i^{\text{th}}$ cosine component in cycles per unit time	[1/s]
$\alpha_i$	the phase of the $i^{\text{th}}$ cosine component	[-]

This expression is called the one-dimensional random phase model (it is one-dimensional because the elevation is only a function of time  $t$ ). In this expression there is only one stochastic value, the phase  $\alpha_i$ . The values of  $\alpha_i$  are stochastic independent values each with a uniform probability distribution function (see Fig.2.10).

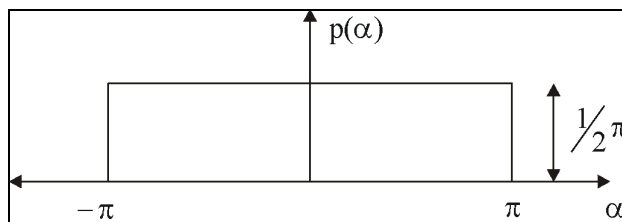


**Figure 2.10 Uniform probability distribution**

The amplitude  $a_i$  and the frequency  $f_i$  are related to each other. Each frequency has its own specific amplitude, which of course depends on the particular wave record. So if the relation between  $a_i$  and  $f_i$  is known, the wave field is known. The problem is how to find this particular relationship.

A spectral analysis (Fourier-transformation) of the surface elevation in one point as a function of time ( $\eta(t)$ ) can be used to find a spectral variance density function  $E(f)$  in which  $f$  is the frequency in cycles per unit time.  $E(f)$  is defined such that its integral, over all positive values of  $f$ , equals the variance of  $\eta(t)$  where the variance of the surface elevation is equal to  $(\sigma_{\eta(t)})^2$ . Because the variance is proportional to the average energy, the spectral variance density function is often called *the wave energy spectrum*. This energy spectrum therefore indicates how the total energy of the wave field is distributed over the various frequencies.

The total average energy of the wave field per unit surface area itself can be found by multiplying the area beneath the energy spectrum curve by  $\frac{1}{2}\rho g$ :

$$\bar{E} = \frac{1}{2} \rho g \int_0^{\infty} E(f) df \quad (2.20)$$

where:

$\bar{E}$	the mean energy per unit surface area	[J/m <sup>2</sup> ]
$f$	the frequency in cycles per unit time	[1/s]

Because the variance and the energy are also proportional to the square of the amplitude of the surface elevation, the spectrum can also be seen as the relation between the amplitude  $a_i$  (actually  $a_i^2$ ) and the frequency  $f_i$ , which we need to know for Eq.(2.20). With this energy spectrum the wave field can be described and reproduced. Here we only want to know certain characteristics of the wave field.

Most of the characteristics can be expressed in terms of moments of  $E(f)$  denoted by  $m_n$ :

$$m_n = \int_0^{\infty} f^n E(f) df \quad n = 0, 1, 2, \dots \quad (2.21)$$

where:

$m_n$	the $n^{\text{th}}$ moment of the spectrum	[-]
-------	--	-----

As we can see  $m_0$  is the area beneath the energy spectrum curve, which was equal to  $(\sigma_{\eta(t)})^2$ :

$$m_0 = \int_0^{\infty} E(f) df = (\sigma_{\eta(t)})^2 \quad (2.22)$$

### Characteristic wave periods

Apart from the amount of energy of a wave, the wave period is important also. Relevant expressions are defined by Battjes [Battjes (1977)].

The 'zero-down crossing wave period'  $T_0$  is the mean time interval between consecutive zero-down crossings (see Fig.2.11):

$$T_0 = \sqrt{\frac{m_0}{m_2}} \quad [\text{s}] \quad (2.23)$$

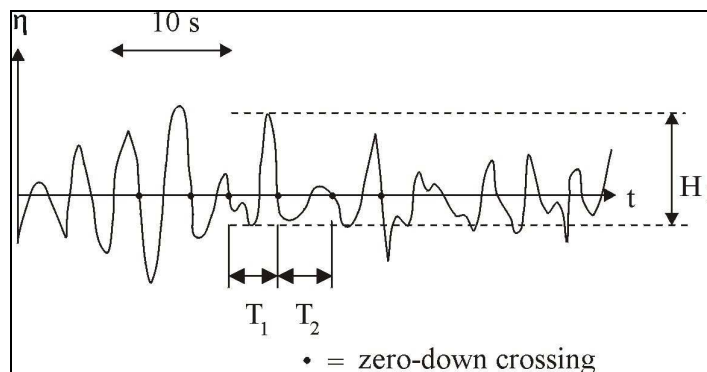


**Figure 2.11 Zero-down crossing periods and wave heights**

The peak-period  $T_p$  is the period at which the spectrum has its maximum energy (see Fig.2.12):

$$T_p = \frac{1}{f_m} \quad [\text{s}] \quad (2.24)$$

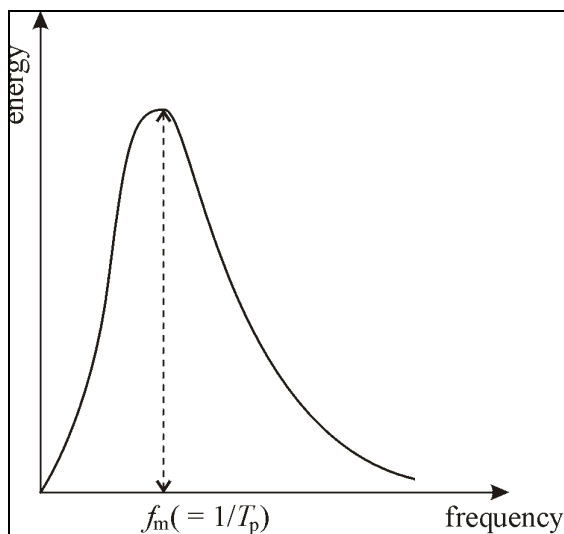


**Figure 2.12 Energy spectrum with peak-period**

The average period of the one-third highest waves  $T_{1/3}$  is called the significant wave period ( $T_{sig}$ ), because this period is very often nearly the same as the visual estimate of the 'characteristic' wave period of a wave field:

$$T_{1/3} = T_{sig} = 0.9 \cdot f_m^{-1} \quad [\text{s}] \quad (2.25)$$

### Characteristic wave heights

A wave height is defined as the difference between the minimum and maximum water level between two zero-down crossings (Fig.2.11).

The mean wave height  $H_{mean}$  often denoted as  $\mu_H$ , is computed from:

$$H_{mean} = \sqrt{2\pi m_0} \quad (2.26)$$

The root mean square wave height, denoted as  $H_{rms}$  is a measure of the average wave energy computed from:

$$H_{rms} = \sqrt{\frac{1}{n} \sum H_i^2} \quad (2.27)$$

If an irregular wave field has to be reproduced by a wave field of monochromatic waves with the same average energy per unit surface area, the monochromatic waves should have the wave height  $H_{rms}$  of the irregular wave field.

$$H_{rms} = 2\sqrt{2m_0} \quad (2.28)$$

The average height of the one-third highest waves  $H_{1/3}$  is also referred to as the significant wave height  $H_{sig}$  as was the case with the significant wave period  $T_{1/3}$ .

$$H_{1/3} = H_{sig} = 4\sqrt{m_0} \quad (2.29)$$

## 2.4.5 Waves and currents combined

Up till now we have discussed waves alone. Very often there will also be a current flowing in an arbitrary direction with respect to the direction of wave propagation. This current will influence some of the wave characteristics, and, in their turn, the waves will influence certain current characteristics.

If the current is in the same direction as the wave propagation direction, the wave height will decrease and the wavelength will increase. If the current is in the opposite direction, the wave height will increase and the wavelength will decrease.

The wave celerity, in the absence of current, is given by Eq.(2.30).

$$c = \frac{\omega}{k} \quad (2.30)$$

where:

$c$	wave celerity	[m/s]
$\omega$	wave frequency, $2\pi/T$	[1/s]
$k$	wave number, $2\pi/\lambda$	[1/m]

so  $\omega = ck$ , and hence  $\lambda = cT$ .

For the combination of waves and current  $v$  (current in wave propagation direction) ‘everything’ will change. Distinction has to be made between observations in a fixed position and observations with a moving reference system (moving with velocity  $v$ ).

The wavelength  $\lambda$  will change in  $\lambda'$  (note:  $\lambda' \neq cT + vT$ ) and the wave height changes in  $H'$ .

In a fixed position still every  $T$  seconds a wave with wavelength  $\lambda'$  is passing. Seen from this fixed position a ‘new’ wave celerity  $c'$  might be defined:

$$\lambda' = c'T \quad (2.31)$$

If the observer is moving with velocity  $v$ , the wavelength  $\lambda'$  will of course not change, but the observed wave period will. Let us call that period  $T_{rel}$ . While moving with  $v$ , also a different wave celerity  $c_{rel}$  is encountered.

$$c_{rel} = c' - v \quad (2.32)$$

Thus:

$$\lambda' = c'T = c_{rel}T_{rel} = (c' - v)T_{rel} \quad (2.33)$$

and:

$$T_{rel} = \frac{c'T}{c' - v} = \frac{T}{1 - \frac{v}{c'}} = \frac{T}{1 - \frac{vT}{\lambda'}} \quad (2.34)$$

With  $\omega_{rel} = 2\pi/T_{rel}$ , Eq.(2.34) can be rewritten as:

$$\omega_{rel} = \omega - k'v \quad (2.35)$$

In the moving system the dispersion relation (see Eq.(2.15)) is now valid:

$$\omega_{rel}^2 = gk' \tanh k'h \quad (2.36)$$

Or, together with Eq.(2.35):

$$\omega - k'v = \sqrt{gk' \tanh k'h} \quad (2.37)$$

For given parameters  $\omega$ ,  $v$  and  $h$ , the wave number  $k'$  (and hence  $\lambda'$ ) can be solved.

In order to determine other wave-related parameters (like the maximum orbital velocity near the bed) in the wave-current system,  $H'$  and parameters associated with the moving reference system have to be used ( $\omega_{rel}$ ;  $n_{rel}$ ).

The modified wave height  $H'$  can be determined using the wave action balance:

$$\frac{Enc}{\omega} = \frac{E'}{\omega_{rel}} (v + n_{rel}c_{rel}) \quad (2.38)$$

See Example 2.1 for an example calculation.

### Example 2.1

*Input parameters:*

Water depth:	$h$	=	3 m
Wave height:	$H$	=	1.0 m (no current)
Wave period:	$T$	=	6 s
Current velocity:	$v$	=	0.5 m/s (in the direction of wave propagation)

*Required:*

Wave height in case of a current

*Output:*

First, compute the wavelength and wave celerity in absence of the current from:

$$\lambda = \frac{gT^2}{2\pi} \tanh kh \approx 30.7 \text{ m}$$

$$c = \frac{\lambda}{T} \approx 5.1 \text{ m/s}$$

Next, compute the modified wave length using Eq.(2.37):

$$\omega - k'v = \sqrt{gk' \tanh k'h} \Rightarrow \lambda' \approx 34.0 \text{ m}$$

The modified wave height  $H'$  can now be computed from the wave action balance:

$$\frac{Enc}{\omega} = \frac{E'}{\omega_{rel}} (v + n_{rel}c_{rel}) \Rightarrow H' \approx 0.89 \text{ m}$$

*Conclusion:*

If a wave with an original height of 1.0 m is combined with a current of 0.5 m/s (in the wave propagation direction), the wave height reduces to 0.89 m and the wavelength increases from 30.7 m to 34.0 m.

### Example 2.1 Wave height in case of a current

To calculate e.g.  $\hat{u}_0$ , the maximum orbital velocity near the bed,  $H'$ ,  $\omega_{rel}$  and  $\lambda'$  should be used. The calculations must be carried out in the moving reference system. Using the linear wave theory (assuming no additional net currents in the moving reference system) yields:

$$u_0 = \hat{u}_0 \sin \omega_{rel} t \quad (2.39)$$

If one considers the near bed water motion in a fixed position, the current velocity component appears as a constant part. An oscillatory contribution with  $\hat{u}_0$  (as determined with the moving reference system) and  $T$  (the original wave period!) has to be added to the constant part.

In the preceding discussion a current in the direction of the wave propagation was the starting point. In general cases (wave propagation and current direction arbitrary) only the component of the current in the wave propagation direction must be taken into account. The component of the current perpendicular to the direction of the wave propagation, is not important in this type of discussions.

## 2.5 Wave deformation

### 2.5.1 Introduction

Now that we can analyse wave fields or predict wave fields, we have to know what happens when these waves approach a coast. Different phenomena will occur:

- Shoaling;
- Bottom friction;
- Wave breaking;
- Refraction;
- Diffraction;
- Reflection.

#### Shoaling, bottom friction and breaking

If a wave approaches water which is gradually becoming shallower (a sandy coast), the wave will be affected by the bottom (friction) when the water depth becomes less than about half the wavelength. Let us further assume that the wave crest is parallel to the depth contours. Nearing the breaker line shoaling occurs: the wave celerity ( $c$ ) and therefore the wavelength ( $\lambda$ ) decreases while the wave height ( $H$ ) increases (approaching from deep water there will be initially a slight decrease in wave height). At a certain water depth the wave height (or in some cases the wave steepness) becomes so large that the wave will break and some wave energy will be dissipated. Because of the orbital motion near the bed also bottom friction will occur. That is important in sediment transport (see Chapter 4).

#### Refraction

If waves approach water which is gradually becoming shallower (a sandy coast), and the wave crests make an angle to the depth contours, the waves will refract. The part of the wave crest, which is already in shallower water, will have a less celerity and therefore the wave crest will bend, diminishing the angle between the wave crest and



the depth contours. This phenomenon is called refraction. Again, when the water depth becomes too small, the wave will break.

### Diffraction

If a wave meets an obstacle (an offshore island, a breakwater), a part of the wave crest will be reflected seaward. The remainder of the wave front will bend around the obstacle and thus penetrate into the zone in the lee of the obstacle. This phenomenon is called diffraction.

Both refraction and diffraction cause the wave crests to bend, however, for different reasons. According to simple refraction theory the energy flux remains constant between wave orthogonals (lines perpendicular to the wave crest extending in the direction of the wave propagation). Because the part of the wave, which is in shallower water, travels more slowly than the part in deeper water, the wave bends. In the case of diffraction the energy flux leaks over a wave orthogonal and as a result the energy in the bending part of the wave is less than the initial wave energy.

In case of diffraction the celerity of the wave crest, and therefore the wavelength, remains the same (because the water depth is assumed to stay constant), the wave height, in contrast to refracted waves, will decrease because of the leaking process.

### Reflection

If the bottom slope has a steep profile like a dam or a dike, the waves will partly break and partly reflect. The steeper the bottom profile, the greater the wave reflection. A vertical wall will reflect practically all the wave energy and a standing wave will develop in front of the wall.

The different phenomena 'breaking', 'refraction' and 'diffraction' will be discussed in more detail in the next sections.

## 2.5.2 Wave breaking

The celerity of waves ( $c$ ) in shallow or transitional water depths is a function of the water depth ( $h$ ). A decreasing water depth yields a decreasing celerity. To find a relation between the wave height ( $H$ ) and the water depth ( $h$ ) we have to examine the energy flux balance. To find the energy that enters or leaves the balance area we need the energy flux. Wave energy flux is the rate at which energy is transmitted in the direction of wave propagation across a vertical plane perpendicular to the direction of wave propagation and extending over the entire depth.

The energy flux is also called the wave power. The average energy flux, per unit wave crest width, follows from Eq.(2.40).

$$U = Ec_g = Enc \quad (2.40)$$

where:

$U$	wave power or energy flux per unit wave crest width	[J/ms]
$E$	wave energy per unit surface area	[J/m <sup>2</sup> ]
$c_g$	wave group velocity	[m/s]
$c$	wave celerity	[m/s]
$n$	ratio $c_g$ to $c$	[-]

By assuming that this energy flux does not change as the wave progresses through water of varying depth, we find:

$$U_2 = U_1 \rightarrow E_2 n_2 c_2 = E_1 n_1 c_1 \quad (2.41)$$

where the subscripts indicate the location at which the parameters are evaluated.

If we choose location 2 in deep water where the wave properties are more easily evaluated, we find:

$$\frac{1}{8} \rho g H_1^2 n_1 c_1 = \frac{1}{8} \rho g H_0^2 n_0 c_0 \quad (2.42)$$

where:

$$H \quad \text{wave height} \quad [\text{m}]$$

For deep water  $n = n_0 = 1/2$  and:

$$H_1^2 n_1 c_1 = \frac{1}{2} H_0^2 c_0 \quad (2.43)$$

This can also be written as:

$$\frac{H_1}{H_0} = \sqrt{\frac{c_0}{c_1} \frac{1}{2n_1}} = K_{sh} \quad (2.44)$$

The parameter  $K_{sh}$  is called the shoaling factor. The shoaling factor can be found in various tables but can also be calculated from Eq.(2.44) or from the more specified equation:

$$K_{sh} = \sqrt{\frac{1}{\left(1 + \frac{2kh}{\sinh 2kh}\right) \tanh kh}} \quad [-] \quad (2.45)$$

where:

$$k \quad \text{wave number } (= 2\pi/\lambda) \quad [1/\text{m}]$$

$$h \quad \text{water depth} \quad [\text{m}]$$

As we see,  $K_{sh}$  is purely a function of  $kh$  and therefore  $h/\lambda$ .

In shallow water the shoaling factor can be reduced (using Eq.(2.44) and  $c_1 = \sqrt{gh}$  and  $n_1 = 1$ ) to:

$$K_{sh} = \sqrt{\frac{c_0}{2\sqrt{gh}}} \quad [-] \quad (2.46)$$

With a bit of algebra this becomes:

$$K_{sh} = \left[ \frac{1}{8\pi} \frac{\lambda_0}{h} \right]^{\frac{1}{4}} = 0.4466 \sqrt[4]{\frac{\lambda_0}{h}} \quad [-] \quad (2.47)$$

Towards the breaker line therefore the wave height increases. This increasing wave height (and decreasing wavelength) gives an increasing wave steepness. As we can imagine there will obviously be an upper limit for the wave height:

- due to a maximum wave steepness ( $H/\lambda$ );
- due to a maximum wave height water depth ratio ( $H/h$ ).

The first criterion, wave steepness, is valid in both shallow and deep water. The wave steepness is defined as the ratio of the wave height to wavelength ( $H/\lambda$ ). From theoretical considerations the limiting steepness is found to be:

$$\left[ \frac{H}{\lambda} \right]_{\max} = \frac{1}{7} \tanh \left[ \frac{2\pi h}{\lambda} \right] \quad (2.48)$$

In deep water Eq.(2.48) reduces to:

$$\left[ \frac{H_0}{\lambda_0} \right]_{\max} = \frac{1}{7} = 0.142 \quad (2.49)$$

which occurs when the crest angle is about  $120^\circ$  (see Fig. 2.13).

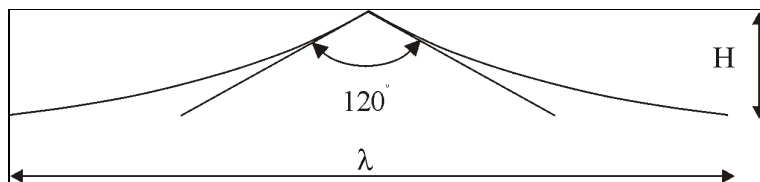


**Figure 2.13 Maximum crest angle**

In shallow water Eq.(2.48) becomes:

$$\left[ \frac{H}{\lambda} \right]_{\max} = \frac{1}{7} \frac{2\pi h}{\lambda} \approx 0.9 \frac{h}{\lambda} \quad (2.50)$$

Therefore  $H_{\max} \approx 0.9h$  from which an upper limit for the second criterion (the wave height to water depth ratio) is found more or less automatically.

The depth at which the wave breaks is called the breaker depth. The ratio breaker wave height to breaker depth is often called the breaker index, denoted by  $\gamma$ .

$$\gamma = \frac{H_b}{h_b} \quad (2.51)$$

Solitary wave theory gives:

$$\frac{H_{\max}}{h} = 0.78 \quad (2.52)$$

The value of  $\gamma$  also depends on the wave steepness. In practice various values of  $\gamma$  are used. For regular waves  $\gamma \approx 0.6 - 0.7$  is often used. If the wave height  $H_b$  in Eq.(2.51) is expressed as  $H_{sig}$ , then values of  $\gamma \approx 0.5 - 0.6$  are reasonable.

All above breaking wave relations have been derived for a horizontal bottom. In reality the bottom will be sloping. Depending on the beach slope:

- the wave will or will not break, or
- different kinds of breaker types will occur.

Battjes proposed a parameter to indicate whether the wave will break or not [Battjes (1974)]. This surf similarity parameter reads:

$$\xi = 2\pi \frac{H}{\lambda_0 \sin^2 \alpha} \quad (2.53)$$

where:

$\xi$	surf similarity parameter	[-]
$H$	wave height	[m]
$\lambda_0$	deep water wavelength	[m]
$\alpha$	beach slope (beach slope is also denoted by $m = \tan \alpha$ )	[-]

If  $\xi > 1$ , breaking will occur.

This is quite similar to Iribarren's approach [Iribarren and Nogales (1949)]. In his approach the parameter reads:

$$\xi = \frac{\tan \alpha}{\sqrt{\frac{H}{\lambda_0}}} \quad (2.54)$$

If  $\xi < \frac{4}{\sqrt{\pi}} \approx 2.3$  breaking occurs.

Waves break in a different way depending on the beach slope and the wave steepness. Three main types of breakers can be differentiated: 'surging breakers', 'plunging breakers' and 'spilling breakers'. The transition from surging to plunging breakers is often referred to as a 'collapsing breaker'. Fig. 2.14 shows how the different breaker types can be recognised. The typical value of the Iribarren parameter  $\xi$  for the breaker type is also given in the figure [Battjes (1974)].

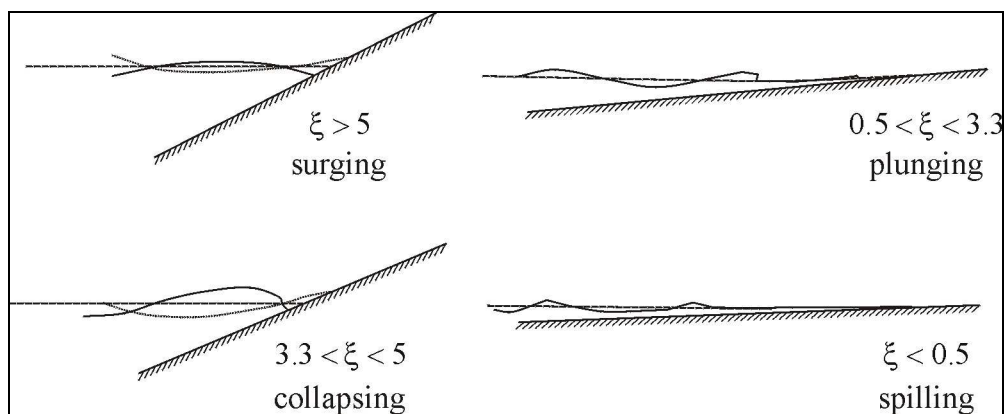


**Figure 2.14 Breaker types as a function of  $\xi$  [Eq.(2.54)]**

### 2.5.3 Refraction

Refraction occurs if, for some reason, one section of a wave crest has a larger celerity than its neighbouring section. Refraction occurs therefore not only in shoaling water

if the waves approach obliquely, but also in cases where there is a gradient in the current velocity e.g., in tidal entrances, in major ocean currents, or in harbour entrance channels.

Refraction in the case of currents is discussed in Chapter 10, which deals with entrance channels and trenches. The present section discusses only refraction caused by shoaling water when the wave crests make an angle with the depth contours.

The process of decreasing wave celerity in decreasing water depth can be considered as similar to the decreasing speed of light in media with increasing density. Snel's Law of geometrical optics has therefore been considered and has shown to give a valid approximation when applied to water wave refraction problems (although in optics the light beam changes speed abruptly while in water wave refraction there is a gradual change in wave celerity).

We consider a long crested, monochromatic wave train approaching at an angle to the shore in a gradually shoaling area with bottom contours that are essentially straight and parallel as shown in Fig. 2.15.

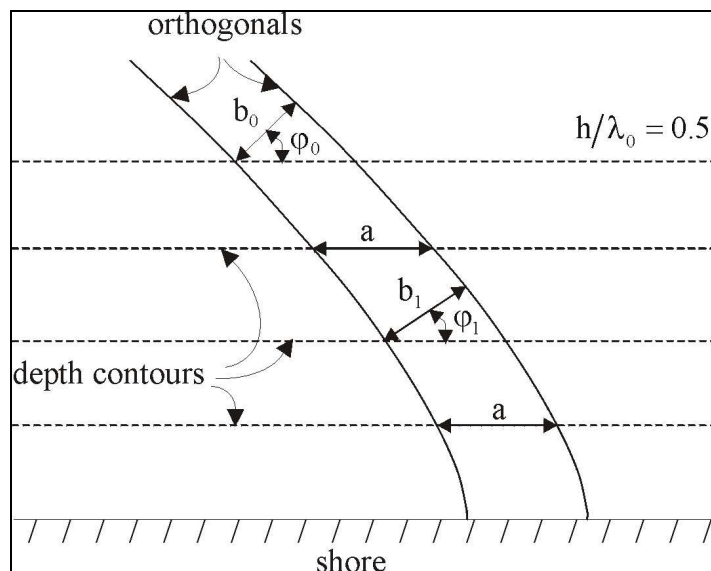


**Figure 2.15** Wave refraction over straight parallel depth contours

The direction of wave propagation is perpendicular to the wave crest i.e., in the direction of the orthogonals. Orthogonals are lines perpendicular to the wave crest extending in the direction of the wave propagation. Orthogonals are sometimes called rays. We assume that the power transmitted between two rays remains constant, in equation of the form:

$$U_1 b_1 = U_0 b_0 \quad (2.55)$$

where:

$U$	the wave power per unit crest length	[J/ms]
$b$	the distance between orthogonals	[m]

Using Eq.(2.40) ( $U = Enc$ ) we get:

$$E_1 n_1 c_1 b_1 = E_0 n_0 c_0 b_0 \quad (2.56)$$

where:

$E$	the wave energy	[J/m <sup>2</sup> ]
$n$	the ratio of wave group velocity to wave celerity	[-]
$c$	wave celerity	[m/s]

Using  $E = \frac{1}{8}\rho g H^2$  and  $n_0 = \frac{1}{2}$  we find:

$$\frac{H_1}{H_0} = \sqrt{\frac{1}{2n_1} \frac{c_0}{c_1} \frac{b_0}{b_1}} = K_{sh} K_r \quad (2.57)$$

where:

$K_{sh}$	the shoaling coefficient (see Eq.(2.44))	[-]
$K_r$	the refraction coefficient, $K_r = \sqrt{\frac{b_0}{b_1}}$	[-]

To find the ratio  $b_0/b_1$  we first make use of Snell's Law to find  $\varphi_1$ :

$$\frac{\sin \varphi_0}{\sin \varphi_1} = \frac{c_0}{c_1} \quad (2.58)$$

For parallel depth contours the distance between given wave orthogonals, measured parallel to the depth contours, remains constant (distance  $a$  in Fig. 2.15). So:

$$\frac{\cos \varphi_0}{\cos \varphi_1} = \frac{b_0}{b_1} \quad (2.59)$$

The computation procedure indicated above is easily carried out for coasts with a simple bathymetry. In reality there will always be a much more complicated pattern of depth contours (Eq.(2.59) does not hold) and then these 'hand' calculations will be impossible. In this case therefore two basic calculating techniques are available for refraction patterns: graphical and numerical. A description of the first method is given in the Shore Protection Manual, Volume I Chapter 2.

Fundamentally all methods of refraction analyses are based on Snell's Law and conservation of wave energy flux.

A refraction diagram is given in Fig. 2.16 as an example of the results of a refraction study. If the wave orthogonals converge there is an accumulation of energy and relatively high wave heights can be expected. In contrast if orthogonals diverge the energy is spread over a larger part of the wave crest so the wave height is reduced.

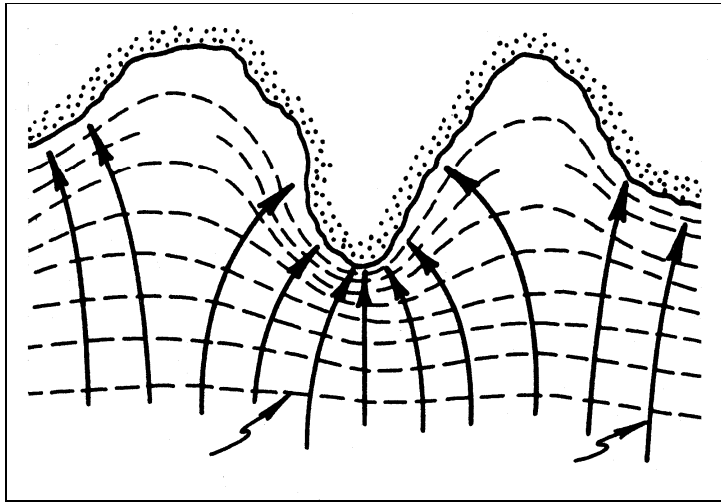


**Figure 2.16** Wave refraction diagram

### 2.5.4 Diffraction

Diffraction occurs when there is a sharp variation in wave energy along a wave crest. When a wave train is passing an obstacle there are, in the first instance, no waves in the lee of the obstacle. There will therefore be a gradient in the wave energy along the wave crest.

The water away from the obstacle has more energy (all the initial wave energy) than the water behind the obstacle (in first instance zero, since there are no waves). Energy is now transported along the wave crest to the part behind the obstacle and bending waves develop in the lee of the obstacle.

The degree of diffraction that occurs depends on the ratio of a characteristic lateral dimension of the obstacle, e.g., the length of a detached breakwater  $L$  to the wavelength  $\lambda$ .

When a thin pile is standing in waves with a large wavelength,  $L/\lambda \ll 1$ , clearly the diffraction will be nearly 100% implying that the wave field is approximately the same as if there is no pile.

In the case of a detached breakwater,  $L/\lambda \gg 1$ , diffraction occurs around each breakwater head. There is a large zone in which diffracted waves develop. The (undisturbed) waves passing the breakwater are diffracted (Fig. 2.17).

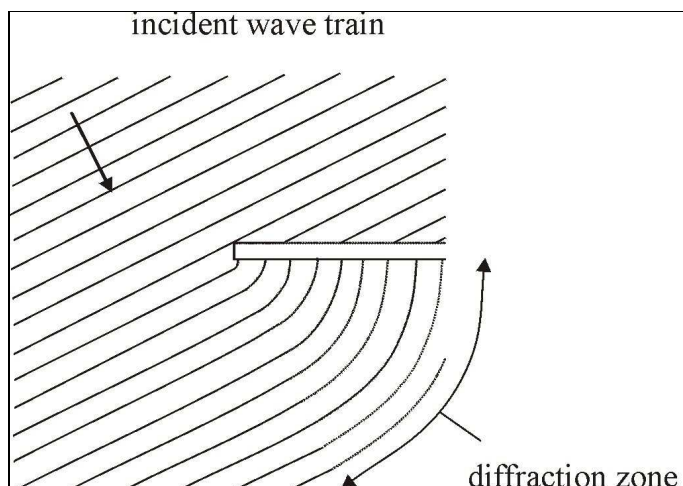


**Figure 2.17 Diffraction of an incident wave train**

As with refraction and shoaling there is a diffraction coefficient which is defined as the ratio of the diffracted wave height to the incident wave height assuming that the latter is not disturbed by the obstacle.

$$K_d = \frac{H_d}{H_i} \quad [-] \quad (2.60)$$

where:

$H_d$	diffracted wave height	[m]
$H_i$	wave height of the incident wave which is not disturbed by the obstacle	[m]

Water wave diffraction is analogous to the diffraction of light in the same way that water wave refraction is analogous to the refraction of light. Using this relation, Wiegel calculated the diffraction coefficient at selected points in the vicinity of the obstacle and tabulated his results [Wiegel (1964)].

Graphical methods are also available for calculating diffraction coefficients. With the Cornu Spiral it is relatively easy to find an approximation of the diffraction coefficient for one or two obstacles.

The use of the Cornu Spiral is explained in certain course documentation and literature on short wave theory [e.g. Battjes (2001)]. Another graphical approach involves the wave diffraction diagrams given in the Shore Protection Manual Volume I Chapter 2.

These diagrams give the diffraction coefficient as a function of position (relative to a semi-infinite rigid impermeable breakwater) and as a function of the breakwater gap width.

The disadvantage of the above methods is that they assume a constant water depth. In reality there will generally be a sloping bottom or an uneven bed and the results will therefore be influenced by this bottom. There are numerical models which take into account diffraction, refraction and reflection.



## 2.6 Software

Various software packages are available to compute wave transformation topics. A few packages developed in The Netherlands are mentioned. Much more packages are available all over the world.

The DIFFRAC software package computes the penetration of a short-crested, monochromatic wave field into harbours. The harbours may consist out of various basins, each with a uniform depth. The effect of partial wave reflection by structures is taken into account.

The ENDEC (ENergy DECay) PC program models the wave propagation on a prismatic coast (depth contours are considered to be straight and parallel). It takes account of wave refraction and dissipation.

ENDEC is also capable of incorporating wind action, and is able to predict commonly required statistics of individual wave height distributions at a given water depth.

HISWA (HIndcast of SShallow WAter waves) is a wave propagation model, especially suitable for coastal regions. The effects of depth, current-refraction and directional spreading are taken into account. Energy dissipation due to bottom friction, wave breaking and energy growth due to wind are also incorporated.

A model still under permanent development, but used all over the world, is SWAN (SImulating WAves Nearshore). The software can be downloaded, and information is available at internet.

The packages mentioned above can be incorporated in larger models. These can combine wave action and e.g. tidal currents, in order to compute sediment transport rates. They will be discussed in Chapter 8.

## 2.7 Wave measurements

There are different types of wave measurements. Which type has to be used depends on what the measurement is needed for. For example, when designing a flexible structure, e.g. a rubble mound breakwater, the failure of which is gradual and repairable, it is common to use the significant wave height as a main criterion. In other cases, for example when designing a fixed rigid structure, e.g. an offshore drilling tower, the total wave spectrum is needed as a main criterion.

In case of an expensive piece of equipment with limited sea keeping ability, the percentage of exceedance of a particular wave height on a day-by-day basis is needed for construction planning.

The most inexpensive method of wave measurements is visual observation. These measurements are made from ships by experienced observers and yield an estimate of  $H_{sig}$ ,  $T_{sig}$  and  $\theta_{sig}$  ( $\theta_{sig}$  is the significant direction of wave propagation). This method of observation is used all over the world. The World Meteorological Organisation (WMO) collects and co-ordinates these measurements.

If more detailed measurements are needed *instrumental observations* must be made.

Fig.2.18 shows the position of various measuring stations at the Dutch part of the North Sea. At these locations wave characteristics are continuously measured. Internet provides online information.

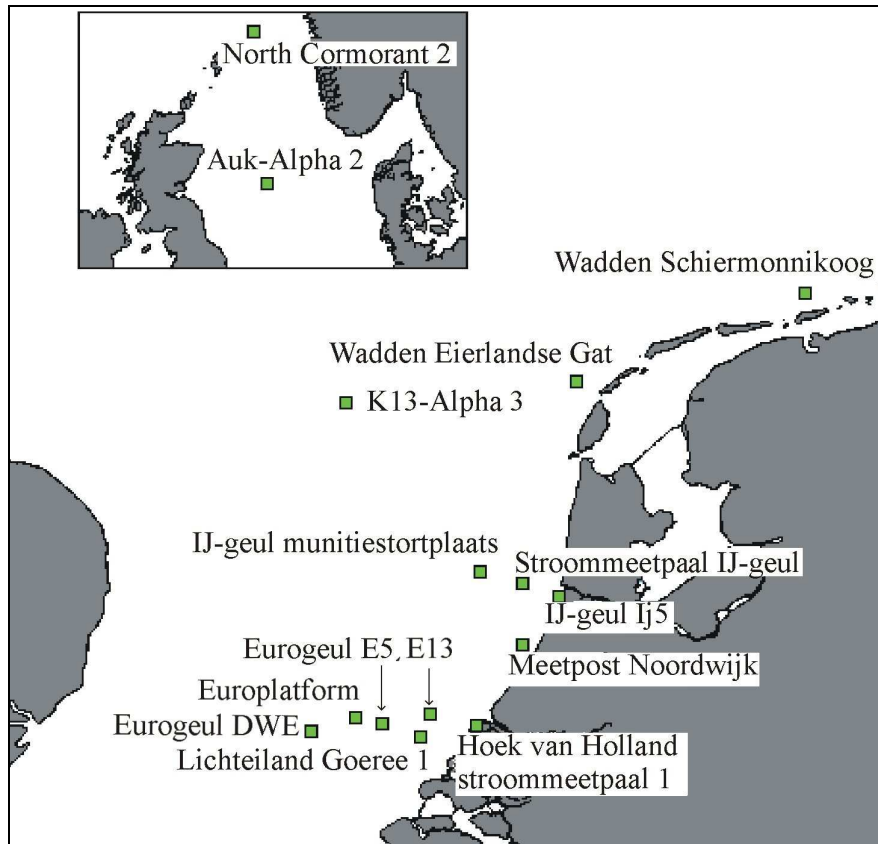


**Figure 2.18** Wave measuring locations

## 3 Coastal Problems

### 3.1 Introduction

Fig.3.1 (next page) shows in plan view schematically a piece of a coastal area with most of the natural conditions, natural features and some examples of man-made interventions in a natural coastal system. Most of the items are dealt with in these lecture notes.

In this chapter some examples of practical cases are to be discussed. In the discussions sediment transport related issues are the starting points. From Fig.3.1 the next items are briefly discussed:

- Cross-shore profile (section A - A in Fig.3.1);
- Morphological development in vicinity of port;
- Pipeline at sea bed;
- Delta near river mouth;
- Tidal inlet;
- Dune erosion during a severe storm surge;
- Large artificial island in open sea.

### 3.2 Cross-shore profile

Fig.3.2 shows the shape of a cross-shore profile as measured perpendicular to a sandy coast at an arbitrary moment. The vertical and horizontal scales of the plot are quite different. Dunes, beach and a part of the shoreface can be noticed. The actual slope of the dune face is 1:3 to 1:4. The slope of the beach is decreasing from the upper part of the beach near the foot of the dunes (1:20) towards the sea; near the waterline the slope is approximately 1:50. At the shoreface some (breaker) bars are present. The average bottom slope becomes flatter with longer distance from the waterline. At the seaward end of the plot (water depth: MSL -8 m) the slope is approximately 1:125.

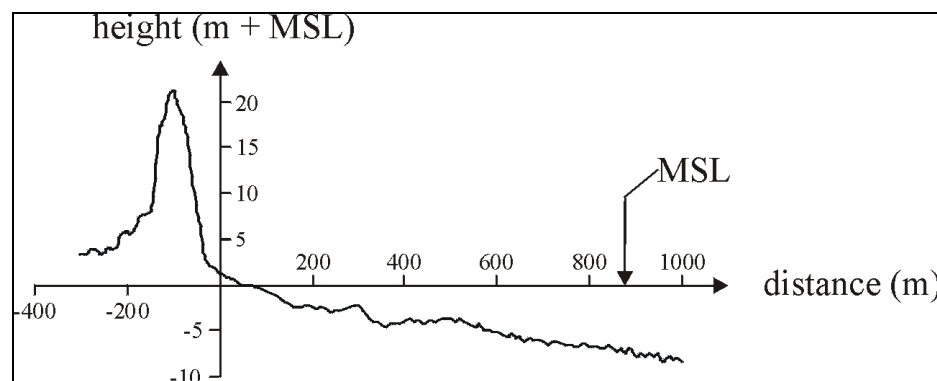


**Figure 3.2 Cross-shore profile (measured at Egmond aan Zee)**

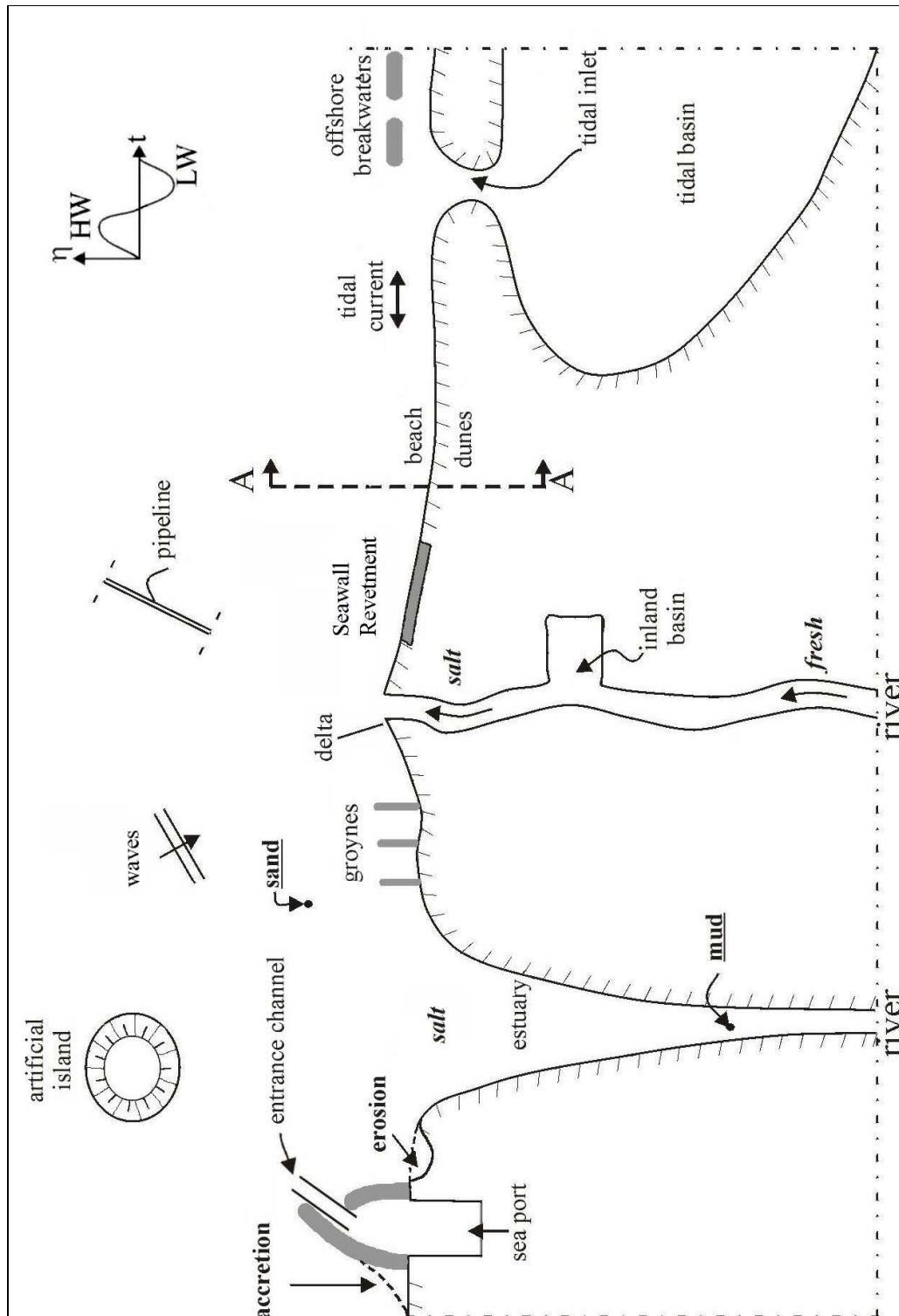


Figure 3.1 Plan view of a coastal area

The water level as indicated in Fig.3.2 reflects the Mean Sea Level (MSL). Effects of tides, wave set-up, and wind set-up are to be superimposed if one likes to find the actual Still Water Level (SWL) at an arbitrary moment. SWL reflects the average water level if the effect of wave motion on the instantaneous water level is time-averaged.

MSL is often used as reference level (Datum). In The Netherlands MSL is almost equal to NAP (Normaal Amsterdams Peil in Dutch). In many nautical maps Low Water Spring (LLWS) is used as reference level. LLWS represents the lowest water level that might occur due to astronomical tides.

The distribution of the particle size over the cross-shore profile of Fig.3.2 is certainly not constant (see for some details Section 4.2). For our discussion, however, we assume a constant particle size all along the bottom of the profile.

A for coasts common size  $D_{50} = 200 \mu\text{m}$  is chosen; 150 million of these particles fit into a volume of 1 litre!

If the body of water as indicated in Fig.3.2 is in rest, nothing will happen. No changes in the shape of the profile will take place.

If the actual water level is equal to MSL and if it is assumed that irregular waves ( $H_{so} = 2 \text{ m}$ ,  $T_p = 10 \text{ s}$ ) approach the coast perpendicularly, the wave height distribution along the profile can be calculated with modern numerical computation models (e.g. ENDEC; see Section 2.6). Fig.3.3 shows this wave height distribution. Notice that the wave height reduces gradually when approaching the waterline. Energy dissipation due to (partial) wave breaking and bottom friction causes this gradual wave height decrease.

[If regular waves would be considered, and only shoaling (constant energy flux outside breaker zone) would be taken into account, the wave height would first reduce slightly and would next increase towards the breaking point, while the waves approach the coast.]

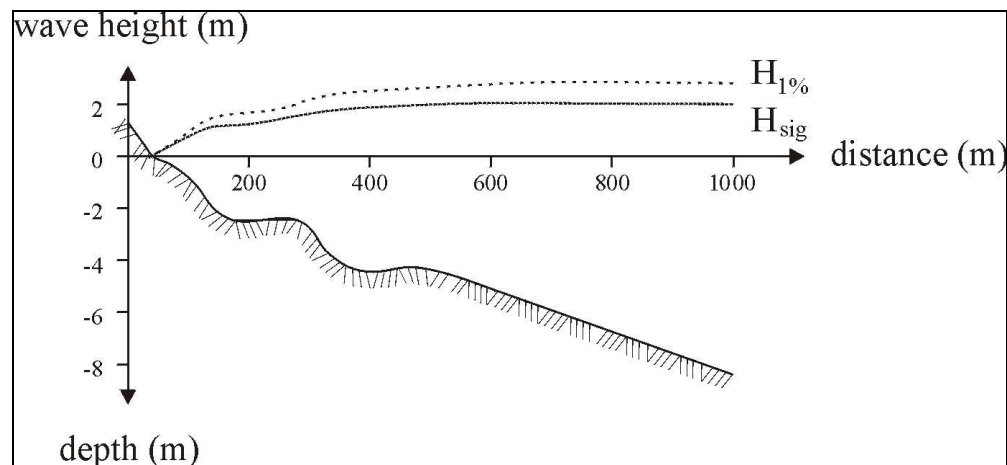


**Figure 3.3 Wave height distribution over cross-shore profile**

In Fig.3.4 the maximum horizontal components of the orbital velocities near the bed are plotted as a function of the position in the cross-shore profile. Notice the rather large magnitudes ( $> 1.0$  m/s at many positions). Realising that the critical velocity in uniform flow for particles with  $D_{50} = 200 \mu\text{m}$  is approximately 0.2 m/s (see Section 4.3), one may understand that the waves in Fig.3.3 are able to stir up many particles in the cross-shore profile. If besides the stirring up of particles also net currents do occur, sediment transport will take place. If differences in net transport will occur in different verticals, it is to be expected that the shape of the profile will change as a function of time if the approaching waves persist. (See Chapter 7 for a discussion of cross-shore transport.) Many practical problems are related to changes in the shape of the profile with time (e.g. dune erosion; behaviour of beach and shoreface nourishments).

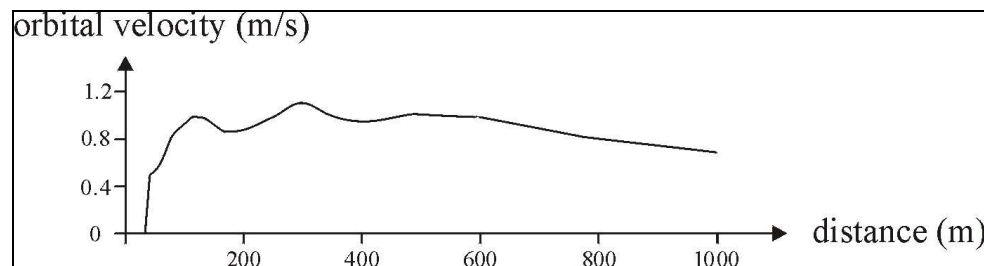


**Figure 3.4 Maximum horizontal velocity components near the bed over cross shore profile**

### 3.3 Morphological development in vicinity of a port

Fig.3.5 shows in plan view a part of a uniform sandy coast. Uniform means that the depth contours are assumed to be straight and parallel. Waves obliquely approach the coast. The wave crests make a changing (changing: due to refraction) angle  $\phi$  with the orientation of the depth contours, or: the direction of the wave orthogonal makes a changing angle with the shore normal. Inside (and a little bit outside) the surf zone, sediment is transported along the coast.

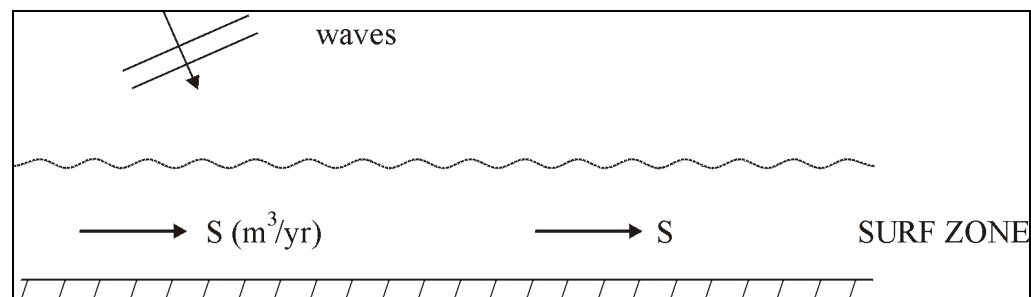


**Figure 3.5 Plan view of a uniform sandy coast**

Waves stir up material from the bed; obliquely approaching waves generate a longshore current; together sediment transport is generated. See Section 4.4 for a more detailed description of the physics involved.

If the coast is uniform indeed, the sediment transport  $S$  is constant along the coast; the coast remains stable.

Let us assume that  $S$  is expressed in  $\text{m}^3/\text{year}$  and that in this case  $S$  is expressed including pores. So if some sediment from the longshore transport rate is settled, it yields automatically an *in situ* volume in the field. [In Section 4.5 other units of sediment transport are discussed.]

If along the uniform sandy coast a port is built with the help of two rather long breakwaters, much longer than the width of the surf zone (see Fig.3.6), the longshore sediment transport will be interrupted. In front of the breakwaters no sediment transport is assumed to occur. At the updrift side of the port accumulation of sand will occur; at the downdrift side (lee-side) erosion will take place.

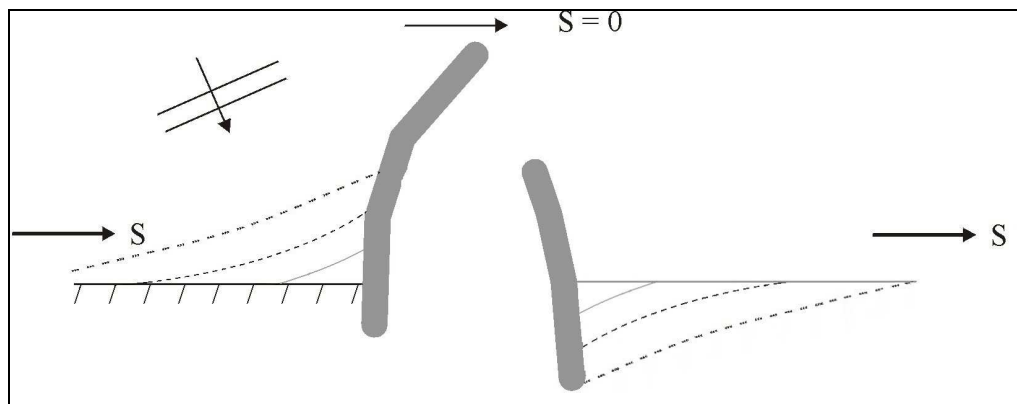


**Figure 3.6 Plan view of a uniform sandy coast with port breakwaters**

One of the aims of these lecture notes is to understand and to describe the shapes of the coastline at updrift and downdrift sides as a function of time. Furthermore it is to be expected that sooner or later the accreting coastline at the updrift side reaches the end of the updrift breakwater; at what time after the construction of the port this will happen? (See Section 6.4.) For the time being it will be clear that as long as no sediment will pass the breakwaters ( $S = 0 \text{ m}^3/\text{year}$  in front of the breakwaters) the total accumulation of sand in  $t$  years after completion of the port at the updrift side will be  $t \times S \text{ m}^3$ . The total erosion at the lee-side will be  $t \times S \text{ m}^3$  as well. In Fig.3.6 already some coastlines have been sketched as a function of time. In most cases the accumulation forms no 'problem'; valuable new land has been gained. The erosion at the lee-side of the port will cause sooner or later serious problems to the coastal zone manager involved. How to resolve such types of erosion problems will be discussed in Chapter 11. An obvious solution will be to artificially transfer volumes of sand from the one side of the port to the other. ( $S \text{ m}^3/\text{year}$  on an average; a so-called sand by-pass system; see Chapter 13.)

In the example of Fig.3.6 the longshore sediment transport was due to obliquely approaching waves only. If also tidal currents do occur along the coast, the

morphological behaviour becomes more complicated. This will be further discussed in Chapter 12.

In order to understand and to predict the morphological impact of a newly constructed port along a sandy coast, the sediment transports induced by waves and currents must be quantified to a reasonable degree of accuracy.

### 3.4 Pipeline at the sea bed

Oil or gas won at offshore production plants is often transported to the mainland by pipelines. At deeper water such pipelines are often just laid at the bottom of the sea. At deeper water sometimes even unprotected; sometimes covered with a layer of stones. Closer to the shore (e.g. crossing the surf zone) it is required in most cases to bury the pipeline so deep into the bottom that, notwithstanding fluctuations with time of the bed level, the pipeline will 'never' lie uncovered.

In Fig.3.7 a piece of an unprotected pipeline at deeper water has been sketched. Since the bottom of the sea is never entirely flat, a newly laid pipeline will never contact the bottom over its entire length. At several parts of the pipeline initial (small) gaps between pipeline and bottom will occur. Due to wave action (orbital motion near the bed) and tidal currents accelerating velocities will occur within the several gaps, as shown in Fig.3.8. Erosion in depth as well as laterally, in the direction of the alignment of the pipeline, will take place. Scour holes will occur.

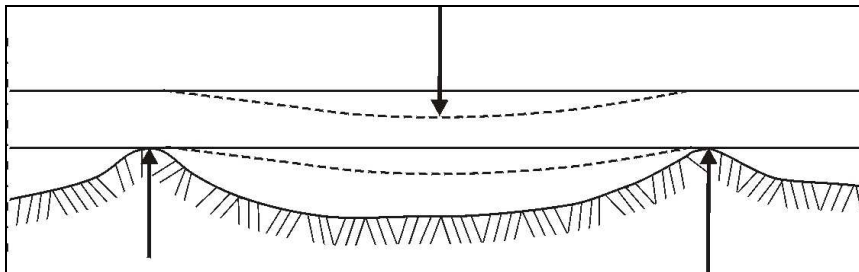


**Figure 3.7 Unprotected pipeline at seabed**

Examples do exist of pipelines, which follow the scour holes in depth; eventually even 'self-burial' might occur. (Even a steel pipeline is flexible to some extent.) So far no serious problems. If, however, along the alignment of the pipeline in the bottom some layers are present which are more resistant to erosion, serious problems might occur. Free spans of the pipeline might occur with eventually breaking of the pipeline.

To be able to quantify the dimensions of scour holes underneath pipelines calls for a proper insight in sediment transports due to waves and currents.



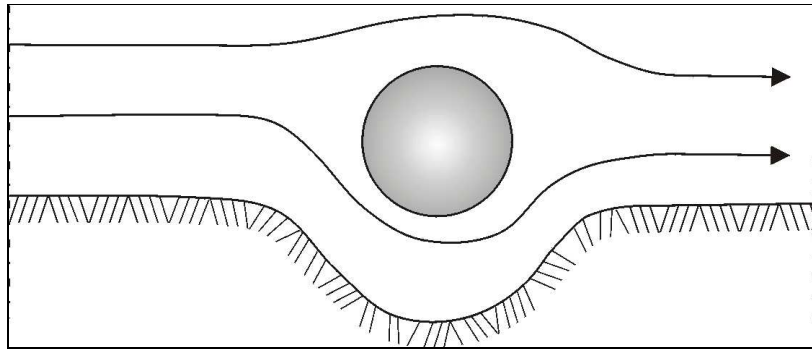


**Figure 3.8 Cross-section of unprotected pipeline at seabed**

### 3.5 Delta near river mouth

Fig.3.9 shows in plan view a piece of a sandy coast with a river outfall. Waves are assumed to approach perpendicular to the (initial straight) coastline. The river discharges a volume water  $Q_r$ ,  $\text{m}^3/\text{s}$  to the sea; at the same time sediment is transported by the river; say  $S_r$ ,  $\text{m}^3/\text{year}$ . ( $S_r$  is expressed in  $\text{m}^3/\text{year}$  since we are looking at large time scales.) Like many rivers all over the world, also the river of Fig.3.9 acts as source of sediments to the coastal system. It is interesting to understand the interaction processes between river and sea and to be able to predict the morphological changes with time, as shown in Fig.3.9. Depending on the power of the waves and the yearly sediment input by the river, different typical cases might develop with time. (See Chapter 8 for a more detailed discussion.) It is quite clear that sediment transport processes due to waves and currents play their role.

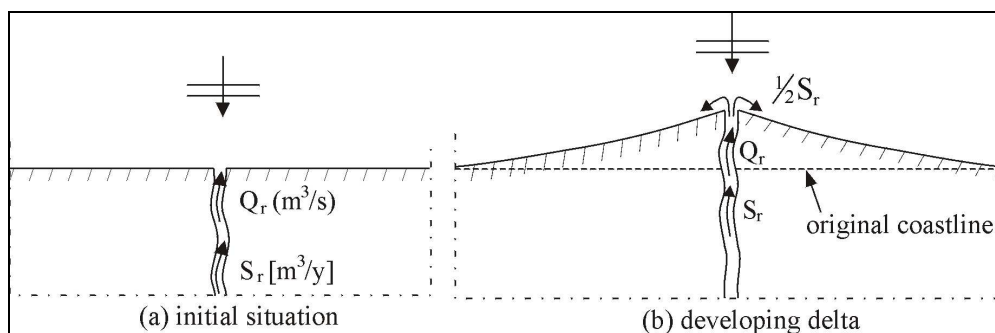


**Figure 3.9 Plan view of a sandy coast with a river outfall in initial situation (a) and with a developing delta (b)**

### 3.6 Tidal inlets

Tidal inlets are very intriguing features in the coastal area. Fig.3.10 shows various tidal inlets in the Wadden Sea, The Netherlands. Essentially for a tidal inlet is the tidal variation at open sea. The tide is the engine that determines most of the occurring features.

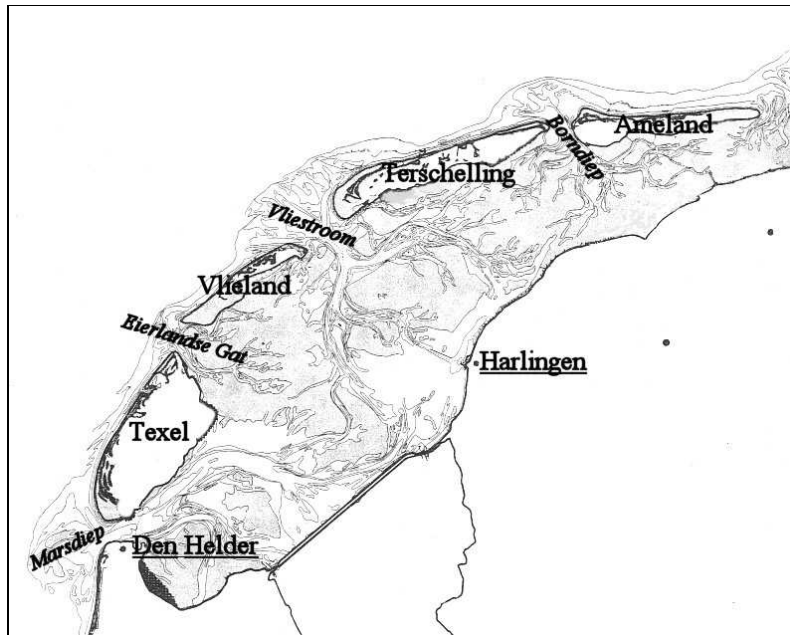


**Figure 3.10 Tidal inlets in the Waddenzee (The Netherlands)**

The tidal range (difference between High Water Level and Low Water Level) and the surface area of the tidal basin together determine in principle the volumes of water that have to flow in and out through the inlet during a tide. This tidal prism is in some cases in the order of magnitude of one billion ( $1 \cdot 10^9$ )  $m^3$ . During one tidal cycle about  $10^9 m^3$  of water enters the Marsdiep (between Texel and Den Helder, see Fig.3.10) and leaves the Marsdiep again.

The position of the different elements of a tidal inlet (e.g. ebb tidal delta, flood tidal delta, flood channels, ebb channels, shoals, tidal flats and gorge) is changing with time. Fig.3.11 shows a schematic plan view of a tidal inlet with some characteristic notions. The system is highly dynamic. This dynamic character is sometimes felt annoying for some practical applications (e.g. navigation through channels or stability of adjacent coasts). At least one has to understand the dynamic behaviour for planning purposes. Sometimes measures are taken to restrict the dynamic behaviour of the morphological system.

The dynamic behaviour of the several elements of a tidal inlet is apparently because of sediment transport by waves and currents.

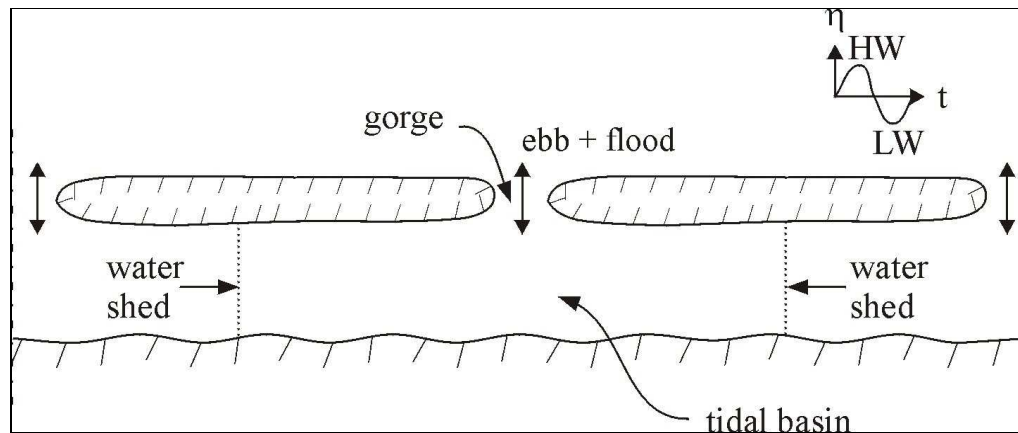


**Figure 3.11 Schematic plan view of a tidal inlet**

### 3.7 Dune erosion during a severe storm surge

Fig.3.12 shows a cross-section of an arbitrary cross-shore profile (comparable to Fig.3.2). Under normal conditions the water level is changing due to vertical tide variations. Every moment a different water level is present. The waves approaching the coast under 'normal conditions' will cause (relatively) small cross-shore transports in a given vertical cross-section; either in offshore or onshore direction.

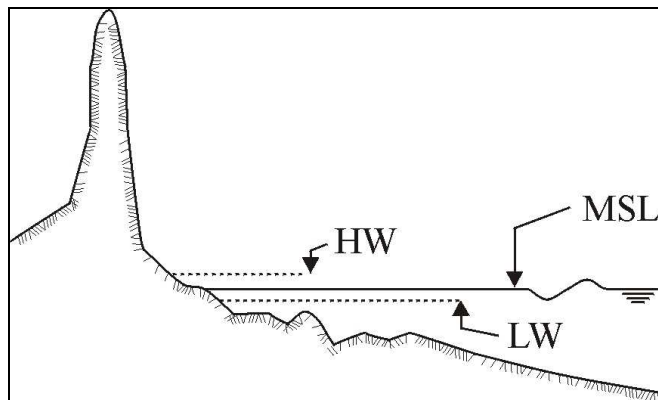


**Figure 3.12 Cross-shore profile under normal conditions**

Due to changing water levels and changing wave characteristics (wave height, wave period and wave direction) from time to time, changing cross-shore sediment transport rates will occur in a given vertical cross-section. The magnitude and even the direction of the resulting sediment transport will change.

During a severe storm the waves generated at open sea will be much higher than normal. Depending on the shape of the sea bordering the coast under consideration, the direction of the wind during the storm and the strength of the wind, the still water level (SWL) can be piled up along the coast. This piling-up of the water level is called surge.

During the severe disastrous storm surge of January 31<sup>st</sup> and February 1<sup>st</sup> 1953 in The Netherlands, the general water level along the Dutch coast was about 2.5 to 3.0 m higher than normal. Along the coasts of the southern part of the North Sea the water was piled up to these levels. The wind associated with this storm came from north-west directions and blew over the funnel shaped North Sea. The rather small gap between United Kingdom and France (The Channel), prevented the piled-up waters to escape from the North Sea (see Fig.3.13).

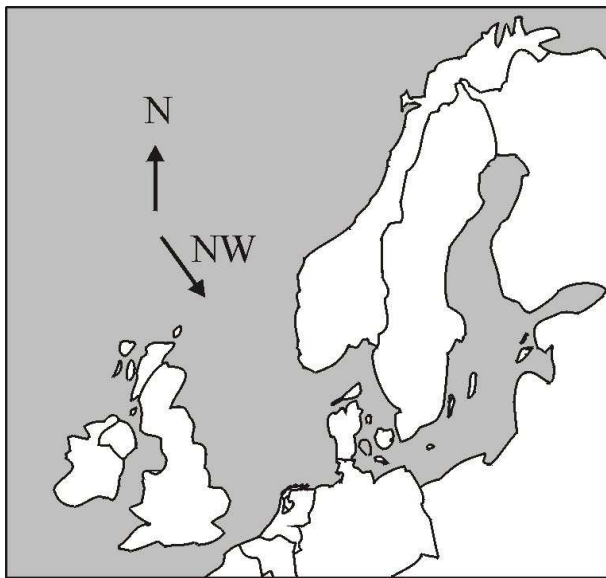


**Figure 3.13 Funnel shaped North Sea**

Fig.3.14 shows some characteristics of the measured and predicted water levels in Flushing (Vlissingen in Dutch). Notice the storm effect (the surge); the difference between the actual measured and the predicted astronomical water level variation. Notice also that the surge lasted in fact a rather small period of time. Within two days the surge level rose from zero to approximately 2.8 m and fell down to zero again.

During the 1953 storm surge many dikes in the south-western part of The Netherlands broke. Nearly 1850 people lost their lives; a large economical loss took place. This disaster triggered the execution of the so-called Delta plan in The Netherlands.

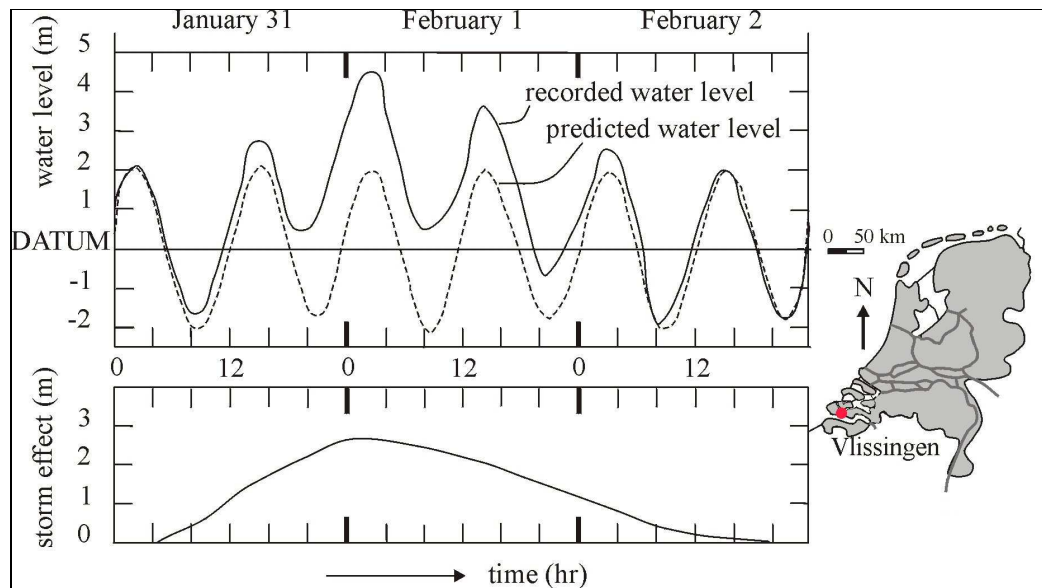


**Figure 3.14 Measured and predicted water levels at Vlissingen (The Netherlands)**

In Fig.3.15 (next page) the same cross-section of Fig.3.12 has been sketched, but now under maximum storm surge conditions. The SWL is much higher than in Fig.3.12 and much higher waves occur. The SWL surpasses even the level of the dune foot; all the beaches have disappeared under water; the waves hit the dunes. In general terms it can be argued that the shape of the cross-shore profile does not fit with the storm surge conditions (the profile shape is far out of equilibrium for these conditions). With large offshore directed sediment transports the profile shape is adapted towards the associated equilibrium shape. The dunes erode; the eroded dune material is settled at deeper water; the shape of the cross-shore profile gradually flattens (see Fig.3.15). In Chapter 7 a more detailed description is given of the associated processes.

For the time being it is sufficient to understand that a coastal zone manager likes to know what will be the loss of dune area under a given set of storm surge conditions e.g. with respect to the safety of properties built close to the brink of the dunes. In The Netherlands even the safety of a large part of the population, living well below MSL behind the dunes, is at stake if a break-through of the dunes will occur.

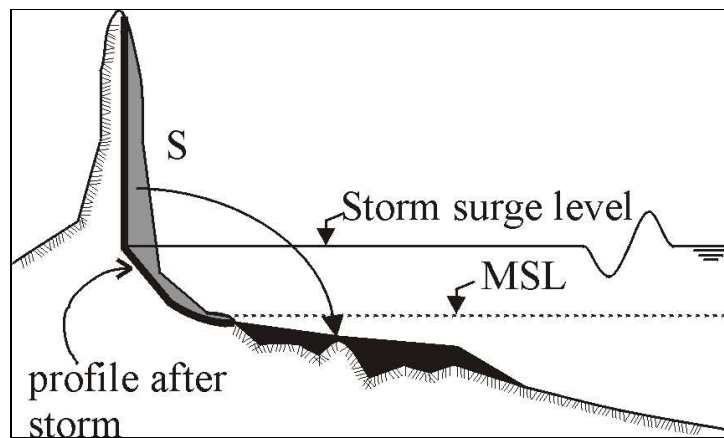


**Figure 3.15 Cross-shore profile directly after storm conditions**

### 3.8 Large artificial island in open sea

In densely populated areas (e.g. Japan, Taiwan or The Netherlands) it is becoming increasingly complicated to find large open areas at the mainland to start new developments (e.g. constructing a new airport, hosting new industries or even housing of growing population).

The open sea in front of the existing coast might be used to build an artificial island. In The Netherlands, for instance, a discussion was going on whether it would be useful to build an artificial island off the coast near IJmuiden for hosting an extension of Schiphol Airport. Such an artificial island in open sea has large morphological implications for the existing coasts. A specific airport-island requires rather large dimensions (e.g. due to the length of runways). A typical size for such an island is 5 km. With respect to the distance of an island from the existing coast, an optimum has to be found taking into account transportation requirements, noise limitations and morphological implications.

Another aspect of an airport-island is that the (tidal) current patterns will be affected in the vicinity of the island. In the shadow area behind the island the wave characteristics will fundamentally change. The island will affect the stability of coasts in a wide area. The adaptation time of the existing coasts and the seabed in the influence area of the island to the new situation is generally relatively long. The water depth off the coast of IJmuiden where an island is probably built, is approximately 15 m. This depth, the required dimensions of an island and the required level above MSL (approximately 5 m) call for huge volumes of sand to construct such an island. (Order of magnitude 600 million m<sup>3</sup> of sand.) These volumes are easily available below the bottom of the North Sea, but call for large borrow pits. Such large borrow pits affect the morphology as well.

During dredging operations also silt will be mobilised, since within the sand deposits at the seabed often small volumes of silt occur (say 2%). With a required volume of 600 million m<sup>3</sup> and 2% silt, this results in 12 million m<sup>3</sup> of silt that is mobilised in the North Sea environment. Ecological effects are to be expected.

It is clear that in the final decision whether to build an artificial island or not, coastal morphology topics have to play their role.

### 3.9 Conclusions of Chapter 3

Only a few real life practical examples have been discussed in the present chapter. From most of the examples it became clear that sediment transports due to waves and currents play their role in the understanding of the phenomena taking place associated with the examples. Without further explications similar examples in coastal engineering practice can be mentioned, namely:

- siltation of (dredged) navigation channels;
- erosion near toe of breakwaters;
- erosion near toe of seawalls;
- erosion near offshore structures;
- natural developments of coasts with time;
- structural / gradual erosion of coasts;
- impact of coastal protection tools, like groyne, offshore breakwaters and seawalls and revetments;
- behaviour of artificial beach and shoreface nourishments.

In all cases sediment transports due to waves and currents are important. Compared to sediment transports due to currents alone (like in rivers), the waves are a complicating additional effect. In Chapter 4 the topic of sediment transport due to waves and currents is discussed in detail.





# 4 Sediment Transport Processes

## 4.1 Introduction

In many cases, coastal engineering problems can be expressed in terms of sediment transport-related problems (Chapter 3). In this approach, changes in the coastal morphology are the logical consequence of spatial gradients in sediment transport. It is therefore crucial to understand the physics behind sediment transport, before going into the more practical details of the coastal engineering profession.

Sediment transport can be defined as the movement of sediment particles through a well-defined plane over a certain period of time. The transport rate depends on the characteristics of the transported material and on the forces which induce such a transport. The primary force behind sediment transport is the bed shear stress exerted by the water motion on the bed. Sediment particles will tend to move when a certain critical bed shear stress is reached. The local bed shear stress can be induced by wind, wave, tide and density driven currents (current-related transport), by the oscillatory water motion itself (wave-related transport) or by a combination of currents and waves. This chapter deals with the basic principles of sediment transport.

Sediment properties which are important for the sediment transport mechanisms are presented in Section 4.2. Next, in Section 4.3, the initiation of motion is considered. There, it is shown that the so-called critical velocity (or critical shear stress) is important to initiate the process of sediment transport. Formulations for these bed shear stresses are given in Section 4.4 for the situations with only a uniform current, waves alone, and the combination of currents and waves.

Sediment transport is generally split up into two modes of transport: bed load and suspended load. If the particles are moved in bed load mode, then they roll, shift or make small jumps over the seabed; they do not leave the bed load layer. Transport in suspended load mode, on the other hand, implies that grains are lifted from the seabed at flows above the critical flow velocity and transported in suspension by the (moving) water. Below a certain flow velocity, the grains settle down again. Section 4.5 describes the basic states of bottom and suspended transport.

Finally, a more detailed elaboration is presented for sediment transport under current conditions, wave conditions and combined waves and currents in respectively, Sections 4.6, 4.7 and 4.8.

## 4.2 Sediment properties

### 4.2.1 General

In these lecture notes we focus on sediments like quartz ( $\text{SiO}_2$ ) and clay minerals (sheets of silicates) which are present in the coastal area as discrete particles. Depending on the particle size we distinguish silt and clay, sand, gravel, stones and boulders.

Clay particles are very small with a large surface area compared to their volumes. This surface area is chemically active, which especially when wet, leads to the typical cohesive (slippery) characteristics of its bulk form. Sand on the other hand is non-cohesive; the grains do not stick together. A handful of pure sand can not be picked up by hand in the way a piece of clay can be picked up.

In these lecture notes we mainly focus on sand. Some fundamentals and related problems for silt and clay are discussed in Chapter 9 separately.

### 4.2.2 Grain size, density and bulk properties

Two important parameters for sediment transport are the mean particle diameter and the grading:  $D_{50}$  and, for example,  $D_{90}/D_{10}$ , where  $D_x$  is defined as the sediment particle diameter (in meters) for which  $x$  % by weight is finer. In American literature, a  $\phi$ -scale is often used to identify the particle dimensions:

$$\phi = -2 \log D \quad (4.1)$$

where:

$$D \quad \text{sand grain diameter} \quad [\text{mm}]$$

Sediment is called well-sorted if  $D_{90}/D_{10}$  is small (say  $<1.5$  although there is no formal classification); for large values of  $D_{90}/D_{10}$  (for instance  $>3$ ) we speak of poorly sorted or well-graded sediment.

In addition to grain size, other parameters are important for sand transport as well, such as: grain shape (the grains are not perfect spheres), grain density, fall velocity, angle of repose and volume concentration.

The grain density  $\rho_s$  depends on the mineral composition of the sand. Most of the world's beach sands consists of quartz (feldspar is the second-common mineral), with a mass density of  $2,650 \text{ kg/m}^3$ . Other minerals are often referred to as heavy minerals since their mass density is usually greater than  $2,700 \text{ kg/m}^3$ .

The fall velocity depends on the grain characteristics as well as on the fluid characteristics (such as water density and viscosity). This has further been worked out in Section 4.2.3. Roughly speaking, the fall velocity of medium-sized sand particles ( $0.1 \text{ mm} < D < 0.5 \text{ mm}$ ) in water varies from 0.01 to 0.05 m/s.

When dry sand is poured onto a flat surface, it will form a mound. The slope of the surface of the mound is called the angle of repose, which depends mainly on the grain size.

The porosity  $p$  is defined as the ratio of pore space (voids) to the whole volume. Natural sands have porosities in the range of 0.25 to 0.50; a frequently applied figure is 0.40 (or 40%). The volume concentration  $n$  is the ratio of the solid mass to the whole volume:  $n = 1 - p$ .

Contrary to the grain density ( $\rho_s$ ) as mentioned above, bulk density is the mass of a unit volume of e.g. a mixture of particles and air or water. The dry bulk density is defined as  $n\rho_s$ . If the whole pore volume is filled with water (density  $\rho$ ), then we obtain the saturated bulk density, which is defined as:  $n\rho_s + p\rho$ . A typical figure for the dry bulk density is  $1,600 \text{ kg/m}^3$ , and for the saturated bulk density  $2,000 \text{ kg/m}^3$ .

### 4.2.3 Fall velocity

When a particle falls in still and clear water, it accelerates until it reaches its fall velocity. Fall velocity is defined as the constant vertical velocity of a single particle in an infinite large volume of water. This velocity can be assessed from the balance between the downward directed gravity force  $F_G$  and the upward directed (retarding) drag force  $F_D$  as indicated in Fig. 4.1.

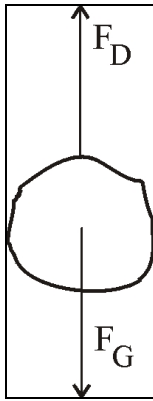


**Figure 4.1** Forces on a “sphere” in clear water

#### Basic equation

In case of a sphere the downward directed gravity force  $F_G$  is equal to:

$$F_G = (\rho_s - \rho) g \left( \frac{\pi}{6} D^3 \right) \quad (4.2)$$

where:

$\rho_s$	mass density of the particle	$[\text{kg/m}^3]$
$\rho$	mass density of the surrounding fluid	$[\text{kg/m}^3]$
$D$	particle diameter	$[\text{m}]$
$g$	acceleration of gravity	$[\text{m/s}^2]$

The term between the brackets refers to the volume of the sphere.

The upward directed force is equal to the so-called drag force denoted by:

$$F_D = c_D \left( \frac{1}{2} \rho w^2 \right) \left( \frac{\pi}{4} D^2 \right) \quad (4.3)$$

where:

$c_D$	the so-called drag coefficient	[-]
$w$	the particle fall velocity	[m/s]

The second term between the brackets refers to the cross-section of the sphere. There is only a drag force in the situation of a fall velocity  $> 0$ .

In equilibrium, both forces are in balance and the fall velocity  $w$  (in m/s) is given by:

$$w = \sqrt{\frac{4(\rho_s - \rho) g D}{3\rho c_D}} \quad (4.4)$$

A particle's fall velocity depends on its size, its specific density and on the magnitude of the drag coefficient  $c_D$ . This drag coefficient depends on the shape of the particle, its roughness but mainly on the Reynolds number, denoted as  $Re$ , being the ratio between the acceleration forces and viscous shear stress forces.

### Dependency on Reynolds number

For low Reynolds numbers ( $Re < 0.1$  to  $0.5$ ) in the so-called Stokes-range, the drag coefficient can be described by (see Fig.4.2;):

$$c_D = 24/Re \quad (4.5)$$

or with:

$$Re = wD/\nu \quad (4.6)$$

where:

$\nu$	kinematic viscosity coefficient	[m <sup>2</sup> /s]
-------	---------------------------------	---------------------

yielding:

$$w = \frac{(\rho_s - \rho) g}{18\rho\nu} D^2 \quad (4.7)$$

In this range, the fall velocity depends on the square of the grain diameter and is dependent upon the kinematic viscosity coefficient (defined as the ratio of the dynamic viscosity  $\eta$  to the fluid density  $\rho$ ). The magnitude of the kinematic viscosity coefficient is largely a function of the temperature.

A characteristic value for  $\nu$  is  $10^{-6}$  m<sup>2</sup>/s.

For high Reynolds numbers ( $400 < Re < 2.10^5$ ), in the so-called Newton range, the drag coefficient becomes a constant ( $c_D \approx 0.5$ ). In that case it follows from Eqs.(4.2) and (4.3):

$$w = 1.6 \sqrt{gD \frac{\rho_s - \rho}{\rho}} \quad (4.8)$$

In this range, the fall velocity depends on the square root of the grain diameter and is independent of the kinematic viscosity coefficient. This is also the case for extremely high Reynolds numbers ( $Re > 2.10^5$ ), where the drag coefficient is (constant) around 0.2.

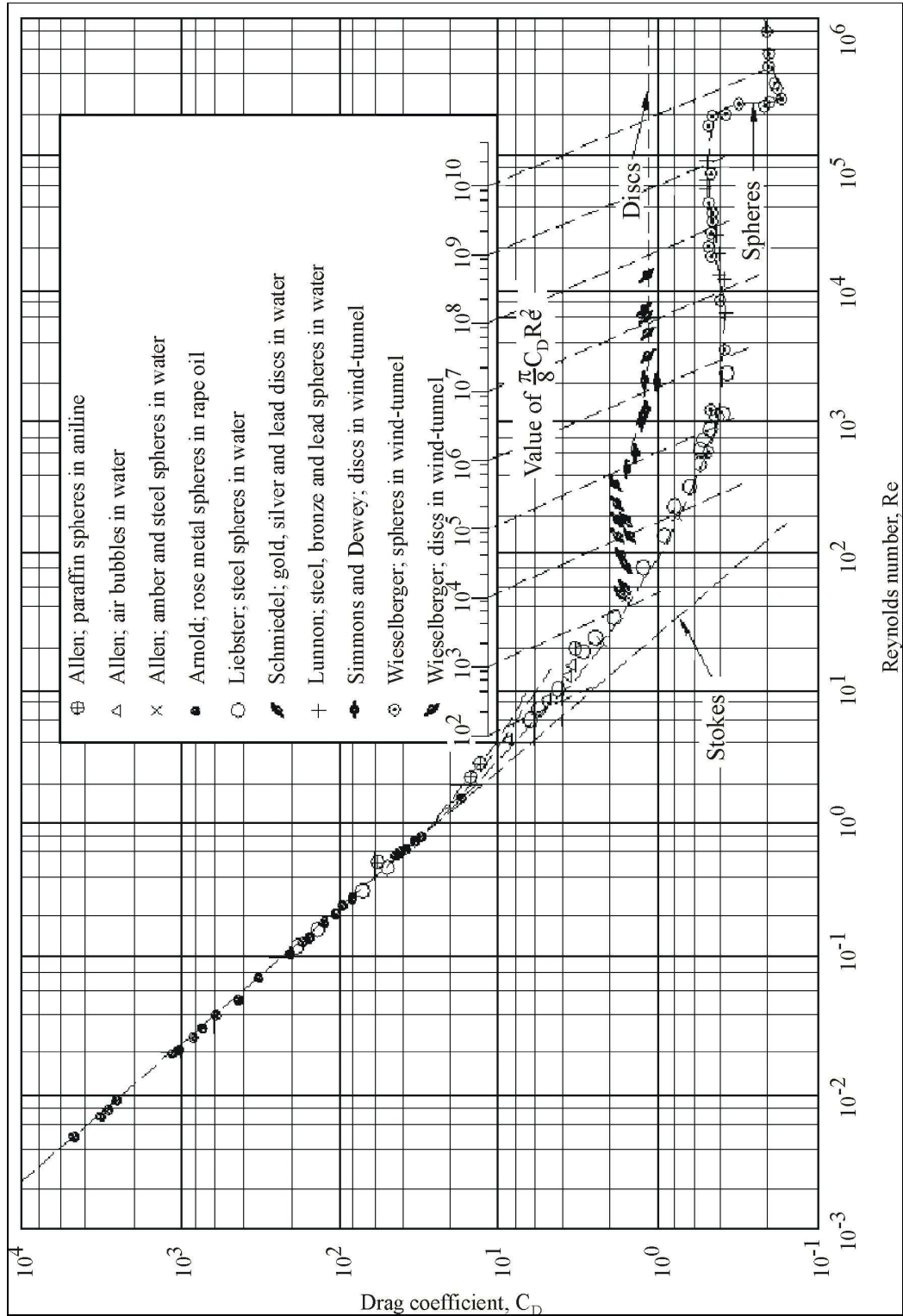


Figure 4.2 Drag coefficient as a function of Reynolds Number (Vanoni 1975)

For quartz spheres falling in still water, a Reynolds number of 0.5 corresponds roughly with a particle diameter of 0.080 mm, while a Reynolds number of 400 corresponds with a diameter of about 1.900 mm. This range (0.080 – 1.900 mm) closely corresponds to all sand particles. So for many often occurring sand particles, neither the Stokes approximation nor the Newton approximation can be used.

For very small particles (silt, clay) the fall velocity is proportional to  $D^2$ ; for gravel size particles the fall velocity is proportional to  $\sqrt{D}$ . For sand, the fall velocity falls in the transition range between a  $D^2$  dependency and a  $\sqrt{D}$  dependency. By lack of a simple relationship for the drag coefficient in this range, it is common practice to use empirical formulae, such as Eqs.(4.9) and (4.10):

Diameter range: 0.050 – 0.300 mm, fresh water, 18 °C

$$\log(1/w) = 0.4949(\log D_{50})^2 + 2.4113(\log D_{50}) + 3.7394 \quad (4.9)$$

Diameter range: 0.050 – 0.300 mm, fresh water, 10 °C

$$\log(1/w) = 0.4758(\log D_{50})^2 + 2.1795(\log D_{50}) + 3.1915 \quad (4.10)$$

In literature, many other formulae can be found [e.g. Van Rijn (1993) and Sisternans (2002)]. These are not reproduced here. The computed fall velocity as a function of the grain diameter is plotted for two formulae in Fig.4.3.

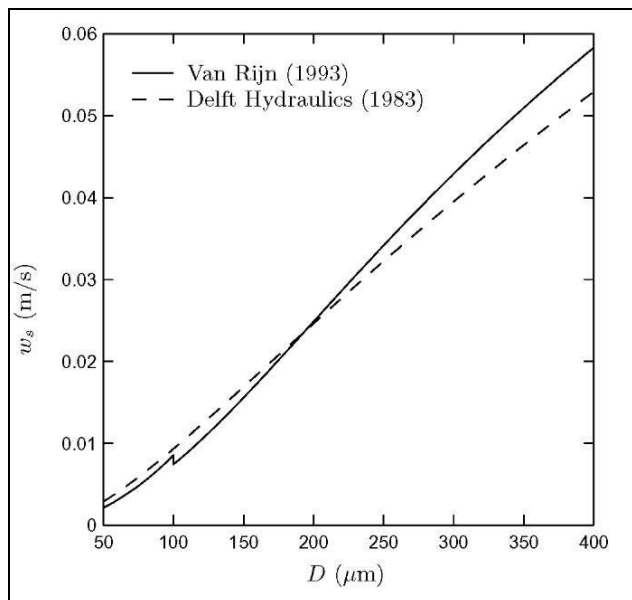


**Figure 4.3 Fall velocities of sediment for fresh water with a temperature of 18 degrees Celsius (after Sisternans, 2002)**

### Other effects

Eq.(4.8) shows that the fall velocity depends on  $\sqrt{((\rho_s - \rho)/\rho)}$ .

For quartz sand ( $\rho_s = 2,650 \text{ kg/m}^3$ ) and for fresh water at 4 °C ( $\rho = 1,000 \text{ kg/m}^3$ ), this factor is 1.28. With a small increase in density of the water like for sea water (for

instance to  $\rho = 1,020 \text{ kg/m}^3$ ), this factor becomes somewhat smaller (1.25). In very turbid water, the ratio may further be reduced (with  $\rho = 1,100 \text{ kg/m}^3$  to for instance 1.19). This shows that the fall velocity in natural environments may decrease due to an increase in water density by not much more than in the order of 7 %. [Starting with Eq.(4.7) slightly different (larger) effects of the ratio  $(\rho_s - \rho) / \rho$  on the fall velocity are found.]

The effect of temperature on the fall velocity has already been indicated by Eqs.(4.9) and (4.10). Temperature has an effect on the water density (small effect), and on the fluid viscosity (large effect). Changes in the fluid viscosity have only a small effect on the fall velocity of smaller particles. The fall velocity increases slightly with increasing water temperatures.

The effect of particle shape becomes relevant only for particles larger than say 0.125 mm (Re larger than about 10). The less spherical the particle, the larger becomes the drag coefficient and thus the smaller becomes the fall velocity. For particles that are far from spherical (like some coral sands or shell fragments), it is best to determine the fall velocity experimentally (for instance with a settling tube).

If the water column contains many sediment particles, then hindered settling may occur. This leads to smaller fall velocities per particle, which can be explained as follows. With each downward grain movement, a similar fluid volume must flow upward. This upward flow slows down the other grains. The effect of hindered settling can be represented by:

$$w_e = (1 - c)^\alpha w \quad (4.11)$$

where:

$w_e$	effective fall velocity	[m/s]
$w$	fall velocity of one grain in clear water in rest	[m/s]
$c$	sediment concentration (volumetric %)	[-]
$\alpha$	coefficient (ranging from 4.6 at low Reynolds numbers to 2.3 at high Reynolds numbers)	[-]

In many engineering cases related to sediment transport, the sediment concentration can be up to say 1 % (where 1% volume gives  $2.65 \text{ kg/m}^3$ ), meaning that the effect of sediment concentration on the fall velocity is small. This is not the case in sheetflow conditions where sediment concentrations can be significantly higher.

## 4.3 Initiation of motion

### 4.3.1 Forces on a single grain

Sediment can only be transported if the water movement is strong enough to move the individual grains. The so-called critical velocity, or critical shear stress, describes the point of initiation of motion. If this condition is exceeded, grains move, roll or be brought into suspension and sediment transport occurs.

In order to assess the critical condition the forces acting on an individual grain have to be taken into account. These forces can be divided into forces which tend to move

the grain, the drag force  $F_D$  and the lift force  $F_L$ , and a force which tries to keep the grain in its place; the gravity force  $F_G$  (see Fig.4.4).

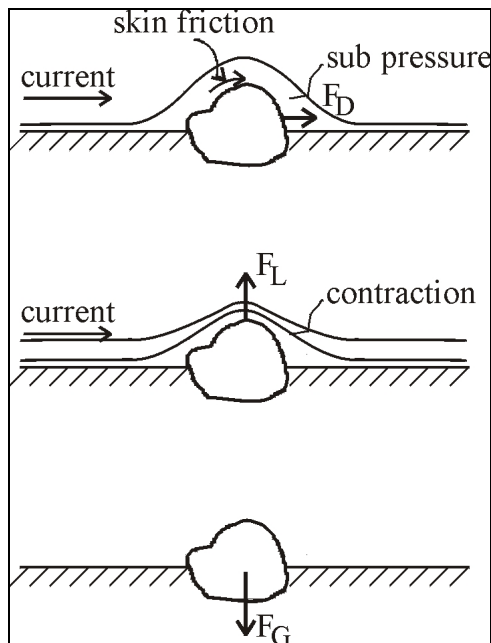


**Figure 4.4 Forces on an individual grain: drag force, lift force and gravity force**

### Drag force

The drag force is caused by the moving water which, in a very schematised way, has to flow around the sediment particle. The disturbance of the streamlines leads to a pressure at the upstream side of the particle, skin friction around the particle and sub pressure at the back of the particle. The drag force is proportional to the particle's surface area ( $\frac{1}{4}\pi D^2$  for spheres) and the momentum of the current ( $\frac{1}{2}\rho v^2$ ):

$$F_D \approx c_D \left( \frac{1}{2} \rho v^2 \right) \left( \frac{1}{4} \pi D^2 \right) \quad (4.12)$$

where:

$F_D$	drag force	[N]
$c_D$	drag coefficient	[-]
$\rho$	water density	[kg/m <sup>3</sup> ]
$v$	water velocity in front of particle	[m/s]
$D$	particle diameter	[m]

The drag force is always directed in the direction of the current. Eq.(4.12) for the drag force is valid for a single particle that is fully exposed to the flow. Sediment particles on top of a flat bed will be hidden to some extent in between the neighbouring particles. The drag force acting upon one particular particle will then be smaller.



## The lift force

The flow around the grain leads to flow contraction above the grain (there is no flow underneath the grain). Higher local flow velocity gives lower local pressure (Bernoulli law). The difference in vertical pressure causes a lift force, which is directed perpendicular to the drag force.

Similar as the drag force, the lift force is proportional to the particle's surface area ( $\frac{1}{4}\pi D^2$  in case of a sphere) and the momentum of the current ( $\frac{1}{2}\rho v^2$ ) (see Eq.(4.13)).

$$F_L \approx c_L \left( \frac{1}{2} \rho v^2 \right) \left( \frac{1}{4} \pi D^2 \right) \quad (4.13)$$

where:

$F_L$	lift force	[N]
$c_L$	lift coefficient	[-]

Vectorial summation of the drag force and the lift force gives the resulting force,  $F_R$ .

## The gravity force

The gravity force is proportional to the (submerged) weight of the grain, which is a function of the mass density of the sediment and of the mass density of water ( $\rho_s - \rho$ ) and the volume of the grain ( $\frac{1}{6}\pi D^3$  for spheres):

$$F_G = (\rho_s - \rho) \left( \frac{1}{6} \pi D^3 \right) g \quad (4.14)$$

where:

$F_G$	gravity force	[N]
$g$	acceleration of gravity	[m/s <sup>2</sup> ]

## Moments

Let us assume that the grain makes contact with its downstream neighbouring grain at one specific point (Fig.4.5). The resulting force  $F_R$  then gives a moment  $aF_R$ ; the gravity force gives a moment  $bF_G$ . It then follows that the grain will move once  $aF_R > bF_G$ . At the critical point of movement:

$$\frac{v^2}{\Delta g D} \approx \frac{4b}{3ac} \quad (4.15)$$

where:

$\Delta$	relative density ( $(\rho_s - \rho)/\rho$ )	[-]
$c$	total drag coefficient ( $\sqrt{c_D^2 + c_L^2}$ )	[-]
$a, b$	arms (see Fig.4.5)	[m]

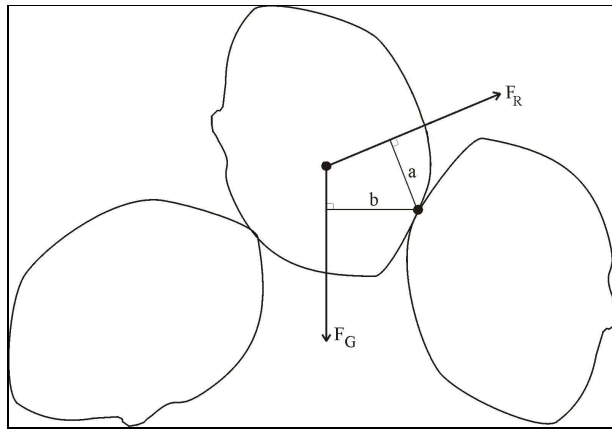


**Figure 4.5 Resulting forces and moments on a grain**

Another way of presenting Eq.(4.15) is by using the bottom shear stress  $\tau$  ( $\tau = \rho g v^2 / C^2$ : see Chapter 2). This leads to the following expression for the critical bottom shear stress (critical in the sense that higher bottom shear stresses lead to the initiation of motion):

$$\frac{\tau_{b,cr}}{(\rho_s - \rho)gD} \approx \frac{2b}{3ac'} \quad (4.16)$$

where:

$c'$	constant ( $C^2 c / 2g$ )	[-]
$\tau_{b,cr}$	critical bottom shear stress	[N/m <sup>2</sup> ]

The factor on the right hand side depends on the hydraulic conditions near the bed (through the  $C$ -value), the shape factor and the particle position relative to the other particles (through  $a$  and  $b$ ), and on the acceleration of gravity.

For perfect spheres and a maximum packing of the grains, it can be deduced that the term on the right hand side of Eq.(4.16) becomes  $\frac{2}{3} \tan(\phi)$ , where  $\phi$  is the angle of repose. (Here we disregard the effect of the lift force.) If we assume  $\phi = 30^\circ$ , then it follows that:

For spheres (no lift force) and neglecting the formal proportionality:

$$\frac{\tau_{b,cr}}{(\rho_s - \rho)gD} = 0.4 \quad (4.17)$$

In practical situations it is not possible to measure the values for  $a$ ,  $b$  and  $c'$ . Fortunately, many experiments have been performed in the past to determine the parameters in Eq.(4.16). The experiments of Shields [Shields (1936)], performed on a flat bed, are the most widely used. He defined the critical bed shear stress as the bed shear stress at which the (extrapolated) measured transport rates were just zero.

### 4.3.2 Shields curve

Fig.4.6 shows the so-called Shields curve (note that the axes are drawn on a log-log scale).

The factor on the left hand side of Eq.(4.16) [which is a dimensionless expression for the (critical) bed shear stress] is put on the vertical axis. The numbers on the horizontal axis are related to the Reynolds number  $Re$  (the subscript  $*$  is used to indicate that the Reynolds number is based on  $v_*$ ).

$$Re_* = \frac{v_* D}{\nu} \quad (4.18)$$

where:

$v_*$	shear stress velocity ( $v\sqrt{g/C}$ )	[m/s]
$D$	diameter of grains	[m]
$\nu$	kinematic viscosity coefficient	[m <sup>2</sup> /s]

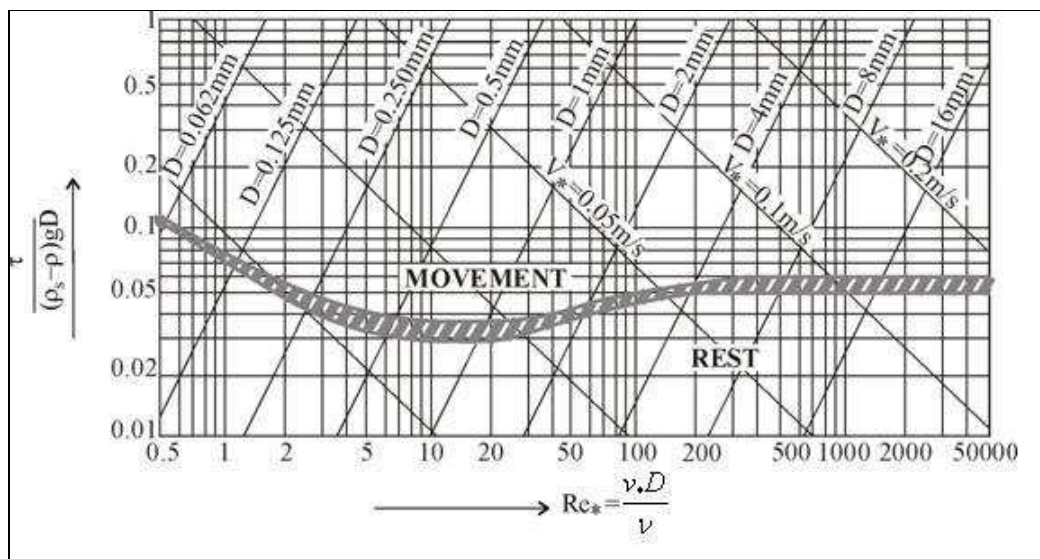


**Figure 4.6 Shields curve**

The shaded band in Fig.4.6 separates two zones: movement of sediment particles was observed in the experiments in the zone above this shaded band; whereas no movement was observed in the zone beneath the shaded band. The shaded band therefore indicates where initiation of motion occurs. Sometimes, the shaded band is represented by a single line, which is then referred to as the Shields curve.

For most practical situations with sand, a flat bed and a uniform current (no waves), critical flow velocities are in the range of 0.2 to 0.3 m/s (see also Example 4.1). During a tidal cycle, such flow velocities are often exceeded for several hours around maximum flood and maximum ebb flow. If we add the effect of orbital motions, the

duration during which the flow velocity exceeds the critical flow velocity, may be considerably extended. Contrary to steady flow conditions, there are no generally accepted relationships for the initiation of motion under oscillatory flow on a plane bed. Information on the initiation of motion for the combined effects of unidirectional and oscillatory flow are very scarce.

#### Example 4.1

*Input parameters:*

Water depth:	$h$	=	3 m
Roughness height:	$r$	=	0.06 m
Grain diameter:	$D_{50}$	=	200 $\mu\text{m}$

*Required:*

Critical velocity for rough bed and flat bed

*Output:*

From the Shields curve it can be found that Eq.(4.17) must be:

$$\frac{\tau_{b,cr}}{(\rho_s - \rho)gD} \approx 0.05$$

The shear stress velocity  $v_*$  equals:

$$v_* = \sqrt{\tau_{b,cr}/\rho} \approx 0.013 \text{ m/s}$$

Hence, the critical velocity equals:

$$v_{crit} = \frac{v_{*,crit}}{\sqrt{g/C}} \approx 0.20 \text{ m/s using } C = 18 \log(12h/r) = 50 \text{ m}^{1/2}/\text{s or}$$

$$v_{crit} = \frac{v_{*,crit}}{\sqrt{g/C}} \approx 0.38 \text{ m/s using } C = 18 \log(12h/D_{50}) \approx 95 \text{ m}^{1/2}/\text{s}$$

*Conclusion:*

With a bed with a roughness height of 0.06 m, the grains of 200  $\mu\text{m}$  start to move with a flow velocity exceeding 0.20 m/s. If a flat bed is considered with a roughness height equal to the particle diameter, the critical velocity becomes almost twice as high.

#### Example 4.1 Critical velocity

The Shields curve indicates that on average the factor on the right hand side of Eq.(4.17) is 0.05, instead of 0.4 as was theoretically determined for perfectly packed spheres. Apparently, it seems to be easier to move 'real grains' than to move perfectly packed spheres.

The 'factor eight' (0.4/0.05) is caused by a number of complicating factors, such as turbulence (which causes higher instantaneous flow velocity than the average flow velocity), bed slopes, graded and non-spherical grains (see below) and the lift force (which was omitted in the determination of the value of 0.4 in Eq.(4.17)).

Gradation of the bed material may play a role, especially for poorly sorted sediment ( $D_{90}/D_{10} > 3$ ). In these cases, the smaller particles will be hidden between the voids of the larger particles, while the larger particles are more exposed. Sometimes, armouring of the bed occurs. This implies that the smaller particles are first being

washed out, leaving a top layer of coarser particles (with higher critical flow velocities).

In case of a sloping bed in the flow direction, it can be argued that the critical flow velocity will be somewhat smaller for downward sloping beds and somewhat higher for upward sloping beds.

Other complicating factors may be the presence of cohesive sediment in the sand material. Cohesive forces between the grains may drastically increase the resistance against erosion. Biological activity and consolidation may be important in this respect as well.

The above illustrates that the Shields curve may yield practical results, but that reality is much more complex. What can be concluded is that the movement of grains depends on the velocity  $v$  (or shear stress  $\tau$  see next Section 4.4) and the grain size  $D$ . These parameters are taken into account in nearly all sediment transport equations.

## 4.4 Bottom shear stress

### 4.4.1 Introduction

In the previous sections it was concluded that the bottom shear stress is important for both the current and the sediment transport distribution. This is why many researchers have tried to formulate applicable and physically sound formulations of the shear stress. Below, we will focus on the rather straightforward approach followed by Bijker (1967), although other methods are also to be found in literature.

### 4.4.2 Shear stress under uniform flow

In a uniform flow there is a balance between the forces that act upon (parts of) the water mass (otherwise there would be an acceleration). The driving force in the case of a free-surface current, is initiated by gravity. This downward force  $G$  depends on the volume and the density of the water (Fig.4.7):

$$G = \rho g \Delta x (h - z) \quad (4.19)$$

where:

$G$	gravity force per unit width	[N/m]
$\Delta x$	length of the element of water	[m]
$h$	water depth	[m]
$z$	vertical axis (bottom: $z = 0$ )	[m]

The component of this force in the direction of the water movement is  $G \sin(i)$  (uniform current), with  $i$  being the bed slope (and water surface slope).

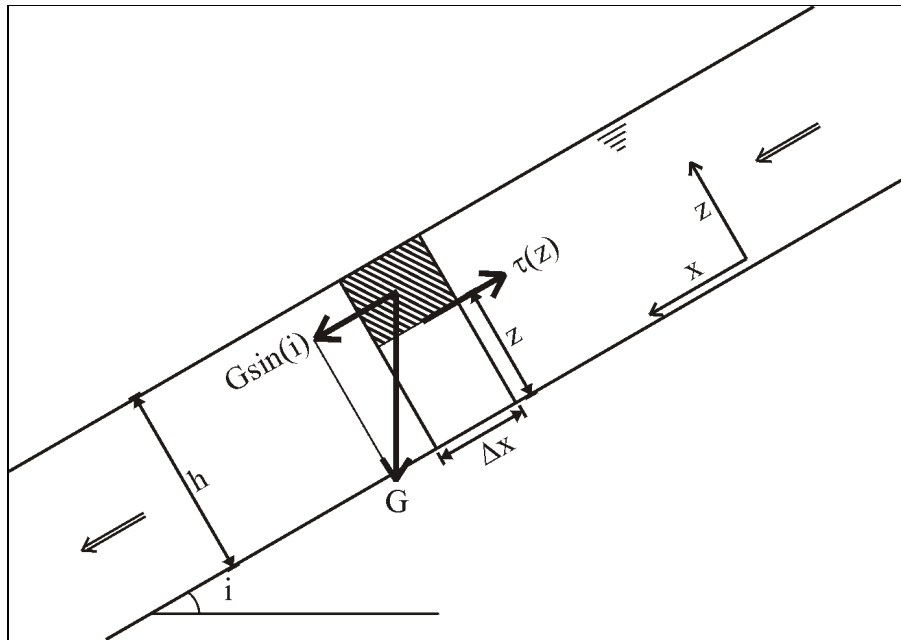


**Figure 4.7 Force balance**

The only opposite force is caused by internal friction, which is referred to as the internal shear stress in the water column, or simply shear stress;  $\tau(z)$ . For equilibrium the shear stress must be equal to  $G\sin(i)$ .

Since  $i$  is generally very small (less than  $10^{-2}$ ), and so:  $\sin(i) = i$ , it follows for the shear stress as a function of the water depth,  $\tau(z)$ , that:

$$\tau(z) = \rho g(h - z)i \quad (4.20)$$

And for the bottom shear stress,  $\tau(z = 0)$ :

$$\tau(z = 0) = \rho ghi \quad (4.21)$$

In many cases, the shear stress is assumed to have a linear distribution over the depth: zero at the water surface and  $\tau_c$  (subscript  $c$  in case of currents alone) at the bottom.

Sometimes the bed shear stress is denoted as  $\tau_b$ , where  $b$  stands for bottom. Other possible subscripts are  $c$  (current),  $w$  (waves),  $cw$  (currents and waves) or  $cr$  (critical). To avoid awkward subscripts like  $b, cw, cr$ , the bed shear stress is denoted with  $\tau$  (and, depending on the case, a single subscript just to clarify the meaning).

For uniform flow we can use the formula of Chézy, so that the expression for the shear stress under currents only,  $\tau_c$  becomes:

$$\tau_c = \rho g \frac{\bar{v}^2}{C^2} \quad (4.22)$$

where:

$\bar{v}$  depth-averaged flow velocity [m/s]

See Example 4.2 for an example calculation of the bottom shear stress under a current.

**Example 4.2**

*Input parameters:*

Water depth:  $h = 3$  m  
 Roughness height:  $r = 0.06$  m  
 Average flow velocity:  $v = 1$  m/s

*Required:*

Bottom shear stress

*Output:*

Using  $C = 18 \log(12h/r) = 50$  m<sup>1/2</sup>/s the shear stress due to the current equals:

$$\tau_c = \rho g \frac{v^2}{C^2} = 3.9 \text{ N/m}^2$$

**Example 4.2 Bottom shear stress under current**

In Eq.(4.22), the shear stress at the bottom is directly coupled to a parameter  $\bar{v}$ , which occurs in fact at a certain distance from the bottom. This is rather strange and not very useful if we later on like to combine the effects of waves and currents. For this reason the bed shear stress will (also) be related to a velocity parameter which is closer to the bed itself. To do so, first the velocity distribution over the vertical must be considered.

Considering the force balance of an element of water in Fig.4.7, it can be understood that the shear stress at a level  $z$  in the water column is somehow related to the gradient in the velocity over the depth. One way to do so is to use diffusivity:

$$\tau(z) = \rho \varepsilon_f \frac{dv(z)}{dz} \quad (4.23)$$

where:

$\varepsilon_f$  fluid diffusion coefficient [m<sup>2</sup>/s]

The fluid diffusion coefficient represents the coefficient for vertical transport of horizontal momentum. It can be regarded as a measure that indicates how 'easily' a certain horizontally moving package of water can move through the water column (up and downwards).

It comprises both the effects of molecular diffusion (induced by density gradients) and by turbulence. The effect of turbulence is generally much larger than the effect of molecular diffusion.

A general expression for the fluid diffusion coefficient can be derived from the mixing length theory of Prandtl (1926):

$$\varepsilon_f = l^2 \frac{dv(z)}{dz} \quad (4.24)$$

where:

$l$  mixing length [m]

Von Karman (1930) developed an equation for the mixing length:

$$l = \kappa z \sqrt{1 - \frac{z}{h}} \quad (4.25)$$

where:

$\kappa$  Von Karman coefficient

Von Karman found that near the bed (for  $z \ll h$ ), the mixing length was proportional to the height above the bed:  $l \cong \kappa z$ . From experiments it was further found that  $\kappa \approx 0.4$ .

Combination of Eqs.(4.23) to (4.25) and by assuming a linear variation of the shear stress over the depth, yields a logarithmic velocity profile. The next step is to introduce the so-called shear stress velocity  $v_*$  defined as:

$$v_* = \sqrt{\frac{\tau_c}{\rho}} \quad (4.26)$$

Using this parameter in the expression for the logarithmic velocity profile gives the well-known Prandtl – Von Karman logarithmic velocity profile:

$$v(z) = \frac{v_*}{\kappa} \ln \left( \frac{z}{z_0} \right) \quad (4.27)$$

where:

$z_0$  the zero-velocity level ( $v = 0$  at  $z = z_0$ ) [m]

The shear stress velocity is the flow velocity that occurs at a certain distance from the bottom, assuming the logarithmic velocity distribution as described by Eq.(4.27).

The zero-velocity level  $z_0$  has no physical meaning. It should be interpreted as a computation parameter, which is necessary because Eq.(4.27) is certainly not valid for depths below  $z_0$  (negative flow velocities are predicted there: see Fig.4.8).

Usually the value for  $z_0$  is related to the bed roughness.

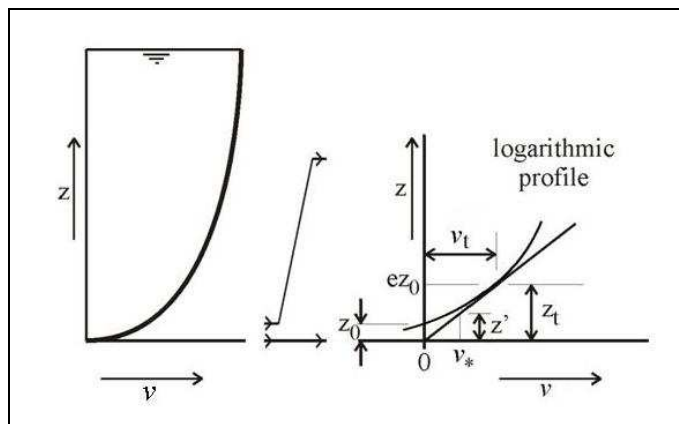


**Figure 4.8** Velocity distribution for a uniform stationary current



For a hydraulically smooth bottom,  $z_0$  is related to the viscous sub layer:

$$z_0 = 0.11 \frac{\nu}{v_*} \quad (4.28)$$

where:

$\nu$  kinematic viscosity [m<sup>2</sup>/s]

For a hydraulically rough bottom, which is generally the case in coastal engineering applications, Nikuradse found experimentally:  $z_0 \approx 0.033k_N$ , where  $k_N$  stands for the Nikuradse bottom roughness, or the equivalent bed roughness denoted as  $r$ .

Basically, we have only shifted the problem of describing the velocity distribution to this last parameter  $r$ . It is very unfortunate that the bed roughness can not be easily determined or measured in practice.

Many attempts have been made to measure the bed roughness in well-controlled laboratory experiments. For flat beds of sand or gravel, for instance, various researchers have related the bed roughness to the diameter of the largest grains on the surface of the bed. Examples are that of Engelund & Hansen (1973):  $r = 2D_{65}$ , and that of Van Rijn (1984):  $r = 3D_{90}$ .

Generally, the bed is not flat. Depending on the hydraulic conditions, different types of bed shapes will develop, like ribbons and ridges, ripples, dunes and bars. In such a case, the bed roughness needs to be related to the bed form, for instance the ripple geometry. An example is that of Swart (1976):

$$r = \frac{25\eta^2}{\lambda} \quad (4.29)$$

where:

$\eta$  measure for the ripple height (trough-crest) [m]

$\lambda$  measure for the ripple length (distance between two neighbouring ripple crests) [m]

The 'actual' velocity distribution under a uniform stationary flow close to the bed can be approximated as follows (see Fig.4.8). A tangent line is drawn from the bottom ( $z = 0$ ), where the velocity is zero, to the logarithmic velocity profile curve as computed with Eq.(4.27). This line touches the velocity profile at a height  $z_t$ , where the velocity is  $v_t$ . This height is related to the zero elevation  $z_0$  as follows:  $z_t = ez_0$ , where  $e$  is the base of natural logarithms (i.e. by approximation 2.72). The velocity at this height follows from Eq.(4.27):

$$v_t = \frac{v_*}{\kappa} \cdot 1 = \frac{\sqrt{g}}{\kappa C} v \quad (4.30)$$

where:

$v_t$  velocity at height  $ez_0$  [m/s]

$v_*$  shear stress velocity [m/s]

$C$  Chézy coefficient:  $C = 18\log(12h/r)$  [m<sup>1/2</sup>/s]

$v$  depth-averaged velocity [m/s]

$\kappa$  Von Karman coefficient (0.4) [-]

Combining Eqs.(4.26) and (4.30) finally gives the following relation between the bed shear stress under a uniform current and the near-bed flow velocity  $v_i$ :

$$\tau_c = \rho \kappa^2 v_i^2 \quad (4.31)$$

Eq.(4.31) might be used in bottom shear stress applications. Compared with Eq.(4.22), Eq.(4.31) has the advantage that the bed shear stress is related to an actual near-bed value of the flow velocity.

#### 4.4.3 Shear stress under waves

As was indicated in Section 4.3.2, initiation of motion is determined by the shear stresses exercised at the bed. The orbital motion under waves alone, so without the presence of a uniform current, also gives a shear stress at the bed. In case of shallow water, the water particles under a propagating wave describe an elliptical orbit. From the surface down to the bottom, the vertical displacement of the water particles reduces to zero, while the horizontal displacement remains almost constant (Fig.4.9).

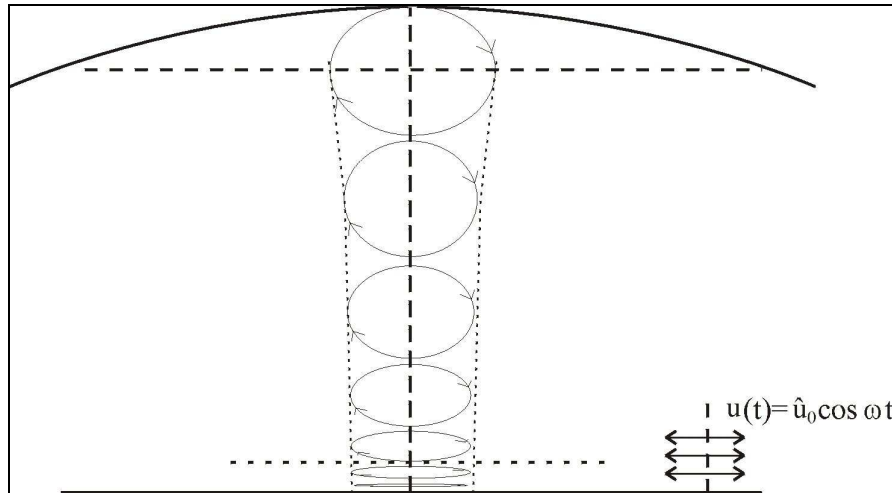


**Figure 4.9** Water particle movement in waves

Applying linear wave theory, the peak value of the orbital velocity  $\hat{u}_0$  and the excursion  $\hat{a}_0$ , at the bed is given by:

$$\hat{u}_0 = \frac{\omega H}{2} \frac{1}{\sinh(kh)} \quad (4.32)$$

$$\hat{a}_0 = \frac{\hat{u}_0 T}{2\pi} \quad (4.33)$$

where:

$\omega$	angular frequency ( $2\pi/T$ )	[Hz]
$H$	wave height	[m]
$T$	wave period	[s]
$k$	wave number ( $2\pi/\lambda$ )	[m <sup>-1</sup> ]

$\lambda$	wavelength	[m]
$\hat{a}_0$	maximum horizontal water particle displacement just outside the boundary layer	[m]

When waves approach shallow water, the shape of the waves will change, leading to non-sinusoidal waves (asymmetrical). For a correct description of the water motion under these waves, higher order wave theories should be used. However, in many computer model applications linear wave theory is also used in shallow water. It has been proved to be a reasonable approximation.

In reality, the orbital velocity at the bed ( $z = 0$ ) must be zero. The above equations are therefore valid from the water level to a small distance from the bed (Fig.4.10). This distance is denoted as  $\delta$ , which is the thickness of the wave boundary layer. The wave boundary layer is the transition layer between the bed and the layer of 'normal' oscillating flow. The thickness is generally between 1 and 10 cm for short period waves ( $T < 10$  s). The reason for this small thickness is that there is not sufficient time for the layer to grow out in vertical direction, because the current regularly reverses.

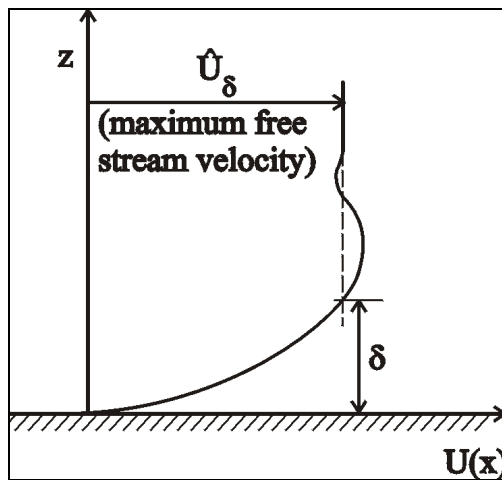


**Figure 4.10** Boundary layer thickness

It is typical for oscillating boundary layers that the maximum flow velocity near the bed is somewhat larger (a few per cent) than the so-called free stream velocity  $\hat{u}_0$ . This is caused by the complex nature of the water movement in and near the wave boundary layer. The boundary layer thickness  $\delta$ , thus defined as the minimum distance between the bed ( $z = 0$ , where  $u = 0$ ) and the level where the velocity equals the free stream velocity  $\hat{u}_0$  (Fig.4.10). Several researchers have experimentally found expressions for the value of  $\delta$ . An example for the situation with laminar flow is that of Nielsen (1985):

$$\delta = 0.5 f_w \hat{a}_0 \quad (4.34)$$

where:

$f_w$  friction factor

For a situation with turbulent flow an example is that of Fredsøe (1984), which is based on theoretical results :

$$\delta = 0.15 \left( \frac{\hat{a}_0}{r} \right)^{-0.25} \hat{a}_0 \quad (4.35)$$

where:

$r$  bottom roughness (under waves) [m]

For a rough bed and turbulent flow it is not easy to determine the bed shear stress.

The presence of ripples and other bed forms make the water motion in and close to the wave boundary layer very complex. Based on experiments, Jonsson (1966) found the following relation for the shear stress under waves:

$$\tau_w = 0.5 \rho f_w (\hat{u}_0)^2 \sin^2(\omega t) \quad (4.36)$$

where:

$\tau_w$  bottom shear stress for waves [N/m<sup>2</sup>]  
 $\omega$  angular frequency [Hz]  
 $\hat{u}_0$  maximum horizontal velocity just outside wave boundary layer [m/s]  
 $f_w$  friction factor [-]

The maximum bottom shear stress, thus is:

$$\hat{\tau}_w = 0.5 \rho f_w (\hat{u}_0)^2 \quad (4.37)$$

Eq.(4.37) relates the bed shear stress under waves directly to a near-bed (orbital) flow velocity. See Example 4.3 for an example calculation.

### Example 4.3

*Input parameters:*

Water depth:  $h = 3$  m  
 Roughness height:  $r = 0.06$  m  
 Wave height:  $H = 1.18$  m  
 Wave period:  $T = 8$  s

*Required:*

Bottom shear stress

*Output:*

From linear wave theory it can be found that the amplitude of the velocity near the bed can be found from:

$$\hat{u}_0 = \frac{\omega H}{2 \sinh(kh)} = 1 \text{ m/s and } a_0 = \frac{\hat{u}_0 T}{2\pi} = 1.27 \text{ m}$$

For a value of  $a_0/r > 1.59$  the friction factor equals:

$$f_w = \exp[-5.977 + 5.213(a_0/r)^{-0.194}] = 0.045$$

The maximum bottom shear stress follows from:

$$\hat{\tau}_w = \frac{1}{2} \rho f_w \hat{u}_0^2 = 22.5 \text{ N/m}^2$$

*Conclusion:*

For a maximum near bed orbital velocity of 1m/s the bottom shear stress due to waves equals 22.5 N/m<sup>2</sup>. This is almost 6 times the value found for the bottom shear stress due to an average current velocity of 1 m/s!

### Example 4.3 Bottom shear stress under waves

The wave friction factor depends on the amplitude of the wave orbital motion at the top of the boundary layer and on the bed roughness:  $\hat{a}_0/r$ . Many researchers have tried to understand and to describe the detailed flow conditions in the boundary layer above a rippled or flat bed. See for instance Fig.4.11 in which measured flow velocities are given of the instantaneous horizontal velocities above the crest and trough of a sand ripple [Du Toit (1982)]. More recently, the attention is focussing more into turbulence modelling.

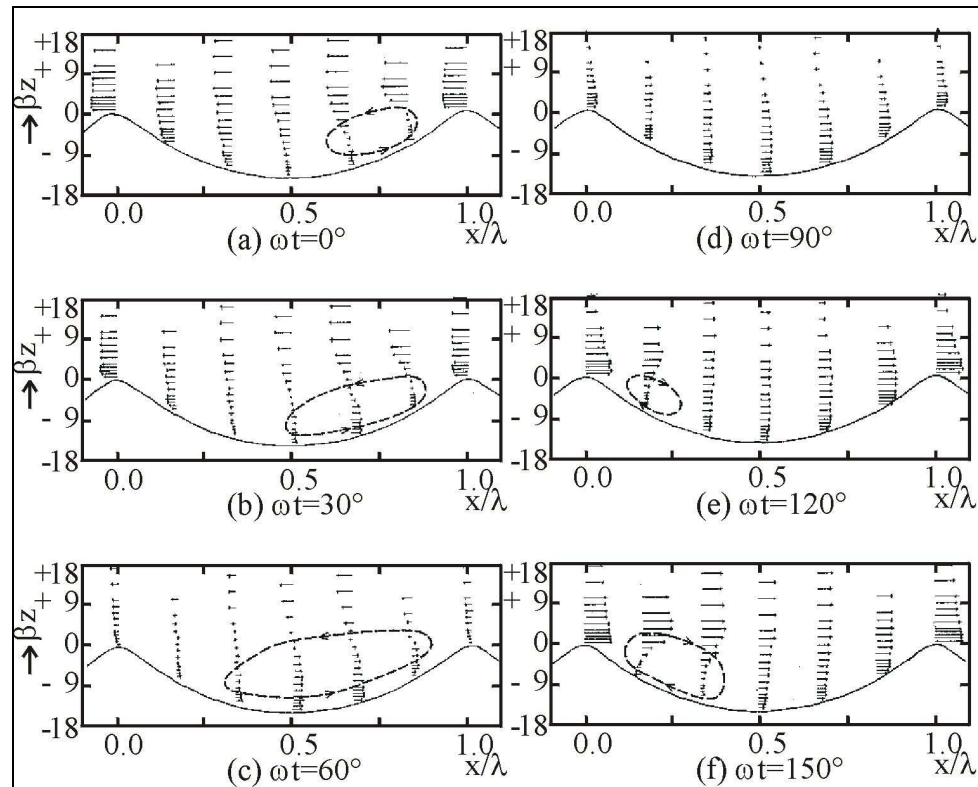


**Figure 4.11 Velocity field near a rippled bed in oscillatory flow (Du Toit, 1982)**

Similar as what was stated in Section 4.4.2, it is unfortunate that the bed roughness turns out to be important for the establishment of a relation for the bed shear stress while this cannot be easily measured in practical applications. This is why results from laboratory experiments are still widely used. A frequently applied example is that of Jonsson (1966), rewritten by Swart (1976) into:

$$f_w = \exp \left[ -5.977 + 5.213 \left( \frac{\hat{a}_0}{r} \right)^{-0.194} \right] \quad (4.38)$$

$$f_w = 0.30, \text{ if } \left( \frac{\hat{a}_0}{r} \right) < 1.59$$

Eq.(4.38) is graphically shown in Fig.4.12 (see next page). The upper limit of  $f_w$  is doubted by various researchers: some suggest that there is no upper limit and that the friction factor remains proportional to  $\hat{a}_0/r$ .

It follows from Fig.4.12, that  $f_w$  increases if  $\hat{a}_0/r$  decreases.

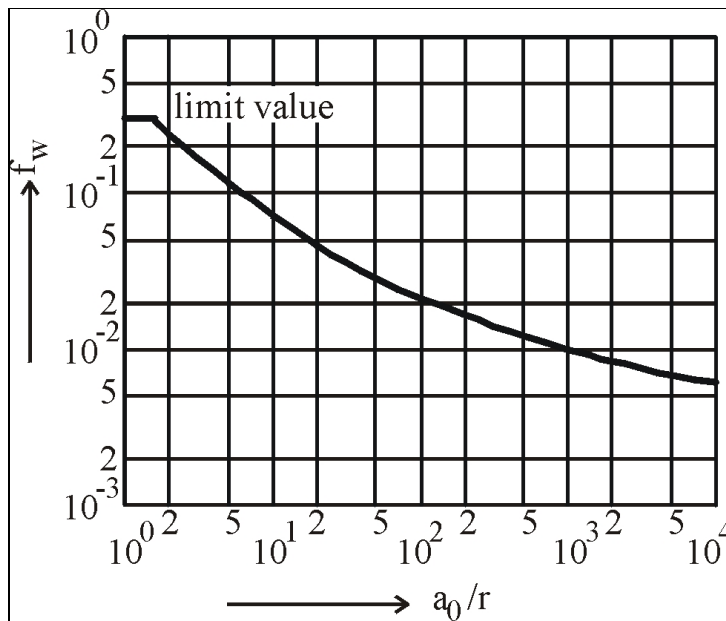


**Figure 4.12 Wave friction parameter**

Let us consider two cases in which  $\hat{u}_0$  is the same but  $T$  differs. For the case with a large value for  $T$ , the value of  $\hat{a}_0$  is larger than in the case with the lower value for  $T$  (Eq.(4.33)). Assuming an equal value for  $r$ , this means that the case with the larger value for the wave period gives lower values for the wave friction factor. This can be understood by considering the development of the boundary layer in time. For the longer wave period there is more time available to develop the boundary layer thickness. Ultimately the gradients in velocity in the boundary layer become smaller and the friction becomes smaller.

#### 4.4.4 Shear stress under combined waves and uniform flow

Wave characteristics, current velocities and shear stresses change when propagating waves encounter currents. The influence of waves on the current velocity distribution has been examined by various researchers. The following general observations were made:

*Waves with opposing current:* increased velocities near the surface, reduced velocities near the bed.

*Waves with following current on a smooth bed:* reduced velocities near the surface, increased velocities near the bed (so the opposite as for waves with opposing current).

*Waves with following current on a rough bed:* reduced velocities near the bed and the surface, increased velocities at intermediate depths.

From experimental data it can be concluded that the current velocities near the bed are reduced by wave-induced vortices in the wave boundary layer. Further,

experiments and theoretical considerations show that flow resistance to the main current will increase due to the presence of waves. The origin for this is turbulence induced by orbital wave motion in the wave boundary layer and water column. By assuming an apparent wave roughness in this case which is larger than the actual physical bed roughness, some researchers straightforwardly describe this effect.

In the previous sections, separate expressions were given for the bed shear stresses under currents and under waves.

Eq.(4.22) relates the bed shear stress under a stationary uniform current to the depth-averaged flow velocity; the depth averaged flow velocity is in fact the actual velocity which is present at a height of about 0.4 times the water depth from the bed. (See Fig.4.13 left panel.) [It was argued that an alternative expression could be derived with a velocity parameter very close to the bed; i.e. the actual velocity at a distance  $ez_0$  from the bottom (where  $z = 0$ )].

Eq.(4.36) relates the bed shear stress under waves to the orbital velocity at the top of the wave boundary layer. (See Fig.4.13 right panel.)

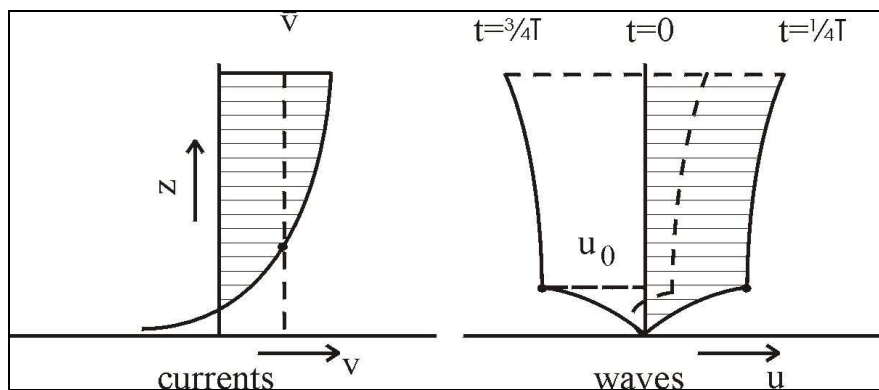


**Figure 4.13 Velocity distribution in stationary current and under waves**

In all bottom shear stress expressions the square of a characteristic velocity is applied. If a combination of current and waves is considered, again a characteristic velocity must be found. Because the position in the water column where the characteristic velocity occurs, is quite different for current and waves, it is clear that a simple addition of the respective velocities is not allowed.

### Bijker approach

Bijker (1967) was one of the first who developed a method in which the bed shear stress under waves and currents can be combined. In this approach the velocity at height  $z_t (= ez_0)$  is determined for both the currents (Section 4.4.2) and the orbital velocity under waves.

For waves Bijker defined the velocity at height  $z_t$  to be proportional to the velocity at the top of the wave boundary layer:

$$u_t = pu_0 \quad (4.39)$$

where:

$u_t$	velocity under waves at elevation $z_t$	[m/s]
$p$	proportionality factor	[-]
$u_0$	velocity on top of boundary layer	[m/s]

For the determination of the bed shear stress Bijker followed the same approach as for currents alone (Eqs.(4.23) to (4.31)). The bed shear stress,  $\tau_w$ , depends on the orbital velocity  $u_t$  (that is at height  $z_t$ ). By using the same 'structure' as Eq.(4.31), it follows that:

$$\tau_w = \rho \kappa^2 u_t^2 \quad (4.40)$$

where:

$u_t$	orbital velocity at height $z_t$ ( $= ez_0$ )	[m/s]
$\kappa$	Von Karman coefficient (0.4)	[-]

By using Eq.(4.40) the maximum bottom shear stress for waves only, is:

$$\hat{\tau}_w = \rho \kappa^2 (p \hat{u}_0)^2 \quad (4.41)$$

From a comparison of the work done by Jonsson (1966) and that of Bijker (1967), it followed that  $p$  is a function of the wave friction parameter  $f_w$ , and the Von Karman coefficient  $\kappa$  (combination of Eqs.(4.41) and (4.37)):

$$p = \frac{1}{\kappa} \sqrt{\frac{f_w}{2}} \quad (4.42)$$

The proportionality factor thus depends on the relative roughness  $\hat{a}_0/r$  as shown in Fig.4.12. The limit value of  $p$  is unity (if  $f_w = 0.3$  then  $p \approx 1$ ), which implies that the maximum orbital velocity at  $z = ez_0$  is then assumed to be equal to the maximum free stream velocity and  $ez_0$  is then equal to the boundary layer thickness  $\delta$ . If  $p < 1$  then the height  $z_t = ez_0$  is somewhere inside the wave boundary layer.

The next step is to combine the velocities under currents ( $v_t$ ) and under waves ( $u_t$ ) as these have been determined separately. In the Bijker approach, the velocities are simply added as vectors. Fig.4.14 shows the co-ordinate system and a plan view of the situation, including the constant current velocity  $v_t$  and the time-varying wave velocity  $u_t$  ( $= pu_0$ ). The combined velocity vector  $v_r$  also varies with time: both in magnitude as well as in direction.

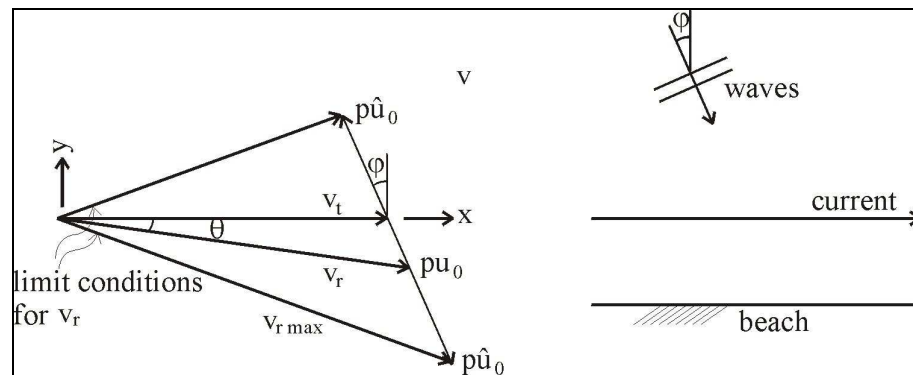


**Figure 4.14 Plan view and specific velocity components at an elevation  $z_t$  above the bottom**



Similar as for the situations with only a current or only waves, the combined bed shear stress can be written as (compare with Eqs.(4.31) and (4.40)):

$$\tau_{cw} = \rho \kappa^2 v_r^2 \quad (4.43)$$

where:

$\tau_{cw}$	(instantaneous) bed shear stress under combined waves and currents	[N/m <sup>2</sup> ]
$v_r$	(instantaneous) combined velocity under currents and waves (at $z_t$ )	[m/s]

Since  $v_r$  varies in time, the same is true for  $\tau_{cw}$  (Fig.4.15). Because of the square of  $v_r$  in Eq.(4.43), the time variation of the magnitude of the shear stress differs from that of the resultant velocity.

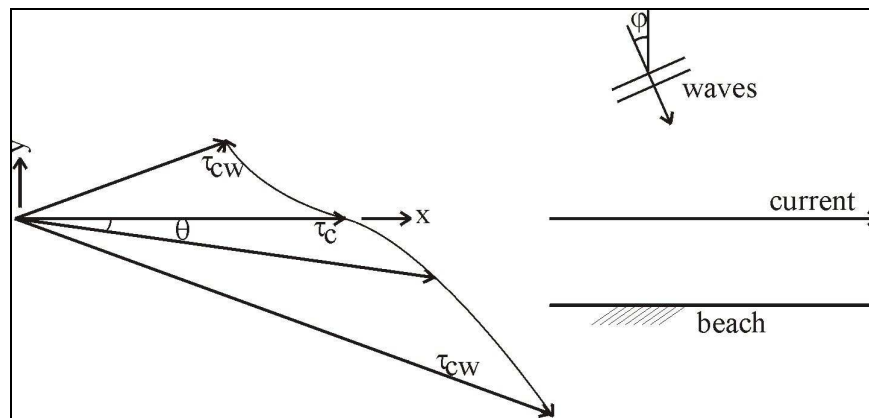


**Figure 4.15 Plan view and bottom shear stress components**

For the initiation of motion and the stirring up of sediment particles from the bed, the critical velocity (or the critical bed shear stress) has to be exceeded. Depending on the actual magnitudes of  $v_t$  and  $u_t$  this exceedance will happen for some parts of the wave period.

The direction of the resulting bed shear stress  $\tau_{cw}$  is varying all the time during a wave period. It can be argued that for some applications in sediment transport the actual direction of the stirring up process of bed particles is not important.

Although one might argue that it is a too straightforward approach, often the time-averaged total bed shear stress, i.e. averaged over the wave period, is used in some sediment transport formulae. Let us consider a quite general case like in Fig.4.15; the current and the waves make an arbitrary angle  $\varphi$  to each other. The time-averaged total bed shear stress reads:

$$\bar{\tau}_{cw} = \rho \kappa^2 \left[ v_t^2 + (p \hat{u}_0 \sin(\omega t))^2 + 2v_t p \hat{u}_0 \sin(\omega t) \sin(\varphi) \right] \quad (4.44)$$

(The over-bar in Eq.(4.44) represents time-averaging.)

The separate components between the brackets in Eq.(4.44) are shown as a function

of time in Fig.4.16. Integration over the wave period eliminates the third component, while integration over the wave period introduces a factor  $\frac{1}{2}$  in the second component. This gives:

$$\bar{\tau}_{cw} = \rho \kappa^2 \left[ v_t^2 + \frac{1}{2} (p \hat{u}_0)^2 \right] \quad (4.45)$$

Or:

$$\bar{\tau}_{cw} = \tau_c + \frac{1}{2} \hat{\tau}_w \quad (4.46)$$

where:

$\bar{\tau}_{cw}$	time-averaged total bed shear stress under currents and waves	[N/m <sup>2</sup> ]
$\hat{\tau}_w$	maximum bed shear stress under waves (Eq.(4.37))	[N/m <sup>2</sup> ]
$\tau_c$	bed shear stress under currents (Eq.(4.22))	[N/m <sup>2</sup> ]

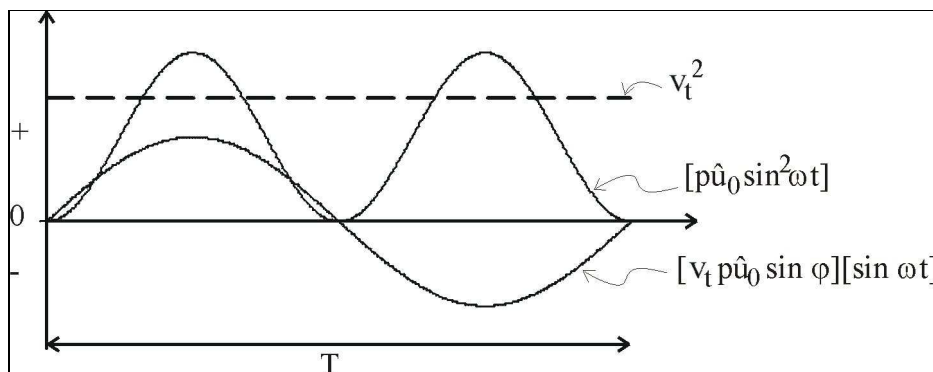


**Figure 4.16 Components of mean shear stress**

See Example 4.4 for an example of the calculation of the time-averaged bottom shear stress under the combined effect of waves and a current.

Time-averaging over the wave period has eliminated the dependency on the wave direction relative to the current direction ( $\phi$  in Fig.4.15). This means that the role of the waves is mere to ease the stirring up of sediment from the bottom. Once the criterion for the initiation of motion has been exceeded, sediment is being transported in the direction of the main current. The contribution of waves to the total bed shear stress can be quite significant in shallow water (easily a factor ten more than the contribution of currents alone). This is why in popular terms one could say that waves stir up the sediment, while currents transport it.

**Example 4.4***Input parameters:*

Water depth:	$h$	=	3 m
Roughness height:	$r$	=	0.06 m
Average flow velocity:	$v$	=	1 m/s
Wave height:	$H$	=	1.18 m
Wave period:	$T$	=	8 s

*Required:*

Time-averaged bottom shear stress

*Output:*

In the previous examples it was found that the bottom shear stress due to the current alone equals  $3.9 \text{ N/m}^2$  and that the maximum value for the bottom shear stress due to waves alone equals  $22.5 \text{ N/m}^2$ . The total time averaged bottom shear stress due to currents and waves follows from:

$$\overline{\tau_{cw}} = \tau_c + \frac{1}{2} \hat{\tau}_w = 3.9 + 11.3 = 15.2 \text{ N/m}^2$$

*Conclusion:*

If (modest) waves are superimposed on the current, the time-averaged bottom shear stress increases by a factor 4!

**Example 4.4 Bottom shear stress under current and waves combined**

In intra-wave modelling applications the time-averaging procedure over the wave period is omitted. An additional problem is then to properly describe the time lag effects. It will take some time before the sediment particles can actually respond to the (quickly) varying magnitude of the combined shear stress. In so-called research models intra-wave modelling is more and more used. In practice, in so-called engineering models, intra-wave modelling is often not yet applied.

Eq.(4.46) can also be written as:

$$\overline{\tau_{cw}} = \tau_c \left[ 1 + \frac{1}{2} \left\{ \xi \frac{\hat{u}_0}{v} \right\}^2 \right] \quad (4.47)$$

where:

$\hat{u}_0$	maximum orbital velocity at top of boundary layer	[m/s]
$v$	depth-averaged velocity (!)	[m/s]
$\xi$	combination of various parameters:	[-]

$$\xi = C \sqrt{\frac{f_w}{2g}} \quad (4.48)$$

### Special case: combined bed shear stress along a coastline

Up till now, we have only considered a situation where, at one specific location, a uniform current and waves are present. If we consider, for instance, a straight coastline, then longshore currents can be generated by tidal forcing (caused by water level gradients), by wind forces (acting upon the water surface) and by obliquely incoming waves (see Chapter 6). The longshore current is counteracted by friction forces, which are expressed in terms of the bottom shear stresses. The bottom shear stress was expressed with the help of velocity vectors at height  $z_t = ez_0$ . This latter is given in Eq.(4.43) or integrated over time in Eq.(4.47). The (instantaneous) direction of  $\tau_{cw}$  coincides with the (instantaneous) direction of the resulting velocity at  $z_t$ . The vector  $\tau_{cw}$  might be decomposed in a component parallel to the shoreline ( $x$ -direction) and a component perpendicular to the shoreline ( $y$ -direction).

For the longshore current, which flows in  $x$ -direction, only the  $x$ -component of the combined shear stress is important. With  $\varphi$  being the angle between the  $y$ -axis and the direction of wave propagation (see Fig.4.15), it then follows:

$$\tau_{cwx} = \tau_{cw} \frac{v_t + p\hat{u}_o \sin(\omega t) \sin(\varphi)}{v_r} \quad (4.49)$$

To obtain the mean value of  $\tau_{cwx}$  (over a wave period), this equation must be integrated over time. This turns out to be not very easy and no analytical solution can be found. Bijker (1967) made numerical experiments and, by fitting an equation to the results, he found:

$$\bar{\tau}_{cwx} = \tau_c \left[ 0.75 + 0.45 \left( \xi \frac{\hat{u}_0}{v} \right)^{1.13} \right], \quad \text{if } 0^\circ < \varphi < 20^\circ \quad (4.50)$$

Eq.(4.50) is only valid for  $|\varphi|$  smaller than  $20^\circ$ . See Example 4.5 for an example calculation.

An even further simplification is possible under the following assumptions:

- $|\varphi|$  is almost zero (which is reasonable in the breaker zone due to wave refraction);
- $\xi \hat{u}_0/v$  is much larger than unity.

With these assumptions, the mean bed shear stress component in longshore direction under combined currents and waves can be derived from Eq.(4.49) as:

$$\bar{\tau}_{cwx} = \frac{\rho}{\pi C} \sqrt{2gf_w} \cdot \hat{u}_0 v \quad (4.51)$$

If we use a shallow water approximation to determine  $\hat{u}_0$  (Chapter 2), then a further simplification is possible, leading to:

$$\bar{\tau}_{cwx} = \frac{\rho g}{\sqrt{2} \cdot \pi C} \gamma \sqrt{h} \sqrt{f_w} \cdot v \quad (4.52)$$

where:

$\gamma$	wave breaking index (= $H/h$ )	[-]
$H$	wave height	[m]
$h$	water depth	[m]

$C$	Chézy coefficient	$[\text{m}^{1/2}/\text{s}]$
$f_w$	wave friction parameter	$[-]$
$v$	depth-averaged flow velocity	$[\text{m}/\text{s}]$

**Example 4.5***Input parameters:*

Water depth:	$h$	=	3 m
Roughness height:	$r$	=	0.06 m
Average flow velocity:	$v$	=	1 m/s
Wave height:	$H$	=	1.18 m
Wave period:	$T$	=	8 s

Angle between the longshore current and the wave crests is small ( $\phi < 20^\circ$ )

*Required:*

Bottom shear stress in longshore direction

*Output:*

In the previous examples it was found that the bottom shear stress due to the current alone equals  $3.9 \text{ N/m}^2$  and that the maximum value for the bottom shear stress due to waves alone equals  $22.5 \text{ N/m}^2$ . The total time averaged bottom shear stress in this special case can be found from:

$$\bar{\tau}_{cwx} = \tau_c \left[ 0.75 + 0.45 \left( \xi \frac{\hat{u}_0}{v} \right)^{1.13} \right] = 7.9 \text{ N/m}^2 \text{ for } \xi = \frac{C\sqrt{f_w}}{\sqrt{2g}} \approx 2.5$$

If  $\xi \frac{\hat{u}_0}{v} \gg 1$  this can be further simplified to:

$$\bar{\tau}_{cwx} = \frac{\rho}{\pi C} \sqrt{2gf_w} v \hat{u}_0 = 6.2 \text{ N/m}^2$$

*Conclusion:*

For this special case of a small angle between the longshore current and the orientation of the wave crests, the bottom shear stress increases by a factor 1.5 - 2.0.

**Example 4.5 Bottom shear stress under longshore current****Conclusion**

Bed shear stresses are important for the initiation of motion and for sediment transport. The presence of waves can increase the bed shear stress significantly, compared to a situation with only a (uniform) current.

Bed shear stresses, however, are also important for counteracting currents that can be tide, wind, density, pressure, or wave driven (or a mixture). This means that we will come back to the topic of bed shear stresses in the remainder of these lecture notes, when hydrodynamics and sediment transport processes are discussed.

## 4.5 Sediment transport modes

### 4.5.1 Introduction

Initiation of motion, transport and deposition of sediment particles are core issues in coastal engineering. Coastal engineers are often mainly interested in the sediment transport integrated over time (such as per year) and over a certain ray (such as a ray perpendicular to the shoreline and covering the entire surf zone). In the following section we will go into the details of sediment transport per m and per s (so:  $\text{m}^3/\text{m/s}$ ). This transport can principally be parallel to the shoreline (longshore sediment transport: Chapter 6) or perpendicular to the shoreline (cross-shore sediment transport: Chapter 7).

The sediment transport at one particular location follows from the integration of the vertical sediment transport distribution over the entire water column. To compute the sediment transport distribution it is first necessary to determine the velocity distribution,  $v(z)$ , and the sediment concentration distribution,  $c(z)$ ; see Fig.4.17.

The sediment transport in a thin layer close to the bed (between  $z = 0$  and  $z = a$  in Fig.4.17) is referred to as bed load transport.

The transport in the upper layer is called suspended load transport.

These two sediment transport modes are briefly introduced in Section 4.5.2.

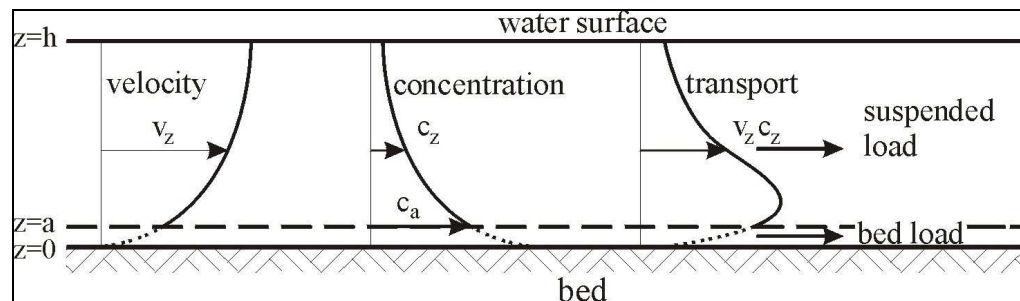


**Figure 4.17 Principle of (suspended) sediment transport computation**

The main focus will be on the description of the concentration distribution, which depends on the shape of the vertical distribution curve and on a so-called reference concentration (i.e. the concentration near the bed: see Fig.4.17). Various shape functions can be found in literature. The reference concentration is often deduced from a (separate) calculation of the bed load transport, for which aim often sediment transport formulae are applied which are also used in river engineering.

### 4.5.2 Basic formulation

Basically, sediment transport can be defined as a quantity of sediment that is moving with a specific velocity through a well-defined (part of a) plane. Expressed in terms of a very simple equation:

$$S = cv \quad (4.53)$$

where:

$S$	sediment transport rate	$[\text{m}^3/\text{s}/\text{m}^2]$
$c$	sediment concentration	[see below]
$v$	velocity of particles (water velocity)	$[\text{m}/\text{s}]$

Here, as in many similar discussions, it is assumed that particles in suspension move essentially with the same speed as the water surrounding the particle; so with the local velocity of the water. The mass of particles in suspension is usually so small, that they are able to follow water velocity fluctuations without a significant time-delay.

Sediment concentration can be defined in two ways: volumetric concentration ( $\text{m}^3$  sediment per  $\text{m}^3$  water; or simply in %), or mass concentration ( $\text{kg}/\text{m}^3$ ). Volumetric concentration thus gives the percentage of the total volume (for instance  $1 \text{ m}^3$ ) which is occupied by grains. This may be with or without voids in between the particles; voids which would be present if the particles would be settled at the bottom. In sediment transport formulae, volumetric concentrations are often directly multiplied by  $1/(1-p)$  ( $p$ : porosity) as that results in direct information on accretion or erosion quantities if the sediment transport rate changes. When we are measuring sediment concentrations, mostly the mass concentration is used as unit ( $c$  in  $\text{kg}/\text{m}^3$  or  $\text{g}/\text{li}$ ). If the mass concentration is used as the unit for the sediment concentration  $c$  in a sediment transport formula, then the results have to be multiplied by  $1/\rho_s$  to get  $\text{m}^3/\text{s}/\text{m}^2$  as unit for  $S$ . ( $\rho_s$ : mass density of particles ( $\text{kg}/\text{m}^3$ .)

Eq.(4.53) can be used if we are interested in the sediment transport rate in a specific point. Usually we are interested in a more integrated measure, for example the total amount of transport between the bed and the water surface. In that case, the sediment transport rate can be described as the same product of sediment concentration  $c$  and water velocity  $v$ , though integrated over the local water depth  $h$ :

$$S = \int_{z=0}^h c(z)v(z) dz \quad (4.54)$$

Both the concentration  $c$  and the velocity  $v$  are allowed to vary as a function of the elevation  $z$  above the bed. This type of equation can be applied for the assessment of the sediment transport rate in e.g. a river in which both concentration and velocity vary only slowly with time.

However, in a coastal environment where waves play an important role, both the velocity and the concentration exhibit large variations in time on the time scale of a wave period. Consequently, latter equations will have to be extended yielding:

$$S = \frac{1}{t'} \int_{z=0}^{h+\eta} \int_{t=0}^{t'} c(z,t)v(z,t) dt dz \quad (4.55)$$

where:

$t'$	the integration period	$[\text{s}]$
$\eta$	the instantaneous water surface elevation	$[\text{m}]$
$h$	average water depth	$[\text{m}]$
$v(z,t)$	instantaneous velocity at height $z$ (in $x$ -direction)	$[\text{m}/\text{s}]$
$c(z,t)$	instantaneous concentration at height $z$	$[\text{m}^3/\text{m}^3]$

For the time interval over which the integration in Eq.(4.55) is carried out, denoted as  $t'$ , a sufficient number of wave periods should be taken into account. For the upper boundary of the integration vertical, the instantaneous level of the water surface should be used.

The local variation in the velocity and consequently the local variation in the sediment concentration are in general related to the oscillating movement of the waves. Bosman (1986) measured sediment concentrations at a constant elevation above the bed and under identical regular waves in a so-called oscillating water tunnel. The results of 99 records are plotted in Fig.4.18.

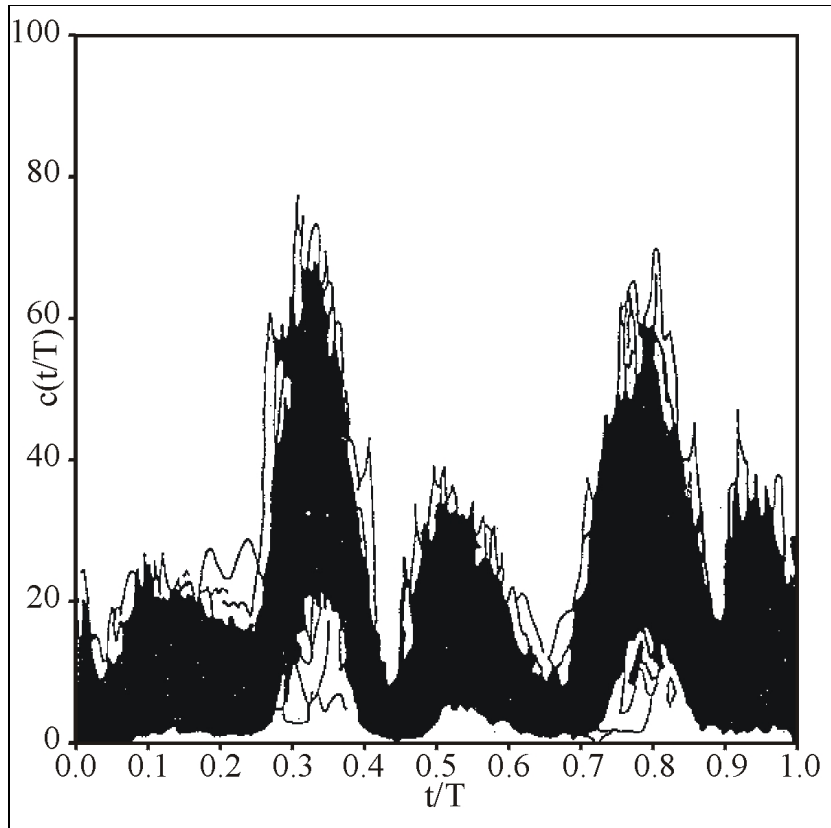


**Figure 4.18 Sediment concentrations as a function of time (99 individual records), Bosman (1986)**

Although some expected tendencies can be seen in Fig.4.18 (e.g. two large peaks, and two smaller peaks in between), the scatter in the measuring results is (unexpectedly) very large. For the time being it is still impossible to find a sound relation for the sediment concentration as a function of time and place for quite general cases (including irregular waves). That means that a sediment transport formula fully based on Eq.(4.55) can in fact not yet be used. By applying some simplifications we are able to derive formulae for special (restricted) cases.

One approach is to distinguish between various transport modes based at the characteristics of the water movement. If, for example, the fluctuations in the magnitude of the velocity (in the direction perpendicular to the plane where we like to quantify the sediment transport rate) are rather small, a quite different situation is



present compared to a situation with large fluctuations. In the coastal area we might make a distinction in sediment transport modes, based at the current characteristics. See further discussion in Sections 4.6 to 4.8 and 5.3.

Another, mainly practical and useful, point is to make distinction in the sediment transport that is occurring in two horizontal transport layers. If one refers to the material that is transported in a layer very near to the bottom, it is the so-called bed load transport. The material transport in the region above this 'bottom layer' is referred to as suspended load transport (Fig.4.17).

Although the actual boundary between the two layers is not always clear, the distinction is considered very practical. Some basic principles of these two types of sediment transport are given in Sections 4.5.3 and 4.5.4.

### 4.5.3 Bed load transport

Bed load transport occurs when the bed shear stress or the bed shear stress velocity ( $v_* = \sqrt{(\tau/\rho)}$ ) exceeds a critical value (initiation of motion). Sediment particles start rolling or sliding over the bed. If the bed shear stress increases further, then the sediment particles move across the bed by making small jumps, which are called saltations. Only if the jump lengths of the saltations are limited to say a few times the particle diameter, this type of motion is still considered as a part of the bed load transport. Otherwise, if the jumps become larger, it looks more like suspended load transport. This illustrates once more that the distinction between bed load and suspended load transport is artificial to some extent. A good reason to do so, is for simplifying the mathematical description of sediment transport.

Bed load transport is concentrated in a layer close to the seabed, the so-called bottom layer with a thickness  $\delta_b$ . The mixing due to (vertical) turbulence is often assumed to be still small in this layer, so that it only slightly influences the motion of sediment particles. The movement of the sediment particles is mainly limited by the effect of gravity.

Many formulae do exist in literature which describe the bed load transport. The oldest is perhaps that of Du Boys (1879!), followed by many others. These formulae were originally developed for rivers, and later adjusted for coastal environments. Most of the formulae 'predict' the rate of bed load transport as a function of logical parameters like current velocity (or bed shear stress), particle size, bed roughness, etc. In Section 4.6.2 an example of a bed load formula is further discussed.

A quite different formulation for the bed load transport would be:

$$S_b = \delta_b c_\delta \bar{v}_\delta \quad (4.56)$$

where:

$S_b$	bed load transport	[m <sup>3</sup> /m/s]
$\delta_b$	thickness of the bottom layer	[m]
$\bar{v}_\delta$	average velocity in the bottom layer	[m/s]
$c_\delta$	(say a constant) concentration in the bottom layer	[m <sup>3</sup> /m <sup>3</sup> ]

It is noted that such a formulation is actually in contradiction with the nature of bed load. In a formulation according to Eq.(4.56) bed load transport is in fact considered as a 'suspended mode'. It refers to a layer of water with an average suspended sediment concentration moving with an averaged velocity. With the help of a reliable

bed load transport formula to find  $S_b$ , and known (assumed) values for  $\delta_b$  and  $\bar{v}_\delta$ , at least a measure for a characteristic near bed sediment concentration  $c_\delta$  can be found. This approach will be used in the following section.

#### 4.5.4 Suspended load transport

When the actual bed shear stress is (much) larger than the critical bed shear stress, the particles will be lifted from the bed. If this lift is beyond a certain level, then the turbulent upward forces may be larger than the submerged weight of the particles. In that case, the particles get into suspension, which means that they loose contact with the bottom for some time.

Now besides gravity, friction forces between the grains in suspension and the grain - water interaction affect the behaviour of the suspended particles.

The suspended transport rate  $S_s$  is found by applying the basic equation according to Eq.(4.55) for the region above the bottom layer (Fig.4.17):

$$S_s = \frac{1}{t'} \int_{z=\delta_b}^{h+\eta} \int_{t=0}^{t'} c(z,t) v(z,t) dt dz \quad (4.57)$$

Notice that Eq.(4.57) is still quite general and realise that we are always interested in the sediment transport through a well-defined plane. The velocity parameter  $v(z,t)$  in Eq.(4.57) refers consequently always to the component of the total velocity perpendicular to the plane as considered. (The component of the total velocity parallel to the plane of the sediment transport, does not contribute to the transport *through* the plane; the particles shear along the plane.)

For the further elaboration of Eq.(4.57) two parameters must be considered into more detail;  $c(z,t)$  and  $v(z,t)$ . In the coastal area both parameters are in general functions of height above the bed and time. Compare for example the effect of the orbital motion of the waves.

In sediment transport applications in coastal engineering it still makes sense to discern between cases where the velocity components are a clear function of time ( $v(z,t)$  must be used) and cases where the time effect might be neglected ( $v(z)$  might be used). The latter case is much easier to handle than the former case. See also Section 5.3.

Let us assume that we can stick to a description of the sediment transport rate where the time effect of the velocity component is not important. (That refers often to cases with tidal currents and/or wave driven longshore currents where we are interested in sediment transports through planes perpendicular to the current direction.)

In these cases we might use of the logarithmic velocity distribution as described with Eq.(4.27). As explained in Section 4.4, a logarithmic velocity distribution 'predicts' negative velocities for  $z < z_0$ , which is of course not realistic. Since we are dealing with suspended load transport, which is by definition above the bottom layer, this is not a real problem. Note that the thickness of the bottom layer  $\delta_b$  has not much in common with  $z_0$  ( $= r/30$ , with  $r$  = bottom roughness). However, both are small relative to the water depth and located just above the bottom.

The second important parameter in the elaboration of Eq.(4.57) is the vertical distribution of the sediment concentration. This depends on various parameters, such

as the wave characteristics, the overall flow velocity, depth, characteristics of the water and the bed material (assuming that the sediment in suspension originates from the local bottom) and the bottom slope. Because all these parameters and sub-parameters influence each other at various time- and space-scales, it is yet impossible to give a formulation for  $c(z,t)$  for an arbitrary combination of conditions. However, in cases where we can stick to a  $v(z)$  description for the current velocity, we also can stick to a  $\bar{c}(z)$  description for the sediment concentration (over-bar: time-averaged).

Sediment transport along a coastline can often be approximated in such a schematised way. Due to wave refraction, the angle of the incoming waves relative to the longshore current, will be small. This means that the variations over the wave period in the velocity component parallel to the coast will also be small. For practical cases, we may use the time-averaged velocity. If we further use the time-averaged concentration, Eq.(4.57) can be rewritten as:

$$S_{s,x} = \int_{z=\delta_b}^{h+\eta} v(z) \cdot \bar{c}(z) dz \quad (4.58)$$

where:

$$S_{s,x} \quad \text{suspended sediment transport in } x\text{-direction} \quad [\text{m}^3/\text{ms}]$$

Reference is made to Chapter 5 where this will be further elaborated.

### Concentration distribution

In the following discussion on sediment concentration we first assume a steady state (like in uniform flow). So fluctuations with time are excluded. The sediment concentration  $c(z)$  is assumed to be only a function of  $z$ ; the over-bar to represent time-averaged conditions is for simplicity reasons omitted.

The grains that cause a sediment concentration  $c(z)$  at height  $z$ , will have a tendency to fall down with their fall velocity  $w$ . The downward transport through a horizontal plane in the water column at level  $z$  above the bed thus is  $wc(z)$ . Local turbulence in the water column leads to upward and downward exchange of water. Averaged over time, of course, there is no net exchange of water. However, since the sediment concentration changes over the water column, more grains will be transported in upward direction than in downward direction. This leads to a turbulent transport of sediment, which depends on the gradient in concentration over the vertical axis. This is why it is referred to as a gradient-type transport.

Turbulence transports – on average – sediment from levels of high concentrations to levels of lower concentrations. So from lower levels to higher levels. An equilibrium situation occurs once the downward transport caused by gravity is compensated by the upward movement of grains by turbulence:

$$wc(z) + \varepsilon_s(z) \frac{dc(z)}{dz} = 0 \quad (4.59)$$

where:

$$\begin{aligned} c(z) & \quad \text{average concentration at level } z \text{ above the bed} & [-] \\ \varepsilon_s(z) & \quad \text{diffusion coefficient for sediment at level } z & [\text{m}^2/\text{s}] \end{aligned}$$

The assumption of a gradient type transport is only valid in situations with small-scale fluid movements. In practical situations, such as a surf zone with breaking waves, this prerequisite will not be met. Under such conditions, large vertical

movements of water take place and diffusion is not the primary process. Still, even in these situations working with Eq.(4.59) proved to be very practical. The parameter  $\varepsilon_s$  however, should then be regarded as a measure for the mixing process.

Note that in Section 4.4.2, the gradient-type transport was also applied for the vertical transport of fluid ( $\varepsilon_f$  in Eq.(4.23)). There, horizontal momentum was exchanged in the vertical direction (instead of sediment grains in this section), ultimately leading to the logarithmic velocity profile.

The most general solution of Eq.(4.59) is:

$$c(z) = c_a \exp \left[ - \int_{z=a}^z \frac{w}{\varepsilon_s(z)} dz \right] \quad (4.60)$$

where:

$c_a$	concentration at level $z = a$ (in fact an integration constant)	[-]
$w$	fall velocity	[m/s]
$z$	height above the bed	[m]

In coastal engineering practice, the reference concentration  $c_a$  is often related to the concentration  $c_b$  inside the bottom layer (see under bed load transport).

If we consider uniform bed material ( $w = \text{constant}$ ), then it follows from Eq.(4.60) that the concentration distribution  $c(z)$  is determined by the reference concentration near the bottom and the distribution of the mixing coefficient  $\varepsilon_s(z)$ .

The mixing coefficient for sediment is likely related to that of the fluid. In simplified format:

$$\varepsilon_s = \beta \varepsilon_f \quad (4.61)$$

where:

$\beta$	factor	[-]
---------	--------	-----

If  $\beta < 1$ , then it is assumed that the sediment particles can not respond fully to the turbulent fluid velocity fluctuations (inertia). If  $\beta > 1$ , then it is assumed that the sediment particles are apparently 'thrown out' of the turbulent eddies. This can be related to the centrifugal forces, which are larger for sediment than for water, due to the higher density of the particles compared to the density of water. Laboratory experiments sometimes give values for  $\beta$  larger than unity, which supports the idea of the dominance of centrifugal forces in the resulting movement of sediment particles through the water.

The value for  $\beta$ , however, remains uncertain. In the following  $\beta = 1$  is used.

Various researchers have suggested distributions for  $\varepsilon_s(z)$ . In Fig.4.19, an overview is given of some suggested  $\varepsilon_s$ -distributions.

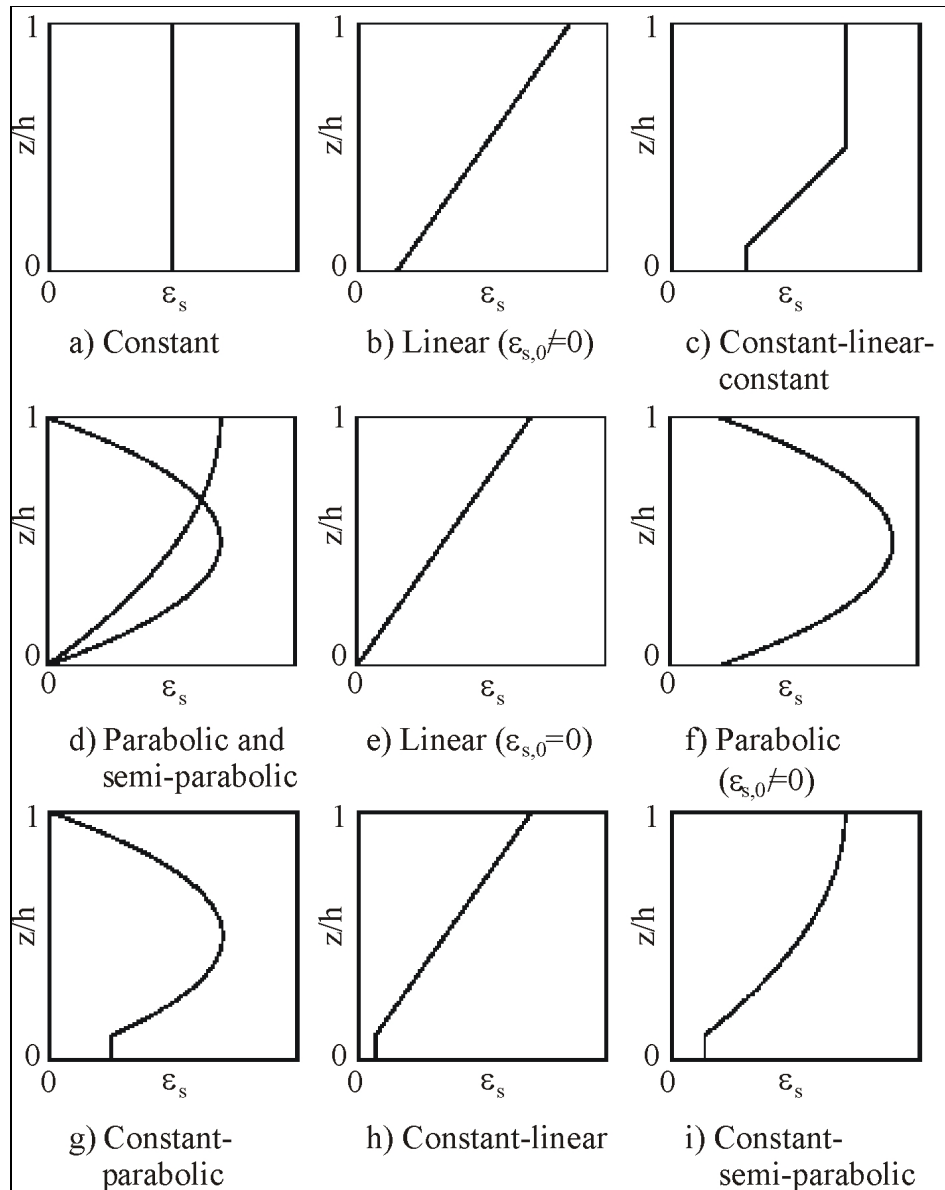


**Figure 4.19 Overview of  $\epsilon_s$  distributions [after Sisternans (2002)]**

Two distributions are discussed in more detail below.

A most simple distribution assumes  $\epsilon_s(z) = \epsilon_s$  is constant all over the water depth. (See Fig.4.19 case a) Constant.) This gives the following solution of Eq.(4.60):

$$c(z) = c_0 \exp\left[\frac{-wz}{\epsilon_s}\right] \quad (4.62)$$

where:

$\epsilon_s$  the constant value for the mixing coefficient  $[\text{m}^2/\text{s}]$

$c_0$  concentration at  $z = 0$  (in this case the integration constant can be taken at level  $z = 0$ ) [-]

The exponential concentration distribution according to Eq.(4.62) predicts finite sediment concentrations at the bottom and at the water surface. (See Fig.4.20) With the help of Eq.(4.62) we easily can see what happens with  $c(z)$  if we assume e.g. more mixing (larger  $\varepsilon_s$ ) or finer bottom material (smaller  $w$ ).

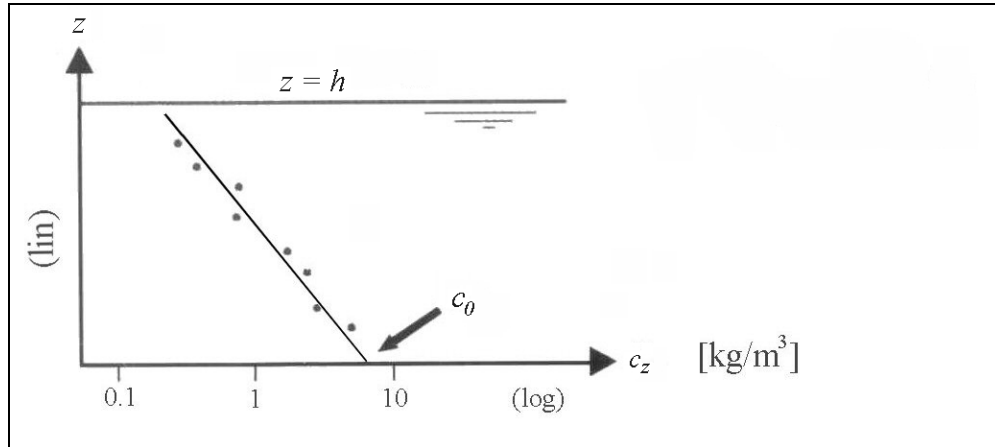


**Figure 4.20 Sediment concentration distribution over water depth (constant mixing coefficient)**

Rouse/Einstein suggested a parabolically changing diffusion coefficient over the water depth (see Fig.4.19 case d):

$$\varepsilon_s(z) = 4\varepsilon_{s,\max} \frac{z}{h} \left[ \frac{h-z}{h} \right] \quad (4.63)$$

where:

$\varepsilon_{s,\max}$  maximum mixing coefficient occurring at half the water depth [m<sup>2</sup>/s]

This results in a concentration distribution denoted as:

$$c(z) = c_a \left[ \frac{h-z}{z} \frac{a}{h-a} \right]^{z_*} \quad (4.64)$$

where:

$a$  thickness of the bottom layer [m]

$c_a$  concentration at reference level  $z = a$  [-]

$z_*$  Rouse number defined as:

$$z_* = \frac{w}{\kappa v_*} \quad (4.65)$$

This concentration distribution leads to infinite values at  $z = 0$  and to zero concentrations close to the surface ( $z = h$ ). (See Fig.4.21) Therefore, a finite concentration near the bottom,  $c_a$  is necessary to determine the whole distribution over the water depth. (In contrary to the use of  $c_0$  as used in Eq.(4.62).)

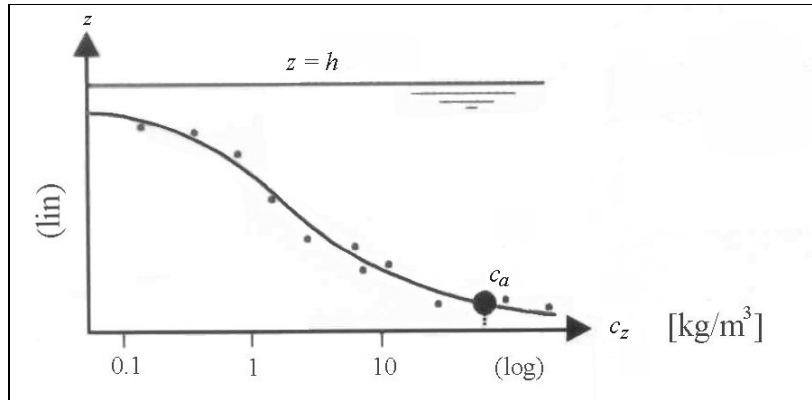


**Figure 4.21 Sediment concentration distribution over water depth (parabolic mixing coefficient)**

It is not known which  $\varepsilon_s$ -distribution is physically most realistic. Various researchers 'promote' various distributions. A given measured sediment concentration distribution over the water depth, can often be equally reliably approximated by various distributions represented in Fig.4.19.

By using the Rouse/Einstein distribution at least some consistency is achieved in the formulations used for the description of the velocity distribution and for the distribution of the sediment concentration. Both for the  $\varepsilon_s$ -distribution and for the  $\varepsilon_f$ -distribution parabolic functions are then assumed. (A parabolic  $\varepsilon_f$ -distribution leads to the well-known logarithmic velocity distribution.)

### Bottom concentration

The *shape* of the concentration distribution depends on the assumed  $\varepsilon_s$ -distribution, whereas the concentration quantities entirely depend on the bottom, or reference concentration. The bottom concentration can be chosen at  $z = 0$  ( $c_0$ ), or at a level  $z = a$  above the bottom ( $c_a$ ). The bed concentration  $c_0$  is used in the concentration distribution with the constant mixing coefficient (Eq.(4.62)); the near bed concentration  $c_a$  is used in the Rouse/Einstein distribution (Eq.(4.64)).

In principle, one may use any level for  $z = a$ . Generally,  $z = a$  corresponds with the surface of the bottom layer, i.e. the narrow zone where the bed load transport takes place. A practical method to find the bottom concentration  $c_a$  is to use one of the many available bottom transport formulae:

$$c_a = \frac{S_b}{va} \quad (4.66)$$

where:

$S_b$	bed load transport	$[\text{m}^3/\text{ms}]$
$v$	average fluid velocity in the bottom layer	$[\text{m/s}]$
$a$	thickness of the bottom layer	$[\text{m}]$

In coastal engineering it is common practice to use the bottom roughness  $r$  as a measure for the thickness of the bottom layer  $a$ , so:  $a = r$ .

Most of the bottom transport formulae relate  $S_b$  to the bottom shear stress and to the particle diameter. If  $S_b$  is determined and  $v$  is computed theoretically,  $c_a$  can also be determined. Some other formulae use more complex formulations, which make it far from easy to determine the value for  $c_a$ . Once a value for  $c_a$  has been established, it is possible to find the entire concentration distribution over the water depth.

### 4.5.5 Total load transport

The sum of the bed load transport rate  $S_b$  and suspended transport rate  $S_s$  equals the total transport rate  $S_t$ :

$$S_t = S_b + S_s \quad (4.67)$$

Such a simple summation of the two transport modes, i.e. bed load and suspended load transport, is allowed because they are driven by different transport processes. They are, however, closely related, for instance via the bottom concentration. In the next sections, sediment transport formulae are presented for both transport modes as well as for the total load transport. From the given examples it will become clear how both transport modes are interrelated.

## 4.6 Sediment transport by currents

### 4.6.1 Introduction

Although we are mainly interested in the sediment transport by waves and currents, we will start our discussion with the (quantification of the) sediment transport by currents only.

The transport of sediment particles by a uniform current is possible in the form of bed load only or in the combination of bed load and suspended load. This mainly depends on the flow conditions and the size of the bed material. Various formulae are available in literature, many of them originating from river engineering. These are not repeated here.

As an example, however, we will describe in some detail a set of formulae. With this set and various assumptions, it is ultimately possible to calculate the sediment transport by currents. (With this basis and some additional assumptions we are later on able to calculate the sediment transport for the combination of waves and currents for some specific cases in coastal engineering).

This approach is first applied by Bijker (1971); we basically follow this approach in these lecture notes (So-called Bijker formula.). Similar approaches have been followed by others.

### 4.6.2 Bed load transport under currents

Kalinske (1947) as well as Einstein (1950) introduced statistical methods for the representation of the turbulent behaviour of the flow. Einstein developed complex formulations for the movement of the particles, whereas Kalinske assumed a normal distribution for the instantaneous fluid velocity at grain level. Frijlink (1952) used a more practical approach and made a fit of various transport formulae. This led to the so-called Kalinske-Frijlink formula for bed load transport (in uniform flow):



$$S_b = \underbrace{5D_{50}\sqrt{\mu}}_{\text{transport}} \cdot \underbrace{v_* \exp\left[-0.27 \frac{\Delta C^2 D_{50}}{\mu v^2}\right]}_{\text{stirring up}} \quad (4.68)$$

where:

$S_b$	bed load transport	$[\text{m}^3/\text{m/s}]$
5	experimentally derived coefficient (fit parameter)	$[-]$
$D_{50}$	mean sediment particle diameter	$[\text{m}]$
$v_*$	shear stress velocity defined as:	
	$v_* = \frac{v\sqrt{g}}{C}$	$[\text{m/s}]$
$v$	depth-average flow velocity	$[\text{m/s}]$
$C$	Chézy friction coefficient	$[\text{m}^{0.5}/\text{s}]$
$\mu$	ripple factor	$[-]$
$g$	acceleration of gravity	$[\text{m/s}^2]$
-0.27	experimentally derived coefficient (fit parameter)	$[-]$
$\Delta$	relative sediment density defined as:	
	$\Delta = \frac{\rho_s - \rho}{\rho}$	$[-]$
$\rho_s$	mass density of sediment	$[\text{kg}/\text{m}^3]$
$\rho$	mass density of water	$[\text{kg}/\text{m}^3]$

Using the expression for the shear stress under currents (Eq.(4.22)) gives:

$$S_b = \underbrace{5D_{50}\sqrt{\mu}}_{\text{transport}} \cdot \underbrace{v_* \exp\left[\frac{-0.27}{\mu} \frac{\rho g \Delta D_{50}}{\tau_c}\right]}_{\text{stirring up}} \quad (4.69)$$

The last part of term between brackets is the inverse of the Shields parameter. The second underlined term in Eq.(4.69) is a measure for the stirring up of sediment particles, which thus mainly depends on the Shields parameter. The first underlined term is the actual (dimensionless) transport term. Apart from the two fit coefficients and the already known parameters, one 'exotic' parameter occurs in both the transport and the stirring parts of the transport equation which needs some explanation: the ripple factor  $\mu$ .

Bottom friction is caused by flow resistance at the bottom. Both the bed forms, like ripples, and the grains contribute to this flow resistance (but on different scales). The actual transport of particles occurs due to the forces (shear stresses) acting on the grains itself (not due to the forces acting on the bottom ripples). With the ripple factor it is meant to specify the actual forces at the grains.

The factor  $\mu\tau_c$  represents the actual shear stress on the grains within the bed, which is a measure for the forces acting on the grains. Since  $\tau_c$  is the bed shear stress (under currents), the ripple factor can be regarded as that part of the available shear stress that can be used to initiate the movement of sediment particles. The remaining part of the shear stress then is a measure for the flow resistance caused by bed forms like ripples.

$$\mu \sim \frac{\tau_{skin,grains}}{\tau_c} \quad (4.70)$$

where:

$\tau_{skin,grains}$  shear stress at skin surface of the grains, defined as:

$$\tau_{skin,grains} = \frac{\rho g v^2}{C_{skin}^2} \quad [\text{N/m}^2]$$

$$C_{skin} \quad 18 \log(12h/D_{skin}) \quad [\text{m}^{0.5}/\text{s}]$$

$D_{skin}$  representative grain size for skin friction [m]

$\tau_c$  total bed shear stress, defined as:

$$\tau_c = \frac{\rho g v^2}{C^2} \quad [\text{N/m}^2]$$

$$C \quad 18 \log(12h/r) \quad [\text{m}^{0.5}/\text{s}]$$

$r$  bottom roughness [m]

In some transport formulations,  $D_{90}$  is used for  $D_{skin}$ , yielding  $C_{skin} = C_{90}$ . However, other formulations can be found in literature as well.

The ripple factor, according to the above definition, is proportional to  $(C/C_{90})^2$ . In practice however, it appears that the following expression is used for the ripple factor:

$$\mu = \left( \frac{C}{C_{90}} \right)^{1.5} \quad (4.71)$$

By using the power 1.5 instead of 2, the factor  $\mu\tau_c$  actually is a combination of the shear stress on the grains (which was the original definition) and the total shear stress:

$$\mu\tau_c = \tau_{skin,grains}^{0.75} \cdot \tau_c^{0.25} \quad (4.72)$$

In the Kalinske-Frijlink transport formula for bed load transport under a uniform flow, it follows that skin friction is assumed to be more important for the transport than the total friction (power 0.75 versus power 0.25).

The physical meaning of the ripple factor is that it indicates, for a certain amount of available shear stress, how 'easily' sediment particles can be stirred up. It is therefore not logical that  $\mu$  (in fact  $\sqrt{\mu}$ ) also appears in the 'transport part' of the Kalinske-Frijlink formula. Bijker (1971) modified the Kalinske-Frijlink formula by indeed leaving out the ripple factor in the 'transport part' of the formula:

$$S_b = 5D_{50}v_* \exp \left[ \frac{-0.27}{\mu} \frac{\rho g \Delta D_{50}}{\tau_c} \right] \quad (4.73)$$

The experimentally derived fit coefficient 5 in the original Kalinkse-Frijlink formula, however, was based including  $\mu$  in the transport part of the formula. With an order of magnitude of  $\mu = 0.4$ , it would mean that this coefficient in the Bijker formula, should be  $\approx 3$  (namely  $5\sqrt{0.4}$ ). But still often a coefficient of 5 is used in real applications.

### 4.6.3 Suspended load transport under currents

Einstein (1950) used the Von Karman – Prandtl logarithmic velocity distribution, and a diffusion equation for the sediment concentration distribution. He further assumed a parabolic distribution of the mixing coefficient  $\varepsilon$ , while he used  $\varepsilon_s = \varepsilon_f$ . As shown in Section 4.5.4 this resulted in the Rouse/Einstein distribution of  $c(z)$ :

$$c(z) = c_a \left[ \frac{h-z}{z} \frac{a}{h-a} \right]^{z_*} \quad (4.64)$$

where:

$a$  thickness of the bottom layer [m]

$z_*$  Rouse number defined as:

$$z_* = \frac{w}{\kappa v_*} \quad (4.65)$$

Einstein assumed a bottom layer thickness ( $a$ ) as twice the grain diameter. He further used his own bed load transport formula (not given here) to find an expression for the reference concentration.

With a logarithmic velocity distribution and Eq.(4.64) for the sediment concentration distribution, the suspended load transport ( $S = v \cdot c$ ) yields:

$$S_s = \int_a^h \frac{v_*}{\kappa} \ln \left[ \frac{z}{z_0} \right] \cdot c_a \left[ \frac{h-z}{z} \frac{a}{h-a} \right]^{z_*} dz \quad (4.74)$$

The integral in Eq.(4.74) cannot be simply solved. Einstein found an expression with two other integrals as a solution:

$$S_s = 11.6 v_* a c_a \left[ I_1 \ln \left( \frac{33h}{r} \right) + I_2 \right] \quad (4.75)$$

where:

$I_1, I_2$  Einstein integrals [-]

$h$  water depth [m]

The Einstein integrals are difficult to solve. Bogaard and Bakker (1977) evaluated the entire term between brackets in Eq.(4.75), referred to as  $Q$ , and listed values for  $Q$  as a function of  $z_*$  and  $r/h$  (see Table 4.1):

$$Q = \left[ I_1 \ln \left( \frac{33h}{r} \right) + I_2 \right] \quad (4.76)$$

[With modern fast computers Eq.(4.74) can be simply approached with a numeric scheme.]

r/h [-]	z* [-]									
	0.00	0.20	0.40	0.60	0.80	1.00	1.50	2.00	3.00	4.00
1·10 <sup>-5</sup>	303000	32800	3880	527	88.0	20.0	2.33	0.973	0.432	0.276
2·10 <sup>-5</sup>	144000	17900	2430	377	71.6	17.9	2.31	0.973	0.432	0.276
5·10 <sup>-5</sup>	53600	7980	1300	239	43.6	14.4	2.28	0.967	0.432	0.276
1·10 <sup>-4</sup>	25300	4320	803	169	42.7	13.6	2.25	0.967	0.432	0.276
2·10 <sup>-4</sup>	11900	2330	496	119	33.9	11.9	2.21	0.967	0.431	0.275
5·10 <sup>-4</sup>	4360	1020	260	74.3	24.6	9.8	2.13	0.962	0.431	0.275
1·10 <sup>-3</sup>	2030	545	158	51.2	19.1	8.4	2.05	0.951	0.430	0.275
2·10 <sup>-3</sup>	940	289	95.6	35.1	14.6	7.0	1.96	0.940	0.428	0.274
5·10 <sup>-3</sup>	336	123	48.5	20.8	10.0	5.4	1.78	0.907	0.424	0.273
1·10 <sup>-2</sup>	153	63.9	28.6	13.8	7.3	4.3	1.62	0.869	0.417	0.270
2·10 <sup>-2</sup>	68.9	32.8	16.5	8.9	5.2	3.3	1.42	0.809	0.404	0.264
5·10 <sup>-2</sup>	23.2	13.1	7.7	4.8	3.1	2.2	1.10	0.694	0.374	0.249
1·10 <sup>-1</sup>	9.8	6.3	4.1	2.8	2.0	1.5	0.84	0.568	0.339	0.236
2·10 <sup>-1</sup>	3.9	2.8	2.0	1.5	1.2	0.9	0.55	0.414	0.317	
5·10 <sup>-1</sup>	0.8	0.7	0.6	0.5	0.4	0.3	0.17			
1	0	0	0	0	0	0	0			

**Table 4.1 Values of Q for different r/h-values**

To find the reference concentration  $c_a$  for the calculation of the suspended load transport Bijker used Eq.(4.56), or:

$$S_b = r v_{bot.layer} c_a \quad (4.77)$$

where:

$r$	thickness of bottom layer	[m]
$v_{bot.layer}$	average velocity in the bottom layer	[m/s]
$c_a$	reference concentration	[-]

The average velocity in the bottom layer follows from integration over the bottom layer thickness of the assumed logarithmic velocity distribution inside the main part of the bottom layer; the part between  $z = 0$  and  $z = ez_0$  is represented by a straight line (see Fig.4.22). It follows that:

$$v_{bot.layer} = 6.34 v_* \quad (4.78)$$

The reference concentration can now be derived from the following equation:

$$c_a = \frac{S_b}{6.34 v_* r} \quad (4.79)$$

In the Bijker approach, values for the bottom layer thickness  $r$  vary from 0.01 m to 0.10 m. He further used the adjusted Kalinske-Frijlink formula (Eq.(4.73)) to find the value for the reference concentration.

With the use of the Rouse/Einstein distribution for the sediment concentration  $c(z)$  and the logarithmic velocity distribution, Bijker followed in fact the Einstein approach for the suspended sediment transport; see formula according to Eq.(4.75).

The main difference between the approaches of Einstein and Bijker is the selection of the height above the bed where  $c_a$  is defined. Bijker used the bottom roughness  $r$  (0.01 – 0.10 m) instead of twice the grain diameter as Einstein did (0.001 – 0.01 m).

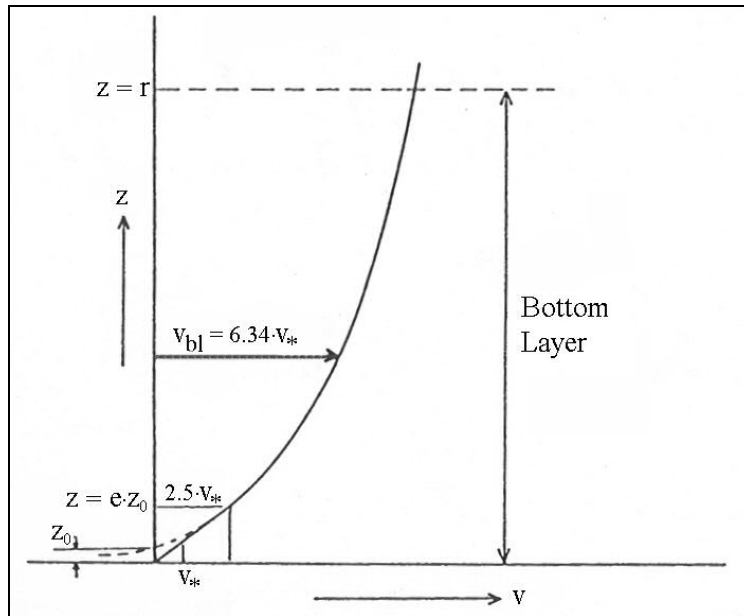


Figure 4.22 Computation of the mean velocity in the bottom layer

#### 4.6.4 Total load transport under currents

The total load transport under currents follows from the summation of  $S_b$  and  $S_s$ . If we use the Bijker formulae, for instance, it follows from Eqs.(4.73) and (4.75) that:

$$S_t = 5 D_{50} v_* \exp \left[ -0.27 \frac{\Delta D_{50} \rho g}{\mu \tau_c} \right] + 11.6 v_* r c_a \left[ I_1 \ln \left( \frac{33h}{r} \right) + I_2 \right] \quad (4.80)$$

Others have developed formulae for the total load transport. An often used formula is that of Engelund-Hansen (1967), which was originally developed for application in rivers (see Eq.(4.81)).

$$S_t = 0.05 v \frac{\tau_c^2 C}{(1-p) \rho^2 g^{2.5} \Delta^2 D_{50}} \quad (4.81)$$

where:

0.05	experimentally derived coefficient	[-]
$v$	depth-averaged velocity	[m/s]
$\tau_c$	bed shear stress under currents	[N/m <sup>2</sup> ]
$p$	voids ratio	[-]

Other formulae exist as well, and most of them generally give reasonable results for river applications. More detailed information can be found in the literature on sediment transport.

## 4.7 Sediment transport by waves

If a wave would be completely sinusoidal and thus perfectly symmetric, the related water motion is able to stir up sediment and generate suspension, but the net transport averaged over a single wave period will be zero by definition. In real cases, however, waves can actually cause transport of sediment.

One mechanism for sediment transport under waves is because of wave asymmetry. It is caused by the non-sinusoidal character of the waves due to higher harmonics in the wave signal. This asymmetry leads to differences in the forward (in the direction of the wave propagation) and the backward direction. Integration over the wave period with these descriptions still gives a zero net velocity. Since sediment transport might be thought to be related to the flow velocity to a power larger than 1, this would mean that more sediment is being moved forward during the wave passage than that is moved backwards. So, although the net movement of water is zero, a resultant movement of sediment remains. The direction of this type of wave asymmetry transport corresponds then with the direction of wave propagation.

Another mechanism is the generation of a (small) net flow by propagating waves even with perfect sinusoidal orbital motion. This is called mass transport or Stokes drift and can be explained as follows. The horizontal movement of a water particle is in general larger higher in the water column than lower in the water column. A water particle under the top of the wave thus moves faster in the direction of wave propagation than a water particle under the trough of the wave runs backward. This makes that the orbital motion is not entirely closed over one wave period: the residual motion is called the Stokes drift. Of course depending on the actual case, the Stokes drift can be up to 0.10 m/s and is directed in the direction of wave propagation.

Along a coastline, with waves propagating perpendicular to the coast, the Stokes drift has to be compensated (otherwise, water is piling up against the coast). This leads to return currents (undertow) close to the bottom in the opposite direction as the Stokes drift. This seaward directed undertow near the bed (in a zone with relatively high sediment concentrations) yields often a seaward directed sediment transport.

The relevancy of Stokes drift related sediment transport is also large in situations with a shallow area with deeper areas behind it. Examples are shallow areas on the outer deltas of coastal inlets, where the Stokes drift is not (entirely) compensated by undertow as the water can flow away at the back of these flats (where often tidal channels are present).

Wave-induced sediment transport plays a role in both cross-shore transport (perpendicular to the coastline: Chapter 7) and longshore transport (parallel with the shoreline: Chapter 6).

## 4.8 Transport by waves and currents combined

### 4.8.1 Introduction

In the case of currents only, the average sediment movement can be large, provided that the current velocities are very high. At open sea, however, the (tidal) currents are often modest in strength. The bed shear stress under tidal currents only is then relatively small, which means that not much sediment will be in suspension, so that transport rates might be low as well.

In the case of waves only, the bed shear stress may be increased significantly. However, since velocities are small, sediment transport rates remain small as well. In most cases, waves and currents are combined along coasts. For instance due to tidal currents and because of the generation of a longshore current by obliquely incident waves along a coastline (littoral drift: Chapter 6).

Various authors have developed methods to calculate the sediment transport under the combined effect of currents and waves. Bijker (1971), for instance, developed a transport formula for a combination of waves and currents, by adjusting a sediment transport formula for currents only. Below we focus on this approach, with the notice that a lot of research has been done and is still going on to find physically more realistic formulations.

### 4.8.2 Bijker approach

Both in the bed load transport formula (Kalinske-Frijlink) and in the description of the sediment concentration distribution (Rouse/Einstein distribution), the bottom shear stress  $\tau_c$  (or the shear stress velocity  $v_*$  which is directly related with  $\tau_c$ ) plays a role, while calculating the sediment transport by *currents only*. Bijker, willing to find a sediment transport formula applicable for the combination of *waves and currents*, followed a quite straightforward approach. He replaced  $\tau_c$  in the formulae simply by  $\bar{\tau}_{cw}$ .

The bottom shear stress under combined waves and currents has been discussed in Section 4.4.4:

$$\bar{\tau}_{cw} = \tau_c \left[ 1 + \frac{1}{2} \left\{ \xi \frac{\hat{u}_0}{v} \right\}^2 \right] \quad (4.47)$$

where:

$\hat{u}_0$	maximum orbital velocity at top of boundary layer	[m/s]
$v$	depth-averaged velocity (!)	[m/s]
$\xi$	combination of various parameters:	[-]

$$\xi = C \sqrt{\frac{f_w}{2g}} \quad (4.48)$$

As partly already discussed in Section 4.6, Bijker modified the Kalinske-Frijlink formula for bed load transport and the Einstein formula for suspended load transport as follows:

- The thickness of the bottom layer (where the bed load transport takes place) is not twice the grain diameter, but equal to the bottom roughness  $r$ ;
- The ripple factor is neglected in the 'transport part' of the Kalinske-Frijlink formula;
- The shear stress in the 'stirring part' of the Kalinske-Frijlink formula is modified to the shear stress according to Bijker under waves and currents:  $\overline{\tau_{cw}}$  (Eq.(4.47)).

This leads to the following bed load transport formula in case of waves and a current:

$$S_b = B D v_* \exp \left[ \frac{-0.27 \Delta D C^2}{\mu v^2 \left[ 1 + \frac{1}{2} (\xi \hat{u}_0 / v)^2 \right]} \right] \quad (4.82)$$

where:

$B$	Bijker coefficient (5, see remarks in Section 4.6)	[-]
$D$	representative particle diameter ( $D_{50}$ )	[m]
$C$	Chézy coefficient	[m <sup>0.5</sup> /s]
$\Delta$	relative density	[-]
$\mu$	ripple factor	[-]

The presence of waves increases the “stirring part” of the sediment transport. It is independent of the wave direction provided that the current velocity is maintained.

Bijker modified the suspended load transport formula by using  $\overline{\tau_{cw}}$  instead of  $\tau_c$ , in calculating the shear stress velocity. This shear stress velocity can be found in the exponent of the concentration distribution according to Rouse/Einstein (Eqs.(4.64) and (4.65)). The shear stress velocity under combined currents and waves becomes:

$$v_{*,cw} = \sqrt{\frac{\overline{\tau_{cw}}}{\rho}} = \sqrt{\frac{\tau_c}{\rho} \left[ 1 + \frac{1}{2} \left\{ \xi \frac{\hat{u}_0}{v} \right\}^2 \right]} \quad (4.83)$$

After substituting the various equations and by using the total Einstein integral term  $Q$  (see Eq.(4.76)), it can be shown that:

$$S_s = 1.83 Q S_b \quad (4.84)$$

This indicates that the suspended sediment transport is directly proportional to the bed load transport. This is not strange as both transport modes are directly coupled via the reference concentration  $c_a$ .

Values of the ratio between suspended sediment and bed load sediment transport ( $S_s/S_b = 1.83 Q$ ) are given in Table 4.2 and plotted in Fig.4.23.

The total transport now follows from the summation of  $S_s$  and  $S_b$ , which yields:

$$S_t = S_b (1 + 1.83 Q) \quad (4.85)$$



r/h	z*=0.00		z*=0.20		z*=0.40		z*=0.60		z*=0.80	
	Q	S <sub>s</sub> /S <sub>b</sub>	Q	S <sub>s</sub> /S <sub>b</sub>	Q	S <sub>s</sub> /S <sub>b</sub>	Q	S <sub>s</sub> /S <sub>b</sub>	Q	S <sub>s</sub> /S <sub>b</sub>
1·10 <sup>-5</sup>	303000	554000	32800	60000	3880	7100	527	964	88.0	161.0
2·10 <sup>-5</sup>	144000	263000	17900	32700	2430	4440	377	689	71.6	131.0
5·10 <sup>-5</sup>	53600	98000	7980	14600	1300	2370	239	438	43.6	98.0
1·10 <sup>-4</sup>	25300	46300	4320	7900	803	1470	169	310	42.7	78.2
2·10 <sup>-4</sup>	11900	21800	2330	4260	496	907	119	218	33.9	62.0
5·10 <sup>-4</sup>	4360	7980	1020	1870	260	475	74.3	136	24.6	45.0
1·10 <sup>-3</sup>	2030	3720	545	998	158	290	51.2	93.7	19.1	34.9
2·10 <sup>-3</sup>	940	1720	289	529	95.6	175	35.1	64.2	14.6	26.7
5·10 <sup>-3</sup>	336	615	123	226	48.5	88.7	20.8	38.1	10.0	18.3
1·10 <sup>-2</sup>	153	280	63.9	117	28.6	52.3	13.8	25.2	7.3	13.4
2·10 <sup>-2</sup>	68.9	126	32.8	60.0	16.5	30.2	8.9	16.3	5.2	9.5
5·10 <sup>-2</sup>	23.2	42.4	13.1	24.0	7.7	14.1	4.8	8.7	3.1	5.7
1·10 <sup>-1</sup>	9.8	18.0	6.3	11.5	4.1	7.5	2.8	5.1	2.0	3.6
2·10 <sup>-1</sup>	3.9	7.1	2.8	5.1	2.0	3.7	1.5	2.8	1.2	2.1
5·10 <sup>-1</sup>	0.8	1.5	0.7	1.3	0.6	1.1	0.5	0.9	0.4	0.7
1	0	0	0	0	0	0	0	0	0	0
r/h	z*=1.00		z*=1.50		z*=2.00		z*=3.00		z*=4.00	
	Q	S <sub>s</sub> /S <sub>b</sub>	Q	S <sub>s</sub> /S <sub>b</sub>	Q	S <sub>s</sub> /S <sub>b</sub>	Q	S <sub>s</sub> /S <sub>b</sub>	Q	S <sub>s</sub> /S <sub>b</sub>
1·10 <sup>-5</sup>	20.0	36.6	2.33	4.26	0.973	1.781	0.432	0.790	0.276	0.505
2·10 <sup>-5</sup>	17.9	32.8	2.31	4.23	0.973	1.781	0.432	0.790	0.276	0.505
5·10 <sup>-5</sup>	14.4	28.2	2.28	4.17	0.967	1.770	0.432	0.790	0.276	0.505
1·10 <sup>-4</sup>	13.6	24.9	2.25	4.11	0.967	1.770	0.432	0.790	0.276	0.505
2·10 <sup>-4</sup>	11.9	21.8	2.21	4.04	0.967	1.770	0.431	0.789	0.275	0.504
5·10 <sup>-4</sup>	9.8	17.9	2.13	3.90	0.962	1.760	0.431	0.788	0.275	0.504
1·10 <sup>-3</sup>	8.4	15.3	2.05	3.76	0.951	1.740	0.430	0.787	0.275	0.503
2·10 <sup>-3</sup>	7.0	12.8	1.96	3.58	0.940	1.720	0.428	0.784	0.274	0.502
5·10 <sup>-3</sup>	5.4	9.8	1.78	3.26	0.907	1.660	0.424	0.776	0.273	0.499
1·10 <sup>-2</sup>	4.3	7.8	1.62	2.96	0.869	1.590	0.417	0.763	0.270	0.494
2·10 <sup>-2</sup>	3.3	6.0	1.42	2.59	0.809	1.480	0.404	0.740	0.264	0.483
5·10 <sup>-2</sup>	2.2	4.0	1.10	2.02	0.694	1.270	0.374	0.684	0.249	0.456
1·10 <sup>-1</sup>	1.5	2.7	0.84	1.53	0.568	1.039	0.339	0.620	0.236	0.432
2·10 <sup>-1</sup>	0.9	1.6	0.55	1.01	0.414	0.758	0.317	0.548		
5·10 <sup>-1</sup>	0.3	0.6	0.17	0.48						
1	0	0	0	0						

Table 4.2 Values for Q and S<sub>s</sub>/S<sub>b</sub> for different r/h-values

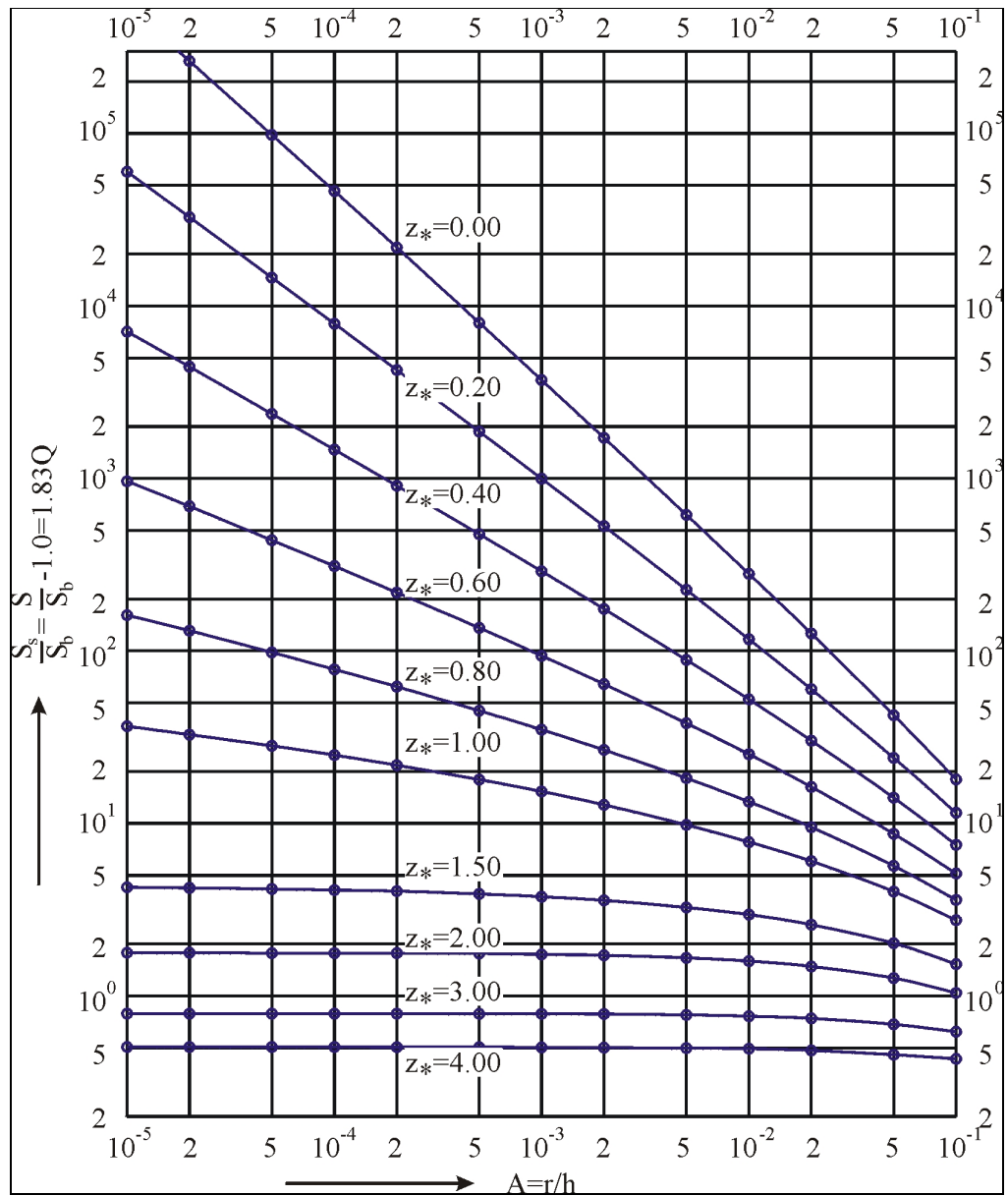


Figure 4.23 Suspended sediment transport parameters

### Some remarks

- With the present approach the sediment transport can only be calculated for a unit plane (from bed to water surface) which is orientated more or less perpendicular to the (net) current direction. E.g. for a plane which is perpendicular to the direction of a tidal current.
- In the bed load transport formula of Kalinske-Frijlink, the shear stress under currents is adapted to that under combined currents and waves by using the time-averaged parameter  $\overline{\tau_{cw}}$ . It would probably be better to first put the shear stress  $\tau_{cw}$  in the formula and then average the entire formula.
- An implicit assumption in the Bijker approach is that the logarithmic velocity distribution over the water depth (which is a fair assumption for a current only case), is also true for the velocity distribution (of the net current part of the total water movement) under waves and currents. Actual measurements have shown that this is not correct in many cases. (It is however for the time being a straightforward and useful assumption.)
- The concentration profile is determined by  $z_*$ , which is directly related to the sediment mixing coefficient  $\epsilon_s$  for which a parabolic distribution has been assumed. In the adapted form, including the wave influence, an increased shear velocity indicates an increased variation in  $\epsilon_s$ . So also in the combination of waves and currents it is assumed that the distribution of  $\epsilon_s$  is still parabolic. This is questionable.
- The ripple factor is not adjusted for the influence of waves, which is questionable as well.
- The value for the Bijker coefficient B (so far equal to 5) has received much discussion. In some actual applications the value of B is changing; e.g. from 2 well outside the breaker zone to 5 inside the breaker zone.

In spite of the above (critical) remarks, the Bijker formula performs rather well in coastal engineering practice.

In Example 4.6 (next pages) the sediment transport is calculated for a case without, and with waves. Waves are according to this example indeed quite effective in yielding rather high transport rates. In coastal engineering practice one cannot neglect the effect of waves.

**Example 4.6***Input parameters:*

Water depth:	$h$	=	3 m
Roughness height:	$r$	=	0.06 m
Average flow velocity:	$v$	=	1 m/s
Particle sizes:	$D_{50}$	=	200 $\mu\text{m}$ ( $w = 0.025$ m/s)
	$D_{90}$	=	300 $\mu\text{m}$
Wave height:	$H$	=	1.18 m
Wave period:	$T$	=	8 s

*Required:*

Sediment transport current only and sediment transport current and waves  
(Bijker formula)

*Current only:*

Total transport is bed load plus suspended load.

We apply Eq.(4.73) for the calculation of the bottom transport:

$$S_b = 5 D_{50} v_* \exp \left[ \frac{-0.27 \rho g \Delta D_{50}}{\mu \tau_c} \right] \quad [\text{m}^3/\text{m per s}] \quad (4.73)$$

Apart from the given and usual parameters,  $v_*$ ,  $\Delta$  and  $\tau_c$  must be calculated.

$$\begin{aligned} C &= 50 \text{ m}^{1/2}/\text{s} \\ C_{90} &= 91.4 \text{ m}^{1/2}/\text{s} \\ \tau_c &= 3.9 \text{ N/m}^2 \\ \mu &= (C/C_{90})^{1.5} = 0.405 \end{aligned}$$

Filled out in Eq.(4.73) yields as bottom transport:  $S_b = 0.000036 \text{ m}^3/\text{ms}$ .

The suspended transport, using Fig.4.23 or Table 4.2, is a function of  $A$  ( $= r/h$ ) and  $z_*$ .  $A = 0.02$ ;  $v_* = \sqrt{\tau_c / \rho} = 0.063$ ;  $z_* = w/(\kappa v_*) \approx 1$ .

Using Fig.4.23:  $S_s \approx 6 S_b = 0.000216 \text{ m}^3/\text{ms}$ .

$S_t = S_b + S_s = 0.000252 \text{ m}^3/\text{ms}$ . [In easily understood units:  $0.9 \text{ m}^3/\text{m per hour}$ .]

*Current and waves:*

Now we must apply Eq.(4.82) for the calculation of the bottom transport.

$$S_b = 5 D_{50} v_* \exp \left[ \frac{-0.27 \Delta D_{50} C^2}{\mu v^2 \left[ 1 + \frac{1}{2} (\xi \hat{u}_0 / v)^2 \right]} \right] \quad (4.82)$$

(continuation next page)

**Example 4.6 (a) Sediment transport by current and by current and waves**

Eq.(4.82) can be rewritten in the form:

$$S_b = 5 D_{50} v_* \exp \left[ \frac{-0.27 \rho g \Delta D_{50}}{\mu \tau_{cw}} \right]$$

$\overline{\tau_{cw}}$  for this case was already calculated in Example 4.4;  $\overline{\tau_{cw}} = 15.2 \text{ N/m}^2$ .

$$S_b = 0.000054 \text{ m}^3/\text{ms}.$$

Again the suspended sediment transport can be found using Fig.4.23, but now with a different (smaller)  $z_*$  value.  $v_* = \sqrt{\overline{\tau_{cw}} / \rho} = 0.123 \text{ m/s}$ ;  $z_* \approx 0.5$ .

In this case  $S_s \approx 25 S_b = 0.001350 \text{ m}^3/\text{ms}$ .

$$S_t = S_b + S_s = 0.001404 \text{ m}^3/\text{ms}. \text{ [Or } 5.1 \text{ m}^3/\text{m per hour.]}$$

*Conclusion:*

By superimposing waves in this example the total sediment transport increases with a factor  $\approx 5.6$ . Waves are indeed very effective in sediment transport. Especially in the case currents plus waves, the contribution of the bottom sediment transport to the total transport is only small ( $\approx 4\%$ ).

#### Example 4.6 (b) Sediment transport by current and by current and waves

### 4.8.3 Other formulae (currents and waves)

In the preceding sections we have discussed a sediment transport formula (Bijker-formula), which is meant to quantify the sediment transport rate through a given unit plane. For the solution of many real life coastal engineering problems a proper insight in such sediment transport rates is helpful. The approach was based on the fair assumption that the sediment transport through such a unit plane might be generally described with the  $S = v \cdot c$  concept. Proper descriptions of the distribution of both the velocity and the sediment concentration over the water depth are then required to achieve at the end of the calculation a reliable answer. Many, often quite uncertain parameters have to be known, before a sediment transport computation can be made. The final result is at the best a fair estimate of the real sediment transport rate.

Results of sediment transport computations compared with actual measurements, not seldom show large discrepancies. A factor 2 - 5 too large or too small, is not exceptional.

Many researchers are trying to improve the computation results, for instance by proposing better and more reliable descriptions of various elements in a formula. At the other hand also simple 'black box' formulae are still used as a help to resolve practical problems in coastal engineering. (Probably also based on the idea that more complicated computations with complex models do not yet yield the real results for

the time being.)

In this section we will discuss some other formulae basically starting from a  $S = v \cdot c$  concept and some more 'black box' formulae.

### Formulae based on a $S = v \cdot c$ concept

The Van Rijn formula [Van Rijn (1993); (2000)] is a good example of a formula (in fact: a formulae suite) based on the  $S = v \cdot c$  concept. The last few years this formula is increasingly used. Much more parameters than for the Bijker-formula have to be known in advance. For many parameters Van Rijn has proposed best estimates or rules of thumb to calculate the relevant parameter.

In case of the combination of waves and currents, the shape of the mixing coefficient for the sediment over the water depth (in order to calculate  $c(z)$ ) differs from the shape of diffusion coefficient (in order to calculate  $v(z)$ ). From a physical point of view this might be strange.

However, the proof of the pudding is in the eating: with the Van Rijn formula often fair results are achieved in actual coastal engineering cases.

The various elements of the Van Rijn formula are not given here (a few pages with formulae); they can be found in literature.

The Van Rijn (and Bijker) formula are implemented in complex morphological computation models (see Chapter 8); amongst others in complex models developed by Delft Hydraulics.

Similar institutes like Delft Hydraulics in The Netherlands, are present in some other European countries. (E.g. *DHI Water & Environment in Denmark* or *Electricité de France, Laboratoire d'Hydraulique* in France and *HR Wallingford* in the United Kingdom.) Such institutes have often developed their 'own' sediment transport formula and apply that formula in their consulting work. (Often they trust the results of their 'own' formula more than the results of other formulae). The result of this is that for the time being many different formulae exist and are used; all pretending to calculate the right answer. Davis *et al.* (2002) show some striking results of intercomparison exercises with various formulae.

### 'Black box' formulae

In coastal engineering and coastal morphology applications still often more or less black box sediment transport formulae are used. The resulting sediment transport is then assumed to depend on only a few physical parameters. The CERC formula and the Bailard formula [Bailard (1981), (1982); Bailard and Inman (1981)] are examples. The notion black box is certainly not used here as some kind of disqualification. Like every 'more sophisticated' formula, also a black box formula has to prove itself. If the ultimate results are fair, then also a black box formula can be used (with care) as a tool in the solution of practical problems.

## 4.8.4 Phase-lag and time-lag effects

Sediment transport formulae have been developed for the combined effect of waves and currents (for both bed load and suspended load transport); such as Bijker (1971), van Rijn (2000) and Bailard. These formulae all have been developed for local transport, i.e. the sediment movements are determined by the local hydraulic conditions.

It is then assumed that the result of the computation refers to a steady state situation. That means that the hydraulic conditions last long enough, and that the bottom conditions in the vicinity are all the same, so that an equilibrium situation with respect to the sediment transport has been achieved. Such a computation result is often referred to as the sediment transport *capacity*.

The assumption that the local transport equals the local capacity is not always true in real life cases. Due to phase-lag and time-lag effects the local transport can be larger or smaller than the local transport capacity. E.g. De Vriend *et al.* (1989) discuss the relevance of not locally determined transport for a tidal flat in the Eastern Scheldt Estuary (Galgeplaat). In order to simulate the observed morphological behaviour of this flat, the use of an adapted suspension transport formulae appeared to be necessary.

Adapted suspension transport formulae have been developed which account for phase-lag and time-lag effects [e.g. Van Rijn (1989) and Gallapatti and Vreugdenhil (1985)]. To estimate the importance of time- and space-lag effects the following formulae can be used [Katapodi and Ribberink (1988)]:

$$L_a = \frac{vh}{w} \quad (4.86)$$

and

$$T_a = \frac{h}{w} \quad (4.87)$$

in which  $L_a$  and  $T_a$  are the so-called adaptation length and adaptation time,  $h$  is the water depth,  $v$  is the average flow velocity, and  $w$  the fall velocity of the sediment.

Increasing values for the adaptation length and time will increase the importance of time- and space-lag. Especially in tidal channels, lag can play an important role (large values of  $h$ ). The same may be true for shallower areas with relatively fine material (small values of  $w$ ).





# 5 Coastal Transport Modes

## 5.1 Introduction

From the examples in Chapter 3 it has become clear that sediment transports due to waves and currents can be seen as important phenomena which are at the basis of day to day coastal engineering issues. In Chapter 4 some general aspects have been dealt with in order to quantify sediment transport rates. A proper insight in the sediment transports involved is often necessary to understand the physics 'behind' a coastal engineering issue. If it regards a coastal engineering problem, also such a proper insight is needed to judge the quality of counter measures to resolve the problem.

Depending on the 'question' related to coastal morphology which has to be answered, or depending on the coastal engineering 'problem' which has to be resolved, it is often useful to use different parameters related to sediment transport. This also refers to the scale of the question / problem involved (see also Section 5.2). E.g. to understand (and at the end to predict) the behaviour of a breaker bar in a cross-shore profile during a storm, calls indeed for a quite different insight in the sediment transports involved, than to understand the long term behaviour of an entire tidal basin.

From Chapter 4 it became clear that, given values for parameters like  $H_{sig}$ ,  $T$ ,  $h$ ,  $D_{50}$  and  $v$ , sediment transport rates ( $S$  in  $m^3/m$  per s) can in principle be calculated with the help of various formulae.

[Although the outcome of the calculations results in one single figure, one has to realise that the 'quality' of the formula as used, and the 'quality' of the input parameters in fact yield as outcome an estimate (a best estimate) rather than the 'truth'.]

To get useful quantities for the understanding and for the solution of real life coastal engineering problems,  $S$  must often be integrated over time (from s to e.g. year) and over length (e.g. from running m to covering an entire surf zone).

Sometimes (again depending on the problem) it is useful to make a distinction between sediment transport rates along a coast and perpendicular to the coast. Section 5.3 gives some reasoning for that distinction.

Understanding of changes in coastal morphology is apparently a key issue in coastal morphology and coastal engineering. Natural or man-induced changes in coastal morphology, which is relevant to the coastal engineer, depend on the spatial and temporal fluctuations in the sediment transport rates. If the net sediment flux from a certain area is negative, meaning that the outgoing sediment flux is larger than the incoming one, then the bottom will 'deliver' the sediment deficit. (We assume that the bottom is erodible.) If the bottom balances the sediment deficit indeed, then a lowering of the bottom occurs (erosion). This may continue until a new situation is reached where sediment input and output is in balance again.

Often, this process towards a new equilibrium takes such a long period of time, that the space-varying sediment transport pattern has already changed again. This principle where the bottom is constantly adjusting to balance momentary spatial differences in the sediment transport, is the basis for coastal morphodynamics.

Besides spatial differences in sediment transport, also time-variations are important for coastal morphology. Today changes in coastal morphology reflect often the historic adaptation process towards new equilibrium. Since such an equilibrium is never static, coastal morphology is always changing on various time and spatial scales. So, for the 'translation' of sediment transport processes towards coastal morphology, it is important to understand the importance of scales (see Section 5.2).

## 5.2 Discussion on scales

A well-known problem in coastal engineering is that morphological developments act on different time scales and spatial scales. Mutual interactions between scales do occur, on their turn with own time and spatial scales. In other words: everything depends on everything. In the analysis of a specific coastal problem, it is often useful to break down the problem in appropriate time and spatial sales.

The spatial scale is generally coupled to the dimensions (in m) of a particular morphological element. (*In fact it is not really a scale, like the scale of a map, but a notion to indicate the extent of the element.*) Examples of spatial scales are:

- A whole tidal inlet system, comprising of a flood basin, an inlet gorge and an outer delta. Dimensions vary between 50 to 700 km<sup>2</sup>. Morphological changes on such a large spatial scale generally take decades to centuries (e.g. the gradual migration of the entire inlet system).
- Large tidal channels and sand banks. Typical surface dimensions are 5 to 20 km<sup>2</sup>, while significant changes generally take place within years to decades (such as the landing of the sand bank 'De Onrust' on the south coast of Texel around 1910).
- Smaller tidal channels and bars, with typical surface dimensions of maximum several km<sup>2</sup>. Significant morphological changes occur within years (such as the development and landing of the 'Bornrif' sand bar on the west coast of Ameland in the Nineties of last century).
- Accretion and erosion patterns at both sides of a port entrance, built with the help of long breakwaters. Several kilometres.
- Smaller bed forms like ripples and (bottom) dunes. The related spatial scales further go down to metres or less, with relevant time periods in which significant changes occur of less than days.

A time scale is generally interpreted as the period of time (e.g. in years) required for characteristic morphological developments. Some researchers relate the time scale to the total duration that a morphological system needs to reach a new equilibrium situation once it has been distorted (by nature or by man). Equilibrium in this sense means that the overall sediment balance of the morphological unit is maintained (no erosion and no accretion).

If a morphological system is out of equilibrium, it is felt that morphological adjustments (because of sediment transports) start to take place immediately; the morphological system reacts to disturbances.

The rate of morphological adjustment has been observed to depend on the magnitude of the still existing disruption (the difference between the actual situation and the equilibrium situation).

Sometimes, morphological changes are induced very abrupt, such as the closure of parts of a tidal basin. Other changes take place more slowly, such as the response of the shape of a cross-shore profile to global sea level rise. Usually, the morphological response to (sudden) changes shows a certain variation with time. The process of morphological response will be fast at first and decelerates when the new equilibrium situation is approached. Often such a morphological adjustment process can be approximated exponentially:

$$V(t) = V_{old} + (V_{new} - V_{old}) \left(1 - \exp\left(-\frac{t}{\tau}\right)\right) \quad (5.1)$$

where:

$V(t)$	characteristic volume in morphological unit at time t	[m <sup>3</sup> ]
$t$	time after the distortion	[year]
$V_{old}$	the (equilibrium) volume before distortion	[m <sup>3</sup> ]
$V_{new}$	the new equilibrium volume	[m <sup>3</sup> ]
$\tau$	morphological time scale	[year]

E.g. Stive *et al.* (1986) and Eysink (1990) use this type of approximation to describe adaptation processes of units with large scales. From Eq.(5.1) it can be derived that the morphological time scale  $\tau$  can be seen as the time that would be required to reach equilibrium, if the initial 'rate of morphological adjustment',  $dV/dt$  at  $t=0$ , would continue during a time  $t = \tau$ :

$$\tau = \frac{(V_{new} - V_{old})}{\left(\frac{dV}{dt}\right)_{t=0}} \quad (5.2)$$

The character of Eq.(5.1) also reflects that within a time  $t$  equal to the morphological time scale already 63 % (namely:  $1-1/e$ ) of the 'way' to reach new equilibrium (namely:  $V_{new} - V_{old}$ ) has been covered.

Implicitly sediment transports rates have been quantified with the help of Eq.(5.1); the term  $dV/dt$  reflects that. It is clear that this type of quantification of sediment transports is quite different from the approach followed in Chapter 4.

Examples of morphological time scales are given in Table 5.1. These examples are related to the observed morphological changes of the outer deltas of several Dutch tidal inlets after abrupt changes in their flood basins. The figures support the general idea that morphological time scales are directly coupled to the spatial scales of the morphological units. This is also illustrated in Table 5.2.

Morphological unit	abrupt change closure of:	surface and flood basin after abrupt change [km <sup>2</sup> ]	Observed morphological time scale [years]
Outer delta Haringvliet	Haringvliet (1970)	120	11
Zoutkamperlaag	Lauwerszee (1969)	200	17
Outer Delta Marsdiep	Zuiderzee (1932)	680	32

**Table 5.1 Examples of morphological time scales**

Barrier system	1,000 - 10,000 yr
Whole backbarrier area	1,000 - 10,000 yr
Barrier chain	1,000 - 10,000 yr
Barrier island	1,000 yr
Tidal system	1,000 yr
Estuary	100- 10,000 yr
Aeolian dune-complex	100 - 1,000 yr
Shore	100- 1,000 yr
Giant subtidal dune	100-?yr
Backbarrier drainage area	100- 1,000 yr
Backbarrier channel system	10- 1,000 yr
Ebb-tidal delta	10- 1,000 yr
Tidal flat system	10- 1,000 yr
Inlet channel	10- 1,000 yr
(Inter)tidal flat	10- 1,000 yr
Tidal marsh	10- 1,000 yr
Creek system	10- 1,000 yr
Marsh shoal system	10- 1,000 yr
Barrier shoal	10- 1,000 yr
Ebb-delta shoal	10- 1,000 yr
Backbarrier channel	10- 100 yr
Backbarrier tidal shoal	10- 100 yr
Channel bend	10- 100 yr
Creek	10- 100 yr
Aeolian dune	10- 100 yr
Saw tooth bar	10- 100 yr
Swash bar	10 yr
Creek bend	1 - 100 yr
Outer channel	1 - 100 yr
Breaker bar	1-10yr
Marginal flood channel	1-10yr
Gully	1-10yr
Mussel bed	1 yr
Ebb- & flood chute	1/2 yr - 10 yr
Subtidal megaripple	neap-spring cycle - 1 yr
Intertidal megaripple	neap-spring cycle - 1 yr
Internal bioturbation	h-1 yr
Marsh shoal layer	h - neap-spring cycle
Hummock	h
Current ripple	minute - neap-spring cycle
Wave ripple	minute - ebb-flood cycle
Aeolian ripple	minutes
Surface bioturbation	seconds - ebb-flood cycle
Faeces & pseudo-faeces*	seconds - ebb-flood cycle

\* Merely existence time outside musselbeds, not active, but passive

**Table 5.2 Order of magnitude of time spans, during which sedimentary features are active [from Oost (1995)]**

Morphological changes on a certain spatial scale can be an autonomous development on that particular scale, or it can be a response to changes on a larger spatial scale. This principle is illustrated in Fig.5.1. The 'circles' stand for morphological developments on various spatial scales. The largest circle illustrates, for instance, the migration of an entire tidal inlet along a barrier coast, or the sudden closure of a part of a flood basin. Within the largest circle smaller circles are drawn. These smaller circles stand for morphological developments of various elements within the larger system.

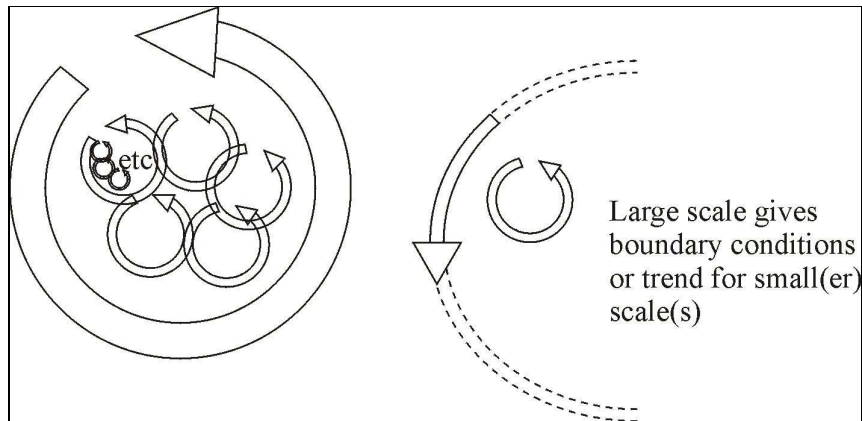


**Figure 5.1 Different scales**

If in the previous example the largest circle refers to the sudden closure of a part of a tidal basin, the smaller circles refer for instance to the migration of a tidal channel on the outer delta, or to the attachment of a sand bank on the barrier coastline. Within these smaller circles even still smaller circles may occur.

The essence of the circle-idea is that morphological changes on the larger scale might be considered to take place more or less independently from the morphological changes on the smaller spatial scales. And, the other way around, that morphological changes on the smaller spatial scales can be examined and analysed without considering the entire morphological evolution on the larger spatial scale. This latter is of course only true as long as the tendencies from the larger scale are being incorporated in the analysis. Conclusions for coastal systems are only valid within the time and spatial scales of that particular system.

### 5.3 Coastal transport modes

Sediment transport in the coastal zone is different from sediment transport in for instance rivers. The reason for this is mainly that in coastal environments short-term fluctuations in the flow conditions become important. In Chapter 4 it was explained how for instance Bijker approached this problem by adjusting the bed shear stress under currents to account for the effect of waves. In general, the net local (thus time-averaged) sediment transport rate through a vertical plane with unit width with an

arbitrary orientation, should be computed from the basic equation Eq.(5.3). In this equation the  $x$ -axis is taken perpendicular to the plane in consideration.

$$S(x) = \frac{1}{nT} \int_{t=0}^{nT} \int_{z=0}^{\eta(x,t)} v(x, z, t) c(x, z, t) dz dt \quad (5.3)$$

where:

$S$	$x$ -component of the net transport	$[m^3/m/s]$
$v$	$x$ -component of the velocity	$[m/s]$
$c$	the sediment concentration	$[-]$
$x$	axis perpendicular to chosen plane	$[m]$
$t$	time	$[s]$
$T$	wave period	$[s]$
$z$	vertical ordinate with respect to $z = 0$ at the (sand) bottom	$[m]$
$\eta$	instantaneous water level	$[m]$
$n$	sufficiently high number	$[-]$

In this formulation  $v(x, z, t)$  refers to the component of the total velocity perpendicular to the plane in consideration. This component indeed contributes to the transport. The velocity component perpendicular to the  $x$ -axis does not contribute to the transport through the plane; the particles transported by that component 'shear' along the plane as considered.

Note that in this formulation already is assumed that the velocity of suspended sediment particles corresponds with the velocity of the fluid particles. Because of the often small mass of the particles this assumption is true to a first approach.

For the solution and elaboration of this equation, one should be able to compute or to describe the time and space variation of both the velocity and sediment concentration properly.

Since no detailed knowledge on these fluctuations [e.g. with respect to the velocity in randomly breaking waves, but especially for  $c(x, z, t)$  under all conditions] is present yet, some simplifications have to be made. Therefore, in the next section this basic expression, viz. Eq.(5.3), is studied in more detail in order to identify different contributions to the net transport rate and, ultimately, to make some reliable simplifications. (Cf. making a distinction between so-called longshore and cross-shore transport.)

## General considerations

The expression for the net sediment transport  $S(x)$  at a particular position  $x$ , can be simplified to:

$$S(x) = \int_h s(z) dz \quad (5.4)$$

in which the mean (time-averaged) transport  $s(z)$  refers to a certain elevation  $z$  above the bottom.

This time-averaged transport rate  $s(z)$  can basically be described by the mean (time-averaged) magnitude of the product of an instantaneous horizontal velocity  $v(t)$  and an instantaneous sediment concentration  $c(t)$  as occurs at the specific level  $z$  of interest, according to:

$$s(z) = \overline{v(t) c(t)} \quad (5.5)$$

in which the overbar denotes time-averaging with an averaging time based on the lowest frequency of the signals involved (actual wave period). Both time functions can be split up into a mean (denoted by an overbar) and a fluctuating part (e.g. orbital motion in case of velocity;  $\tilde{v}$  added) according to:

$$v(t) = \bar{v} + \tilde{v} \quad (5.6)$$

and:

$$c(t) = \bar{c} + \tilde{c} \quad (5.7)$$

[In Eqs.(5.6) and (5.7) only two terms are taken into account; a mean part and a fluctuating part. The fluctuating part is in that case at the time scale of the wave period. To be complete Eqs.(5.6) and (5.7) could be extended with additional terms representing fluctuations at turbulence scale.]

The net transport rate  $s(z)$ , according to Eq.(5.5), can be elaborated further as:

$$s(z) = \underbrace{(\bar{v} + \tilde{v})(\bar{c} + \tilde{c})}_{(1)} = \underbrace{\bar{v}\bar{c} + \bar{v}\tilde{c} + \tilde{v}\bar{c} + \tilde{v}\tilde{c}}_{(2)} = \underbrace{\bar{v}\bar{c} + \tilde{v}\tilde{c}}_{(3)} \quad (5.8)$$

Since the mean value of  $\tilde{v}$  and  $\tilde{c}$  equals zero by definition, the second and third term of part (2) in Eq.(5.8) become zero, so that part (3) remains.

Consequently, the net transport at a certain level above the bottom consists out of two contributions, namely a mean component of time-averaged velocity times time-averaged concentration and a more complex correlation component, thus:

$$\begin{aligned} - \text{mean component} & \quad s(z)_{mean} = \bar{v}\bar{c} \\ - \text{correlation component} & \quad s(z)_{corr} = \overline{\tilde{v}\tilde{c}} \end{aligned}$$

The mean component is sometimes also called the current related component. The correlation component in case of waves is mainly because of the effect of fluctuations due to orbital motion; this component is consequently often called the wave related component of the sediment transport.

For a proper quantification of sediment transports through arbitrary planes, both the mean component (current related) and the correlation component (wave related) must be determined and taken into account. [Notice that Eq.(5.8) only holds for level  $z$  above the bed. By applying Eq.(5.4) the total suspended sediment transport is achieved.]

A still big 'problem' in coastal sediment transport quantification is that the correlation component is very difficult to determine. It especially calls for a proper description of  $\tilde{c}$  (concentration as a function of time; wave period scale; at various levels above the bed). At the moment no reliable calculation methods are available to calculate  $\tilde{c}$  for arbitrary conditions (see also Fig.4.18).

Next it makes sense to make a distinction in the direction of sediment transport one likes to describe. In some real life cases, one is mainly interested in the sediment transport along the coast; longshore transport. In other cases the problem to be resolved calls for a proper description of the cross-shore sediment transport (see Fig.5.2 for a sketch).

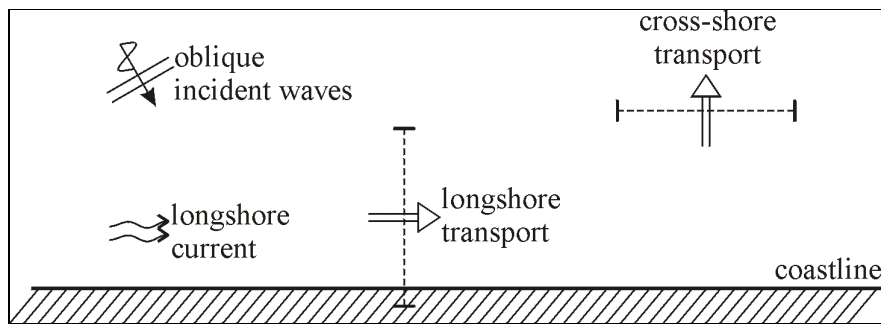


**Figure 5.2 Distinction between longshore and cross-shore transport**

### Longshore transport

If we like to describe longshore sediment transport the  $x$ -axis as was used in Eq.(5.3) must be directed parallel to the coast. The factor  $v(x,z,t)$  in Eq.(5.3) refers in that case to the velocity components parallel to the coast. Especially in the area not too far from the shoreline the tidal and/or wave driven currents are parallel to the shoreline and can be assumed to be constant at the time scale of a number of wave periods. (At deeper water in open sea it is not for sure that the currents are parallel to the shoreline.)

Due to refraction the angle of the wave crests with the orientation of the coast (or the angle between the wave direction and the shore normal) is in most cases rather small in shallow water. That means that the component of the orbital motion in the  $x$ -direction is also rather small. The fluctuations of  $v(x,z,t)$  with time are consequently rather small. The correlation or wave related contribution to the total suspended sediment transport might then be neglected. Only the current related contribution to the sediment transport remains. This simplifies a reliable description of longshore sediment transport to a large extent. We can stick to a proper description of the time-averaged sediment concentration distribution over the water column.

Although our insight in  $\overline{c(z)}$  distributions over the water depth in wave and current cases for arbitrary boundary conditions, is still far from perfect, it is far better than our insight in  $c(z,t)$  distributions.

Longshore sediment transport due to waves and currents is thus rather 'easy' to be described according to this approach.

### Cross-shore transport

If we like to describe cross-shore sediment transports (onshore or offshore transport) the  $x$ -axis as was used in Eq.(5.3) must be directed perpendicular to the coast. The factor  $v(x,z,t)$  in Eq.(5.3) refers in that case to the velocity components perpendicular to the coast.

Longshore currents (tidal and/or wave driven currents) do not contribute to the factor  $v(x,z,t)$ . What certainly remain are the fluctuations in velocity due to the orbital motion of the waves. Due to refraction in this case the orbital motion crosses almost perpendicularly the plane where we like to describe the sediment transport. The wave



related contributions cannot be neglected and must be taken properly into account for a reliable description of the cross-shore sediment transport. That considerably complicates a proper description of cross-shore sediment transport.

Although tidal and/or wave driven longshore currents do not contribute to time-averaged components of  $v(x,z,t)$ , still time-averaged velocity components might occur in a direction perpendicular to the coast due to wave action. While in e.g. a simple linear wave theory no net currents through a vertical plane are predicted (the wave height is assumed to be infinitively small in this theory), in reality, with a given wave height, time-averaged currents appear in the water column. (See also Section 4.7.) Looking at a vertical plane a mass transport towards the coast takes place in the part between wave crest and wave trough, and in a two dimensional case (like in a laboratory wave flume), the same mass of water has to return to the sea again. In the lower part of the water column this results in a so-called undertow or return flow. (See Fig.5.3.) In non-breaking waves the undertow is rather small (but cannot be neglected); in breaking waves the mass transport towards the coast might be quite large, resulting in rather large undertow velocities.

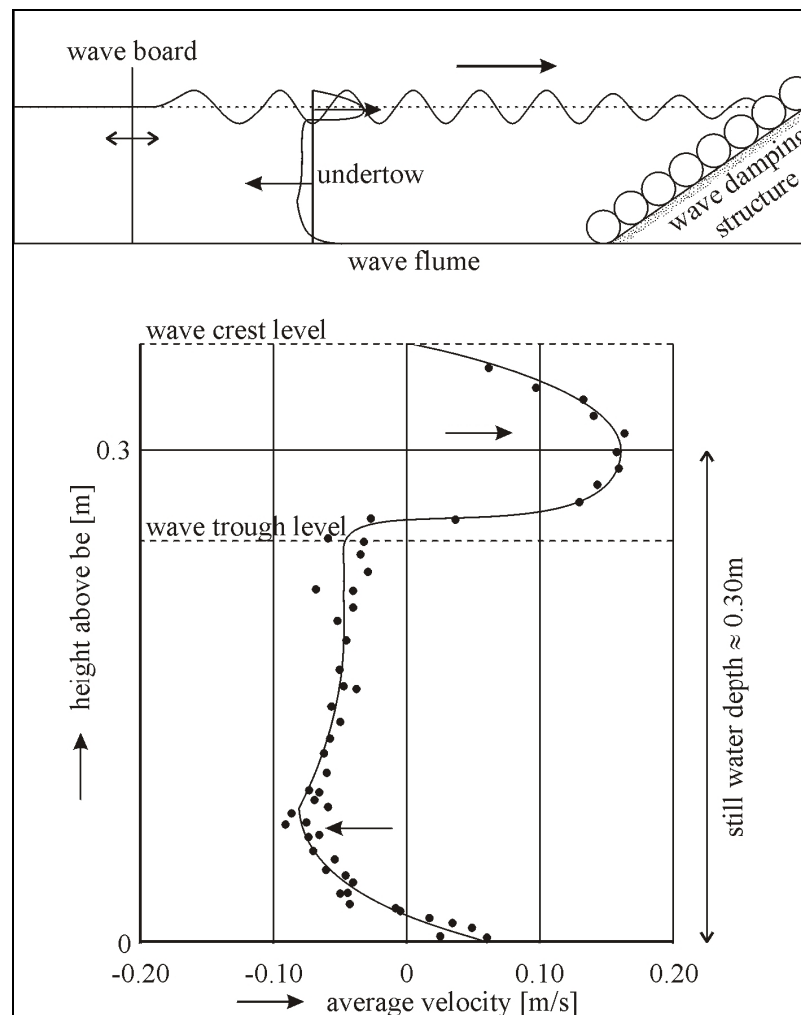


**Figure 5.3 Measured velocities under a propagating wave**

So for a proper description of the cross-shore sediment transports, current related and wave related components must be taken into account. The fact that we are hardly able to quantify the wave related component, considerably complicates a proper description. See also Chapter 7.

### Strategies to component assessment

Especially for a proper description of cross-shore sediment transport due to waves and currents, both the current related and wave related contributions must in principle be taken into account. Of course it is relevant to know the possible quantitative relationship between both contributions. There are several methods by which one can get some insight in the relative importance of the transport components, viz.:

- Using analytical and mathematical approximations;
- Conducting detailed intra-wave measurements;
- Comparing measured transport rates with a computed contribution based on the current related transport.

Some preliminary approaches to assess the contributions to the net transport rate by using analytical and mathematical approximations will be elaborated in the next Chapters 6 (longshore transport) and 7 (cross-shore transport).

With respect to the above second method, some results are available for neat laboratory conditions [Chen (1992); Ribberink and Chen (1993); Al-Salem (1993); Dohmen-Janssen (1999)].

In the third approach, the mean component to the transport rate  $S_{mean}$  is computed from measured time-averaged  $\overline{v(z)}$  and  $\overline{c(z)}$  signals directly and subsequently compared with measured  $S$  values. It is assumed that any (systematic) discrepancy in the outcomes of computations and measurements thus must be due to the effect of the depth-integrated correlation component  $S_{corr}$ .

In many cases for cross-shore sediment transport quantification, a quite confusing result is achieved. In some cases the wave related contribution is apparently small compared to the current related contribution. In other cases the wave related part is of the same order of magnitude compared to the current related part. Also with respect to the direction of the wave related sediment transport some confusion exists. Sistermans (2002) reports the results of a series of careful tests in a laboratory wave flume (irregular waves with a following current; horizontal bottom). In his tests the direction of the wave related sediment transport turned out to be opposite to the direction of the current related sediment transport. [The (absolute) magnitude of the wave related contribution turned out to be approximately 1/3 of the current related sediment transport.]

Indeed, a lot of research is still necessary to clarify these aspects.

# 6 Longshore transport

## 6.1 Introduction

Littoral transport is sediment transport that occurs in the littoral zone, i.e. the zone of the sea nearby the coastline. The definition is not very clear but includes certainly the surfzone. Although the subdivision is somewhat artificial, one generally speaks of cross-shore transport (i.e. perpendicular to the coastline and the depth contour lines) and longshore transport (i.e. parallel to the coastline and the depth contour lines). Changes in cross-shore sediment transport are responsible for fluctuations in the coastal profile: sediment is being moved in onshore and offshore direction principally maintaining the sediment balance of the entire cross-shore profile. Sediment moved by longshore transport, on the other hand, may actually lead to negative (erosion) or positive (accretion) sediment balances along a certain stretch of coastline. This only happens if there is a so-called gradient in the longshore sediment transport ( $dS/dx \neq 0$ ).

Littoral transport is initiated and maintained by hydrodynamic forces. Particularly (breaking) waves, are very effective in increasing the bed shear stress, so that sediment particles can be stirred up and be brought into suspension. Local currents actually transport the stirred and suspended sediment particles. Local currents can be generated by wind forces, density-gradients, tides or by progressive waves. Breaking waves which enter a shoreline under a certain angle (oblique incident waves) are very effective in generating a longshore current. The basic principles of such hydrodynamic forcing of sediment transport in the littoral zone, is discussed in Section 6.2.

Next, in Section 6.3, various longshore transport formulae are presented (in particular the CERC and Bijker formulae).

Variations in longshore transport on various time and spatial scales, natural or man-induced, will cause the position of the coastline to constantly adjust. This may interfere with human interests (for instance if erosion of the coastline is threatening the stability of houses), in which case we might speak of a coastal ‘problem’. Examples of coastline changes and possible related problems are discussed in Section 6.4.

## 6.2 Longshore current

### 6.2.1 Introduction

Currents in the littoral zone are caused by so-called hydrodynamic forces. The most important forces in the littoral zone are radiation stresses, tidal forces and wind forces. These are discussed in Sections 6.2.2 to 6.2.4. Turbulent forces (Section

6.2.5) tend to smooth out gradients in the cross-shore distribution of the longshore current.

By the hydrodynamic forcing a longshore current is generated and as soon as a current exists also a counter-force (bottom shear stress) is present. Without such resistance force, the flow would accelerate until unrealistic values (Section 6.2.6). The longshore current can be calculated from a force balance (Section 6.2.7). The longshore current (velocity speed and cross-shore distribution) is an important input parameter in longshore sediment transport computations.

## 6.2.2 Radiation stress

### General introduction

The radiation stress theory was originally posed in a series of papers by Longuet-Higgins and Stewart (1962), (1963), (1964). The theory describes how propagating waves exert a force on vertical surfaces. Additionally to the well-known hydrostatic force, this force, called radiation stress, is always present when waves migrate through a body of water. However, its effect is most eminent in the littoral zone, where relatively strong longshore currents can be generated by radiation stresses (for instance 1 m/s under some conditions).

The second law of Newton prescribes that the transfer of momentum ( $d(mv)/dt$ ) is equivalent to a force. So under waves the effect of orbital motion (transfer of momentum) can be ‘translated’ to a force. Let us consider the forces and the flux of horizontal momentum across a vertical plane with unit width from bed to water surface. ( $M$  can also be seen as the instantaneous force acting on that plane.)

$$M(X,t) = \int_0^{h+\eta} (p + \rho u^2) dz \quad (6.1)$$

where:

- $X$  the direction of wave propagation (note that the mentioned vertical plane is assumed to be directed perpendicular to the direction of wave propagation)
- $\eta$  instantaneous water level
- $p$  pressure (function of time and  $z$ )
- $\rho u$  measure for ‘mass’ ( $m$ ) passing the vertical plane
- $\rho u^2$  flux of horizontal momentum ( $mv$ ) (function of time and  $z$ )

The radiation stress is defined as the mean value of  $M(X,t)$  with respect to time, minus the hydrostatic force onto a vertical plane in the water in rest:

$$S_{XX} = \int_0^{h+\eta} (p + \rho u^2) dz - \int_0^h p_0 dz \quad (6.2)$$

where:

- $S_{XX}$  radiation stress in the direction of wave propagation [N/m]
- $p_0$  hydrostatic pressure in water in rest [N/m<sup>2</sup>]

Note:  $S_{XX}$  is called radiation *stress* (unit of stress:  $[\text{N}/\text{m}^2]$ ), but it is in reality a force per unit width acting over the total water depth ( $[\text{N}/\text{m}]$ ).

Eqs.(6.1) and (6.2) show the two contributions to the horizontal momentum flux: (horizontal) pressure and orbital motion.

Let us first consider the pressure. If we consider a body of water in rest, then we have a hydrostatic water pressure distribution. This pressure is at the bottom equal to  $\rho gh$ , with  $h$  being the water depth. The total depth-integrated hydrostatic force then is  $\frac{1}{2}\rho gh^2$ .

Now, we superimpose a wave. Then the water pressures compared to the hydrostatic pressures are enlarged under the wave crest and decreased under the wave trough (Fig.6.1). Integration of these pressure fluctuations (over the wave period and the water column) is generally not zero, but positive.

In *deep water* (Fig.6.1a), it can be argued that this net effect will be very small (pressure fluctuations occur over a relatively small portion of the water column only). In deep water the pressure contribution to the radiation stress  $S_{XX}$  is often neglected.

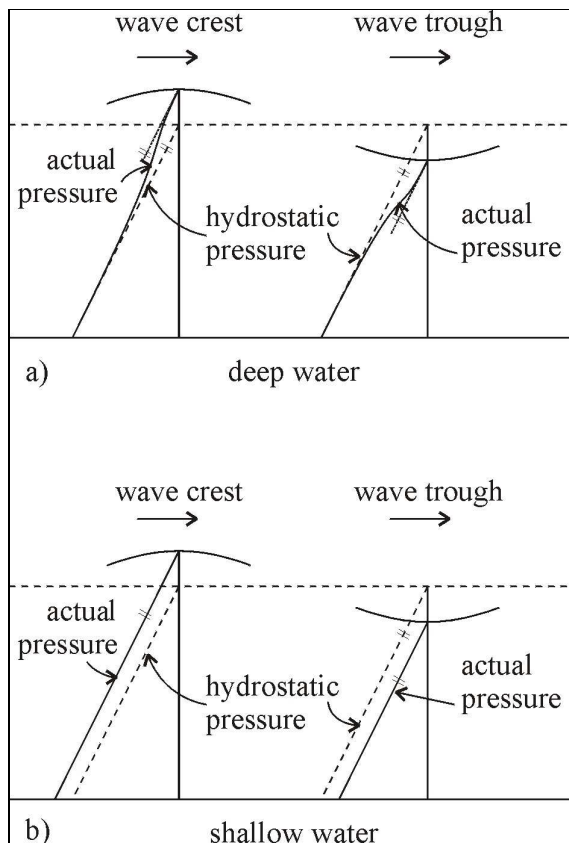


**Figure 6.1** Wave-induced changes in pressures compared to hydrostatic pressure under still water

In *shallow* water (Fig.6.1b) the pressure fluctuations due to wave action are felt over the entire water column and are even felt at the bottom. Both under a wave crest and under a wave trough, hydrostatic pressures can be assumed to occur. Under these conditions (Fig.6.1b) it is quite clear that the net effect over a wave period (formal integration) results in a net force (contribution to  $S_{XX}$ ) in wave propagation direction.

Let us now consider the contribution of the orbital velocity to the radiation stress.

Under a wave *crest* the orbital velocities are directed in the positive  $X$ -direction (to the right in this discussion). The term  $\rho u^2$  then results in an increase of  $\overline{mv}$  at the right side of the plane. That is to be seen as a force in positive  $x$ -direction.

Under a wave *trough* a mass  $\rho u$  is moving with velocity  $u$  from right to left through the vertical plane ( $\overline{mv}$ ). The  $\overline{mv}$  at the right side of the plane has *increased* by this action (just like under a wave crest). So also under a wave trough a force in positive  $X$ -direction is acting on the plane by the wave action.

Over the entire wave period a formal integration with time has to be carried out.

Longuet-Higgins and Stewart (1964) combined both contributions to the radiation stress and expressed the radiation stress in terms of the total wave energy:

$$S_{XX} = \left[ \frac{1}{2} + \frac{2kh}{\sinh 2kh} \right] E \quad (6.3)$$

where:

$S_{XX}$	radiation stress in the direction of wave propagation	[N/m]
$k$	wave number ( $2\pi/\lambda$ )	[m <sup>-1</sup> ]
$\lambda$	wavelength	[m]
$E$	wave energy defined as: $E = \frac{1}{8}\rho g H^2$	[J/m <sup>2</sup> ]
$H$	wave height	[m]

In Eq.(6.3) the parameter  $E$  appears (total energy in water column per m<sup>2</sup>; [J/m<sup>2</sup>]). The dimension of radiation stress is force per unit length (N/m) acting over the entire depth. J/m<sup>2</sup> can be rewritten to N/m; the dimension of Eq.(6.3) is correct.

The radiation stress is actually a vector. The transverse radiation stress  $S_{YY}$  has a similar definition as  $S_{XX}$  above, but holds now for the transverse  $Y$ -direction, i.e. perpendicular to the wave propagation direction. (Note that in the  $Y$ -direction the orbital motion does not play a role.)

The annotation for radiation stresses is  $S$  with two subscripts (like  $S_{XX}$ ). The first subscript is in this lecture note related to the direction of the plane on which the radiation stress acts; the second subscript is related to the direction in which the radiation stress acts. The direction of wave propagation is defined as the  $X$ -direction; the direction of the wave crests is defined as the  $Y$ -direction. This leads to  $S_{XX}$  and  $S_{YY}$  forces acting at a column of water presented in top view in Fig.6.2.

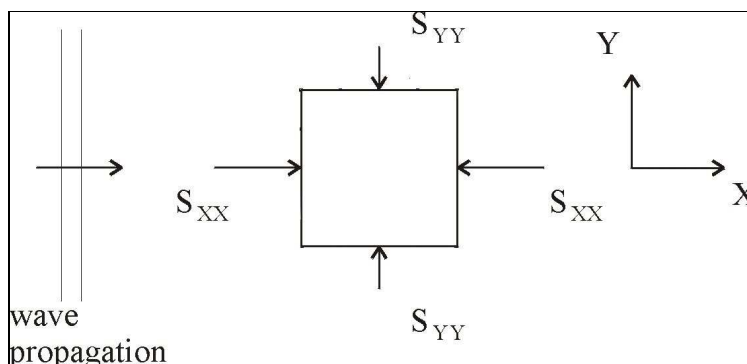


**Figure 6.2 Principal radiation stresses**

*Remark:* In the explanation of  $S_{XX}$  we so far considered the processes in wave propagation direction yielding e.g. the radiation stress  $S_{XX}$  acting at the left plane of the water column of Fig.6.2. A quite similar discussion with hydrostatic pressures and momentum transfer due to  $\rho u^2$  can be held for the force  $S_{XX}$  acting at the right plane of the water column. It results in a force in opposite direction. Also with the notion *action = reaction* it can be understood that the forces at both sides of the water column of Fig.6.2 are acting in an opposite direction.

The transverse radiation stress  $S_{YY}$  can be found in a similar way as  $S_{XX}$  and reads:

$$S_{YY} = \left[ \frac{kh}{\sinh 2kh} \right] E \quad (6.4)$$

As was explained in Chapter 2, the ratio between the wave group velocity and the individual wave celerity is denoted as  $n$  ( $n = c_g/c$ ). If we use this parameter in Eq.(6.3),  $S_{XX}$  can be re-written as:

$$S_{XX} = \left[ 2n - \frac{1}{2} \right] E \quad (6.5)$$

Likewise,  $S_{YY}$  can be written as (also see Fig.6.2):

$$S_{YY} = \left[ n - \frac{1}{2} \right] E \quad (6.6)$$

In *deep* water where  $n = 1/2$ , it follows:

$$S_{XX} = \frac{1}{2} E, \text{ and } S_{YY} = 0$$

In physical terms this can be understood as in deep water the only remaining contribution to the radiation stress is the orbital velocity (in the direction of the wave propagation). The contribution of the varying pressures in deep water is nil (in the wave propagation direction ( $X$ -direction), but of course also in the  $Y$ -direction).

In *shallow* water, on the other hand, where  $n = 1$ , it follows from Eqs.(6.5) and (6.6) that:

$$S_{xx} = \frac{3}{2}E, \text{ and } S_{yy} = \frac{1}{2}E$$

Here both contributions add to the total radiation stress. (The pressure part is equal to  $S_{yy}$ .)

The radiation stress in shallow water is clearly larger than in deep water. And, it has two components in shallow water: parallel and perpendicular to the direction of wave propagation.

In deep water the radiation stresses ( $S_{xx}$ ) are generally only a small fraction of the depth-integrated hydrostatic pressure (maximum in the order of ‰). In shallow water, on the other hand, the fraction can be quite significant (in the order of 10% or more).

The magnitude of the radiation stress depends mainly on the wave height, via the wave energy ( $E \sim H^2$ ). In shallow water (surf zone) wave breaking processes determine to a great extent the (remaining) wave energy. As such a spatial gradient will develop in the radiation stresses. Gradients in radiation stresses cause wave set-down and wave set-up and radiation stresses are main driving forces behind a littoral current.

### Wave set-down and wave set-up

We first consider a situation with normally incident, purely shoaling waves (no bottom friction, refraction, diffraction or breaking).

The magnitude of the radiation stress  $S_{xx}$  depends on the water depth, the wave number and the wave height (Eq.(6.3)). If dissipation of wave energy can be neglected outside the breaker zone, then in this region, the energy flux ( $Ec_g = Enc$ ) is constant. With linear wave theory it can be shown that  $S_{xx}$  increases with decreasing depth in the region outside the breaker zone. This is the region referred to as intermediate depths; further offshore in really deep water, the radiation stress  $S_{xx}$  is constant.

An increasing  $S_{xx}$  in landward direction means that at a water column a resulting force due to radiation stresses is acting in seaward direction. By a (small) difference in water level at both sides of the water column, equilibrium of forces can be achieved again. This phenomenon is called wave set-down, which means that outside the breaker zone in intermediate water depths, the water level at the landward side of a water column is a little bit lower than at the seaward side.

Inside the surf zone the magnitude of  $S_{xx}$  decreases rapidly due to wave breaking while moving towards the waterline. Looking at a water column inside the surf zone the  $S_{xx}$  component at the seaward side of the column is larger than at the landward side. To achieve equilibrium again, the water level at the landward side of the column should be higher than at the seaward side (wave set-up).

In general the equilibrium between radiation stress change and the average water level slope yields the following first order differential equation:

$$\frac{dS_{xx}}{dx} = -\rho g(h+h') \frac{dh'}{dx} \quad (6.7)$$

where:

$x$  co-ordinate axis pointing from land to sea



- $h$  water depth at point  $x$  (in absence of waves)
- $h'$  average water level change at point  $x$

Note that in Eq.(6.7), because of the chosen  $x$ -co-ordinate, inside the surf zone the term  $dS_{xx}/dx$  is positive yielding a negative water level gradient ( $dh'/dx$ ) (downward sloping water surface from land to sea). This is just opposite to the physical feeling: moving inside the surf zone towards the waterline, the term  $S_{xx}$  becomes smaller and the still water surface becomes higher (wave set-up).

Just outside the breaker zone (assuming regular waves), by integration of Eq.(6.7) starting at deep water, it can be shown that the total wave set-down equals (see also Fig.6.3 and Fig.6.4):

$$h'_b = -\frac{1}{16} \gamma H_b \tag{6.8}$$

where:

- $h'_b$  water level change at the point of wave breaking [m]
- $\gamma$  wave breaking index ( $H_b/h_b$ ) [-]
- $H_b$  wave height at point of breaking [m]
- $h_b$  still water depth at point of breaking [m]

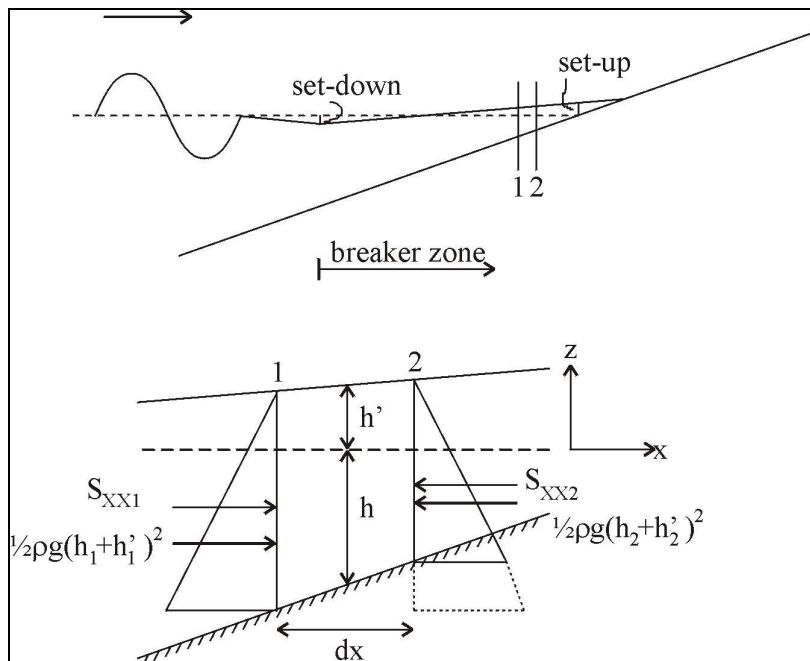


**Figure 6.3** Effect of changes in the radiation stress component  $S_{xx}$

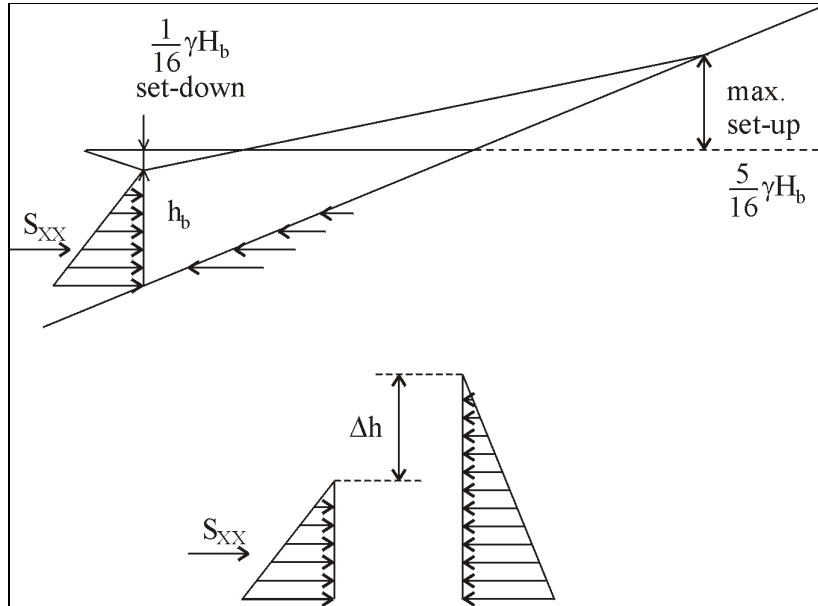


**Figure 6.4 Equilibrium of forces in the entire breaker zone**

Inside the breaker zone we may assume that the wave height is proportional to the local water depth. If we further use the shallow water equations ( $n = 1$ ), then it follows that  $S_{xx}$  is decreasing from the breaker line towards the coastline. Similar as was mentioned above, this causes landward directed resulting forces acting at a water column. This will be balanced by a water level increase (in landward direction) over the water column. In this straightforward approach, increasing water levels from the breaker line towards the coastline can be expected. It can be proven that the water level difference between the breaker line and the point of maximum water level rise (wave set-up) equals:

$$\Delta h = \frac{3}{8} \gamma H_b \quad (6.9)$$

where:

$\Delta h$  change in water level across the breaker zone [m]

Keeping in mind that the maximum set-down at the breaker line is  $(1/16)\gamma H_b$ , this means that the maximum wave set-up relative to the still water level is  $(5/16)\gamma H_b$ . According to the shallow water approximation ( $n = 1$ ), the water level slope inside the breaker zone is constant (assuming a constant bottom slope and a constant breaker index.) Wave set-up can be quite significant, as is illustrated in Example 6.1.

**Example 6.1***Input parameters:*

Offshore wave height:	$H_0$	=	5 m
Wave period:	$T$	=	12 s
Offshore wave direction:	$\varphi_0$	=	0° (perpendicular to the coastline)
Breaker index:	$\gamma$	=	0.7

*Required:*

Maximum wave set-up relative to the still water level

*Output:*

The first step is to compute the wave height at the breaker line.  $H_b$  depends on shoaling and (though not in this case) refraction. Computer programs can be used or the generalized description as given in Example 6.2. It follows that  $H_b = 5.5$  m.

The maximum wave set-up then becomes 1.19 m

*Conclusion:*

If we assume an average beach slope of 1:50, then almost 60 m of beach width is 'lost' by the effect of wave set-up.

**Example 6.1 Maximum wave set-up relative to still water level**

For various reasons wave conditions can vary along a certain stretch of coast. For instance, due to wave refraction on a non-uniform nearshore region, or due to wave diffraction in the lee side of a breakwater. This leads to varying wave set-ups along the coastline, which produces a pressure gradient along the coast. These pressure gradients can form an important contribution to the driving force of a longshore current.

The actual situation in a breaker zone is much more complex than what has been described here above. This is proven by the fact that experimental results often do not agree with the theoretically predicted values for wave set-up. Some complicating factors are the following:

- By assuming that inside the surf zone there is a direct relationship between the local wave height and local water depth, it means that the build up of the wave set-up just starts at the (first) point of breaking. In reality there is some delay.
- $S_{XX}$  is not evenly distributed over the water column: it is larger near the water surface due to higher orbital velocities than near the bed. The excess hydrostatic pressure (excess because of the wave set-up), on the other hand is distributed evenly over the water column. Inside the breaker zone, this difference contributes to a 2DV circulation with a surface current running towards the coast and a seaward current near the bottom.
- Bottom shear stresses have not been considered so far, but they can add a horizontal force.
- Waves are irregular. For the computation of the wave set-up for a wave spectrum, the root mean square wave height  $H_{rms}$  is generally applied.

- In an irregular wave field periods (say a few waves) with relatively small wave heights and periods with relatively large wave heights do occur. That means that the magnitude of the radiation stress is varying with time. This varying force generates water level fluctuations with a time scale much longer than the wave period (long waves).
- Breaking waves generate a layer of air-water mixture, which moves in landward direction in the upper parts over the water column. This roller may also contribute to an additional horizontal force component.
- Linear wave theory has its limitations, especially in the breaker zone.
- Waves generally approach the coastline under a (small) angle, which means that  $S_{XX}$  is not directed perpendicular to the coastline (see below). Moreover, the wave angle changes across the breaker zone.

### From wave directions to coastline orientations

Until now, we have only considered the so-called principal radiation stresses  $S_{XX}$  and  $S_{YY}$ . The directions of these stresses are related to the direction of wave propagation ( $X$ -direction).

In coastal engineering practice it is common to work with longshore and cross-shore orientated axes. As shown in Fig.6.5, the  $x$ -axis is defined parallel to the shoreline, where the  $y$ -axis is perpendicular to the shoreline. The  $X$  and  $Y$ -axes which were used above (capital  $X$  and  $Y$ ) were related to the direction of the wave propagation.

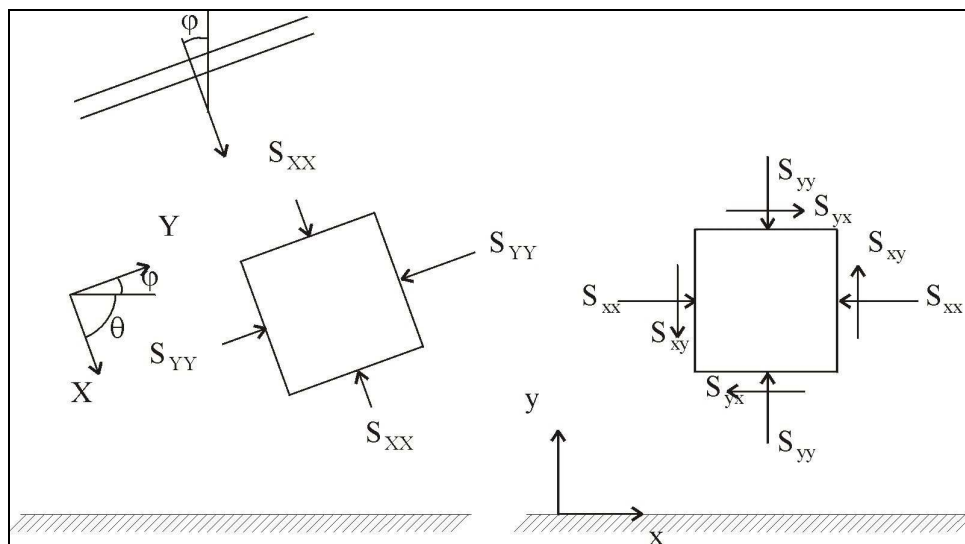


**Figure 6.5 Radiation shear stresses**

Just like in Applied Mechanics we might consider the element in the left side of Fig.6.5 as a situation with only principal forces (only normal forces). At the element at the right side, in the same medium, but with a different orientation, then apart from normal forces also shear stresses appear. On each plane then two radiation stresses are found:  $(S_{xx}, S_{xy})$  and  $(S_{yy}, S_{yx})$ . With the Mohr-circle or looking at the equilibrium of the hatched element in Fig.6.6 the next expressions can be derived:

$$S_{xx} = \frac{(S_{xx} + S_{yy})}{2} + \frac{(S_{xx} - S_{yy})}{2} \cos(2\theta) \quad (6.10)$$

$$S_{yy} = \frac{(S_{xx} + S_{yy})}{2} - \frac{(S_{xx} - S_{yy})}{2} \cos(2\theta) \quad (6.11)$$

$$S_{xy} = (S_{xx} - S_{yy}) \sin \theta \cos \theta = (S_{xx} - S_{yy}) \cos \varphi \sin \varphi = S_{yx} \quad (6.12)$$

where:

$\theta$  re-orientation of the two axis systems (Fig.6.5) [rad]

$\varphi$  angle between wave crest and coastline, or  
angle between direction of wave propagation  
and shore normal [rad]

$\varphi = \pi/2 - \theta$

$S_{yx}$  radiation shear stress in the direction of the  
coastline acting on a plane which is parallel to  
the coast [N/m]

*Remark:* It looks like that the radiation shear stress  $S_{yx}$  acting on a plane parallel to the coastline results according to Eq.(6.12) from a straightforward Applied Mechanics operation. With the 'physics' of wave motion in mind in reality the orbital motion, while crossing a plane parallel to the coastline under an angle, transfers momentum in  $x$ -direction (the direction along the coast), which can be seen as a shear stress. (The pressure component of the radiation stress does not contribute to the radiation shear stress.)

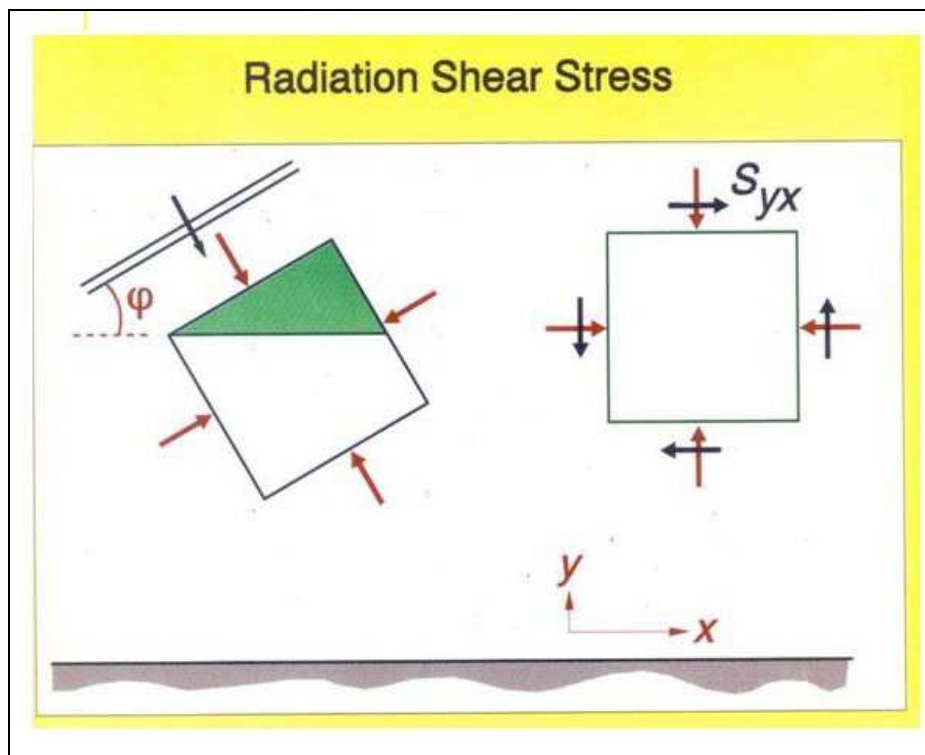


**Figure 6.6 Radiation stresses for oblique approaching waves**

The two squares in Fig.6.5 represent in fact entire columns of water. Only the contribution of the radiation stresses to the total forces acting on the four planes have been given (the hydrostatic forces belonging to a situation without waves are of course also present).

If the conditions (wave and other conditions) are such that the radiation (shear) stresses at opposite planes are just identical, then the influence of radiation stress on the hydrodynamics is zero. Only if the conditions differ, a resultant radiation stress (resultant force on a water column) occurs which will affect the local hydrodynamics.

This is the case especially in the littoral zone, where wave refraction, shoaling, diffraction and wave breaking occur. A few pages back (see also Fig.6.3 and Fig.6.4), we already showed how wave set-down and wave set-up can be explained in terms of changes in the principal radiation stress  $S_{xx}$  (which corresponds to  $S_{yy}$  for a situation with normally incident waves). Below, we consider the influence of changes in  $S_{yx}$  ( $dS_{yx}/dy$ ) on the hydrodynamics in the surfzone.

### Longshore radiation stress component $S_{yx}$

The radiation stress component  $S_{yx}$  acts in longshore direction and is only present in situations where the waves approach the coastline under a certain angle  $\varphi$  (Fig.6.5).

Let us first consider the situation in deeper water, i.e. outside the breaker zone. From Eqs.(6.5), (6.6) and (6.12) it can be deduced that:

$$S_{yx} = En \sin \varphi \cos \varphi \tag{6.13}$$

From refraction theory (without wave breaking and energy dissipation due to bottom friction) it follows that the energy flux between two wave rays (lines along which the waves propagate) is constant:

$$E c_g b = \text{constant} = E_0 c_{g,0} b_0 \tag{6.14}$$

where:

$c_g$	group velocity of the waves (= $nc$ )	[m/s]
$b$	width between two wave rays	[m]

The subscript  $_0$  refers to deep water conditions.

If we further assume the validity of Snel's law and that the depth contours are all parallel to the coastline (a so-called uniform coast), then it follows that seaward of the surfzone (no energy dissipation is assumed),  $S_{yx}$  is constant. So although outside the surf zone the wave conditions are constantly changing (wave height; wave direction), the radiation shear stress is constant.

Inside the breaker zone the  $S_{yx}$  determining parameters change (especially the wave height is changing due to wave breaking) so that  $S_{yx}$  will also change. This yields on a column of water inside the surf zone a resultant force (N/m) in longshore direction, dependent on the value of  $dS_{yx}/dy$ .

How can this resulting longshore force be balanced?

One option would be a hydraulic pressure gradient (similar to what was described for the wave set-up inside the breaker zone). In that case, the water surface has to develop a certain slope in longshore direction. (In cross-shore direction this indeed happens as the coast itself forms a closed barrier.) If we consider an infinitely long

non-interrupted coastline, then no such hydraulic pressure gradient can develop. If a resulting force in the direction along the coast is acting on a column of water (water in rest), then that column will accelerate ( $F = m.a$ ). But as soon as the column has a velocity, bottom shear stresses are generated. So another option for a 'counter force' to restore equilibrium of forces in longshore direction, is the generation of bottom shear stress due to moving water. This happens indeed; a so-called longshore current is generated.

So the conclusion is that the gradient in  $S_{yx}$  ( $S_{yx}/dy$ ) in the breaker zone generates a longshore current. This longshore current leads to a bottom shear stress, which counter-acts the driving force. Equilibrium is reached once, via the longshore current, the bottom shear stress equals the cross-shore gradient in  $S_{yx}$ .

From Eq.(6.13), combined with Snel's law and the criterion of wave breaking ( $H = \gamma h$  across the entire breaker zone) it can be shown that inside the breaker zone:

$$S_{yx} = \frac{1}{8} \rho g \gamma^2 h^2 n \frac{c \sin \varphi_0}{c_0} \cdot \cos \varphi \tag{6.15}$$

where:

$\varphi$  wave angle [rad]  
 $c$  wave velocity [m/s]

The subscript 0 refers to deep water conditions.

In the breaker zone, the parameters  $n$ ,  $c$ ,  $h$  and  $\varphi$  are a function of  $y$ . If we use the shallow water approximations:  $n = 1$  ( $dn/dy = 0$ ),  $\varphi$  is small and  $c = \sqrt{gh}$ , then it can be proven that:

$$\frac{dS_{yx}}{dy} = \frac{5}{16} \rho \gamma^2 (gh)^{1.5} \frac{\sin \varphi_0}{c_0} m \tag{6.16}$$

where:

$m$  the slope of the seabed inside the breaker zone ( $dh/dy$ ) [-]

As mentioned above the radiation shear stress  $S_{yx}$ , is constant seaward of the border of the breaker zone. It decreases inside the breaker zone to zero at the waterline [see Example 6.2 (next page) and Fig.6.7].

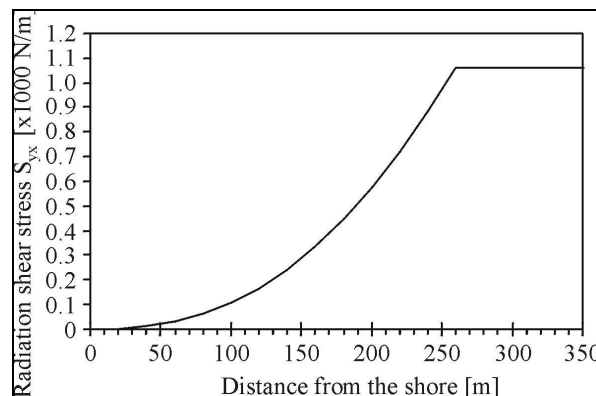


**Figure 6.7** Computed radiation shear stresses

**Example 6.2***Input parameters:*

Offshore wave height:	$H_0$	=	2 m
Wave period:	$T$	=	7 s
Offshore wave direction:	$\varphi_0$	=	30°
Bottom slope:	$m$	=	1:100
Breaker index:	$\gamma$	=	0.8
Roughness height:	$r$	=	0.06 m

*Required:*Radiation shear stresses and gradients in  $S_{yx}$  for various positions*Output:*

Depth contours are assumed to be parallel. The first step of the solution is to define the outer edge of the breaker zone. The non-linear character makes a direct analytical solution impossible; instead, the following iterative scheme can be used:

1. Guess a breaker depth,  $h_b$  and compute  $h_b/\lambda_0$
2. Using the tables of wave functions (or computations) to determine the shoaling coefficient  $K_{sh}$  and the ratio of wave speeds  $c/c_0$
3. Determine the angle  $\varphi$  using:  $\sin(\varphi) = (c/c_0)\sin(\varphi_0)$
4. Compute the wave height at guessed water depth  $h_b$  from:

$$H' = H_0 K_{sh} \sqrt{[\cos(\varphi_0)/\cos(\varphi)]}$$

5. Check whether  $H'/h_b = \gamma = 0.8$ . If yes: o.k.; if no: return to step 1 with a better guess of  $h_b$

For the computation of  $S_{yx}$  Eq.(6.13) is used. For the computation of  $dS_{yx}/dy$  Eq.(6.16) is used. The results of the computations can be found in the table.

y	h	$\lambda$	c	k	n	$\varphi$	H	Limit H	$S_{yx}$	$dS_{yx}/dy$
[m]	[m]	[m]	[m/s]	[-]	[-]	[°]	[m]	[m]	[N/m]	[N/m <sup>2</sup> ]
0	0.0	0.00	0.00	--	--	0	--	0	--	0.00
"z:10	0.1	6.92	0.99	0.91	1.00	2.59	4.38	0.08	0.35	0.09
20	0.2	9.78	1.40	0.64	0.99	3.66	3.70	0.16	1.99	0.25
40	0.4	13.79	1.97	0.46	0.99	5.17	3.12	0.32	11.15	0.71
60	0.6	16.84	2.41	0.37	0.98	6.32	2.84	0.48	30.41	1.31
80	0.8	19.40	2.77	0.32	0.98	7.28	2.65	0.64	61.78	2.01
100	1.0	21.62	3.09	0.29	0.97	8.12	2.52	0.80	106.83	2.81
120	1.2	23.62	3.37	0.27	0.97	8.88	2.42	0.96	166.79	3.70
140	1.4	25.44	3.63	0.25	0.96	9.57	2.34	1.12	242.71	4.66
160	1.6	27.12	3.87	0.23	0.96	10.21	2.28	1.28	335.44	5.69
180	1.8	28.69	4.10	0.22	0.95	10.81	2.22	1.44	445.70	6.79
200	2.0	30.16	4.31	0.21	0.95	11.37	2.18	1.60	574.09	7.95
220	2.2	31.54	4.51	0.20	0.94	11.89	2.14	1.76	721.12	9.17
240	2.4	32.85	4.69	0.19	0.94	12.40	2.10	1.92	887.22	10.45
260	2.6	34.09	4.87	0.18	0.93	12.87	2.07	2.08	1061.98	0.00
280	2.8	35.28	5.04	0.18	0.93	13.33	2.04	2.24	1061.98	0.00
300	3.0	36.41	5.20	0.17	0.92	13.77	2.02	2.40	1061.98	0.00
320	3.2	37.50	5.36	0.17	0.92	14.19	2.00	2.56	1061.98	0.00
340	3.4	38.54	5.51	0.16	0.91	14.59	1.98	2.72	1061.98	0.00
360	3.6	39.54	5.65	0.16	0.91	14.98	1.96	2.88	1061.98	0.00

**Example 6.2 Radiation stresses and gradients in  $S_{yx}$  for various positions**



For many day to day wave conditions, this gradient in  $S_{yx}$  causes resulting longshore stresses (forces) which are in the same order of magnitude as the bottom shear stress in rivers: in the order of 1 to 10  $\text{N/m}^2$  (the dimension is now that of a real stress:  $dS_{yx}/dy$ ). The gradient in the longshore radiation stress  $S_{yx}$  is therefore an important driving force in the littoral zone. (Further reference is made to Section 6.2.7.)

### 6.2.3 Tidal forces

Also tides can generate a longshore current (see Fig.6.8). The direction of this current normally turns when going from ebbing tides to flooding tides and vice versa.

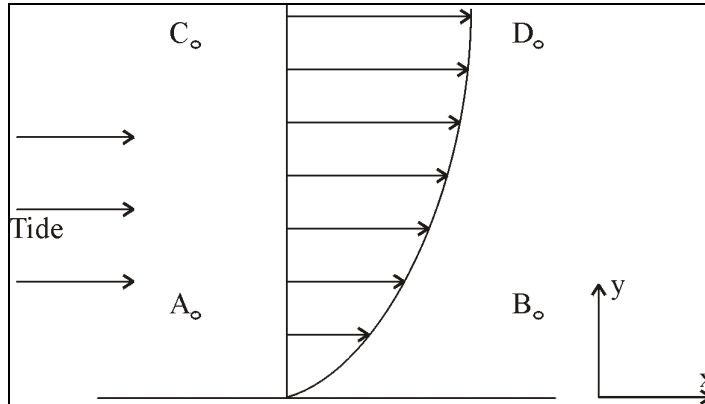


**Figure 6.8 Tidal current along the shore**

Tidal forces are deterministic, that means that they are independent of weather or climate conditions. Once the tidal constituents (amplitudes and phases) are known from measurements, tidal forces can be forecasted. This is contrary to radiation stresses as the waves, which are generated by wind, are of a stochastic nature. The equation of motion of a tidal wave propagating along a coastline follows from the long wave theory (see Eq.(6.17)).

$$\frac{\delta v}{\delta t} + v \frac{\delta v}{\delta x} + g \frac{\delta Z}{\delta x} = -\frac{gv|v|}{C^2 h} \quad (6.17)$$

where:

$v$	depth-averaged tidal velocity	[m/s]
$Z$	tidal elevation (relative to still water level)	[m]
$g$	acceleration of gravity	[ $\text{m/s}^2$ ]
$C$	Chézy coefficient	[ $\text{m}^{0.5}/\text{s}$ ]
$h$	(still) water depth	[m]
$x$	co-ordinate along the coast	[m]

The three terms on the left hand side are responsible for the tidal force. The dimension of these terms is  $\text{m/s}^2$ . To obtain forces (in  $\text{N/m}^2$ , so actually stresses), these three terms need to be multiplied with the water depth and with the density of the water (the dimensions then become  $\text{kgm/s}^2$  per  $\text{m}^2$  which is the same as  $\text{N/m}^2$ ). Now we make a few simplifications. First of all, we assume a sinusoidal behaviour of the tidal elevation  $Z$  and the tidal velocity  $v$ , with a possible phase difference

between these two. If this phase difference is zero,  $v$  is maximum at zero tidal elevation and vice versa. It is further assumed that inertia and the water surface slope (hydraulic pressure gradient) are the two biggest contributions to the tidal force. This means that advection is neglected (generally a factor ten smaller). With these assumptions the tidal force (in  $\text{N/m}^2$ , so actually a stress) can be written as:

$$F_{tide} \approx \rho h \left[ \hat{v} \Omega \cos(\Omega t - kx - \varphi) + gk\hat{Z} \sin(\Omega t - kx) \right] \quad (6.18)$$

where:

$\Omega$	tidal frequency	$[\text{s}^{-1}]$
$k$	wave number ( $2\pi/\lambda_{tide}$ )	$[\text{m}^{-1}]$
$\lambda_{tide}$	length of tidal wave	$[\text{m}]$
$\varphi$	possible phase angle between $v$ and $Z$	$[\text{rad}]$
$t$	time	$[\text{s}]$
$\hat{v}, \hat{Z}$	amplitude value (of $v$ and $Z$ )	

A way to solve the simplified Eq.(6.18) is by using data from measurements made simultaneously at different points along the coast. During these measurements, no waves must be present, since these influence the bottom friction forces, even when no wave-driven longshore current is generated (i.c. perpendicular incoming waves).

If the tidal velocity at one particular water depth is known, for instance from measurements, then a very practical method for finding the cross-shore distribution of the velocities is by using the Chézy formula:  $v = C\sqrt{hi}$ . This implies that the streamlines must be parallel to the coast and that the water surface slope is the main driving force for the tidal current. If a constant  $C$  value is assumed Eq.(6.19) can be applied:

$$v_2 = v_1 \sqrt{\frac{h_2}{h_1}} \quad (6.19)$$

where:

$v_{1,2}$	tidal current velocities at cross-shore positions 1 and 2	$[\text{m/s}]$
$h_{1,2}$	still water depth at points 1 and 2	$[\text{m}]$

See also Fig.6.8. Note that in this approach it is assumed that  $i$  at deeper water is equal to  $i$  at shallow water (head between  $D$  and  $C$  equal to head between  $B$  and  $A$ ).

Following this simple approach, a tidal longshore velocity of 0.7 m/s at a water depth of 10 m yields a tidal velocity of 0.3 m/s at a water depth of only 2 m.

In this shallow region with 2 m water depth, waves can be very effective in increasing the bed shear stress. Consequently, the tidal velocities in the wave-influenced littoral zone will even be smaller than what follows from Eq.(6.19).

## 6.2.4 Wind stresses

Due to shear stresses between the water surface and the moving air, the upper parts of the water layers will start to move more or less in the same direction as the occurring wind direction.

In case the wind is seaward directed, a seaward directed current is generated in the upper water layers, the velocity of which is determined by the duration of the particular wind condition and its force. Similarly, a landward directed wind will induce a landward current in the upper layers. The coastline forms a barrier for this landward current. Therefore, to compensate for the landward (or seaward) directed water mass movement in the upper layers, an opposite directed water mass transport follows in the lower water layers. In addition to these 'compensation currents', a water level set-up or set-down can develop near the coast to compensate for the respective wind-induced shear stresses.

In case the wind is directed parallel to a (long) coast, a longshore current is generated. The wind stress  $\tau$  exerted on the water surface by the moving air is:

$$\tau = C_w \rho_a W^2 \quad (6.20)$$

where:

- $C_w$  drag coefficient depending on wind velocity.  
 $C_w = (0.63 + 0.066W)10^{-3}$  for  $2 < W < 21$  m/s on the North Sea [Verlaan *et al.* (1993)]
- $\rho_a$  density of air ( $1.25 \text{ kg/m}^3$ )
- $W$  wind velocity at the water surface in longshore direction

The vertical distribution of the wind-generated current differs largely from the current generated by a water level gradient (Fig.6.9). The highest flow velocities occur at the water surface, with usually a rapid decrease in downward direction (much more than with the logarithmic velocity profile).

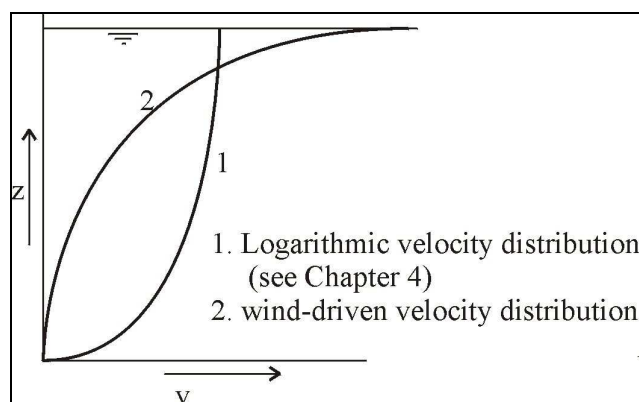


**Figure 6.9 Typical velocity distribution for wind-driven current**

During storms, this stress may have an important effect on the residual longshore current. Often, however, the effect of wind stress on the longshore current in the littoral zone is neglected (small contribution to the longshore current and small velocities near the bottom where the highest sediment concentrations occur).

Wind stresses are of greater importance in, for instance, coastal lagoons. The Dutch Wadden Sea, comprising of several inlets, is an example of a series of tidal basins in which wind-driven currents may play an important role. For dominant SW winds, a significant volume of water and sediment can be transported towards the east. This

may lead to a gradual, but over the years continuing, shift of the water sheds between the barrier islands and the mainland. FitzGerald *et al.* (1987) appoint this primarily wind-generated transport as the primary force behind inlet migration in the German Wadden Sea.

### 6.2.5 Turbulent forces

In general, turbulent forces are activated in situations where spatial gradients occur (like density gradients, or gradients in the flow velocity). For the longshore current, it is not a real driving force, nor a resistance force. It tends to smooth out sharp local changes in the longshore current distribution.

Let us consider a coastline with a cross-shore gradient in the longshore velocity: ( $dv/dy$ ). Due to turbulent forces, 'velocity' is transferred from areas with high current speeds to areas with low current speeds. This momentum transfer can be expressed as a turbulent shear stress:

$$\tau_{yx} = \rho v' u' = \rho \varepsilon_y \frac{dv}{dy} \quad (6.21)$$

where:

$v$	velocity component parallel to the coastline ( $x$ -direction)	[m/s]
$v'$	turbulent velocity fluctuation in $x$ -direction	[m/s]
$u'$	turbulent velocity fluctuation in $y$ -direction	[m/s]
$\varepsilon_y$	turbulent diffusion coefficient, also called eddy viscosity, defined as: $\varepsilon_y = l_y u'$	[m <sup>2</sup> /s]
$l_y$	mixing length	[m]

The eddy viscosity thus depends on a characteristic horizontal scale and on a characteristic velocity. In the littoral zone, both are related to the wave motion. The horizontal wave orbital motion, for instance, can be regarded as a measure for the characteristic velocity  $u'$ , whereas the depth may be used for the characteristic (mixing) length. Typical values for the eddy viscosity are  $10^{-2}$  m<sup>2</sup>/s.

### 6.2.6 Bottom friction

In a hydraulic equilibrium situation (i.e. no accelerations), the hydrodynamic driving forces are balanced with a force in the opposite direction, generally caused by bottom friction. On an energetic level this means that in a hydraulic equilibrium situation, wind energy (waves, currents) and lunar energy (tides) are transformed into heat (bottom friction and internal friction).

The bottom friction depends on the flow velocity, which consists of a 'constant' velocity component and a rapidly changing flow velocity component caused by (breaking) wave motion. It is still difficult to describe the bottom friction accurately if these two components are considered in detail. One method is to use the formulations of the shear stress presented in Section 4.4. The bottom friction can be expressed by considering the actual velocities at an elevation  $z_t$  above the bottom. For the combined waves and currents action in the longshore direction, with the assumption that the waves obliquity is less than 20°, Bijker determined (Section

4.4.4, Eq.(4.50):

$$\bar{\tau}_{cwx} = \frac{\rho g v^2}{C^2} \left[ 0.75 + 0.45 \left( \xi \frac{\hat{u}_0}{v} \right)^{1.13} \right] \quad (6.22)$$

Since this is a rather difficult equation to work with, it might be further simplified by assuming that wave incidence is almost perpendicular ( $\varphi \approx 0^\circ$ ), that  $\xi \hat{u}_0/v \gg 1$ , and that linear wave theory can be applied. In shallow water this leads to (Eq.(4.52)):

$$\bar{\tau}_{cwx} = \frac{\rho g}{\sqrt{2} \cdot \pi C} \gamma \sqrt{h} \sqrt{f_w} \cdot v \quad (6.23)$$

The above descriptions deal with the time-averaged bottom shear stress; they disregard the momentary shear stresses that may occur within the wave period. Leaving out the intra-wave bottom shear stress fluctuations in the determination of the hydrodynamics seems acceptable for many coastal engineering applications. The intra-wave velocity fluctuations might be important for the longshore sediment transport. In the quantification of sediment longshore transport these processes are tried to model as good as possible.

## 6.2.7 Longshore current by oblique waves (uniform coast)

In a hydraulic equilibrium, there is a balance between the driving forces and the resistance force. Seaward of the surf zone there is to a first approximation no gradient in the radiation shear stress. So no longshore current is generated outside the surf zone.

Inside the surf zone a gradient in  $S_{yx}$  does exist.

The first step is to find the balance between the gradient in the radiation shear stress and the bottom friction. If the waves and the shore geometry are constant along the coast, then the hydraulic forces are constant as well (often referred to as a uniform coast). Eq.(6.16) gives the expression for the driving force, which must be balanced by the resisting friction force given by Eq.(6.22); see also Fig.6.10:

$$\frac{dS_{yx}}{dy} = \bar{\tau}_{cwx} \quad (6.24)$$

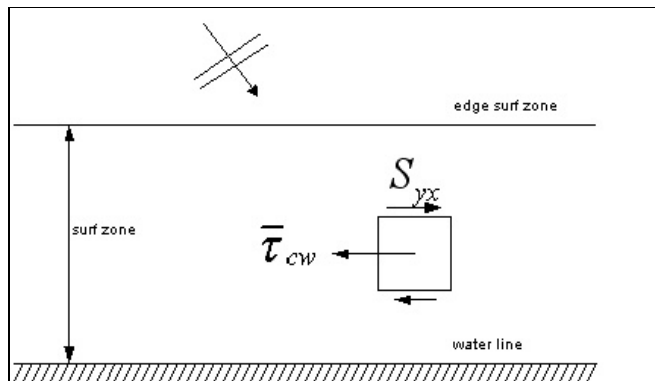


**Figure 6.10** Forces acting on water column

Solving Eq.(6.24) gives the value for  $v$ , which is the longshore velocity at a given point in the breaker zone. However, with using Eq.(6.22),  $v$  cannot be solved explicitly; iterative solution techniques must be used. A much simpler approach uses Eq.(6.23) instead of Eq.(6.22). This leads to the following expression for the longshore velocity  $v$ :

$$v = \frac{5\pi}{8\sqrt{2}} \cdot \frac{\sin \varphi_0}{c_0} \cdot \frac{C}{\sqrt{f_w}} \cdot \gamma \cdot \sqrt{g} \cdot h \cdot m \tag{6.25}$$

where:

- $\varphi_0$  angle of wave approach in deep water (relative to the shore normal) [°]
- $c_0$  wave velocity in deep water:
 
$$c_0 = \frac{g}{2\pi} T$$
 [m/s]
- $T$  wave period [s]
- $C$  Chézy friction coefficient [m<sup>1/2</sup>/s]
- $f_w$  friction factor for waves [-]
- $\gamma$  breaker index [-]
- $g$  acceleration due to gravity [m/s<sup>2</sup>]
- $h$  water depth [m]
- $m$  beach slope (vertical distance / horizontal distance) [-]

The following parameters in Eq.(6.25) are principally functions of the cross-shore position in the breaker zone:  $C$ ,  $f_w$ ,  $h$  and  $m$ . If we assume a given roughness height and application of linear wave theory,  $C$  and  $f_w$  can be calculated for various positions perpendicular to the coast. It then follows that the velocity distribution in the breaker zone is almost a linear function of the distance from the waterline. With this (too) simple formula the maximum velocity occurs at the breaker line; seaward of the breaker line the longshore velocity is zero (since  $dS_{yx}/dy$  equals zero). Reference is made to Fig.6.11 and Example 6.3.

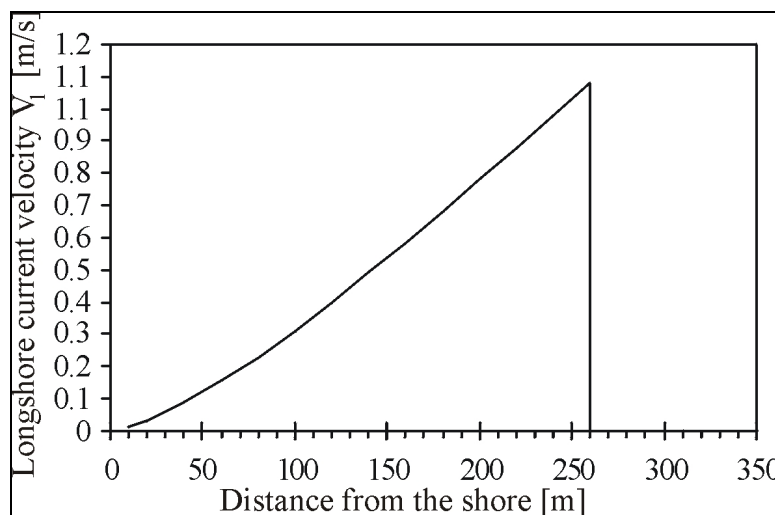


**Figure 6.11 Longshore velocity distribution (regular wave field)**

**Example 6.3***Input parameters:*

Offshore wave height:	$H_0$	=	2 m
Wave period:	$T$	=	7 s
Offshore wave direction:	$\varphi_0$	=	30°
Bottom slope:	$m$	=	1:100
Breaker index:	$\gamma$	=	0.8
Roughness height:	$r$	=	0.06 m

*Required:*

Distribution of the depth-averaged longshore current

*Output:*

This example is a continuation of Example 6.2. In addition to the already computed parameters the friction parameters have to be computed using the following equations:

$$a_0 = \frac{1}{2} H (\sinh(kh))^{-1}$$

$$f_w = \exp[-5.977 + 5.213(a_0/r)^{-0.194}]$$

$$C = 18 \log(12h/r)$$

The velocity follows from Eq.(6.25). The results can be found in the table.

y	h	$\lambda$	k	n	$\varphi$	H	$a_0$	$f_w$	C	V
[m]	[m]	[m]	[-]	[-]	[°]	[m]	[m]	[-]	[m <sup>1/2</sup> /s]	[m/s]
0	0.0	0	--	--	0	--	--	--	--	--
10	0.1	6.92	0.91	1.00	2.59	0.08	0.44	0.088	23.4	0.01
20	0.2	9.78	0.64	0.99	3.66	1.81	0.96	0.053	56.6	0.03
40	0.4	13.79	0.46	0.99	5.17	0.32	0.87	0.056	34.3	0.09
60	0.6	16.84	0.37	0.98	6.32	0.48	1.06	0.050	37.4	0.16
80	0.8	19.40	0.32	0.98	7.28	0.64	1.22	0.046	39.7	0.23
100	1	21.62	0.29	0.97	8.12	0.80	1.36	0.044	41.4	0.32
120	1.2	23.62	0.27	0.97	8.88	0.96	1.48	0.042	42.8	0.40
140	1.4	25.44	0.25	0.96	9.57	1.12	1.59	0.040	44.0	0.49
160	1.6	27.12	0.23	0.96	10.21	1.28	1.69	0.039	45.1	0.58
180	1.8	28.69	0.22	0.95	10.81	1.44	1.78	0.038	46.0	0.68
200	2	30.16	0.21	0.95	11.37	1.60	1.87	0.037	46.8	0.78
220	2.2	31.54	0.20	0.94	11.89	1.76	1.94	0.036	47.6	0.88
240	2.4	32.85	0.19	0.94	12.40	1.92	2.02	0.035	48.3	0.98
260	2.6	34.09	0.18	0.93	12.87	2.07	2.08	0.035	48.9	0.00
280	2.8	35.28	0.18	0.93	13.33	2.04	1.96	0.036	49.5	0.00
300	3	36.41	0.17	0.92	13.77	2.02	1.86	0.037	50.0	0.00
320	3.2	37.50	0.17	0.92	14.19	2.00	1.77	0.038	50.5	0.00
340	3.4	38.54	0.16	0.91	14.59	1.98	1.69	0.039	51.0	0.00
360	3.6	39.54	0.16	0.91	14.98	1.96	1.62	0.040	51.4	0.00

**Example 6.3 Distribution of the depth-averaged longshore current**

To ultimately find the simple expression according to Eq.(6.25), many assumptions and approximations had to be made. With the present-day computer models 'smooth' velocity distributions can be easily computed for cases without many simplifications.

Although Eq.(6.25) must be considered as a too simple representation of the truth, it is however still useful to inspect the dependency of the velocity to various parameters.

Let us, for instance consider the dependency of the velocities inside the breaker zone to the wave parameters: wave height  $H$ , wave period  $T$  and wave direction  $\varphi$ .

The *wave height* is not a direct parameter in Eq.(6.25), but it is evident that the wave height must play an important role. No waves: no wave driven currents. The width of the surf zone (where the wave driven currents are generated) is, however, largely determined by the wave height ( $h_b = H_b/\gamma$ ). If we disregard other effects, then we could simply conclude that the width of the surf zone doubles, with a doubling of the wave height. Assuming a triangularly shaped cross-shore distribution of the longshore flow (for a constant slope as beach profile) this leads to a factor 2 higher velocity at the breaker line and a factor 8 higher discharge in the surf zone. Wave height thus is indeed an important parameter.

The *wave period* appears in Eq.(6.25) via  $c_0$ . If we double the wave period, then it follows from Eq.(6.25) at first sight, that the flow velocity reduces (since  $c_0$  increases). However, a larger wave period also gives a wider surf zone.

If we look at the effect of the *wave direction* the following remarks can be made: no longshore current is generated if the angle of wave incidence is zero (waves enter the shore perpendicularly). If the angle is small, then the longshore current velocity at a specific water depth within the surf zone, becomes a linear function of  $\varphi_0$  (since:  $\sin(\varphi_0) \approx \varphi_0$ ). The maximum velocities occur for  $\varphi_0 = 45^\circ$ .

The (too) simple formula according to Eq.(6.25) also allows us to get an idea of the effect of the beach slope  $m$ . A steeper slope, at the one hand, results in (linearly) higher velocities. At the other hand the width of the surf zone becomes also linearly smaller. The discharge through the entire surf zone is then constant to a first approach.

The effect of turbulent forces is indicated in Fig.6.12.

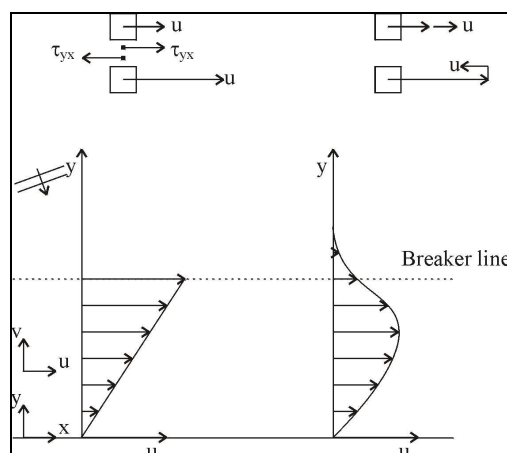


**Figure 6.12** Effect of turbulence on the velocity profile



Since the largest velocity gradient occurs at the breaker line, the maximum transfer of horizontal momentum will occur here. This leads to a reduction in the maximum velocity, a landward shift of the position of maximum velocity and to a situation where also outside the breaker zone longshore velocities occur. The distribution of  $\varepsilon_y$  (eddy viscosity) now also determines the velocity distribution. Various distributions  $\varepsilon_y$  can be motivated: the effects of a few of them on the resulting velocity distribution are shown in Fig.6.13.

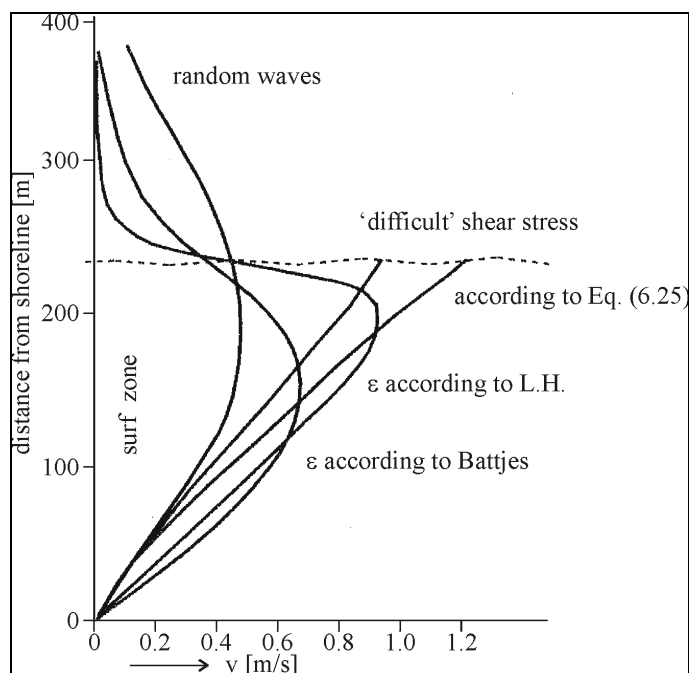


**Figure 6.13** Examples of velocity profiles

Until now we have only considered regular waves. In reality, of course, waves are irregular. Waves of various heights and periods enter the breaker zone and contribute to the longshore current. For each 'individual' wave, the driving force starts at the breaker line of each 'individual' wave. If we (simply) add the contributions of each 'individual' wave condition that may occur in a wave spectrum, then a very smoothed resultant velocity distribution results. This is also illustrated in Fig.6.14 (next page), which shows the output of a computation with the computer model Unibest-LT (input:  $H_{s,0} = 2$  m;  $\gamma = 0.7$ ;  $\varphi_0 = 30^\circ$ ;  $T_p = 8$  s). The effect of wave irregularity on the velocity distribution looks very similar to the effect of turbulence (wider and less sharply peaked).

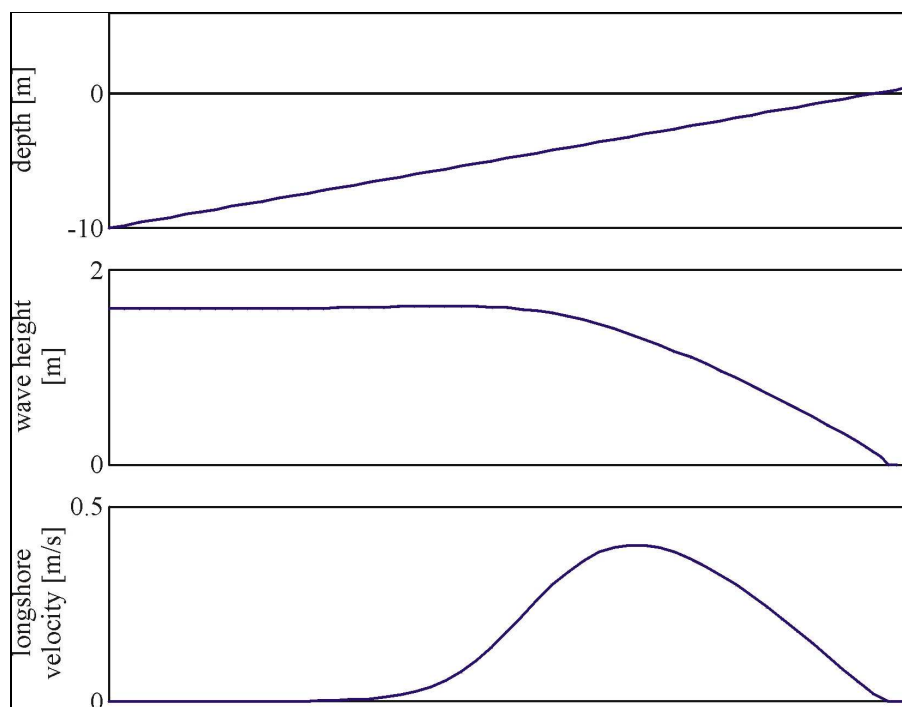


**Figure 6.14** Wave driven velocity computed with UNIBEST-LT

If we have a coastal profile with a breaker bar, then the determination of the velocity distribution gets more complicated. In a simplified approach, we can distinguish between a breaker zone at the seaward side of the breaker bar (if waves indeed start to break here) and a breaker zone near the shoreline where the remaining wave energy is dissipated. This simplification would lead to a zero longshore velocity in the deeper section between both breaker zones. Also in such a situation, both lateral transfer of horizontal momentum and the irregularity of the waves will smooth out the velocity distribution.

The next step is to include the effect of tidal forces. One complicating factor here is that the direction of the tidal velocity changes twice during one tidal cycle. The appropriate way to include the effect of tides is first to combine the driving forces (during ebb and flood periods) and then to calculate the velocity. Simply adding the tidal velocity to the wave-induced longshore current is not correct (that would only be possible if the velocity is a linear function of the driving forces which is generally not the case).

Fig.6.15 shows sketches of the resulting velocity distribution if the wave generated currents are combined with ebb tidal velocities and with flood tidal velocities. The maximum tidal velocity occurs outside the breaker zone, but the effect inside the breaker zone can be quite substantial. If the tidal force is in the same direction as the wave-driven current, then the maximum longshore flow velocity increases (and shifts towards the breaker line). If the tidal force is in the opposite direction, then the maximum velocity decreases (and shifts towards the shoreline). The longshore current in the breaker zone, although reduced in velocity, might then be in the opposite direction as the tidal current present further seawards.

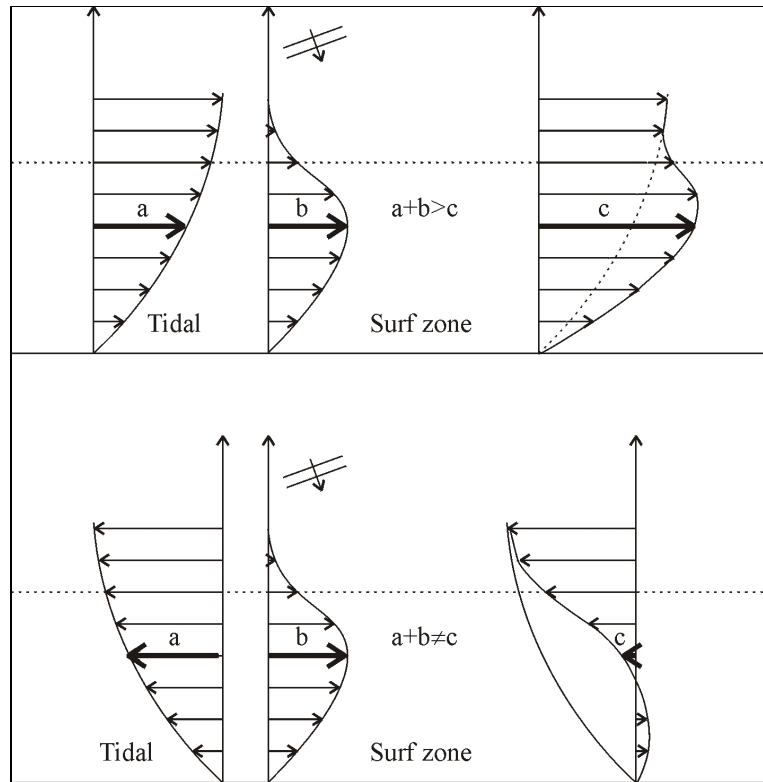


**Figure 6.15** Inclusion of tidal currents

If the radiation stresses are large enough relative to the tidal forces, it is even possible that the direction of the current in the breaker zone does not reflect anymore the direction related to the tide.

Tidal currents may significantly complicate the determination of the longshore current in the breaker zone. In practical cases, like for instance for the Dutch coastline, it will be necessary to establish the longshore current throughout the entire tidal cycle. Only in areas with weak tidal forces (like for instance the Mediterranean) the effect of tides on the water movement in the breaker zone can often be neglected.

## 6.3 Longshore sediment transport

### 6.3.1 Introduction

Longshore sediment transport is the net movement of sediment particles through a fixed vertical plane perpendicular to the shoreline. The direction of this transport is parallel to the shoreline and the depth contour lines. Without further specifications it is often meant to be the total transport in longshore direction (e.g. the total transport along a coast in the entire surf zone).

Longshore sediment transport depends amongst others on the hydrodynamics in the breaker zone (Section 6.2) and on the sediment properties (Section 4.2). Only if moveable sediment is available in a certain area, actual sediment transport may

occur. If the seabed is fixed (for instance by bottom protection, by bio-chemical processes or by vegetation) the local transport *capacity* (based on the hydrodynamics) might not be satisfied and a lower actual transport rate develops. The sediment properties as well as the local seabed and shoreline characteristics, are thus equally important for the longshore sediment transport as the transport-generating hydraulic forces.

In Chapter 4 it was argued that the longshore sediment transport (through a plane with unit width in this case) can be determined from the following equation:

$$S_x = \int_0^{h+\eta} v(z) \cdot \bar{c}(z) dz \quad (6.26)$$

where:

$S_x$	longshore sediment transport	[m <sup>3</sup> /m/s]
$v(z)$	the longshore current velocity at height $z$ above the bottom	[m/s]
$\bar{c}(z)$	the time-averaged sediment concentration at height $z$	
$h$	local (still) water depth	[m]
$\eta$	instantaneous water surface elevation	[m]

If we like to quantify the total transport in e.g. the surf zone, we must integrate the outcome of Eq.(6.26) over the width of the surf zone.

Many investigators have attempted to find a solution of Eq.(6.26). This is not an easy task, as both the longshore velocity and the sediment concentration depend on various often interrelated parameters. (See also Section 4.8.)

Below, two longshore transport formulae are presented in particular: the CERC formula and the Bijker formula. These formulae as well as most other formulae, are developed for sand only. Transport of mud and silt is further complicated by the cohesive behaviour of the sediment particles (see further Chapter 9). Also the transport of gravel and stones (when cohesion can be neglected similarly as for sand) is more complicated in reality, since the initiation of motion requires larger hydrodynamic forces than those for sand. The existing longshore transport formulae thus are (mostly) sand transport formulae.

### 6.3.2 The CERC formula

The CERC-formula has been developed by the Coastal Engineering Research Center (USA). It gives the total longshore sediment transport over the breaker zone, generated by the action of waves approaching the coast under an angle. The distribution of the sediment transport over the surf zone is not described.

The CERC formula is not predicting the sediment concentration nor the longshore velocity (as required in Eq.(6.26)). The development of this formula took place (in the late 1940's) well before the longshore current theory was developed. The formula has based on prototype and laboratory measurements and considers only wave generated currents (not tidal currents or other phenomena).

There is basically not much 'physics' involved in the CERC formula, but its application in real cases is rather straightforward and illustrative. The CERC formula is classified as a bulk energy formula. It is interesting to note that afterwards, American researchers have continued developing transport formulae based on the

available energy, while European researchers have focussed more on a description of the sediment concentration and the flow velocity. In this respect we might speak of an 'American School' and an 'European School'.

The CERC formula is based on the observation that the longshore sediment transport is proportional to 'the longshore component of the wave energy flux per meter of coastline present at the outer edge of the breaker zone':

$$S_x = A' P \quad (6.27)$$

where:

$S_x$	total longshore sediment transport through breaker zone	[m <sup>3</sup> /s]
$A'$	coefficient	[see further]
$P$	longshore component of wave power (energy flux) entering the breaker zone	[W/m]

Note: the notion 'longshore component of the wave energy flux' suggests that the wave energy flux is a vectorial quantity. That is not true; it is a scalar quantity which formally cannot have a component.

From a dimension analysis of Eq.(6.27) it follows that the coefficient  $A'$  is actually not dimensionless.

The wave power (or energy flux) for a unit crest length is given by:

$$P = \frac{1}{8} \rho g H^2 c_g \quad (6.28)$$

where:

$H$	wave height	[m]
$c_g$	wave group celerity (= $nc$ )	[m/s]
$n$	ratio of wave group celerity and wave propagation speed	[-]

If the angle of the wave crest and the coast at the breaker line is denoted as  $\phi_b$ , then the wave power per unit length of beach is:

$$P \cos(\phi_b) = \frac{1}{8} \rho g H_b^2 n_b c_b \cos \phi_b \quad (6.29)$$

Here, the subscript  $b$  stands for the value of the respective parameter at the breaker line.

The longshore sediment transport depends, according to the basic idea of the CERC formula on the 'longshore component of Eq.(6.29)', so on  $\sin \phi_b$  times Eq.(6.29). The CERC formula now reads:

$$S_x = A \cdot H_b^2 n_b c_b \cos \phi_b \sin \phi_b \quad (6.30)$$

Note that in this equation the coefficient  $A$  is now a dimensionless coefficient (contrary to  $A'$  in Eq.(6.27)).

Using the CERC formula in real applications must be done carefully (like of course with all types of sediment transport formulae). In particular the value for the coefficient  $A$ , and the value for the wave height in case of an irregular wave train, requires carefulness. Both parameters are related. If one uses the root mean square wave height to represent an irregular wave field, then the value for  $A$  must be a factor

two *larger* compared with the value of  $A$  if one uses the significant wave height instead (note that for a Rayleigh distribution:  $H_s = \sqrt{2} \cdot H_{rms}$ ).

Based on work by among others Komar (1976) and Van de Graaff and Van Overeem (1979), it was concluded that the value for the coefficient  $A$  should be around 0.04 if one uses  $H_s$  (and so 0.08 if one uses  $H_{rms}$ ).

The CERC formula can be written in various ways, by introducing formulations from linear wave theory or by using geometry. This makes it even more important to find out which value for the coefficient needs to be applied. In all cases, at least one wave parameter at the breaker line is required.

### Physical justification and drawbacks

A kind of physical justification of the CERC formula can be found by considering the radiation shear stress. In Section 6.2 it was explained that the radiation shear stress is the main driving force for the longshore current in the breaker zone. If we use the wave conditions at the edge of the breaker zone, then Eq.(6.13) reads:

$$S_{yx} = E_b n_b \cos \varphi_b \sin \varphi_b \quad (6.31)$$

where:

$E_b$  the wave energy at the breaker line ( $= 1/8 \rho g H_b^2$ )

Comparing Eq.(6.30) with Eq.(6.31) shows that both formula are almost identical; the only difference is the (additional) parameter  $c_b$  in Eq.(6.30). So the CERC-formula might be considered as the product of a radiation shear stress term and the wave velocity at the breaker line. The wave velocity at the breaker line can be approximated by:

$$c_b \approx \frac{2}{\gamma} \hat{u}_0 \quad (6.32)$$

where:

$\gamma$  breaker index ( $= H_b/h_b$ ) [-]  
 $\hat{u}_0$  maximum orbital velocity at  $z = 0$  [m/s]

The radiation shear stress  $S_{yx}$  can be regarded as a measure for the longshore velocities in the breaker zone: these velocities are the transporting agents of the longshore sediment transport. The orbital velocity  $\hat{u}_0$  on the other hand might be regarded as a measure for the wave stirring, so for the sediment concentration. Apparently the CERC formula also multiplies a 'velocity' measure with a 'concentration' measure, in agreement with the quite general formulation of  $S = v \cdot c$ .

An important drawback of the CERC formula is that it does not give any information on the transport distribution. Such information is often required, for instance if bars are present in the coastal profile, or if coastal structures are considered that do not entirely cover the breaker zone (like groynes: see Chapter 11).

Another drawback of the formula is that it does not take into account the properties of the sediment. (Some researchers propose a particle size dependent value for  $A$  in Eq. (6.30).) The CERC formula was originally derived for beaches with uniform sand ranging between 175  $\mu\text{m}$  to 1000  $\mu\text{m}$ . The CERC formula does not take into account the slope of the beach profile. And it is noted that the CERC formula does not make a distinction between bed load and suspended load transport.

The CERC formula can not be used if other driving forces such as tidal currents become important.

### The $(S, \varphi)$ -diagram

The effect of the angle of wave incidence can be examined by considering the relation between  $S_x$  and the deep water wave angle  $\varphi_0$ . The CERC formula according to Eq.(6.30) can be rewritten as follows by assuming a value 0.04 for the coefficient  $A$ , assuming straight depth contour lines parallel to the shoreline, assuming  $n_0 = 0.5$  and by using refraction theory:

$$S_x = 0.02 H_0^2 c_b \sin \varphi_0 \cos \varphi_0 = 0.01 H_0^2 c_b \sin(2\varphi_0) \tag{6.33}$$

where:

- $H$  significant wave height [m]
- $0, b$  subscripts for deep water and at the breaker line

The wave propagation speed at the breaker line depends on the deep water wave angle as it depends on the wave refraction from deep water to the breaker line. In Example 6.4 (see next page) a whole range of sediment transports are computed for varying values of  $\varphi_0$ . ( $H_{rms}$  is used in Example 6.4!) Computed parameters for this example are also shown in Fig.6.16 (also see the iterative scheme presented in Example 6.4).

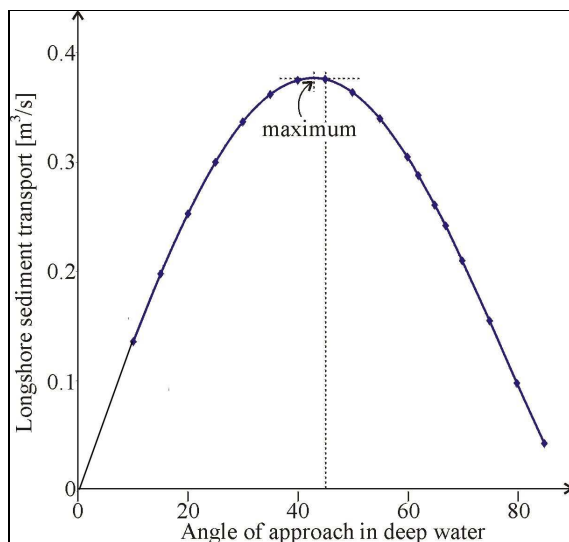


**Figure 6.16 Results of Example 6.4**

If we plot the longshore sediment transport in a graph against the wave angle in deep water, then a so-called  $(S, \varphi)$ -diagram is obtained. The results from the example indicate that the maximum longshore transport takes place for an angle just smaller than an angle of  $\varphi_0 = 45^\circ$ .

Although the term  $\sin(2\varphi_0)$  in Eq.(6.33) would suggest that the maximum of  $S_x$  occurs at exactly  $\varphi_0 = 45^\circ$  this is not true because the wave propagation speed at the breaker line also depends on the deep water wave angle.

**Example 6.4***Input parameters:*Offshore wave height:  $H_{rms} = 2$  mWave period:  $T = 7$  sBreaker index:  $\gamma = 0.8$ *Required:*Sediment transport rate  $S_x$  for different values of  $\varphi_0$ *Output:*

Choose  $\varphi_0$ . Calculate  $\varphi_b$  by trial and error (choose  $h$ , calculate  $H$ , check  $H/h > \gamma$  or  $H/h < \gamma$ , choose new  $h$ , repeat process). The results for various values of  $\varphi_0$  are presented in the table below. The sediment transport rate can now be computed using Eq.(6.33), but with coefficient times two since we are using  $H_{rms}$  instead of  $H_s$ . The results can be found in the table.

$\varphi_0$ [°]	$h_b$ [m]	$\varphi_b$ [°]	$c_b$ [m/s]	$S_x$ [m <sup>3</sup> /s]	$S_x$ [m <sup>3</sup> per year]
10.00	2.71	4.52	4.96	0.136	4,300,000
15.00	2.69	6.73	4.95	0.198	6,200,000
20.00	2.66	8.87	4.93	0.253	8,000,000
25.00	2.63	10.91	4.90	0.300	9,500,000
30.00	2.59	12.85	4.86	0.337	10,600,000
35.00	2.54	14.64	4.82	0.362	11,400,000
40.00	2.48	16.26	4.76	0.375	11,800,000
45.00	2.40	17.69	4.70	0.376	11,900,000
50.00	2.31	18.87	4.61	0.364	11,500,000
55.00	2.21	19.79	4.52	0.340	10,700,000
60.00	2.09	20.42	4.40	0.305	9,600,000
62.00	2.04	20.57	4.35	0.288	9,100,000
65.00	1.95	20.69	4.26	0.261	8,200,000
67.00	1.89	20.70	4.20	0.242	7,600,000
70.00	1.79	20.58	4.09	0.210	6,600,000
75.00	1.59	19.99	3.87	0.155	4,900,000
80.00	1.35	18.77	3.57	0.098	3,100,000
85.00	1.01	16.46	3.11	0.043	1,400,000

*Conclusion:*

The computed annual transports are rather high. In practical cases a net longshore transport of 1 million m<sup>3</sup> per year is already considered as a ‘heavy’ case. Often smaller net yearly transport rates occur. The reason for the high computed values are the rather severe conditions:  $H_{rms}$  of 2 m, from *one* direction, constantly present for the whole year.

**Example 6.4 Sediment transport rate  $S_x$  for different values of  $\varphi_0$** 

The  $(S, \varphi)$ -diagram also shows how the longshore transport reduces to nil for wave angles of 0° (perpendicular to the coastline: only wave stirring: no longshore current). For  $\varphi_0$  (nearly) 90° (waves run nearly parallel to the coastline): hardly any



wave energy reaches the coast by wave refraction; the radiation shear stress component is nearly 0 and due to the very small wave heights hardly any stirring occurs.

The  $(S, \varphi)$ -diagram further shows that the longshore transport changes almost linearly with the wave angle for small angles (to approximately  $20^\circ - 30^\circ$ ).

The practical use of  $(S, \varphi)$ -diagrams is further explained in Section 6.4.

### 6.3.3 The Bijker formula

In contrast to the bulk transport formula like the CERC formula, Bijker [Bijker (1971)] developed as one of the first a formula that is based on the concept of velocity times concentration (Eq.(6.26)) independent of the driving forces and could be used to determine the distribution of the longshore transport over the breaker zone. Later researchers have derived other transport formulae as well, but the Bijker transport formula is still a useful formula in longshore sediment transport computations.

The Bijker approach has been introduced in Section 4.4.4. There, it was explained how Bijker combined the effects of currents and waves on the bed shear stress. In Section 4.8 the Bijker transport formula has been described. It was shown that Bijker makes a distinction between bed load and suspended load transport.

The bed load transport formula of Bijker is based on the Kalinske-Frijlink transport formula which was originally developed for river applications:

$$S_b = BD_{50}v_* \exp \left[ \frac{-0.27\Delta D_{50}\rho g}{\mu\bar{\tau}_{cw}} \right] \quad (6.34)$$

where:

$B$	Bijker coefficient (5, see remarks in Section 4.6)	[-]
$D_{50}$	representative particle diameter	[m]
$v_*$	shear stress velocity	[m/s]
$\Delta$	specific density	[-]
$\mu$	ripple factor = $(C/C_{90})^{1.5}$	[-]
$C$	Chézy coefficient	[m <sup>0.5</sup> /s]
$C_{90}$	Chézy coefficient based on $D_{90}$	[m <sup>0.5</sup> /s]

The suspended load transport formula of Bijker was based on the suspended sediment transport formula of Einstein and could be expressed in terms of the bed load transport as follows:

$$S_s = 1.83QS_b \quad (6.35)$$

where:

$Q$	$[I_1 \ln(33h/r) + I_2]$
$I_1, I_2$	Einstein Integrals
$h$	water depth
$r$	bottom roughness

The total load transport follows from the summation of the bed load and the suspended load transport:

$$S_t = S_b (1 + 1.83Q) \quad (6.36)$$

The distribution of the longshore sand transport across the breaker zone denoted as  $s_x$  can be found by computing  $S_t$  for various positions in the cross-shore profile. This is illustrated in Example 6.5, where as a first step the longshore velocity distribution following Eq.(6.25) is used (triangularly shaped distribution with the maximum velocity at the breaker line)

With the Bijker formula the combined effect of waves and currents is taken into account. (Currents: irrespective the 'source' of the current; so e.g. tidal currents and/or wave driven currents.) This makes the formula more generally applicable than for instance a formula like the CERC formula. The Bijker formula can be applied 'everywhere' in the sea where the sediment transport can be approximated by the  $S = v.c$  concept with time averaged parameters.

If we like to compute with the Bijker formula the total longshore sediment transport in the surf zone, we can use any combination of driving forces for the computation of the longshore velocity.

Furthermore, the formula takes into account the effect of the sediment properties.

As explained in Section 6.2.7, many methods are available to compute the distribution of the longshore current velocity. These alternative methods obviously result in different transport distributions as well. See Fig.6.17; the transport distributions of Fig.6.17 have been calculated with the velocity distributions according to Fig.6.13.

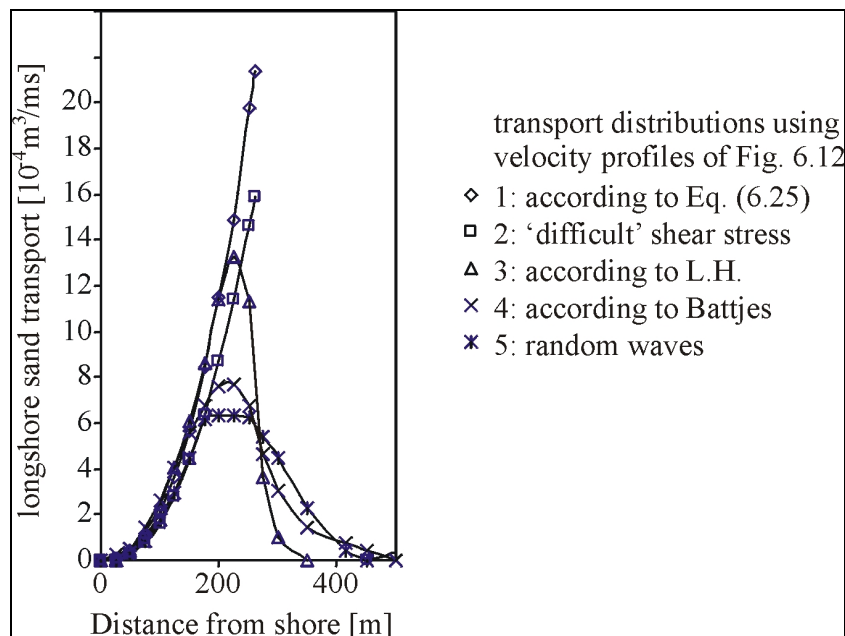


**Figure 6.17** Examples of transport distributions

**Example 6.5**

*Input parameters:*

- Offshore wave height:  $H_0 = 2$  m
  - Wave period:  $T = 7$  s
  - Offshore wave direction:  $\varphi_0 = 30^\circ$
  - Bottom slope:  $m = 1:100$
  - Breaker index:  $\gamma = 0.8$
  - Roughness height:  $r = 0.06$  m
  - Mean sand diameter:  $D_{50} = 200$   $\mu\text{m}$
  - 90% sand diameter:  $D_{90} = 270$   $\mu\text{m}$
  - Specific water density:  $\rho = 1000$   $\text{kg/m}^3$
  - Specific sand density:  $\rho_s = 2650$   $\text{kg/m}^3$
  - Particle fall velocity:  $w_s = 0.0252$  m/s
- Velocity distribution as computed in Example 6.3

*Required:*

Sediment transport using the Bijker formulation

*Output:*

For the computation of the sediment transport using the Bijker method, it is needed to compute the following parameters:  $C_{90}$ ,  $\mu$ ,  $\hat{u}_0$ ,  $\xi$ ,  $\tau_c$ ,  $\bar{\tau}_{cw}$ ,  $v^*_{cw}$ ,  $z^*$  and  $A (= r/h)$ .

Using Table 4.1 we can now find a value for  $Q$  and, after computing the value for the bottom transport  $S_b$ , the total transport  $S_t$ . Results of the computations can be found in the following table.

y	h	H	$\hat{u}_0$	V	$\mu$	$f_w$	$\xi$	$V^*_{cw}$	$z^*$	r/h	$S_b$	Q	S
[m]	[m]	[m]	[m/s]	[m/s]	[-]	[-]	[-]	[m/s]	[-]	[-]	[ $\text{m}^3/\text{ms}$ ]	[-]	[ $\text{m}^3/\text{ms}$ ]
											$\times 10^{-5}$		$\times 10^{-4}$
0	0	--	--	--	--	--	--	--	--	--	--	--	--
25	0.25	0.2	0.62	0.05	0.27	0.06	1.76	0.08	0.79	0.24	0.3	0.96	0.1
50	0.50	0.4	0.87	0.12	0.31	0.05	1.87	0.10	0.62	0.12	0.8	2.26	0.4
75	0.75	0.6	1.06	0.22	0.33	0.05	1.92	0.12	0.54	0.08	1.4	3.67	1.1
100	1.00	0.8	1.22	0.32	0.35	0.04	1.95	0.13	0.49	0.06	2.1	4.18	1.8
125	1.25	1.0	1.35	0.42	0.36	0.04	1.98	0.14	0.45	0.05	2.7	6.84	3.7
150	1.50	1.2	1.47	0.54	0.37	0.04	2.00	0.15	0.42	0.04	3.4	8.60	5.7
175	1.75	1.4	1.58	0.65	0.38	0.04	2.02	0.16	0.39	0.03	4.1	10.71	8.4
200	2.00	1.6	1.67	0.78	0.38	0.04	2.03	0.17	0.37	0.03	4.8	12.62	11.5
225	2.25	1.8	1.76	0.90	0.39	0.04	2.04	0.18	0.36	0.03	5.5	14.24	14.9
259	2.59	2.1	1.87	1.08	0.39	0.03	2.06	0.19	0.34	0.02	6.5	17.41	21.3

**Example 6.5 Sediment transport using the Bijker formulation**

The suspended sediment transport for the conditions of Example 6.5 is quite significant relative to the bed load transport. This is particularly the case closer to the

breaker line (greater depths). The high orbital velocities in the deeper sections of the breaker zone result in large transport rates. The large effect of the waves on the bed shear stress was already noticed in Chapter 4.

If we integrate the computed sediment transport distributions according to Fig.6.17 across the entire transport zone (that is the area where longshore transport has been computed: this includes at least the entire breaker zone), we get computation results for the total longshore transport. In spite of the significant differences in the distribution, the ultimate results show that the total computed sediment transport rates are not very sensitive to the distribution involved. The computed transports turn out to be all in the same range. From an energetics point of view, this may not be so surprisingly as in every computation the same amount of 'transport generating energy' is available. So if due to the selection of a certain velocity distribution the velocities (and the transport rates) reduce at the one place along the cross-shore profile, the velocities (and the transport) will increase at the other place.

### Sensitivity computations

In Example 6.5 only one set of input parameters was used. In practical cases it is worthwhile to examine the sensitivity of the output to varying values of certain input parameters. This is important as one generally does not exactly know the value for the bottom roughness, the grain size, the breaker index, or even the beach slope.

To get some feeling for the sensitivity of various parameters we have computed the total sediment transport (integrated across the transport zone) for varying values of  $r$ ,  $D_{50}$ ,  $m$  and  $\gamma$ . Note that these four parameters are no input parameters in the CERC formula.

The results are shown in Fig.6.18.

On the vertical axis the computed total transport is given divided by the reference transport rate ( $S_{ref} = 0.146 \text{ m}^3/\text{s}$ ). [The reference case holds for:  $H_{s,0} = 2.8 \text{ m}$ ,  $\varphi_0 = 30^\circ$ ,  $D_{50} = 200 \mu\text{m}$ ,  $\gamma = 0.8$ , roughness height  $r_w = r_c = 0.06 \text{ m}$  and slope 1:100.] On the horizontal axis of Fig.6.18, the value for the respective parameter divided by the reference value has been plotted.

The dots in the figure are the actual computational results; the lines have been drawn to connect these dots. This way of presentation is useful if one wants to show the relative effect of varying input conditions.

From the sensitivity computations it follows that the total transport reduces significantly with increasing values for the bottom roughness. Fig.6.18 also shows the large influence of the grain size. An increase in the grain diameter leads to a decrease in total transport. This may seem strange if one considers the position of  $D_{50}$  in the bottom sediment transport formula [Eq.(6.34)]. However, the grain diameter also influences the fall velocity (important for the suspended sediment transport part), the ripple factor and it occurs in the exponent part of Eq.(6.34). This is why the influence of the grain diameter on the transport is complex.

A steeper beach slope leads to a more narrow breaker zone and thus to a more narrow sediment transport zone. However, the sensitivity computations show that the total transport, i.e. integrated across the entire transport zone, hardly changes.

Finally, the results show that also the effect of the breaker index is not significant for the total transport; however, it does have a great influence on the transport distribution.

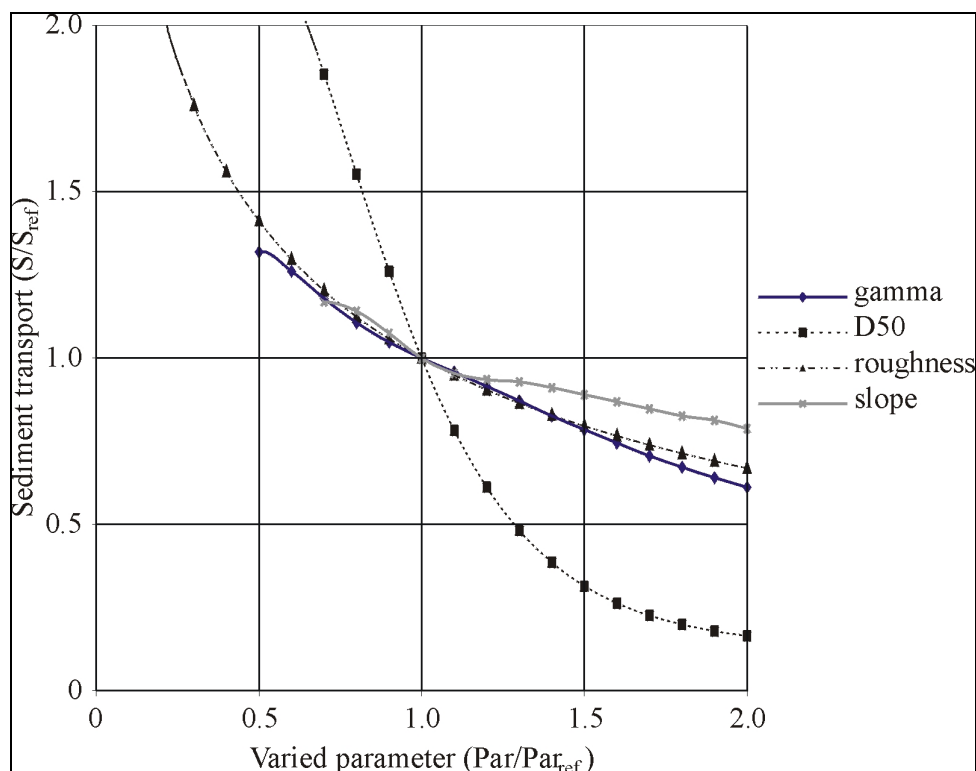


**Figure 6.18 Sensitivity analysis with UNIBEST-LT**

### 6.3.4 Other longshore transport formulae

Similar as what Bijker did, other researchers have also modified sediment transport formulae that were already available for river applications.

The various formulae differ particularly in the way the influence of the waves has been schematised. Each formula has a different sensitivity for varying input parameters. Differences in total transport between the various transport formulae can easily be up to a factor ten! This illustrates the absolute need for calibration data before results from computer computations can be used in specific coastal engineering cases.

Examples of such calibration data are observed coastline changes following a certain 'event' (such as the construction of a new harbour along a coastline, or the damming of a river and the subsequent erosion of the shoreline of the river delta).

## 6.4 Shoreline dynamics

### 6.4.1 Introduction

In the previous sections we have primarily focussed on a description of the longshore sediment transport and its underlying driving mechanisms. In Chapter 5, it was indicated that coastline changes may occur along coastal sections where gradients in the longshore transport occur. If we disregard sediment transport in cross-shore direction (to and from deeper water and to and from the hinterland), then the shoreline will recede in a situation where the longshore transport increases along the shoreline (erosion). The shoreline will move seawards if the longshore sediment transport decreases in the transport direction (accretion).

Changes in the position of the shoreline can be natural or man-induced, and can occur on various time- (for instance seasonal) and spatial scales.

Shoreline dynamics, which is the topic of this section, is a vital element of coastal engineering practice. The basic concept is that of a sediment balance analysis (Section 6.4.2). This concept has further been worked out in the single and multiple line theories which are presented in Sections 6.4.3 and 6.4.4.

Fig.6.19 shows typical examples of cases where the position of the coastline may change drastically.

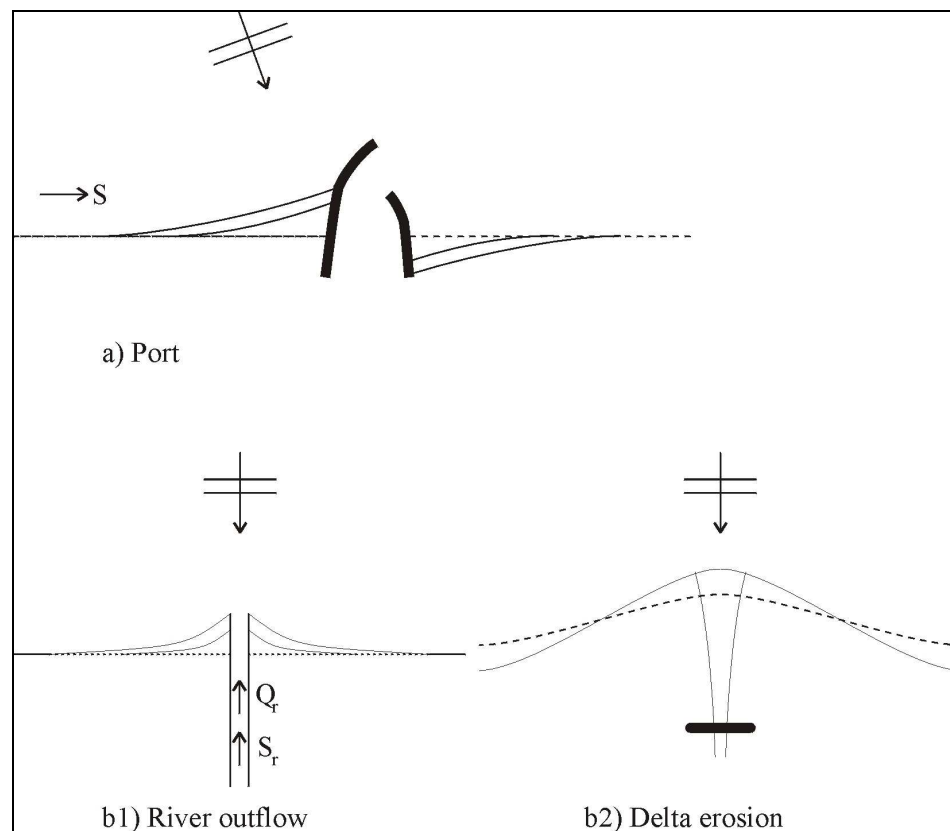


**Figure 6.19 Typical cases of possible drastic coastline change**

The first case considers a coastline with a wave driven resultant longshore transport from 'left' to 'right'. The construction of a traditional port with breakwaters leads to a blocking of this longshore sediment transport. As a result, the coastline to the left of the port will tend to move seawards (accretion), whereas the coastline on the right side (in this example) will tend to move landward (erosion).

The accretion is not always considered to be a problem, but if the accretion becomes too much and reaches the end of the breakwater it may reduce the water depth at the entrance of the port.

The erosion, on the other hand may undermine existing infrastructure, like roads and houses.

The second case in Fig.6.19 (b1) considers a prograding delta. This progradation is caused by the deposition of sediment which is being transported to the delta by the river discharge.

If a dam is constructed somewhere upstream the river, then the river discharge distribution changes. In many cases this means a significant lowering of the peak discharge (with a more or less constant mean discharge). The effect is that less sediment is being carried to the river mouth with shoreline erosion as result (b2). Such erosion may threaten the low-lying land of the delta and is often experienced as a serious problem.

In the example cases it is important to understand the observed coastline changes and to make reliable predictions of the future coastline changes.

If we plot the computed longshore sediment transport against the angle of wave incidence, then we get a so-called  $(S, \phi)$ -diagram (as introduced in Section 6.3). Such a diagram has proven to be useful in the analysis of (observed) shoreline changes. How this works is explained in Section 6.4.5. Concluding remarks are given in Section 6.4.6, where the role of cross-shore sediment transport is mentioned (further described in Chapter 7) and where complicating matters are briefly mentioned (further described in Chapter 8).

## 6.4.2 Sediment balance

Consider a stretch of coastline which is bounded by the high water mark (the dry beach) and the seaward end of a selected longshore transport zone (e.g. some distance further seaward than the width of the breaker zone). The stretch of coastline is further arbitrarily bounded on both sides (Fig.6.20).

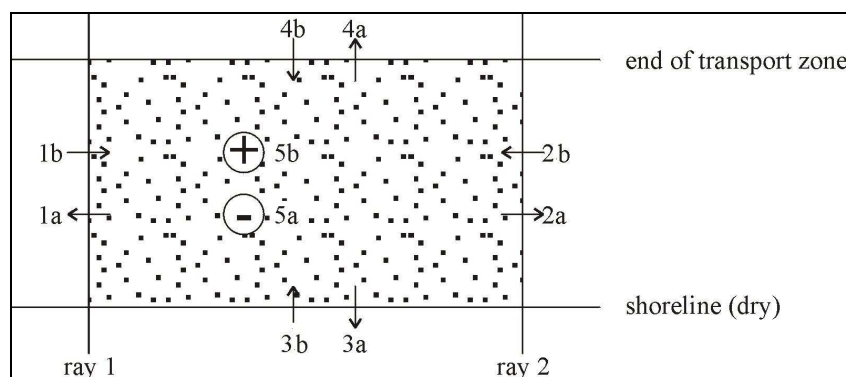


**Figure 6.20 Sediment balance** (*not to scale*)

Depending on the topic to be studied or the problem to be resolved, the mutual distance between ray 1 and ray 2 might vary. While the cross-shore distance in Fig.6.20 might be say 1 km, the longshore distance might be say 10 km. The sketch of Fig.6.20 is in that case certainly not to scale. (If we like to analyse the behaviour of a single cross-shore profile, the distance between ray 1 and ray 2 is only 1 m.)

If we compute, measure or determine somehow the sediment transport through each of these borders, then we can make up the sediment balance of the area. Also the time scale is important: short term sediment deficits (more sediment transported out of the area than is transported into the area), may occur while the longer term sediment balance is positive (accretion).

The longshore transports occurring during a given period of time (e.g. HW - LW cycle; month; year) are denoted with 1a, 1b, 2a and 2b in Fig.6.20 ('a' represents: out; 'b': in). Two comparable quantities (e.g. 1b and 2a) can be different for many reasons. For instance, because the wave angle relative to the shore orientation is different for ray 1 and ray 2, or because of longshore differences in the prevailing wave conditions.

The longshore transport under one specific wave condition (with a given  $H$ ,  $T$  and  $\phi$ ) generates a longshore transport in only one direction.

However, the occurrence of waves along a coast depends on the wind climate, which is often of stochastic nature. During a certain (long) period of time, for instance one year or one winter season, waves will occur that generate transports in two opposite longshore directions. Furthermore the effects of tidal currents on the sediment transports must often be taken into account.

If we add all the longshore transports occurring in one direction and also in the other direction, then we find two contributions to the net transport in opposite directions. These contributions have been shown in Figure 6.20. For the sediment balance it is important to know both. Summation of the two contributions to the transport rates through rays 1 and 2 gives the net sediment transport through these rays. The dimension of this net transport depends on the period of time over which the wave and other relevant hydraulic conditions are considered. If this is one year, we get [ $\text{m}^3/\text{y}$ ] for the dimension of the sediment transport. As a reference: the net yearly transport in the central part of the Dutch coast (Wassenaar - Zandvoort) is often assumed to be approximately 200,000  $\text{m}^3/\text{y}$  in northward direction.

The sediment balance is not complete without considering the transport in the cross-shore direction.

Aeolian (wind-induced) sediment transport, for instance, is the basic mechanism for the formation of dunes. Aeolian transport takes place on a dry surface and can be quite substantial in some cases. Several Aeolian transport formulae have been developed by different researchers. Reference is made to Swart (1986); Swart gives an overview of them. Clearly, Aeolian transport can also contribute to the sediment balance of the coastal area; e.g. transport 3a in Fig.6.20 representing a loss of material out of the balance area.

Depending on the (own selected) position of the landward border of the balance area, the sediment transport rates 3a and 3b refer to Aeolian transport only, or to a combination of Aeolian and hydraulic transport.

Also the sediment transport that crosses the lower border of the selected coastal area must be known. These onshore-offshore sediment transport mechanisms are



discussed in Chapter 7. Similar as for the longshore sediment transport, two direction related contributions to this cross-shore transport will take place within a certain period of time. The time scales of the governing processes behind longshore and cross-shore sediment transport are generally not the same. Cross-shore profile changes develop generally more rapidly (days) than changes in the shoreline (years). Anyway, for the sediment balance of the selected area, the resultant cross-shore transport ( $4a+4b$  in Fig.6.20) is important.

The sediment balance is further influenced by local influences inside the considered coastal area (indicated in Fig.6.20 with transport modes 5a and 5b). In agreement with the other annotations, 5a represents all possible sediment sinks, while 5b represents possible sediment sources.

Examples of sediment sinks are sediment mining or subsidence of the subsoil. At various places around the world, sand excavation from the beaches (for instance used for construction purposes) is an important reason for shoreline retreat. Sometimes, rather unusual mechanisms contribute to the sink term in the sediment balance, for instance the presence of a deep canyon from where any deposited sediment can not return.

Examples of sediment sources are dredge disposal or sediment input from rivers. The input from rivers can be highly season dependent (rainy season or not). There are numerous examples where the construction of a dam greatly reduced the sediment transport to the sea, which changed the sediment balance of the receiving coastal area into a negative one. Erosion of (parts of) the shoreline is the ultimate result (Section 6.4.4).

After we have determined the various contributions to the sediment balance for a certain stretch of coastline (1a to 5a as sediment losses and 1b to 5b as sediment sources), then we can determine the final result.

$$in + out = \sum_{i=1}^{i=5} (ib - ia) = \text{variation in sediment balance} \quad (6.37)$$

Although the balance area of Fig.6.20 might be quite arbitrary, if the area includes the coastline, it might be interesting to look what is the effect of the outcome of Eq.(6.37) to the position of the coastline. There are different ways to compute these coastal changes. In the simplest approach it is assumed that the shape of the coastal profile itself does not change over the considered period of time. The coast is then schematised as one single line, which moves seaward (accretion) or landward (erosion) depending on the sediment balance. The one-line theory is based on this approach (Section 6.4.3).

Multiple line theories (Section 6.4.4) are based on the same principle, but now the coastal (cross-shore) profile is split up into a number of sections (depth zones), which can each be represented by one line. This is a simple method to account for the fact that different depth zones respond differently to changing sediment budgets.

The basic ideas behind keeping the sediment balance of an area like in Fig.6.20 is also used in complex morphological computer models. To that end we cover a total area of interest with a large number of linked small balance areas; the area is covered by a fine grid. By doing so, we compute the sediment balance of a great number of small coastal areas.

Such detailed morphological models are generally used in complex areas or in

complex applications (Chapter 8). They are generally expensive to run, use a lot of computer power and require professionally skilled people to interpret the computation results and to apply the results in practical problems. Since this Section 6.4 is only meant to present some fundamentals of shoreline dynamics, these models are not discussed any further here.

### 6.4.3 Single line theory

The first one who described the single line theory was Pelnard-Considère [1956].

The basic assumption is that the shape of the cross-shore profiles does not change while the position of the coastline is changing with time. The entire profile moves seaward or landward with a horizontal distance  $a$  depending on the sediment balance. Fig.6.21 shows that this assumption requires also the assumption of a more or less horizontal part in the underwater profile; otherwise, unrealistic large quantities of sand might be required for a small seaward movement of the shoreline.

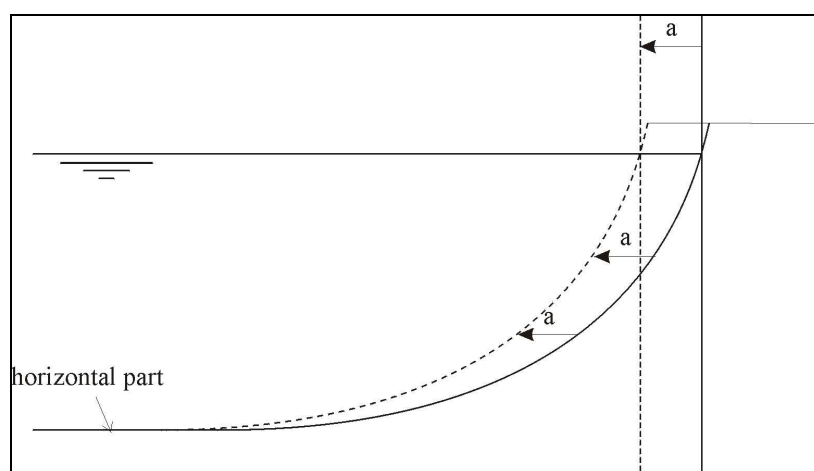


**Figure 6.21** Single line theory

In practical applications, one usually takes the so-called closure depth as the lower limit of the coastal profile. Depth changes seaward of this closure depth are then assumed not to directly contribute to the shoreline dynamics. The closure depth can be regarded as the depth where, for the considered period of time (normally years), only relatively small cross-shore sediment transports take place.

The closure depth can be determined by considering the highest waves that may occur during a relevant period of time. For an order of magnitude of the closure depth one might think at the range between MSL  $-6$  m to MSL  $-12$  m.

The upper limit to be taken into account of a cross-shore coastal profile in a single line theory, depends on the question whether the coast is eroding or not.

If the coast is eroding, the upper limit is often the height of the dunes. The dunes should, in case of erosion, be a part of the sediment balance area.

In case of accretion, the upper limit is determined by the representative wave run-up added to the high water level. This is usually about 1 m to 3 m above MSL.

In the discussions below, this subdivision is not made; it is assumed that the profile moves horizontally over a height  $d$  independent of the question whether it is an accreting or an eroding coast.

## Equations

We consider a coastal section with length  $dx$ , which 'receives' a longshore sediment input  $S_x$  from the left border and 'loses' a longshore sediment transport  $S_x + dS_x$  from the right border (Fig.6.22). Starting at time  $t$ , the shoreline moves until  $t + dt$  over a distance  $dy$ . This movement occurs over the profile height  $d$ .

The continuity equation now follows from the notice that the inflow (of sediment) minus the outflow equals the volume accumulated (from which the shoreline movement can be determined):

$$\frac{dS_x}{dx} = -d \frac{dy}{dt} \quad (6.38)$$

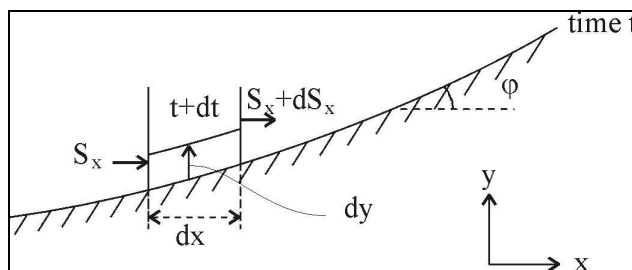


**Figure 6.22** Definition sketch for single line theory

Since we are interested in shoreline dynamics, thus in  $dy/dt$ , we need another equation to determine the left term in Eq.(6.38). For this we can use the 'equation of motion'. The longshore transport may vary along the coast for various reasons. Here we assume that the wave conditions do not vary; only the wave angle with respect to the orientation of the coastline varies because of changes in the orientation of the shoreline (and depth contours). In Section 6.3, the  $(S, \varphi)$ -diagram was introduced. It was indicated that as long as the wave angle is small and the changes in wave angle remain small (along the shoreline), the change in the longshore transport per unit change in wave angle, is constant. In fact, we then use the tangent of the  $(S, \varphi)$ -diagram at the point in the diagram where  $\varphi = 0^\circ$ . The equation of motion then becomes:

$$\frac{dS_x}{d\varphi} = -s \quad (6.39)$$

where:

$s$  coastal constant defined by Eq.(6.39)  $[(m^3/y)/rad]$

From Fig.6.22 it can be seen that  $\varphi = dy/dx$ . This means that as long as  $d\varphi$  remains small:

$$\frac{d\phi}{dx} = \frac{d^2 y}{dx^2} \quad (6.40)$$

Combination of Eqs.(6.39) and (6.40) gives the following parabolic differential equation for one-line modelling:

$$-s \frac{d^2 y}{dx^2} + d \frac{dy}{dt} = 0 \quad (6.41)$$

To resolve this equation we need one initial boundary and two boundary conditions. Very often these conditions are the position of the coastline at  $t = 0$  (the initial situation) and the sediment transport on both borders of the coastal area as a function of time.

Computer programs are available to resolve Eq.(6.41) and, (even more directly) also Eq.(6.38). Below, we consider a simplified analytical solution to show the principles of shoreline changes near a breakwater.

### Application to accretion near breakwater or jetty

Consider the (sudden) construction of a breakwater or a jetty running perpendicular to an initially straight shoreline (Fig.6.23). If the longshore transport is from left to right, then very often the coast to the left of the structure is called the 'updrift' coast, whereas the coast to the right of the breakwater is called the 'downdrift' coast.

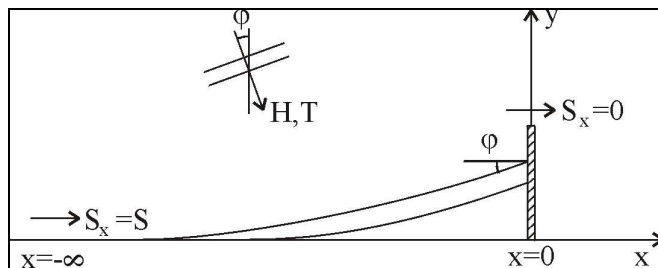


**Figure 6.23 Accretion of the shore near a breakwater. The wave conditions given in the sketch refer to the conditions at the assumed horizontal part in the coastal area**

The length of the breakwater is assumed to reach so far into the sea that the head of the breakwater is situated somewhere in the (more or less) horizontal part of the cross-shore profile as was indicated in Fig.6.21. If we further assume that the breakwater is impermeable for sand (no sand particles slipping through the pores of the breakwater), then the local longshore transport at the breakwater must be zero (100% blocking). This means that the wave angle at this particular point along the coastline with respect to the orientation of the coastline, must be zero as well. As the wave conditions at the horizontal part of the coastal area do not change, the only option is that the coastline rotates in such a way that the wave angle relative to this rotated coastline becomes zero (Fig.6.23).

The changes in the coastline will not (immediately) influence the shoreline over large distances. So, at a point at a great distance away from the breakwater the sediment transport remains the same.

With the help of Eq.(6.41), applying the reference system of Fig.6.23 and using the following initial and boundary conditions, the shape of the coastline of the updrift side of the breakwater can be calculated as a function of time.

- Starting (initial)condition:  $y = 0$ , for  $t = 0$  and for  $-\infty < x < 0$
- Left boundary condition:  $S_x = S$ , for  $x = -\infty$  and for all  $t$
- Right boundary condition:  $S_x = 0$ , for  $x = 0$  and for all  $t$

Note that the shoreline at the breakwater moves seaward, which means that the relative length of the breakwater, that is the distance between the actual position of the shoreline and the head of the breakwater, gets smaller. As a consequence the breakwater may, after some time of shoreline accretion, no longer block the whole transport zone. Sediment will start to by-pass the breakwater, so that the third boundary condition is no longer fulfilled (the solution 'stops').

In this example, however, we assume that the length of the breakwater is still long enough for the time being.

The resulting solution to Eq.(6.41) is:

$$y(x,t) = \varphi \sqrt{\frac{4at}{\pi}} \left[ \exp(-u^2) - u\theta\sqrt{\pi} \right] \quad (6.42)$$

where:

$x$  distance along the beach ( $x = 0$  at the breakwater) [m]

$y$  position of the shoreline (see Fig.6.23) [m]

$t$  time [y]

$d$  profile height [m]

$$a = \frac{s}{d} = \frac{S}{\varphi d} \quad [(\text{m}^3/\text{y})/\text{rad m}]$$

$$u = -\frac{x}{\sqrt{4at}}$$

$$\theta = 1 - \frac{2}{\sqrt{\pi}} \int_0^u \exp(-u^2) du$$

With the solution according to Eq.(6.42) it can be shown that the influence of the breakwater (in terms of accretion of the shoreline relative to the accretion at the breakwater) is negligible at a distance  $5\sqrt{at}$ . So, the influenced shoreline is longer in situations with larger undisturbed sediment transport, with smaller wave angles and with smaller profile heights. The influenced coastal area, of course, also expands in time.

If we focus on the accretion of the shoreline at the breakwater  $L(t)$ , then it can be derived that:

$$L(t) = 2\sqrt{\frac{\varphi S}{\pi d}} \cdot \sqrt{t} \quad [\text{m}] \quad (6.43)$$

Since time is present under the square root in Eq.(6.43), the progress of the shoreline slows down with time. Time needs to be multiplied by four to double a certain accretion length at the breakwater.

Eq.(6.43) further shows that accretion occurs more rapidly in situations with a large sediment transport (which is very logical).

The total surface area updrift of the breakwater is a function of  $L^2$ . From Eq.(6.43) it follows that this is inversely proportional to the profile height.

The effect of the wave angle can also be explained with Eq.(6.43). Assuming that in two cases (large and small wave angle) the same longshore sediment transport takes place, the case with the large wave angle yields a larger accretion at the breakwater than the case with the small wave angle, given a same time lapse. On the other hand, accretion at larger distances from the breakwater is larger for small wave angles.

An application of the above analytical solution is given in Example 6.6. Example 6.6 also gives the coastline accretion as computed with the computer program Unibest. The two approaches (i.e. analytical equations and numerical solution of Eq.(6.41)) give similar results.

Note that the annual sediment transport in Example 6.6 is  $10.6 \cdot 10^6 \text{ m}^3/\text{year}$ . This is a very high yearly sediment transport rate. (Rather high waves were assumed, occurring the entire year.) If the wave conditions as were given, will last e.g. for half a year (in remaining months no wave action is then assumed), the annual transport reduces with a factor 0.5. The time for the morphological developments to reach the end of the breakwater doubles in that case from 15 years to 30 years. Once more it is underlined how important it is to properly estimate the annual sediment transport rate.

In determining the coastline changes computed with the analytical approximation it is assumed that no sediment by-pass occurs at the head of the breakwater (right boundary condition  $S = 0$ ). This is not such a strict requirement in a numerical model. In a numerical model the transport zone might extend further seaward. Consequently, the by-pass gradually builds up in the numerical model, which also influences the orientation of the coastline. Further reference is made to Section 6.4.5.

The coastline changes at the lee side of the breakwater ('downdrift', or 'downstream') can also be calculated with the help of Eq.(6.41). (Realize that for this situation an 'own' set of initial and boundary conditions must be formulated.) With a similar set of conditions as for the updrift side, then the coastline changes at the downdrift side show essentially a mirror image of the coastline changes at the updrift side. The total volume of accreted sediment equals the total volume of eroded material. This is illustrated in Fig 6.24, where the dashed line shows the mirrored position of the eroded coastline.

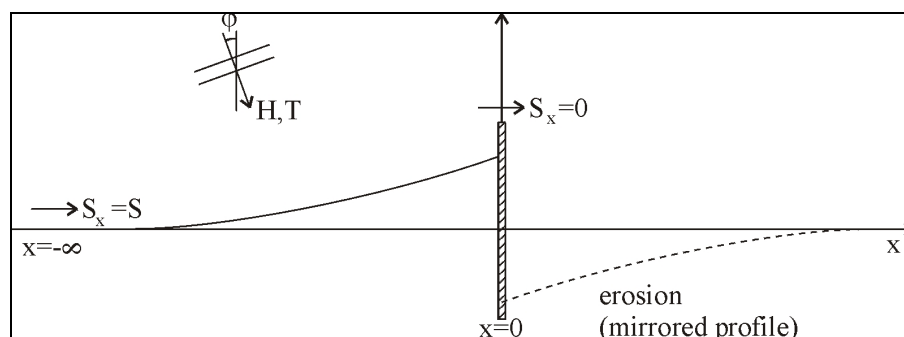


**Figure 6.24 Shoreline development at the lee side of a breakwater (simplified)**

**Example 6.6***Input parameters:*

Offshore wave height:	$H_0$	=	2 m
Wave period:	$T$	=	7 s
Offshore wave direction:	$\varphi_0$	=	30°
Bottom slope:	$m$	=	1:100 to a depth of 7 m, thereafter

horizontal bed for a significant length.

Parallel beach contour lines in undisturbed situation.

Breaker index:	$\gamma$	=	0.8
Breaker depth:	$h_b$	=	2.59 m (see Example 6.4)
Breaker angle:	$\varphi_b$	=	12.85° (see Example 6.4)
Sediment transport:	$S$	=	10.6·10 <sup>6</sup> m <sup>3</sup> /year (see Example 6.4)
Breakwater length:	$L$	=	3250 m
Breakwater end slope:	$m_b$	=	1:3

*Required:*

Number of years needed before the sediment transport starts to by-pass the breakwater and the coastline development during this time-span.

*Output:*

First compute the effective blocking length of the breakwater. This is determined by the breaker depth  $h_b$ , the length of the breakwater and the slope values:

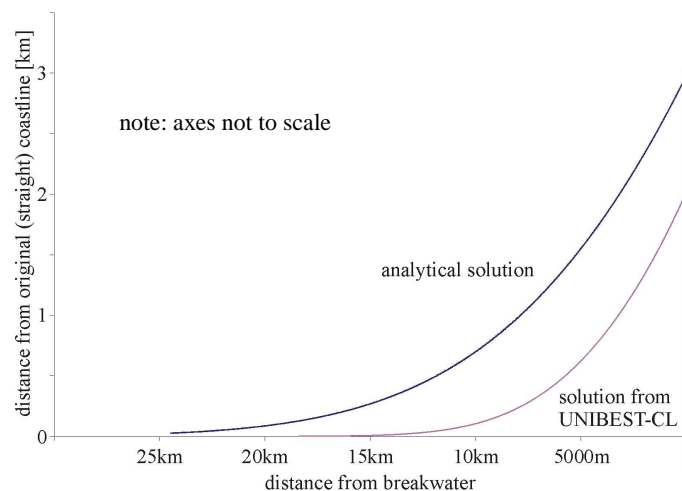
$$L_{\text{blocking}} = L - (1/m - 1/m_b) \cdot h_b = 3250 - (100 - 3) \cdot 2.59 \approx 3000 \text{ m}$$

The wave angle at the beginning of the beach slope can be found using the approach described in Example 6.3 and is found to be:  $\varphi' = 20^\circ$ . The time needed for the sand to accumulate to the point that it is no longer blocked by the breakwater is found using a rewritten Eq. (6.43):

$$t = 0.785 \frac{L^2 d}{S \varphi'} = 0.785 \frac{(3000)^2 (8)}{(10.6 \cdot 10^6)(0.35)} \approx 15 \text{ year}$$

Note that  $\varphi'$  has been expressed in radians in the above expression. The height  $d$  (8 m) is found by the water depth of 7 m and a wave run-up of 1 m.

This has also been computed with the computer model Unibest-CL, but now by using the Bijker transport formula. The longshore transport is less than 50% of that according to the CERC result. This is why the position of the coastline after 15 years based on UNIBEST-CL differs from the analytical solution (see figure below).

**Example 6.6 Application of single line theory to a breakwater**

The total surface of the accretion and the erosion areas are not equal by definition. This can be understood by considering the profile height in the accreted and the eroded areas. Accretion normally takes place over the height of the active part of a cross-shore profile added by a modest part of the profile related to water level fluctuations and wave run-up. Erosion also takes place in the higher parts of the coastal profile (upper parts of the beach and ultimately even the dunes). The profile height of an erosion area is usually larger than that of an accretion area, so that the surface of the erosion area is smaller than that of the accretion area.

The presence of the breakwater influences the wave conditions at the lee side of the breakwater. Sheltering of incoming waves leads to an area close to the breakwater where less wave energy occurs than on a fully exposed part of the coastline. Diffraction and directional wave spreading are two mechanisms that bring part of the wave energy into the sheltered area. The consequences are lower wave heights and altered wave directions and complicated transport patterns in the very downdrift side of the port.

The differences in wave conditions will lead to differences in wave set-up as well. Differences in wave set-up lead to a slope in the water level in longshore direction, which generates a longshore flow towards the breakwater. With this longshore flow sediment is being carried into the sheltered area. The resulting coastline development is shown schematically in Fig 6.24.

### Critical review of one-line theory

The single-line theory of Pelnard-Considère makes it possible to make hand (analytical) computations of coastline changes, and by doing so, to make a tentative assessment of the impact of certain coastal structures on the shoreline development. However, the single line theory has important restrictions, because of the assumptions that have to be made.

Consider, for instance, the shoreline accretion updrift of a breakwater with length  $L$ . According to the single line theory, the accretion near the breakwater ( $L(t)$  in Eq.(6.43)) continues till the moment that  $L(t) = L$ . (Till that moment  $S = 0$  in front of the breakwater is assumed.)

In reality, however, the accretion of the coastline near the breakwater (according to Eq.(6.43)) will slow down when the coastline approaches the head of the breakwater. The underwater profile, and the zone where sediment transport might occur, extend beyond the head of the breakwater (which creates unrealistic bottom slopes in front of the breakwater). Sediments will be transported in front of the head of the breakwater; however, the accretion at some distance updrift from the breakwater will continue as there are still gradients in the longshore transport.

Sediment by-pass around the head of the breakwater increases with increasing time. Basically this means that the right boundary condition ( $S_x = 0$  for all  $t$ ) does not hold anymore, and consequently that the wave angle (or the shoreline orientation) at the breakwater is gradually shifting from  $\varphi$  to  $0^\circ$  at  $t = \infty$  (which was the original shoreline orientation). This can not be simply handled with the equations of Pelnard-Considère.

Another restriction is that we can not account for variations along the coast, for instance, in the wave angle (or the shoreline orientation with fixed offshore wave angle), sediment characteristics, cross-shore profiles (note that the shape of an



accreting profile often differs from the shape of an eroding profile); nor can we take tidal influences into account. For these reasons, the equations following the single-line theory of Pelnard-Considère are not often used in real coastline engineering cases. However, computer programs like for instance Litpack, Genesis or Unibest, are all based on the single line theory. These models use numerical solutions of Eq.(6.41) [or even better Eq.(6.38)] and these models have the option to include the above-mentioned items. The use of these computer programs can only be done by skilled people who are aware of the weaknesses of the single-line theory.

#### 6.4.4 Multiple line theory

If we use multiple lines instead of one single line to schematize the coastal profile, then we can take cross-shore exchange of sediment into account. Even for a two-line approach, it becomes difficult to find analytical expressions for the movement of the two depth contours (Bakker (1968) did so for a two-line approach). Instead, numerical solution techniques are generally followed as, for instance programmed in the computer model PonTos [Steetzel *et al.* (1999)].

For instance the multi-layer model PonTos is based on the assumption that the cross-shore profile can be schematised as a number of mutually coupled layers, defined between fixed (but freely to be chosen) profile depths (Fig.6.25).

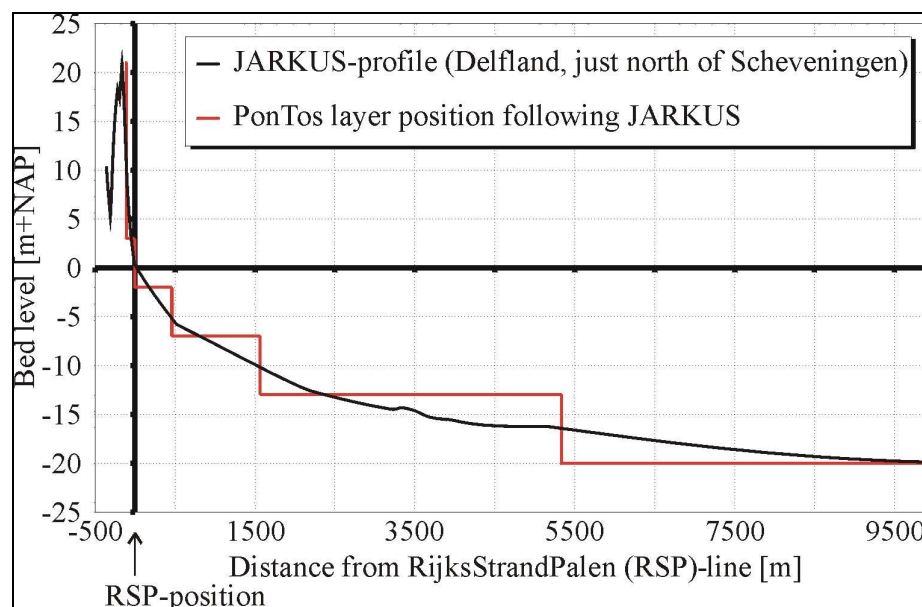


**Figure 6.25 PonTos layer schematisation**

The actual shape of a cross-shore profile is schematized as some kind of a staircase with steps of different (chosen) heights and lengths (lengths: depending on the actual shape of the cross-shore profile). The model intends to cover a large part of the coast; so many cross-shore profiles have to be schematized.

The ultimate aim of the model is in fact to properly predict the behaviour with time of the various vertical parts of the steps of the various cross-shore profiles. The

PonTos model is primarily meant to be used for the simulation of the coastal behaviour over long periods of time

Consider the positions of the vertical lines a, b and c of the staircase with respect to the reference line in Fig.6.25. The vertical line b represents in fact the sloping part of the cross-shore profile between the horizontal lines 1 and 2 in Fig.6.25. The position of line b might change due to gradients in the longshore sediment transport over the sloping part of the cross-shore profile represented by vertical line b.

Furthermore the position of line b might change due to cross-shore transport processes. The position of line b will change by cross-shore transports from step a to b over line 1 (and vice versa) and from step b to c over line 2 (and vice versa). The power of models like PonTos is that the quantification of the transport rates for the many time steps of a model simulation occurs very efficiently. E.g. for the quantification of the cross-shore transport between the steps a and b in Fig.6.25 use is made of the length of the horizontal part of the step between a and b. If that length is for instance smaller than the so-called equilibrium length (the cross-shore profile is then locally steeper than the equilibrium shape) a seaward directed transport is calculated. If that length is larger than the equilibrium length, a transport from step b to a is expected.

(More details concerning cross-shore sediment transport are discussed in Chapter 7.)

The model needs a series of site specific constants. In the present set-up of the model these constants are determined within the model on the basis of external conditions such as wave climate, tidal conditions, bathymetry and sediment characteristics. In this way a user-friendly behaviour-oriented model has been formulated [Steetzel (1997c), (1998)]. The model is still constantly improved and extended to involve more physical processes and effects (like diffraction, etc.).

#### 6.4.5 Application of a $(S, \varphi)$ -diagram

In the previous sections we considered coastline changes caused by spatial gradients in the longshore transport, where these transports were generated by a single wave condition. It was shown that the relation between the longshore transport  $S$  and the wave angle  $\varphi$  could be approximated by a linear function as long as the wave angle was small enough (less than  $20^\circ$  -  $30^\circ$ ). In real applications we are not particularly interested in the effect of one single wave condition, but in the effect of a full wave climate.

A local wave climate is schematised as a set of individual conditions. These individual conditions are described by a number of parameters, namely:

- the significant wave height  $H_s$  (e.g. at the deep water boundary);
- the accompanying peak wave period  $T_p$ ;
- the angle of wave approach  $\varphi$ ;
- the storm-related set-up  $h_s$ ;
- the fraction of occurrence of the combination of previous four parameters.

The wave climate consists of a distinct number of individual conditions for which the sum of all fractions of occurrence equals 1 (or 100 per cent, or 365 days per year). The longshore variation of the yearly wave climate might be taken into account by relating a specific wave climate to a specific longshore position.

For each of the occurring wave conditions it is possible to determine the relation between  $S$  and  $\varphi$ . If we further combine all results taking into account the

percentages of occurrence of each considered wave condition, we then can compute the year-averaged  $(S, \varphi)$ -curve. Usually, one uses computer programs, like Unibest-LT for this purpose. Example 6.7 shows the computed  $(S, \varphi)$ -curve using the input data as specified (with all non-mentioned input parameters set in Unibest-LT at 'default-values'). The longshore transport for the reference coastline orientation ( $\varphi = 0^\circ$ ) in this fictive example, is 490,000 m<sup>3</sup>/y. This reduces to zero if the coastline rotates over 15°.

The angle for which  $S = 0$  is sometimes called the equilibrium orientation. This is in fact a somewhat confusing term; every specific coastline section with no net sediment gain or net loss is in equilibrium. (Equilibrium:  $S_{in} = S_{out}$  even if  $S_{in} = S_{out} \neq 0$ .) Equilibrium or not is not related to sediment transport rates, but to gradients in the sediment transport.

In areas where the wave conditions are affected by non-uniform bottom topographies, by natural coastal features like headlands, or by man-made structures like breakwaters, the shape of the  $(S, \varphi)$ -curve might change as a function of the position along the coastline. This is illustrated in Example 6.8 (page 165). If we have in case of the conditions of Example 6.7 a long breakwater in mind which interrupts the net sediment transport, in the very leeside of the breakwater the waves from the wave direction sector +45° will not be present: they are shielded off by the long breakwater. If we eliminate the waves from sector + 45°, then the longshore transport for the original reference orientation reduces to 110,000 m<sup>3</sup>/y. The 'zero-transport' orientation is reached in this case after a rotation of the coastline of only 3°. The two computed  $(S, \varphi)$ -curves, one for the fully exposed coast and the other for the coasts with selective wave shielding, are plotted in Example 6.8.

The coastline 'behaviour' depends on the local  $(S, \varphi)$ -curve. Since  $(S, \varphi)$ -curves may vary along the coastline, also the coastline dynamics may be different from the one position to the other along the coast.  $(S, \varphi)$ -curves are a helpful tool to analyse coastline dynamics as will be illustrated in the examples of the coast with (long) breakwater.

**Example 6.7**

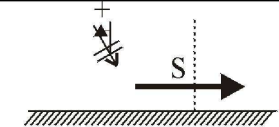
*Input parameters:*

Bottom slope:  $m = 1:100$  from MSL to MSL -20 m

Wave input at MSL -20 m; transport zone from MSL -10 m

Wave conditions:

	direction with respect to shore normal			
$H_s$	-45°	-15°	15°	45°
0.5	10	10	25	8
1.0	8	15	35	16
2.0	4	10	21	11
4.0	1	1	4	2



positive wave angles give positive sediment transports

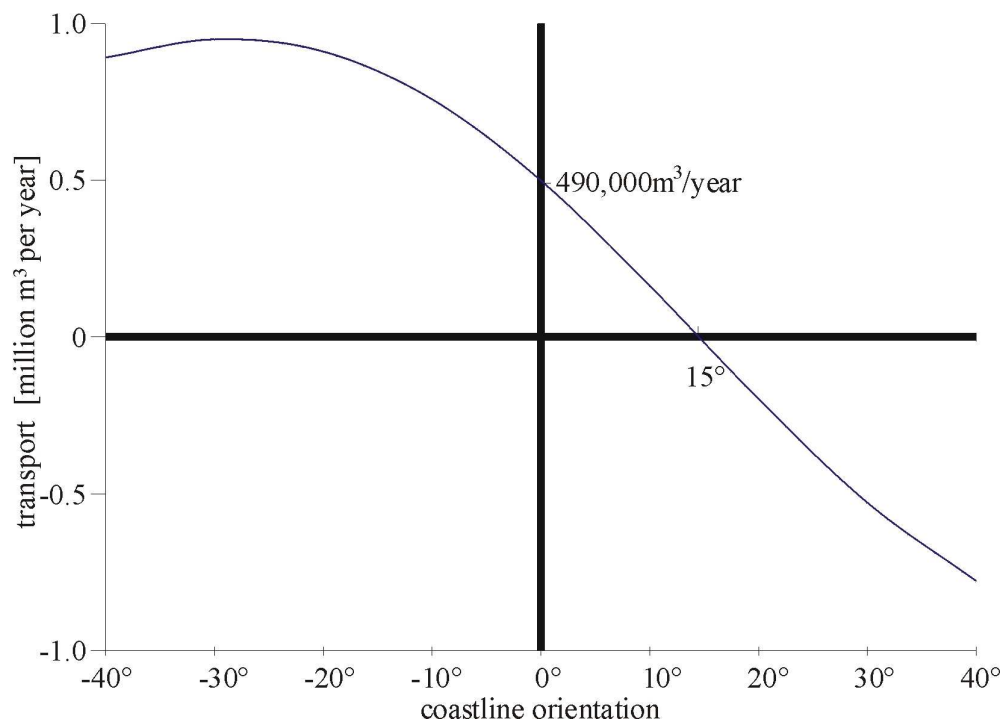
Number of days per year with no (onshore directed) waves:  $365-181=184$

Sediment properties:  $D_{50} = 200 \mu\text{m}$

*Required:*

$(S, \varphi)$ -curve

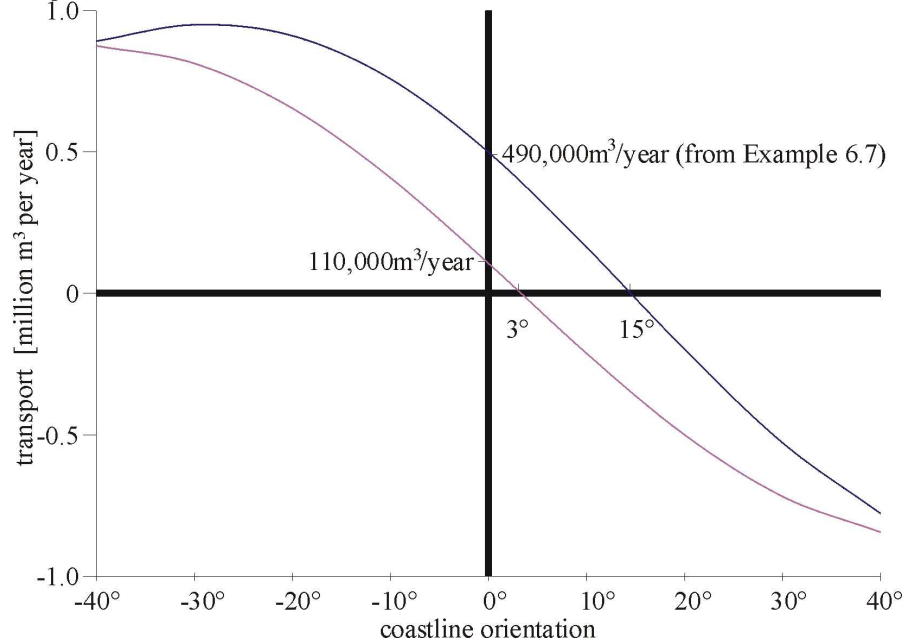
*Output:*



*Conclusion:*

- 1) For the reference coastline orientation the yearly longshore transport is  $490,000 \text{ m}^3$ .
- 2) If the coastline rotates over  $15^\circ$ , the total longshore transport becomes  $0 \text{ m}^3/\text{year}$ .
- 3) The relation between transport  $S$  and coast orientation  $\varphi$  is not linear.

**Example 6.7  $(S, \varphi)$ -curve**

**Example 6.8***Input parameters:*As in Example 6.7, but without waves from direction  $45^\circ$ *Required:*Changes in  $(S, \varphi)$ -curve*Output:**Conclusion:*

- 1) Shielding of waves from direction  $+45^\circ$  gives a yearly longshore transport of  $110,000 \text{ m}^3$ . This is a reduction of 75%!
- 2) The angle for which  $S = 0 \text{ m}^3/\text{year}$  changes from  $15^\circ$  to  $3^\circ$ .

**Example 6.8  $(S, \varphi)$ -curve (partial blocking of waves)****Coast with (long) breakwater**

Consider a (long) straight coastline with an incoming longshore transport  $S_m$  which equals the outgoing longshore transport  $S_{out}$  (see Fig.6.26; next page). The coastline is in equilibrium (there is just a constant sediment transport along the coast.) The 'equilibrium' orientation of the coastline (orientation of the coastline for which the sediment transport is zero) follows from the  $(S, \varphi)$ -curve that can be computed for the fully exposed coast (see line 'ray 1 (= ray 8)' in Fig.6.27).

Let us assume that this is the starting situation as drawn in Fig.6.26. Next, we consider the effect of a breakwater. This breakwater is assumed to be long enough to block the longshore transport for a certain period of time. The sediment by-pass around the head of the breakwater can be neglected for the first period of time.

The annual offshore wave conditions cover a wide range of wave directions. Only the wave directions that can actually reach the coast will be taken into account when computing the  $(S, \varphi)$ -curve.

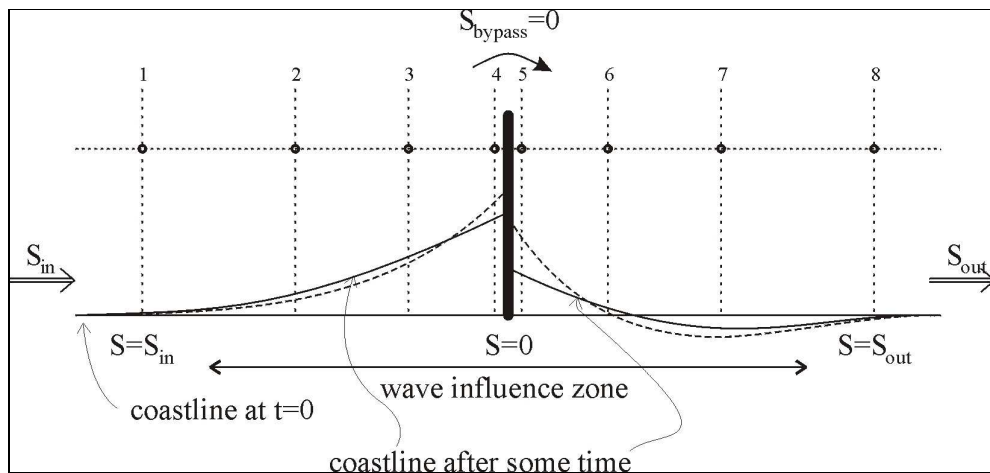


**Figure 6.26 Coastline development with breakwater**

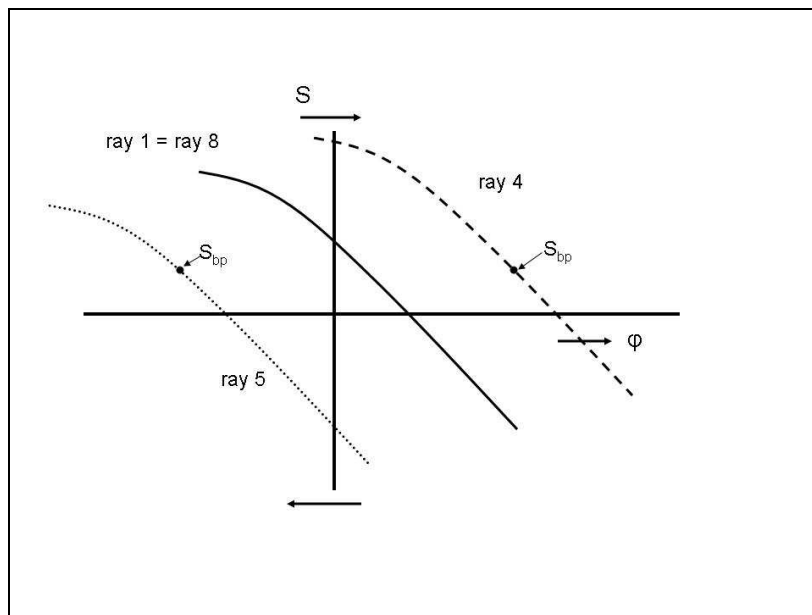


**Figure 6.27 ( $S, \phi$ )-curves for various cross-sections of Fig. 6.26**

In Fig. 6.26 eight rays (cross-sections) have been drawn. The small dots represent the seaward boundary of the transport zone. The local wave climates for these eight locations can be computed with the use of numerical models.

Consider, for instance, the local wave climate at ray 4. The most simple approach is to assume that all waves from the 'right quadrant' are blocked by the breakwater. Leaving these wave conditions out of the computations leads to a modified local ( $S, \phi$ )-curve; see line 'ray 4' in Fig. 6.27. The local equilibrium angle for ray 4 can be read from its ( $S, \phi$ )-curve at the transect where  $S = 0$ . To achieve a zero sediment transport for ray 4, an anti-clockwise rotation of the coastline is required. (In this

example the orientation of the coastline for which  $S = 0$  is for ray 4 larger than for e.g. ray 1.)

The 'equilibrium' coastline orientations ( $S = 0$ ) are in this example different for each of the eight cross-rays. Starting with ray 1 at the updrift side of the breakwater and going to ray 4 an increasing anti-clockwise direction is expected. At the downdrift side for ray 5 a clockwise rotation for the 'equilibrium' orientation is expected; see line 'ray 5' in Fig.6.27. The required rotation of the orientation of the coastline to achieve a zero sediment transport gradually changes towards ray 8 in an anti-clockwise rotation (again) for ray 8.

The position of the coastline after some time depends on the variations in the sediment transports along the coast which could be derived from the local  $(S, \varphi)$ -curves. The dotted lines in Fig.6.26 are the expected coastlines after some time, based on an analysis of the  $(S, \varphi)$ -curves and by maintaining the sediment balance. The full line in the updrift side is given as comparison; this line would result if all along this part of the coast the same  $(S, \varphi)$ -curve is assumed (compare Section 6.4.3). Note that the downdrift erosion 'somewhere' needs to bend back to the original coastline position. Where this occurs is basically a matter of time. The eroded coastline gradually extends further away from the breakwater.

Another notice is that the coastline downdrift adjacent to the breakwater, may initially accrete. After some time, this may turn into erosion again, particularly when the sediment by-pass remains small and does not nourish the downdrift coast.

If the accretion of the coast at the updrift side of the breakwater extends so far seaward that part of the transport zone extends beyond the head of the breakwater, then sediment by-pass occurs. How this affects the coastline development is sketched in Fig.6.28.

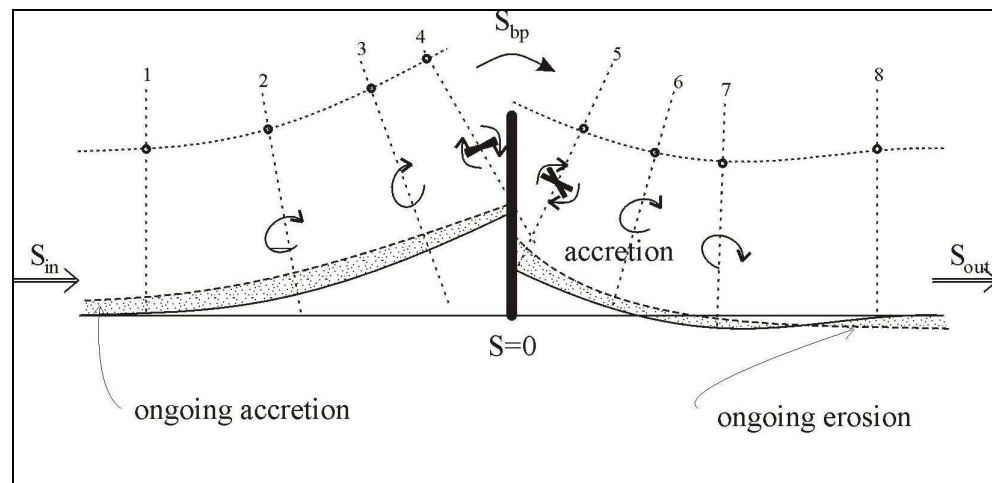


**Figure 6.28 Prolonged coastline development with breakwater**

Let us first consider the updrift ray 4, for which the local  $(S, \varphi)$ -curve was shown in Fig.6.27. After the construction of the breakwater, the coastline shifted as indicated above, since the local transport reduced to zero near the breakwater.

If sediment by-pass occurs, the sediment transport in ray 4 is apparently not zero anymore, but has increased to say  $S_{bp}$  (the by-pass transport; also indicated in

Fig.6.27). From the local  $(S, \varphi)$ -curve it follows that the coastline will then reorientate towards a smaller angle. In this phase of time there will be still progress of the position of the coastline along the breakwater in seaward direction, but with a slower speed than in the period of time that no by-pass took place.

Once sediment by-pass occurs, it follows that the zone with the largest accretion moves away from the breakwater.

While the coastline near the breakwater is shifting with time in seaward direction, the by-pass transport  $S_{bp}$  will increase further.

After an infinitely long period of time, the coastline at ray 4 will have reached the head of the breakwater and will ultimately reach the same orientation again as at time  $t = 0$ . In that situation the by-pass transport  $S_{bp}$  has increased to  $S_{in}$ .

Next, we consider the downdrift situation at ray 5.

During the first stage when no sediment by-pass occurs, it was concluded that the coastline rotated in a clockwise direction. If sediment by-pass starts to occur, a further clockwise rotation will take place. In order to achieve a balance between sediment input and sediment output, there must be a local transport capacity (equal to  $S_{bp}$ ), and for that a certain coastline orientation is required (see the by-pass transport  $S_{bp}$  as indicated at line 'ray 5' in Fig.6.27). The effect on the coastline changes is that instead of ongoing erosion, accretion may take place just downdrift close to the breakwater (see Fig.6.28). Further downdrift, the erosion will of course still continue.

After an infinitely long period of time, when  $S_{bp}$  equals  $S_{in}$ , the downdrift coastline will have its original (straight) orientation (as at  $t = 0$ ). In that infinite final stage, the entire coastline will be straight again, but with a 'step inland' at the location of the breakwater.



# 7 Cross-shore transport

## 7.1 Introduction

In the description of sediment transport in the littoral zone, a distinction can be made between longshore and cross-shore transport. In Chapter 6, longshore transport and related coastline dynamics were discussed. In the current chapter, we focus on cross-shore transport and related profile dynamics.

Cross-shore transport means transport in onshore or offshore direction. This may change the shape of the coastal profile, however, without actually changing the total sediment content (in  $\text{m}^3/\text{m}$ ) of the profile. Sand is being moved up or down the profile, without leaving the profile. Only, if one considers a small section of the profile, then for a certain period of time, the sediment balance may be disturbed, leading to a deepening, a re-shaping or a shallowing of the bottom. Profile dynamics, in this respect, is similar to shoreline dynamics which is governed by spatial gradients in the longshore transport. Examples of profile changes are given in Section 7.2. In that section also the concept of equilibrium profiles is introduced.

The driving mechanism behind profile changes is cross-shore transport. It is very difficult to develop cross-shore transport formulae for instance in the way longshore sediment transport formulae have been developed. This is partly because of the complex hydraulic driving forces, but especially because of the time scales involved (intra-wave, so on the time scale of wave periods).

The cross-shore sediment transport can be described according to the basic equation of sediment transport [see also Eq.(4.55)]:

$$S_y = \frac{1}{t'} \int_{z=0}^{h+\eta} \int_{t=0}^{t'} v(z,t)c(z,t) dt dz \quad (7.1)$$

where:

$t'$	integration period	[s]
$\eta$	instantaneous water surface elevation	[m]
$h$	average water depth	[m]
$v(z,t)$	instantaneous velocity at height $z$ (in $y$ -direction)	[m/s]
$c(z,t)$	instantaneous concentration at height $z$	$[\text{m}^3/\text{m}^3]$

Basically, the computation of a local net sediment transport rate  $S_y$  should be based on a both time- and depth-integrated product of flow velocity and sediment concentration, which can be schematised as  $S = v.c$ . In this equation both  $v$  and  $c$  are characteristic values of the cross-shore flow velocity and the sediment concentration respectively.

In Chapter 5, it was argued that both effects of currents and waves are incorporated in the basic equation for sediment [see Eq.(7.1)]. In particular, the wave-related part is very difficult and even to-day impossible to resolve. Consider in this respect the

instantaneous sediment concentration throughout the wave period, which still can not be determined.

The examples in Section 7.2.1 show the importance of being able to quantify cross-shore sediment transport. This is the reason that several researchers have developed simplified equations to approximate the basic equation [Eq.(7.1)]. Some of these are mentioned in Section 7.3.

Finally in Section 7.4, we focus in somewhat more detail on the issue of dune erosion, which is an important issue in the coastal defence of The Netherlands.

## 7.2 Cross-shore morphology of beaches

### 7.2.1 Relevancy

Fig.7.1 shows a typical coastal profile, and how the various depth zones are often referred to. Note that in literature other descriptions are found as well, but in these Lecture Notes, we use the definitions as in Fig.7.1.

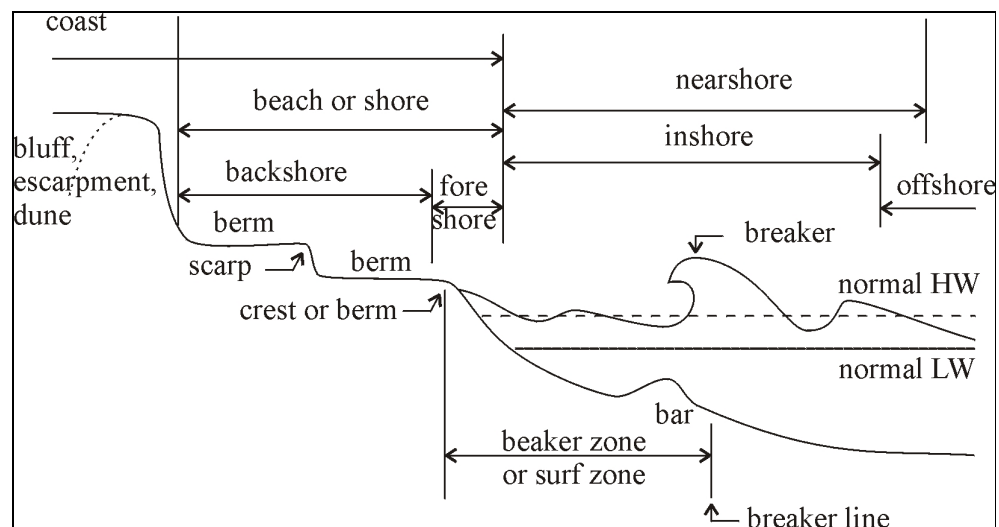


**Figure 7.1 Profile schematisation and indication of different zones**

Sometimes a coastal profile exhibits breaker bars: sometimes even more than one. Fig.7.2 shows a 3D image of the Dutch coastline based on measurements (Jarkus). These measurements are made every year at fixed positions along the Dutch coastline (starting from the early 1960's). Bars may develop under certain hydraulic conditions and disappear again during other conditions. Or they migrate across the profile, get lower, or higher, more peaked or less peaked, and so on. Both barred and non-barred profiles change their shape almost constantly under the occurring hydraulic conditions.

One may argue that cross-shore morphology is not particularly relevant if it does not influence the sediment balance as a whole. The following examples, however, show the relevancy of cross-shore transport and related profile adjustments. Moreover, if

one is interested in a certain part of the coastal profile, for instance the area between the dunes and depth contour MSL  $-5$  m, then for the assessment of the coastal changes it is important to know the cross-shore sediment transport (see sediment balance in Fig.6.20).

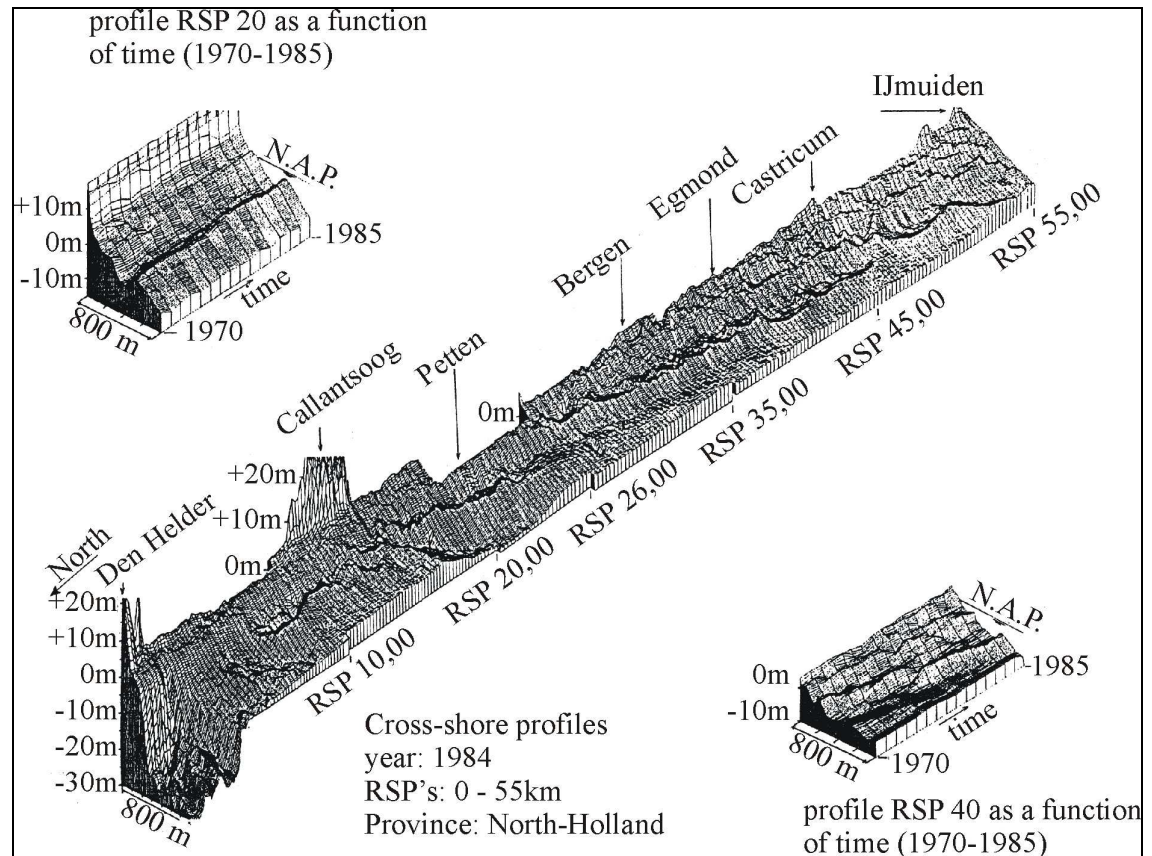


**Figure 7.2 3D image of the coast of Holland**

### Summer – winter profiles

Generally, most storms occur during the winter season. Since sediment transport, in general is highest under intense hydraulic forcing (whatever the mathematical description), one may expect that cross-shore transport rates are relatively large during a storm. If the profile is not yet adjusted to the rough hydraulic conditions, so if large spatial gradients in the cross-shore transport occur, then sediment is moved from the upper parts of the profile to the lower parts. This may lead to the development of a bar at some distances from the shoreline, as indicated in Fig.7.3 (next page). In popular terms, one speaks of a typical summer profile (the steeper profile with more sand 'high' in the profile) and a typical winter profile (with more sediment stored further offshore).

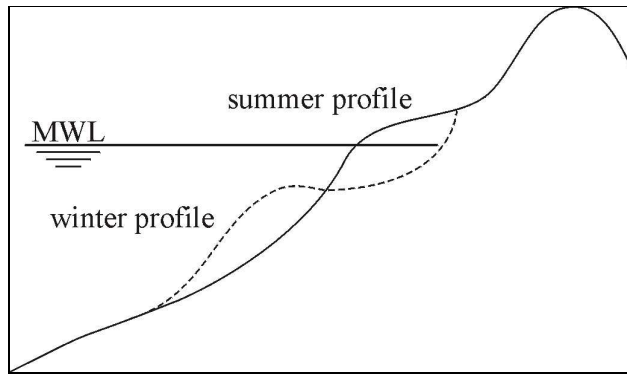


**Figure 7.3 Summer and winter profile**

The slopes of the winter profile are gentler, particularly in the area where most storm waves actually break. The dissipation of wave energy then takes place over a large area, resulting in less intense wave attack on the beach.

Field observations indicate that under more tranquil conditions, sediment is being transported back again from the lower parts of the profile to the upper parts of the profile. The temporary deposition of sand not too far away from the beach effectively prevents ongoing sediment losses to deep water, from where perhaps it could not be recovered.

### Dune erosion

If during a specific storm, the water level is raised so far, that the waterline moves to the forefront of the dunes, then dune erosion will take place (Fig.7.4). The steep dune profile will then 'collapse' and large quantities of sand are transported from the dunes to the beach. The effect of dune erosion is that the slope of the beach gets gentler, so that wave energy gets (partly) dissipated before it reaches the eroded dune front during the erosion process (Section 7.4).

For a natural restoration of this type of profile change, aeolian transport is required (i.e. wind-blown transport over a dry sandy surface). Coastal managers will tend to take measures to restore the dunes for instance by using bulldozers or (in many cases) by planting beach grass (in Dutch: helm) or by placing wind fences.

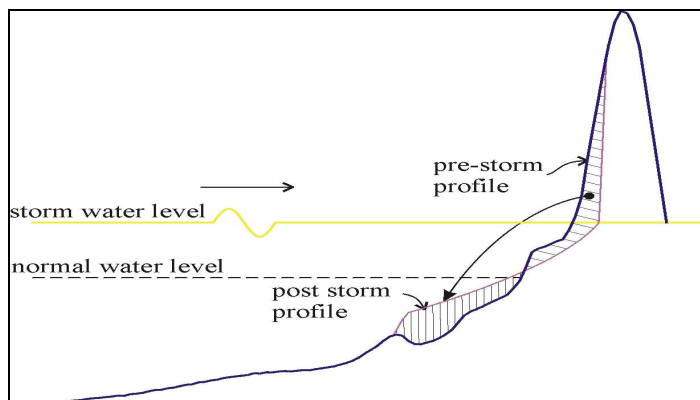


**Figure 7.4 Dune erosion during severe storm**

## Scour

Consider a situation with an artificial 'hard element' somewhere in the coastal profile. This can be an offshore breakwater (parallel to the shoreline), a ship wreck, or a seawall higher in the profile (Fig.7.5).

In case of a seawall directly attacked by waves, wave reflection will increase the bed shear stress just in front of the seawall, which leads to an increase in sediment transport. Sediment will be transported in offshore direction until a new equilibrium is reached with a deeper bottom just in front of the seawall (scour hole). For the design of such a structure it is crucial to know beforehand the maximum depth of the possible scour hole during design conditions (to avoid undermining).

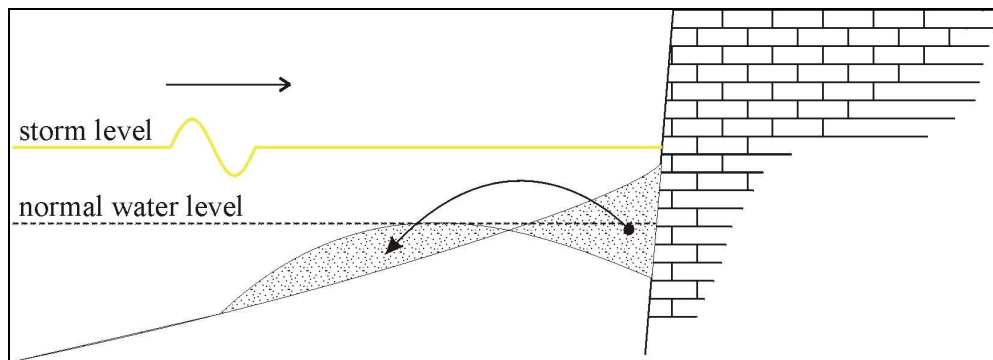


**Figure 7.5 Erosion in front of an almost vertical wall**

## Shoreline adjustment

If a certain stretch of coastline accretes (for instance updrift of a breakwater as described in Section 6.4), then sediment is deposited 'somewhere' in the cross-shore profile. This 'somewhere' initially relates to the distribution of the longshore transport, which is mainly in the upper parts of the coastal profile (Fig.7.6 next page). This may lead to unrealistic steep profiles after some time. Cross-shore sediment transport re-distributes the deposited sediment next over the whole profile. Since, this usually occurs on a different time scale than the time scale involved with the initial accretion, its effect may be felt at a later stage. A similar sediment redistribution due to cross-shore profile adjustments occurs in the situation of shoreline retreat.

## Sea level rise

The direct effect of sea level rise is that the whole coastal profile moves landward (Fig.7.7 next page). Note that this is similar to the effect of land subsidence; in many cases one speaks of *relative* sea level rise, which includes the effect of land subsidence. In a situation with a raised sea level, adaptations in the shape of the cross-shore profile will occur. Over a longer period of time, that is on the time scales of sea level rise and land subsidence (decades to centuries), cross-shore transport will redistribute sand from the dunes across the profile.

If this redistribution can actually 'follow' the relative sea level rise, then the effect is that the whole profile, so including the width of the beach, will remain the same. In

the end, the dunes have delivered the sand for the coastal profile to follow the relative sea level rise. This effect is often referred to as the 'Bruun-rule' [Bruun (1954), (1962)].

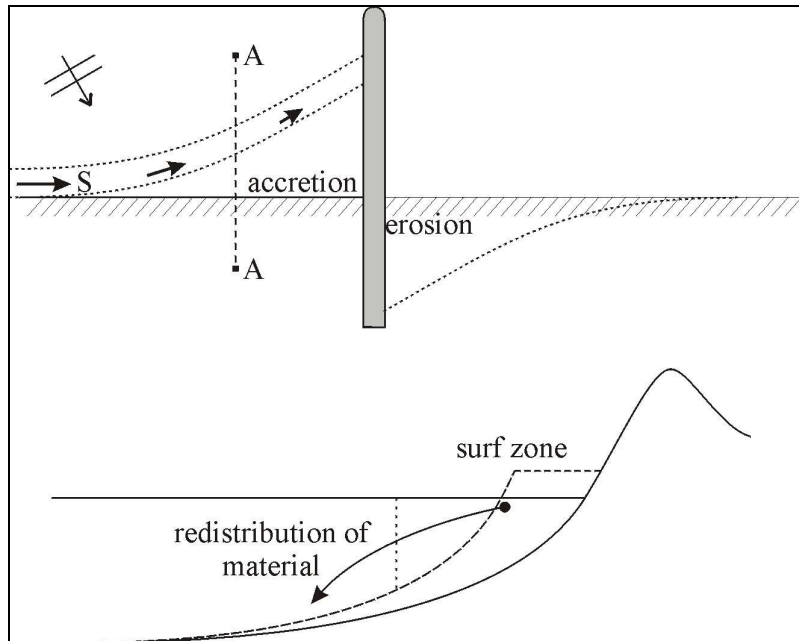


**Figure 7.6 Redistributing material due to cross-shore transport**

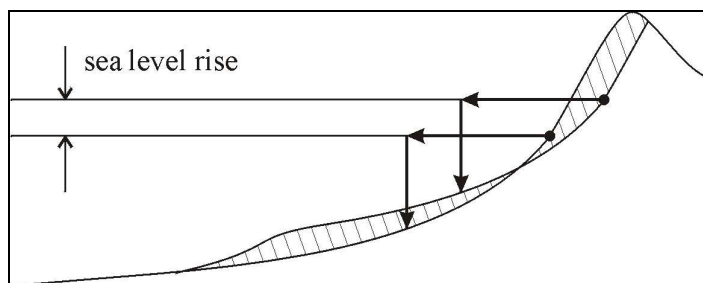


**Figure 7.7 Sea level rise: Bruun rule**

### Land reclamation

In the design of a land reclamation project, one always has to consider offshore sediment losses. By moving only the upper part of the profile in seaward direction, one gets a rather steep part of the coastal profile in the transition zone between the original sea bed and the under water part of the reclaimed land. A steeper profile generally leads to more offshore directed sediment transport (Section 7.3) than a

mildly sloping profile. This may cause a net offshore sediment flux, which may lead to shoreline erosion of the reclaimed land as well.

To combat such shoreline retreat, one may consider artificial (beach) nourishments to balance the offshore sediment losses. On the long run, this policy leads to a coastal profile without sharp bends in the underwater slopes. In this context, one speaks of 'postponed construction'. Alternatively, one would also directly place the sand at the deeper sections of the reclamation profiles, but this is not very attractive as these (large) quantities of sand have to be paid directly.

### Shoreface nourishments

Artificial shoreface nourishments (see also Chapter 13) are increasingly used as an alternative for artificial beach nourishments. One of the basic ideas behind the application of shoreface nourishments is that at the end of the day (a part of) the nourished sand will be transported to the beach area. That is because of cross-shore sediment transport processes. The volume of nourished sediment on the shoreface is to be considered as a disturbance of the equilibrium profile; the coastal processes flatten out the disturbance. To estimate the speed of this beach-feeding process, one needs a proper insight in cross-shore sediment transport processes.

In all of the above examples it is important to know the cross-shore sediment transport and the related coastal profile dynamics.

## 7.2.2 Scales

The relevancy of cross-shore transport and profile dynamics in coastal engineering practice has been indicated. Next it is important to consider the scales on which cross-shore processes take place.

Three distinct types of coastal processes are considered, which might be characterized by decreasing scales, viz.:

- Shoreface evolution;
- Surf zone evolution;
- Dune erosion.

The evolution of the shoreface profile takes place on relatively large scales. Typical scales are decades for the time scale and of the order of several kilometres for the (cross-shore) space scale.

Profile evolution in the surf zone (say in between the outer bar and the dune face) takes place on middle scales. Typical evolutions, including bar and berm features, take place over wave climate seasons like a summer and winter season, while return periods in profile evolution may occur between one and several years. Significant profile variations extend to depths of about twice the wave height extreme which is exceeded for example a few hours per year, relative to the mean sea level; see e.g. Hallermeier (1978).

The process of dune erosion is characterised by relatively small scales. Significant profile variations are established on a time scale of hours: the extent of these variations being limited to a depth of less than about the incident significant wave height relative to the storm surge level.



### 7.2.3 Equilibrium profile models

Basically an equilibrium profile can be defined as a cross-shore profile of constant shape which is reached if it is exposed, for a sufficiently long time, to constant wave and water level conditions. Many researchers take this notion as a basis for further considerations, e.g. Swart (1974) and Steetzel (1993).

The existence of an equilibrium profile was already long ago proved to be a valid concept under (probably constant) laboratory conditions by Waters (1939) and Rector (1954) and many other researchers.

However, since in nature the profile-forcing hydraulic conditions will definitely not be constant in time, an absolute equilibrium shape (with zero transport rates all across the profile) will not exist in nature. In fact, one has to deal with some sort of average shoreface profile and, consequently, the term 'dynamic equilibrium profile' could be a safe alternative. A critical review on the concept of shoreface equilibrium is given by Pilkey *et al.* (1993), who question both the validity of the concept of equilibrium profiles as used in standard coastal engineering practice in the United States as well as the general application of one equilibrium profile equation to describe all shoreface profiles. Nevertheless, some handy formulations of equilibrium profiles can be found in literature.

#### Bruun

Bruun [Bruun (1954)] developed a predictive equation for an equilibrium beach profile by studying beaches along the Danish North Sea coast and the California coast and proposed a simple power law to relate the water depth  $h$  to the offshore distance  $y$ , according to:

$$h = A y^m \quad (7.2)$$

where:

$m$	exponent equal to $m = 2/3$	
$h$	water depth	[m]

The non-dimensionless constant  $A$  (which dimension depends on the magnitude of the  $y$ -exponent) denotes a so-called shape factor, depending on the stability characteristics of the bed material. Bruun found that  $A = 0.135 \text{ m}^{1/3}$  provided the best correlation for North Sea beaches in the Thyborøn area in Denmark. Bruun applied his empirical equation in 1962, to estimate the amount of erosion to occur along the Florida coast as a result of long-term sea level rise [Bruun (1962)]. This approach is nowadays known as the 'Bruun-rule' (see Fig.7.7 and Section 13.2).

#### Dean

The Bruun hypothesis (simple power law) was supported by Dean [Dean (1977)] on theoretical grounds by reasoning that nature aims at a uniform energy dissipation  $D_{eq}$  (loss in wave power) per unit volume of water across the surf zone (in  $\text{W}/\text{m}^3$ ). So:

$$\frac{1}{h} \frac{d(Ec_g)}{dy} = -D_{eq} \quad (7.3)$$

where:

$E$	wave energy	[J/m <sup>2</sup> ]
$c_g$	group velocity	[m/s]



Based on monochromatic waves and a constant breaker index  $\gamma = H/h$ , the magnitude of the exponent  $m$  in Eq.(7.2) can be derived and the same  $2/3$ -power curve is found for the shape of a cross-shore profile.

Furthermore, for this case the non-dimensionless shape factor  $A$  (in  $\text{m}^{1/3}$ ) can be described by:

$$A = \left( \frac{24}{5} \frac{D_{eq}}{\rho g \sqrt{g} \gamma^2} \right)^{2/3} \quad (7.4)$$

in which the equilibrium energy dissipation rate  $D_{eq}$  (in  $\text{W}/\text{m}^3$ ) depends on both the particle diameter and shape.

The magnitude of the related shape factor  $A$  varies from  $0.079$  to  $0.398 \text{ m}^{1/3}$  [Dean (1977)]. Hughes and Chiu (1978) show that  $A = 0.10 \text{ m}^{1/3}$  provided the best correlation for beaches along the coast of Florida.

The empirical shape parameter  $A$  was later related to the median grain size by Moore (1982), showing that a coarser grain size implies a larger value of  $A$  and thus a steeper cross-shore profile. Later on Dean (1987) showed that this relation could be transformed to a relation using the fall velocity  $w$  as a parameter, viz.:

$$A = 0.067 w^{0.44} \quad (7.5)$$

For general applications, however, the constant  $A$  remains an unknown factor which is likely to be also dependent on several other variables, like wave climate, water level variations and coastal currents. Ergo, a universal application of 'Dean'-profiles seems troublesome, although some applications of equilibrium profiles are presented in e.g. Kriebel (1990) and Dean (1991).

Note that a formula like  $h = Ay^m$  (a parabola) results in a vertical slope of the beach profile at the waterline ( $y = 0$ ). This is far from realistic. In some practical applications therefore the top of the parabola is taken at a level somewhere above the waterline. This results in more reasonable slopes at the waterline.

## Vellinga

A well-known Dutch example of the application of equilibrium profiles is the 'erosion profile' approach, presented by Vellinga (1986). Vellinga extended the earlier work of Van de Graaff (1977). (Although an *erosion profile* is not identical with an *equilibrium profile*, the same basic principles are applied.) This erosion profile method is presently still basically used to check the safety of the Dutch dunes [TAW (1984)/CUR (1989)].

Based on a scale relation showing the effect of the grain size on the shape of an erosion profile according to:

$$\frac{n_l}{n_h} = \left( \frac{n_h}{n_w^2} \right)^{0.28} \quad (7.6)$$

a power curve can be derived according to:

$$h = Ay^{0.78} \quad (7.7)$$

where:

$A$  non-dimensionless shape factor  $A = 0.14$  [ $\text{m}^{0.22}$ ]

In Eq.(7.6)  $n_x$  represents the ratio between two cases with different scales of a parameter  $x$ . If in a laboratory a small-scale physical model is made of a part of reality (the 'prototype') scales are involved to mould the physical model. The following scales are used in Eq.(7.6):

$n_l$	ratio between a horizontal distance in prototype and the equivalent distance in the model
$n_h$	ratio between water depth in prototype and the water depth in the model
$n_w$	ratio between fall velocity of bottom material in prototype and fall velocity of bottom material in model

Using the scale relation of Eq.(7.6), a general expression for the shape factor can be found according to:

$$A = 0.39w^{0.44} \quad (7.8)$$

or:

$$A = 0.70 \left( \frac{H_0}{\lambda_0} \right)^{0.17} w^{0.44} \quad (7.9)$$

where:

$H_0$	deep water wave height	[m]
$\lambda_0$	wavelength at deep water	[m]
$w$	fall velocity bed material	[m/s]

The quotient of the wave height  $H_0$  and wavelength  $\lambda_0$  denotes a characteristic offshore wave steepness. Both a coarser grain size and a larger wave steepness imply a larger value of  $A$  and thus a steeper beach [Vellinga (1986)]. It should be noted that this particular erosion profile is definitely not in equilibrium (most likely even not in 'near-equilibrium') shape, since the period of wave attack is limited by the duration of the specific storm surge considered.

From the definition of equilibrium profile shapes it is almost for sure that equilibrium profiles are not directly suited to compute the detailed effect of the impact of an arbitrary storm event (which only lasts several hours or one day at most) on an arbitrary initial cross-shore profile. Moreover, if there is any equilibrium profile at all, it will definitely not be reached within such a short time interval. However, as in many cases: 'the proof of the pudding is in the eating'.

It is interesting to quote Bruun (1992) who states that: "*Dean's as well as Bruun's assumptions may be more academic than real in a highly three-dimensional and irregular environment. That they give the same result may be incidental, but neither Dean's nor Bruun's results should be extended beyond their capacity. A beach/bottom profile is a very dynamic feature subject to considerable variances. Its behaviour may be better described in statistical, rather than in physical terms.*"

## 7.2.4 Dynamic equilibrium profile models

A space-integrated, though instantaneous concept is also based on the assumption of the existence of an (at least local) equilibrium profile as discussed in the former section. This equilibrium shape will be approached when the cross-shore profile is exposed to fixed hydraulic conditions for a sufficiently long time.

The rate of change in a quasi-equilibrium approach is related to the deviation of the actual situation from a pre-defined equilibrium condition. Typically, this approach results in a negative exponential development of the profile (for constant hydraulic conditions).

Swart (1974) proposed a definition of an equilibrium profile determined by the deep water wave height, the deep water wave steepness and the particle diameter. The offshore transport, at any location in a cross-shore profile which is out of equilibrium, at any time, is proportional to the difference between the equilibrium profile shape and the actual shape.

Larson (1988) developed the SBEACH-model that simulates the macro-scale profile change, such as growth and movement of bars and berms. Based on an extensive analysis of two large wave-tank experiments (with regular waves), a number of semi-empirical transport rate relations have been developed for different regions of the cross-shore profile [Larson and Kraus (1989a)].

Roelvink developed a quasi-equilibrium version of the original DUROS-model of Vellinga, known as the DUIN-model. The preliminary research version of this model was used by a few authorities to simulate the behaviour and effectiveness of measures on beach and dune [Delft Hydraulics (1990d)].

Although approaches based on equilibrium notions are quite instructive, the application in practical cases is often cumbersome; many parameters have to be estimated/determined beforehand. A more promising approach for a reliable assessment of the development of a cross-shore profile due to arbitrarily varying hydraulic conditions starts with formulae describing the local transport rate as will be discussed in more detail in the next section.

### 7.3 Cross-shore sediment transport

In order of increasing simplification one can identify a number of possible approaches to solve Eq.(7.1), namely:

- indeed using the basic equation;
- using best estimates of both  $v$  and  $c$  to compute  $S_y$ ;
- using an estimate of  $v$  and assuming  $c$  to be related to (some power of)  $v$ ;
- assuming  $c$  to be related to wave energy dissipation;
- assuming  $S_y$  to be related to wave energy dissipation;
- assuming  $S_y$  to be related to (bottom) shear stress;
- estimating  $S_y$  by an empirical relation;
- estimating only the sign of  $S_y$  by an empirical relation.

It is obvious that the first method is preferable, although elaboration of the detailed transport equation is troublesome, and today still impossible, because our knowledge of especially the factor  $c(z,t)$  is quite insufficient.

#### Classification formulae

Empirically based relations have been derived to predict only the direction of the cross-shore sediment transport. They can be used in order to classify a particular beach state. In fact they present the transition between erosion and accretion. In actual coastal

engineering problems one often needs to know (much) ‘more’ than only the direction of sediment transport.

The various formulae typically use dimensionless parameters, such as wave steepness  $H/\lambda$  and the relative grain size  $D/H$ . A well-known example is presented by Dean (1977), viz. the  $(H/Tw)$ -ratio. Also a number of Japanese criteria are present, see e.g. Shibayama and Horikawa (1982), Kajima *et al.* (1982) and Shimizu *et al.* (1985).

### Empirical transport formulae

These formulae show empirical relationships for the computation of the transport rate. An example is Larson's SBEACH-model as already mentioned [Larson and Kraus (1989a)].

### Shear stress related transport rates

These kinds of formulae are based on bottom shear stress equations. Examples are the relations presented by Madsen and Grant (1976), Shibayama and Horikawa (1980) and Watanabe (1982). Since suspended sediment transport is predominant, it is doubtful whether shear stresses only, are sufficient to quantify cross-shore sediment transport.

### Energy dissipation related transport

These formulae use the wave energy dissipation rate to estimate sediment transport rates. According to Dean (1977), offshore transport continues until the wave energy dissipation per unit volume of water is constant and equal to a pre-described value over the entire surf zone. Based on this consideration, the rate of local cross-shore sediment transport in the surf zone can be expressed in terms of the difference between the actual and the equilibrium condition of wave energy dissipation in the surf zone [Kriebel and Dean (1985)]. Consequently, the local cross-shore transport is expressed according to Eq.(7.10).

$$S_y = K (D - D_{eq}) \quad (7.10)$$

where:

$S_y$	the rate of (cross-shore) sediment transport	$[\text{m}^3/\text{m}/\text{s}]$
$K$	a non-dimensionless parameter	$[\text{m}^5/\text{W}/\text{s}]$
$D$	the actual energy dissipation per unit volume of water	$[\text{W}/\text{m}^3]$
$D_{eq}$	the energy dissipation per unit volume of water for equilibrium profile conditions	$[\text{W}/\text{m}^3]$

This computational model comprises two unknown coefficients, namely  $A$  in the power curve [Eq.(7.2), or  $D_{eq}$  in the shape parameter of Eq.(7.4)] and  $K$  in the transport formula. Although for a specific location and condition the magnitudes might be known, both constants vary from site to site and from one condition to another. It is clear that there should be a relation with sediment characteristics and hydraulic conditions. Additional results and some extensions of this model are presented by Kriebel (1986), (1987), (1990).

### Energy dissipation related suspension

These formulae use the wave energy dissipation rate to compute sediment loads. Next, the actual transport is computed from the product of this load with the mean velocity as

occurs under breaking waves (the so-called undertow). An example of this kind of approach is presented by Dally (1980).

### Velocity related transport (energetics approach)

These formulae use an energetic approach to compute the sediment concentration from the velocity field, basically starting with a relation for the concentrations according to:

$$c = m|v|^n \quad (7.11)$$

where:

$m$	arbitrary non-dimensionless parameter;	
	dimension depending amongst others on $n$	[?]
$n$	exponent	[-]

Bagnold (1962), (1966) developed formulae for calculating sediment transport rates based on this energy approach for application in rivers and made a distinction between bed load and suspended load. His elementary work has been refined afterwards for application in coastal environments, including cross-shore transport sediment transport calculations. This refers to the so-called Bailard formula; Bailard and Inman (1981), Bailard (1982). The Bailard formula was (and is still) widely applied by several others. See for instance Stive (1987), Roelvink and Stive (1989) and Nairn (1990).

Assuming a direct relation between velocity and sediment transport (bottom and suspended) to be valid within the wave period, the effects of asymmetry of the orbital velocity and e.g. a steady current (cf. the undertow) on the transport rate, can next be accounted for. The transport vector due to the combined actions of steady current, wave orbital motion and bottom slope effect can now be elaborated.

The total near bed velocity can be split-up into a mean and a time varying velocity component:  $u = \bar{u} + \tilde{u}(t)$ ; thus separate terms for the wave orbital motion  $\tilde{u}$  and the steady current  $\bar{u}$ . The sediment transport according to the Bailard formulation uses different exponents  $n$  in the expressions for bottom transport  $S_{y,b}$  and suspended transport  $S_{y,s}$ :

$$S_{y,b,s} \approx \overline{(\bar{u} + \tilde{u}(t))^n} \quad (7.12)$$

For a horizontal bed:  $n = 3$  (bottom) and  $n = 4$  (suspended). If a sloping bed is considered, additional terms must be included. A term with exponent  $n = 5$  appears. With expressions for  $\bar{u}$  and  $\tilde{u}(t)$  (e.g. sinusoidal expressions including higher harmonics) the bottom and suspended sediment transport contributions can be determined with Eq.(7.12). Formal integration over time (wave period) results in many terms. See e.g. Stive (1988a) and Roelvink and Stive (1989).

### Models based on $S_y = v.c$ concept

Consider a pure 2DV case; e.g. a test in a wave flume with a cross-shore profile. Applying a simple linear wave theory with an infinitesimal small wave height results in closed orbits of the orbital motion; so without resulting water motions in a vertical cross-section. In reality, however, wave heights are finite. Even in non-breaking waves this results in a mass transport towards the coast in the upper part of the water column. In a closed system (cf. in a wave flume) the same volume of water has to flow in seaward direction in the lower part of the vertical; the so-called return flow.

In breaking waves both the landward directed, as the seaward directed flows increase.

So in conclusion: real waves lead to net currents in a 2DV case. This allows us to develop a sediment transport description where at least the *current related* sediment transport contribution ( $s(z) = \bar{v} \bar{c}$ ; see Section 5.3) is taken into account. [The wave related contribution ( $s(z) = \overline{\tilde{v} \tilde{c}}$ ) is in most calculation methods neglected; mainly because this contribution can yet not be reliably quantified.]

Approaches to quantify cross-shore sediment transport rates based on this concept are amongst others Unibest-TC and DUROSTA (both developed by Delft Hydraulics).

## Computer models

In order to efficiently apply any of the concepts as were mentioned above in practical cases, various computer models have been developed.

An example of such a model is Unibest-TC, which is part of the Unibest Coastal Software Package, developed by Delft Hydraulics. It is designed to compute cross-shore sediment transports and the resulting profile changes along any coastal profile of arbitrary shape under the combined action of waves, longshore currents (e.g. tidal and wave driven) and wind. The model is frequently used to assess the stability of a beach nourishment (see Chapter 13), to estimate the impact of sand extraction on the cross-shore bottom profile and to estimate the cross-shore profile development due to (seasonal) variations in the incoming wave field. The Unibest-TC module has been tested using wave flume measurements [Roelvink and Stive, 1989]. The module is frequently improved in new releases of the software. Within the newest releases of the Unibest-TC model the total sediment transport over the water depth is computed for many positions in the cross-shore profile. The suspended sediment contribution is based on the  $S = v.c$  principle. An example computation using Unibest-TC is given in Example 7.1.

## 7.4 Dune Erosion

### 7.4.1 Introduction

River and sea dikes are good examples of structures to protect low-lying areas from flooding. Also a dune area (dune row) serves that aim in some cases. E.g. the safety of large parts of The Netherlands, often with ground levels even below Mean Sea Level (MSL), relies on dikes but also on dunes for their protection against flooding.

Visiting the beach and the coastal zone in The Netherlands under normal weather conditions would easily give the impression that the dunes are certainly strong enough to properly protect the hinterland. However, during a severe storm surge, with under design conditions water levels at sea which are approximately 5 - 6 m above MSL and together with the much more severe wave conditions than normal (cf. wave heights  $H_s \approx 7 - 9$  m and peak periods  $T_p \approx 12 - 18$  s), the dunes will be eroded in a very short period of time. Existing design rules in The Netherlands yield erosion rates of 80 - 100 m of the dunes during design storm conditions. (The rates of 80 - 100 m are given as an order of magnitude value only to facilitate the further

discussion; the actual erosion rates under design conditions depend on the specific local conditions; e.g. shape of initial cross-shore profile and particle size.) It must be realized that because of the specific Dutch conditions, the design conditions in The Netherlands are very strict (see Section 7.4.2).

[In Chapter 11 dune erosion problems in coastal engineering practice are discussed, under less severe boundary conditions.]

### Example 7.1

*Input parameters:*

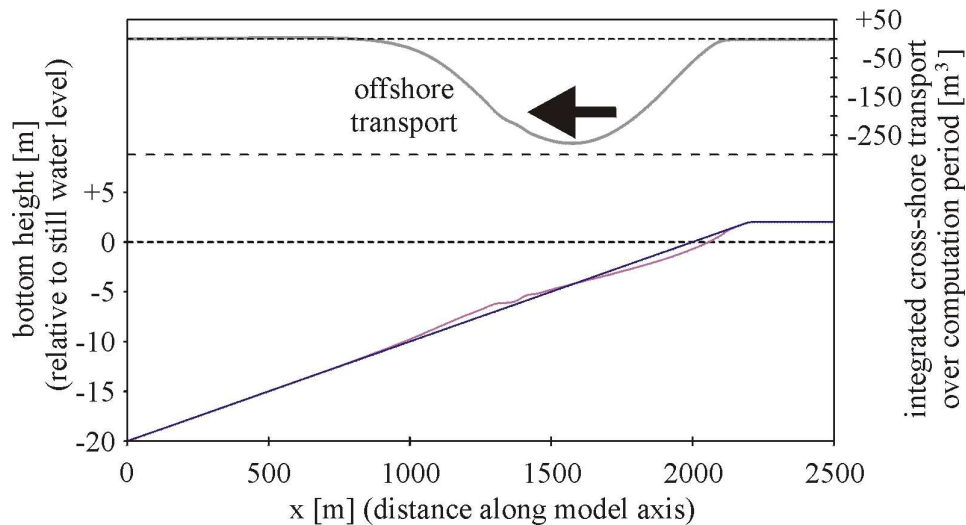
Wave climate and bottom profile as in Example 6.7 (see page 164)

*Required:*

Bottom profile development due to cross-shore transport

*Output:*

The results are computed using the model Unibest-TC. In the figure below the profile development after half a year has been given. In the upper graph, the total integrated cross-shore transport during the computation period (half a year) has been given.



*Conclusion:*

With the given climate and profile, sediment is mostly transported in offshore direction.

### Example 7.1 Unibest-TC calculation

Often the dune areas in The Netherlands are wide enough to accommodate 80 - 100 m of dune erosion during a single severe storm surge. In some cases, however, the



row of dunes is rather slender; a careful judgement has to be passed whether the dunes provide the required rate of protection. Is a break-through expected under design conditions?, and if yes: what reinforcement is necessary to fulfil the requirements?

So far in the discussion the safety problem of people living behind the dunes was raised as the main issue. In Section 7.4.2 it will be shown that more issues related to dune erosion are relevant to a coastal zone manager. Aspects like the safety of single houses and hotels in the erosion zone are dealt with. Also topics like how to deal with structural erosion and global sea level rise are relevant topics for a coastal zone manager. They are briefly discussed in this section with the present Dutch policy and insights as starting points. In Chapter 11 a more detailed discussion follows.

From the discussion in Section 7.4.2 it will become clear that for many reasons a proper insight in the rates of dune erosion as a function of the boundary conditions is necessary. Section 7.4.3 will deal with the dune erosion process and the methods to quantify the rates of erosion during a severe storm surge.

## 7.4.2 Large and small scale safety problems

Fig.7.8 shows schematically what happens with a (in this case: rather slender) dune during a severe storm surge. The initial cross-shore profile, which might be considered to be in a more or less dynamic equilibrium condition with the normal occurring boundary conditions, will be reshaped during the severe storm surge. The much higher water levels and the much higher wave heights and peak periods call for a quite different shape of an equilibrium profile than the shape of the initial profile. Offshore directed sediment transports will occur, especially with sediments from the dunes. Sand is eroded from the dunes and is settled at the foreshore again. During these reshaping processes the slopes of the cross-shore profile gradually decrease, and consequently it can be understood that the rate of dune erosion will decrease with time during the storm surge. It is, however, not expected that a real equilibrium profile will develop during the storm surge. The time available during the storm is too short to achieve such a real equilibrium profile, but the developments are in the direction of achieving equilibrium. The shape of a cross-shore profile as encountered after the storm surge is often called 'erosion profile'.

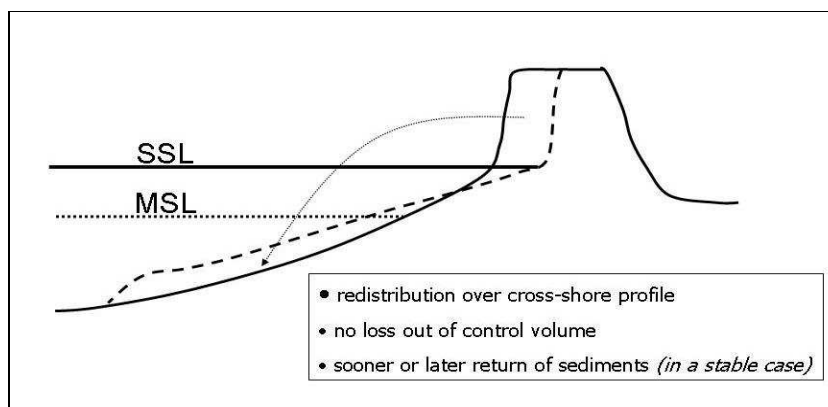


**Figure 7.8 Dune erosion during a severe storm**



Right after a severe storm surge, when the boundary conditions are normal again, the shape of the (erosion) profile does not fit with these normal conditions. Onshore directed sediment transports will occur; wind will blow sand from the beach to the dunes; the 'old' situation will gradually be restored. Dune erosion because of severe storm surges is thus a temporary and a reversible process.

### Large scale safety problem

If, like in Fig.7.8, the dunes are really slender and landward of the row of dunes the ground levels are even below MSL (like in some places in The Netherlands) a *large scale* safety problem might occur. A break-through of the dunes causes flooding and will cause loss of lives and results in a lot of damage in the densely populated low-lying areas of The Netherlands.

Given the dimensions of a row of dunes and the specific design conditions, the coastal zone manager has to judge whether the dunes are 'safe' or not. 'Safe' is in this respect in fact a relative notion. 'Safe' means that the strength (width, height) of the dunes fulfils the requirements. Absolute safety does not exist in many cases; often a set of even more extreme boundary conditions is conceivable which will result in a break-through of a row of dunes which was judged just 'safe' enough. The chance that such a set of boundary conditions will occur, is then, however, apparently smaller than has agreed.

For the judgement of the safety of a row of dunes, a proper computation model is necessary and (a set of) design conditions. Section 7.4.3 will deal with these computation models.

For the further discussion in the present section it is good to realize that because of the many (stochastic) parameters which ultimately determine the rate of erosion, a probabilistic approach seems to be appropriate (see e.g. Van de Graaff, 1986). In a probabilistic approach an acceptable chance of failure must be the starting point instead of a single set of design conditions. Because of the high importance of the low-lying hinterland, a probability of failure for dunes of  $10^{-5}$  per year (return period 100,000 years) has been agreed in The Netherlands for the most important parts of the country. This chance seems rather small, but compared to other threats (e.g. accidents with nuclear power plants, air planes or large industrial plants) the probability of failure is not that small taking into account the number of human lives and the high investments that are at stake.

The probability of failure of  $10^{-5}$  per year holds for the most important parts of The Netherlands; in some more rural areas larger probabilities of failure are the (legal) norm. Fig.7.9 (next page) shows a schematic plot of the relationship between the rate of erosion RD (distance RD is in Fig.7.8 the distance between the initial edge of the dune and the edge of the dune after the storm surge) and the frequency of exceedance. According to Fig.7.9 there is a chance of  $10^{-5}$  per year that a rate of erosion of 85 m is reached or will be surpassed.

The safety problem of large parts of The Netherlands, in so far the problem depends on the protection by dunes (*large scale* problem), seems thus solvable if a proper insight is available in the possible occurring conditions in the (very) small chances range. However, this also introduces many uncertainties. E.g. reliable measurements of (maximum) water levels of the sea in measuring stations near the coast (cf. in ports) are available since approximately 1850. So for only 150 years. With such an in

fact restricted data set, it is hard to estimate water levels which are associated with frequencies of exceedance in the range of  $10^{-3}$  to  $10^{-5}$  per year.

Data sets of reliable measurements of wave characteristics cover even shorter periods of time. Nevertheless, these kinds of uncertainties have been taken into account to arrive at figures like Fig.7.9.

Based on a legal norm, with the help of a proper computation method, and for a given situation (cross-section of cross-shore profile and dune area) one is next able to judge whether the cross-section meets the requirements; i.e. whether the cross-section is safe enough or not. If not: iteratively an improvement scheme for the dune area can be developed; e.g. a strengthening of the dunes at the landward side.

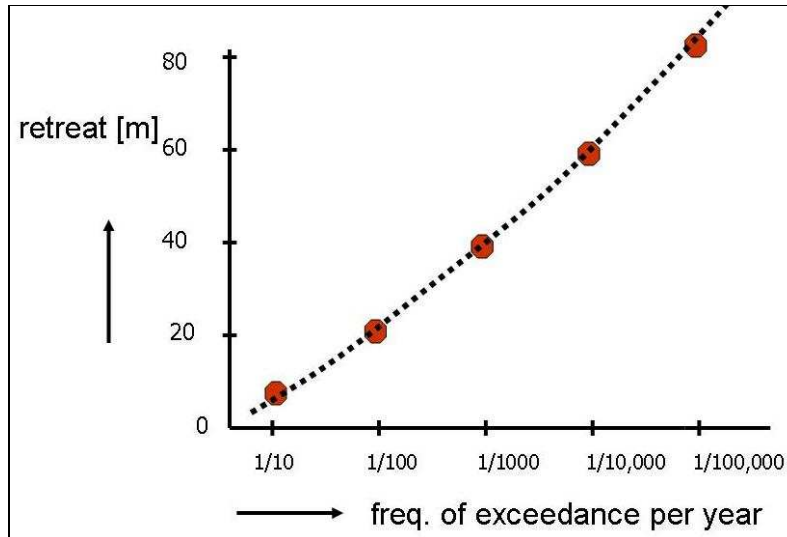


**Figure 7.9** Rate of erosion as function of frequency of exceedance

### Small scale safety problem

If the width of the row of dunes is rather large (or at least large enough to meet the legal safety standard), the safety problem for the hinterland is not a real issue (any more). That holds for many stretches of the Dutch coast. If these stretches concern bare dunes, loss of dune area will occur during a severe storm surge and some damage to e.g. nature will occur.

However, along the Dutch coast (like along many coasts elsewhere) at some places coastal villages and holiday resorts do exist with roads, houses and hotels built very close to the seaward brink of the dunes. And even if the dunes are safe enough to protect the hinterland, the (required or wanted) safety of single houses and hotels built in the zone prone to erosion during a severe storm surge, might be an issue. This safety problem might be classified as a *small scale* safety problem.

It is to the direct interest of a large part of the Dutch population that the *large scale* safety problem is properly dealt with. Legal norms are available. The responsibilities of the various parties (Water Boards, Provinces, Central Government) have been legally embodied.

The *small scale* safety problem directly regards a rather restricted part of the Dutch population. E.g. owners of houses and hotels built (or to be built in future) in the

zone prone to erosion during a severe storm surge, but also governmental agencies are directly involved as owners of infrastructure like roads, promenades and car parks. The government must also formulate and maintain a set of rules to avoid unbridled developments in the zone prone to erosion during a severe storm surge.

It must be realized, however, that within the zone which is 'necessary' during the design conditions for the safety of the hinterland, a distinction can be made in chances that a property will be lost. Close to the seaward brink of the dunes (say RD = 20 m according to Fig.7.9) the chance of loss of property is larger than at the landward side of the potential erosion zone (say RD = 60 m).

The coastal zone very close to the brink of the dunes has high socio-economic potentials; many people would like to build houses and hotels with 'sea view' in this zone or would buy existing buildings. Owners of such properties are primarily responsible for possible damage to their properties by a severe storm surge. From this point of view the role of a coastal zone manager would be a limited one in this respect. It is conceivable, however, that 'society' calls for some regulation. Too often (say: on an average of every 10 years) loss of many properties in the coastal zone might be unwanted. A lot of commotion is to be expected; owners of properties who at once lost 'everything' might be considered as 'poor and innocent' fellow-citizens. At the other hand there seems to be no reason to avoid damage in the zone prone to erosion during a severe storm surge to chances comparable with the chance of failure of the dunes as sea defence. To find an acceptable compromise between these limits is a very difficult task for a responsible coastal zone manager. Many managers 'struggle' with this issue. E.g. financial, legal and insurance aspects might be helpful to be considered while developing a proper policy.

So far the discussion referred to the erosion of the dunes due to a single storm surge (episodic effect). However, seen over a long period of time, the position of sandy coasts often show some distinct tendencies. It refers to either accreting, or eroding coasts (structural erosion), although also a more or less stable position with time of a coast might occur. Especially structural eroding coasts seriously complicate the coastal zone management task in dune areas where coastal villages or holiday resorts do exist. If the structural erosion is 'accepted', the zone prone to erosion during design conditions during severe storm surges is then continuously shifting in landward direction. It is good to realize that the effect of structural erosion (e.g. a few m *per year*), is quite different from the effect of a really serious storm surge: up to tens of meters *per (really severe) event*. (See also Chapter 11.)

If structural erosion is not accepted, proper protection measures must be applied: see further Chapters 11-13.

### 7.4.3 Dune erosion process and quantification

Both for the *small scale* safety problem, but especially for the *large scale* safety problem a reliable quantification method for the rate of dune retreat during severe storm surge conditions is necessary. Rather much effort has spent on this quantification topic in The Netherlands.

Although 3D effects are undoubtedly important in the dune erosion process, for the time being often a 2D approach is adopted. In that case the dune erosion process can be considered as a typical offshore directed cross-shore sediment transport problem. Sand from the dunes is transported to deeper water and is settled there. To a first

approach a closed sediment balance in cross-shore direction can be assumed. The same volume of sand which is eroded from the dunes and the very upper part of a cross-shore profile (in  $\text{m}^3/\text{m}$ ) is accumulated elsewhere in the cross-shore profile. [Because of differences in porosity of the eroded dune material (often relatively loose packed) and of the settled material (often slightly denser packed), the sediment balance is not always strictly closed.]

During really severe storm surges, with a serious increase of the water level (compare Fig.3.14; an increase of the water level with approximately 2.8 m was measured in that case) huge volumes of sand from the dunes are transported in offshore direction. And because dune erosion is a rather short lasting process, some computation methods take only offshore directed transports into account.

A rather straightforward computation procedure uses the concept of a so-called 'erosion profile' (see also Section 7.4.2). The upper part of the shape of a cross-shore profile right after a (rather severe) storm surge is thought to be known in such a method. In the procedure still in use in The Netherlands, the shape of an erosion profile with the maximum storm surge level as reference, depends on the occurring wave height and the particle size of the dune/beach material. Once the characteristics of the erosion profile are known, the relevant dune retreat is easily to be determined with a closed sediment balance method. This concept forms the heart in a further probabilistic method taking into account the stochastic character of several dune erosion determining parameters. (E.g. water level, wave height, wave period, shape of initial cross-shore profile, estimated accuracy of computation method, duration of storm surge.) In TAW (1984) / CUR (1989) the approach followed in The Netherlands is described. In Van de Graaff (1986) some background information has been presented.

A serious drawback of such a straightforward computation method with a 'known' profile is that hardly any physics is involved. E.g. only the 'end' profile after the storm surge is thought to be known; the development with time is unknown. Effects of varying water levels and varying wave characteristics during the storm surge cannot be accounted for.

But also dune erosion during a severe storm surge is a real cross-shore sediment transport process.

Based on theoretical and a lot of experimental work, Steetzel has developed the so-called DUROSTA computation model in which at many positions in a cross-shore profile actual sediment transports are calculated with a  $S = v.c$  concept. [Steetzel (1993)]. Although in the mathematical descriptions of the cross-shore sediment transport the so-called *wave related* transport (see Section 5.3) is neglected, only the *current related transport* is taken into account, the results of the model compared with e.g. the 'reality' of large scale model tests in the Delta Flume of Delft Hydraulics are rather good. (See Fig.7.10.)

During storm surge conditions the rather high breaking waves cause a considerable return flow ( $v$  in  $S = v.c$ ) in the lower part of a water column in the surf zone. The fierce wave conditions result also in high sediment concentrations within the water column ( $c$  in  $S = v.c$ ). Gradients in calculated sediment transport rates allow next for a bottom up-date. And so on. With the DUROSTA model the development with time of a bottom profile during a storm surge can be calculated and studied.

Also with computation models like UNIBEST-TC (developed by Delft Hydraulics) in principle dune erosion computations can be made. With the present day (mid 2006) versions of UNIBEST-TC the results are not yet satisfying.

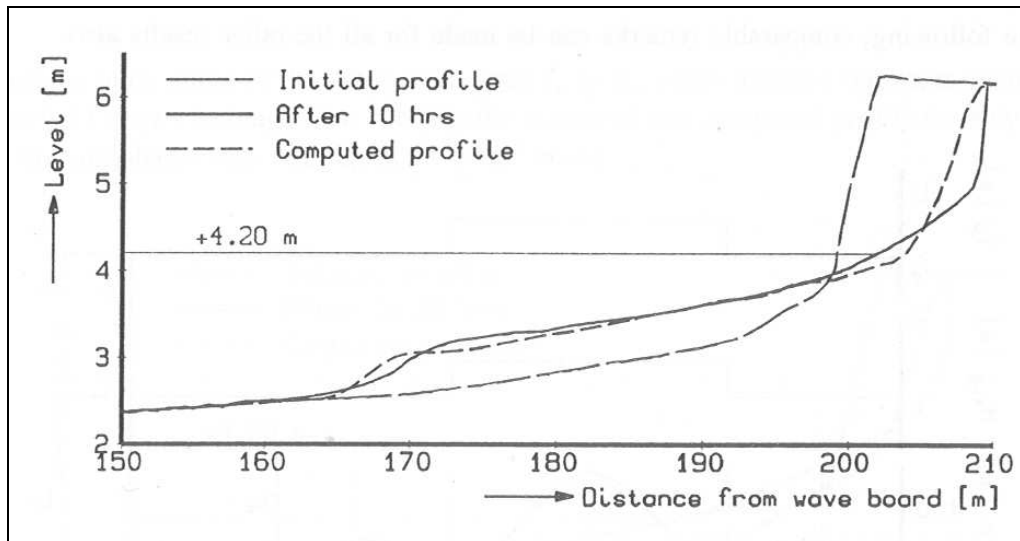
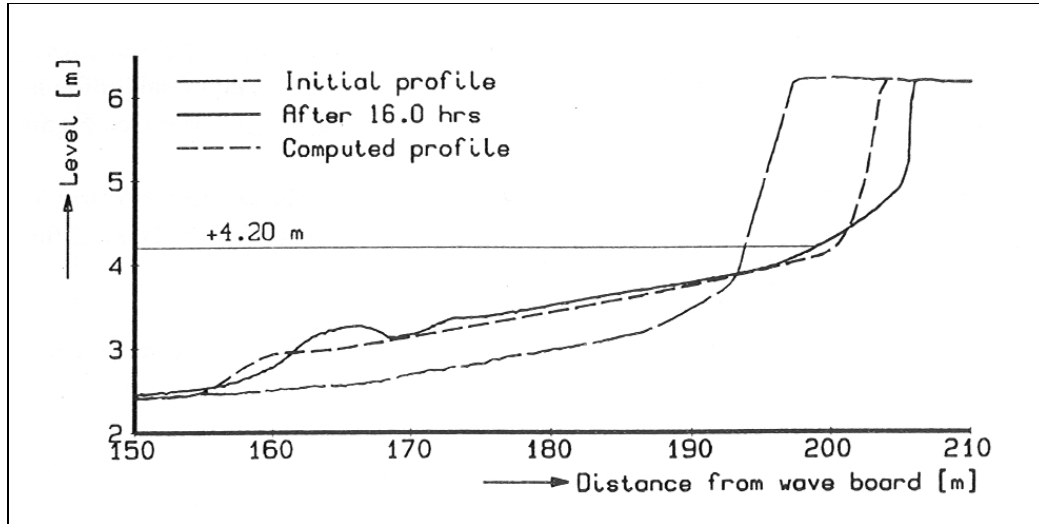


Figure 7.10 DUROSTA versus Delta Flume results [Steezel (1993)]



# 8 Combination of Longshore and Cross-shore Transport

## 8.1 Introduction

In many real life coastal engineering 'problems' sediment transports (and the associated morphological developments of a coastal area) play an important role. Compare the examples as have been given in Chapter 3.

This means that, at least a part of, a solution to a coastal engineering problem relies on a proper insight into the morphological development of the relevant piece of the coast. In the Chapters 6 and 7 a distinction has been made between longshore and cross-shore sediment transport processes. It has turned out that it seems easier to quantify longshore sediment transport rates than cross-shore sediment transport rates. For some real life coastal engineering issues it may be imagined that they could be (more or less properly) schematized as a mainly longshore transport topic or a mainly cross-shore transport topic. However, for many other issues such a schematization would lead to a too simple representation of reality. That calls for integrated computation models.

Fig.8.1 shows the basic set-up of a complex morphological computation model.

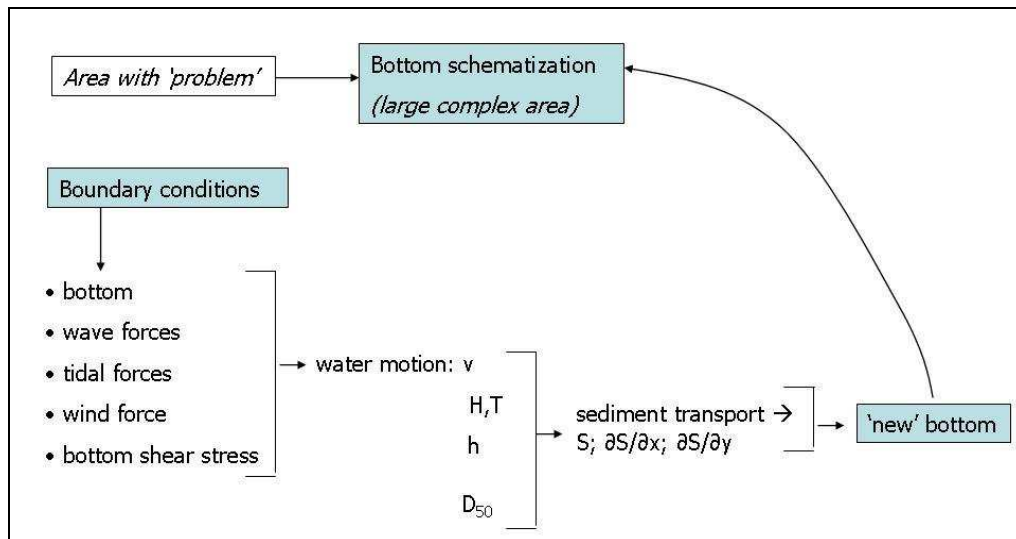


**Figure 8.1** Basic set-up of complex morphological computation model

The following points are relevant in the set-up of a complex morphological computation model:

- A large area, surrounding the specific 'problem' area, is taken into account.
- The area is overlain with a computation grid (grid points and grid cells).
- The initial bottom position of the area is transferred to water depths belonging to the grid points.
- With specific models for water motion and wave propagation (including interaction between water motion and wave action), the boundary conditions to be known at the boundaries of the computation area, are 'translated' to the grid points.
- Next sediment transports are calculated for the planes bordering a grid cell.
- With the sediment transports as determined, and a time step, the change in bottom position of a grid cell can be calculated.
- A 'new' bottom position is determined.
- With the 'new' bottom position the previous procedures are repeated.
- Many loops are required to achieve the wanted final situation.

The previous basic set-up is rather straightforward. But one has to realize that one often is interested in morphological developments covering many years. Although the computers are becoming faster and faster, this basic set-up requires still an unacceptable computing time. However, a *skillful designer* of such a morphological computation model is able to apply various methods and tricks to efficiently handle the very complex reality in order to reduce the computation time. For instance:

- Nested grids; i.e. smaller grid sizes in the most important area.
- Time steps as large as possible.
- Finding a fair balance between accuracy and computing time.
- Taking advection and diffusion effects into account; i.e. the actual sediment transport rate does not (only) depend on the local conditions, but also on transport rates 'upstream'.
- Short cuts in the loops; e.g. with still small bottom variations it is not necessary to run the water motion model each time. Knowing the discharge through a plane of a grid cell from a previous computation with an 'old' bottom, a fair estimate of the 'new' velocity for a 'new' bottom is found by assuming that the discharge has not (yet) changed.

A *skillful user* of such a morphological computation model should be able to efficiently handle the boundary conditions. One has to realize that in reality in nature the boundary conditions are changing 'every moment' [wave characteristics; wave direction; water levels (vertical tide); water velocities at the boundaries (horizontal tide); wind effects; density effects]. An efficient reduction of the various 'cases' as input in the model is required to reduce the computing time. For instance:

- Using a so-called morphological tide (e.g. 1.1 times an average tide to represent a full spring - neap tide variation).
- Taking together the various wave directions in a restricted number of wave direction classes.
- Taking together various wave heights in a restricted number of wave height classes.
- Etc.



Depending on the nature of the coastal engineering 'problem' one has to resolve, one might stick to a 2D approach of the water motion (average velocity through a plane of a grid cell), or one has to run the model in a full 3D mode (detailed description of the velocity distribution over the water column). In the latter case the water depths in the model are split in e.g. 10 layers. Much more computing time is required in a 3D mode compared to a 2D mode.

Various integrated models are (commercially) available. E.g. Delft3D model suite developed by Delft Hydraulics; MIKE 21 / MIKE 3 developed by Danish Hydraulic Institute.

The further developments into this type of models are going very fast. New, improved, versions are frequently released. Notwithstanding these fast developments and improvements this type of models is still not yet 'fool-proof'. Experienced and skillful people are necessary to judge the outcomes of this type of models. It remains recommended if one likes to compute the effect of a new proposed change in the morphological system (e.g. the effects in future of an extension of a set of breakwaters on the adjacent coastlines), first to re-calculated the present situation (e.g. the effect of the present set of breakwaters as shown and measured in the past). The applied computation model has to be validated.

*Chapter 8 is not yet finished at this stage (September 2006). For the time being this chapter is finished with an example of the application of a complex morphological computation model. It refers to a reprint of a paper from the Proceedings of the International Conference on Coastal Engineering 1998.*

## North-Coast of Texel: A Comparison between Reality and Prediction

Rob Steijn<sup>1</sup>

Dano Roelvink<sup>2</sup>

Dick Rakhorst<sup>3</sup>

Jan Ribberink<sup>4</sup>

Jan van Overeem<sup>5</sup>

### Abstract

*For an efficient protection of the north coast of the Dutch Waddensea island Texel, a long dam was constructed in 1995. The position of this dam is on the southern swash platform of the ebb tidal delta of the Eijerlandse Gat: the tidal inlet between the two Waddensea islands Texel and Vlieland. The long dam changed the hydrological conditions in this tidal inlet. The changes in the inlet's morphology have been monitored through regular bathymetry surveys. This paper describes some of the most remarkable changes that occurred in the inlet after the construction of the long dam. The impact of the long dam on the inlet's morphology and the adjacent shoreline stability has been examined with the use of a medium-term morphodynamic model. From a comparison between the observed and predicted morphological changes it followed that the model was able to simulate the large-scale morphological response of the inlet system. However, on a smaller scale there were still important discrepancies between the observations and the predictions.*

### Introduction

The Dutch Government decided in 1990 to maintain the coastline at its 1990-position by means of artificial sand nourishments. However, at certain coastal sections, where nourishments appear to be less effective, alternative coastal protection methods could be considered. The north-coast of Texel (Figure 1) appeared to be such a coastal section.

---

<sup>1</sup> Alkyon Hydraulic Consultancy & Research, P.O. Box 248, 8300 AE Emmeloord, The Netherlands; fax: +31 527610020

<sup>2</sup> WLIDelft Hydraulics, P.O. Box 177, 2600 MH Delft, The Netherlands; fax: +31 152858582.

<sup>3</sup> Ministry of Public Works, Rijkswaterstaat, regional Directorate North Holland; P.O. Box 3119, 2001 DC Haarlem, The Netherlands; fax: +31235301752

<sup>4</sup> University of Twente, P.O. Box 217, 7500 AE Enschede, The Netherlands; fax: +31534894040

<sup>5</sup> Alkyon Hydraulic Consultancy & Research, P.O. Box 248, 8300 AE Emmeloord, The Netherlands; fax: +31 527610020

Over a distance of some 6 km, the north-coast of Texel has lost in the last decades on average about 0.5 million m<sup>3</sup> sand per year. Before 1995 the maximum coastline retreat was 5 - 10 m/year at the most severely eroded northern sections. According to the formalised Dutch Coastal Defence Policy (Rijkswaterstaat, 1990), this erosion was combatted through regular sand nourishments. However, these nourishments became less and less effective. Alternative coastal protection measures were considered for this coast, like groynes, offshore breakwaters, long dams, revetments; most of them in combination with initial beach nourishment. Detailed numerical model studies were carried out to investigate the effect of the alternative measures and their cost efficiency to combat the erosion. A long dam (700 m from the MLW-line) was finally chosen (Rakhorst, De Wilde and Schot, 1997).

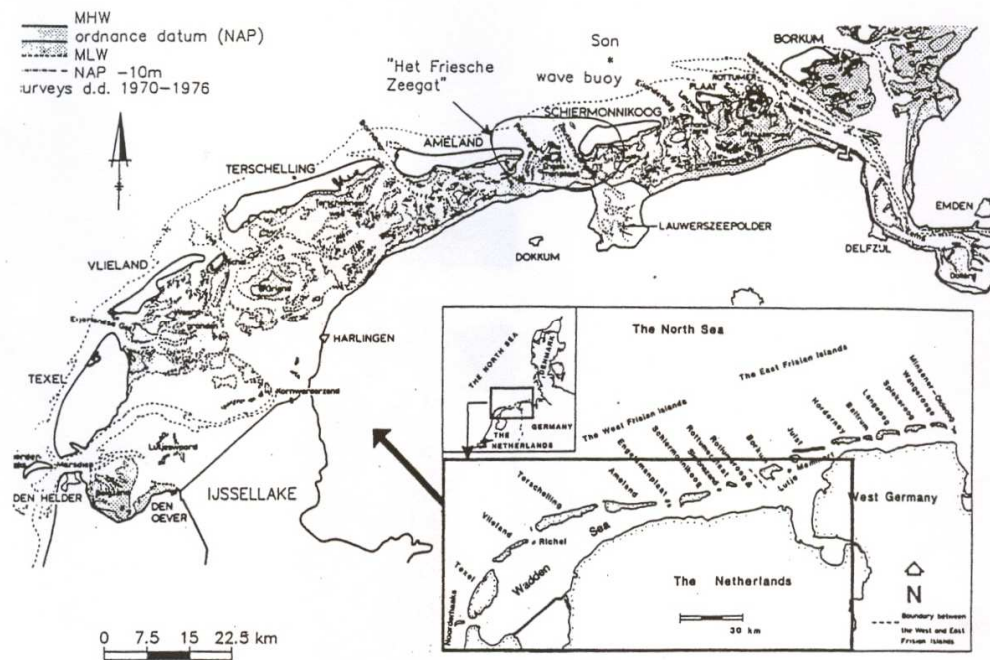


Figure 1 Geographical setting

The long dam was constructed in 1995 at the northern end of the north-coast of Texel (at RSP 30.5 km), in combination with nourishment and dredging works. The morphological changes that took place afterwards were monitored, which gave valuable data for a comparison between predicted and actually observed morphological tidal inlet responses.

In recent years, process-based morpho-dynamical modelling has developed rapidly. In the present study the available dataset for the long dam case has been used to check and validate the model. The model parameters were set as much as possible identical as the ones in the "old model" from 1993; however this time with the latest versions of the applied software DELFT3D (Roelvink, Boutmy and Stam, 1998). A comparison between the renewed predictions (improved hindcast) and the field

observations was made and valuable information was obtained on how to set up and operate similar models and to know their weak and strong points.

### The tidal inlet "Eijerlandse Gat"

The ebb tidal delta, the inlet throat and the flood tidal basin are shown in Figure 2 (situation as in 1993; before the dam construction). On the ebb tidal delta, the pattern of tidal channels can clearly be recognised, as well as the presence of shallow areas and delta bars. The ebb-dominant inlet throat channel "Robbengat" will be of special importance for the present study. The flood tidal basin is, in contrast to the other Waddensea flood tidal basins, a closed basin: only during storms, exchange of water takes place across the watersheds.

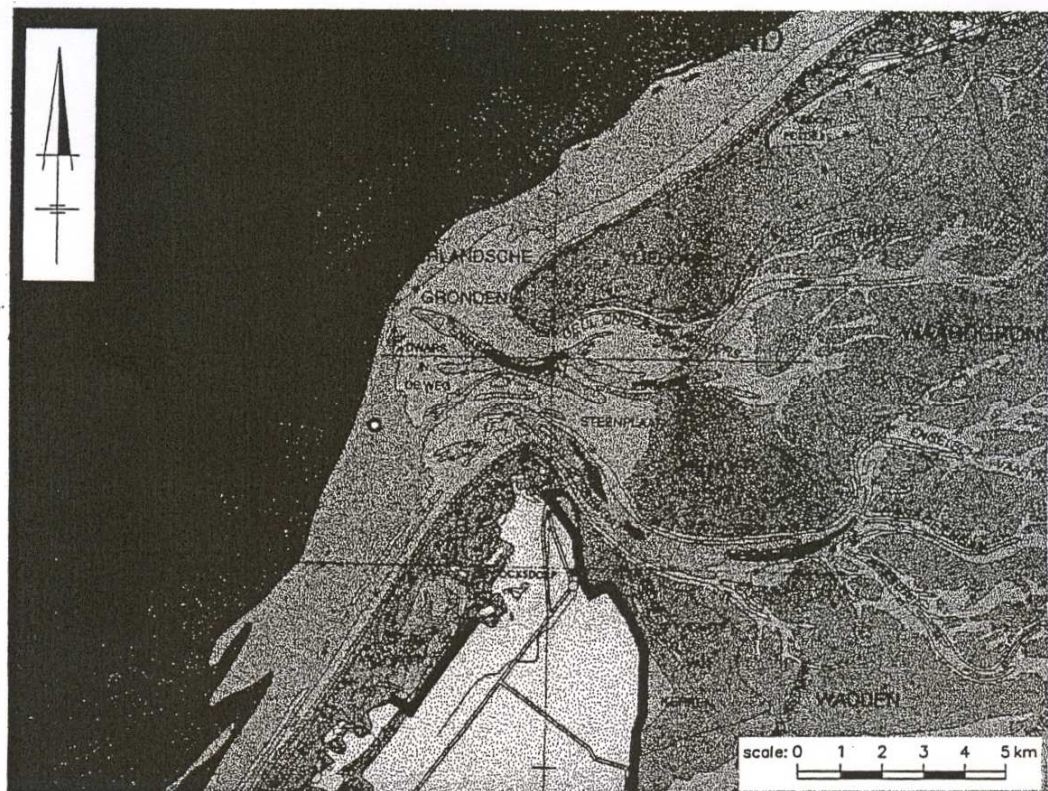


Figure 2 The tidal inlet "Eijerlandse Gat"

The particles size of the seabed and the beach sediments ranges between 150 and 350  $\mu\text{m}$ : coarser in the tidal channels than on top of the shallow areas or on the beaches.

The tide is semi-diurnal with neap, mean and spring tidal ranges of, respectively, 1.35 m, 1.70 m and 1.90 m. Tidal wave propagation is from south to north. Waves are moderate, with a mean annual wave height (at deep water) of  $H_s = 1.2$  m. The yearly average wind speed is 7 m/s from south-southwesterly directions. Storms (larger than 7 Beaufort) mainly come from northwesterly directions.

### What has been done in the last decades?

The southward migration of the Robbengat was stopped successfully in 1948 and 1956 with the construction of two slope-protection schemes on the north-side of Texel (inside the inlet throat). Ongoing erosion of the north coast of Texel (south of the above-mentioned slope-protection works) was combatted in 1979, 1985 and 1990 by artificial sand nourishments of 2.5 to 3 million m<sup>3</sup>, each time. The actual lifetime of the last nourishment was shorter than what was expected beforehand.

In the period 1990 - 1993 different studies were carried out to find more efficient methods to protect the north-coast of Texel (e.g. Negen, 1993, Ribberink and de Vroeg, 1991, 1992, Hartsuiker, 1991, Ribberink, de Vroeg and van Overeem, 1993, Rakhorst and Pwa, 1993 - all of them in Dutch and Ribberink, Negen and Hartsuiker, 1995). A first attempt for a full morpho-dynamic simulation of the tidal inlet, including a long dam alternative, was made by Negen (1993). Based on these effect studies, which also included ecological and cost-benefits studies, it was concluded that a long dam at the northern end of Texel would be the most cost-effective for maintaining the north-coast of Texel.

In 1994 a 1.3 million m<sup>3</sup> sand nourishment was carried out on the north-coast of Texel. This was necessary as the 1994-position of the coastline had already receded behind the reference 1990-position. The sand for this nourishment was reclaimed from a borrow area below the MSL -20 m depth contour (i.e. below the closure depth, so from outside the active coastal system).

Construction of the long dam at position RSP 30.5 km (Figure 3) commenced in April 1995. By July 1995, the dam had reached its most seaward tip at 700 m from the most seaward MLW-line; or 800 m from the dunefoot. Also in early 1995, an additional 0.7 million m<sup>3</sup> sand was replenished along the north-coast of Texel. Another 0.4 million m<sup>3</sup> sand was placed in the neck of the dam (Figure 3), also to make the construction site better accessible for construction equipment. This 1.1 million m<sup>3</sup> sand was borrowed by a cutter suction dredger from an area between the expected scour hole and the inlet channel Robbengat (Figure 3). The idea behind this was to initiate the development of a new ebb tidal channel in southward direction, and consequently to let the ebb tidal delta develop more in front of the north-coast of Texel, which on the longer term could also benefit the sand balance of the north-coast of Texel.

### Observations

The long dam and dredging works changed the tidal flow regime and wave conditions around and in the immediate vicinity of the dam. It also affected the tidal flow to and from the flood basin. Figure 4 shows for the area around the dam, the observed pattern of erosion and sedimentation between 1995 and 1997 (two-years period).



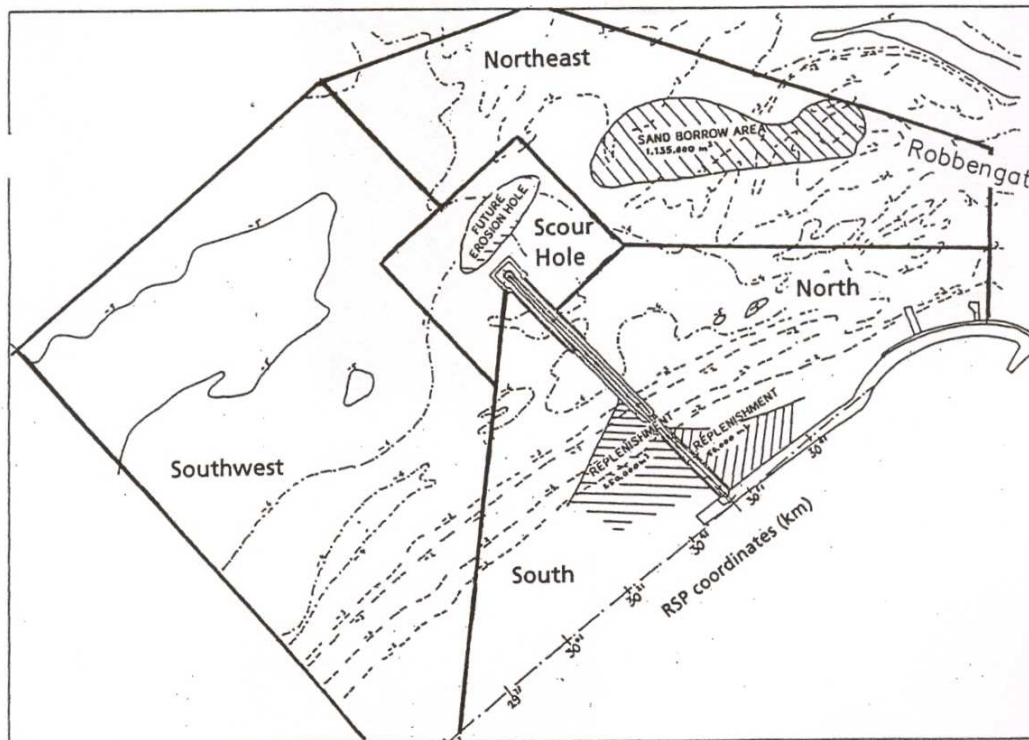


Figure 3 Drawing of the long dam and dredging works

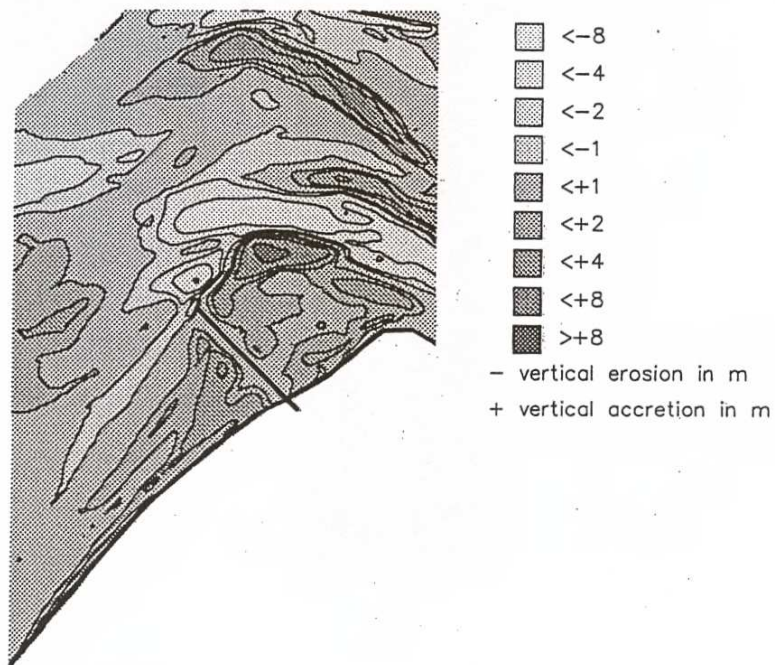


Figure 4 Observed sedimentation and erosion 1995 - 1997

The figure shows areas with significant erosion (such as in front of the tip of the dam, and to the north of the dredged borrow area), as well as areas with significant accretion (such as in the dredged borrow area and to the southwest of the ebb tidal delta). The figure also clearly shows the accretion along the coastlines on both sides of the dam. Below, some details of the observations are given:

**Scour hole**

The scour hole in front of the tip of the dam developed more rapidly than expected. The maximum depth reached MSL -18 m already in September 1995, that is only two months after the dam was finished (note that the local depths at this point were only MSL -5 m). The slopes on the dam-side of the scour hole are very steep, namely 1:2 to 1:3 (vert:hor), which led to the placement of an extra rubble layer after completion of the dam and later again in December 1996 (Rakhorst, De Wilde and Schot, 1997). The wet volume of the scour hole in m<sup>3</sup> below MSL -5m is given in Table 1.

Wet volume below MSL -5 (m <sup>3</sup> )	Time after dam construction (months)	Max. depth (MSL -m)
0	0	-5
250,000	2.5	-18
350,000	8	-16
300,000	14	-15
300,000	20	-13

Table 1 Development of the scour hole

The maximum depth reduced considerably in the winter of 1996/ 1997, where it is noted that the winter of 1995 / 1996 hardly had any westerly storms (which is an anomaly). Without the occurrence of high waves, the scour hole apparently developed first in vertical direction, before it widened in horizontal direction.

**Dredged hole**

The borrow area north of the dam (Figure 3), which was intended to develop into a tidal ebb-channel, indeed changed in that direction. The maximum dredged depths down to MSL -15 m reduced rapidly to not deeper than MSL -10 m two years later. While the MSL -7 m depth contour of the dredged borrow area and that of the inlet channel Robbengat were not connected in June 1995, they were in March 1997 (see Figure 5). Once the borrow area stretched in east-west directions and became "connected" with the inlet channel Robbengat and with the scour hole, it migrated in northward direction under the influence of the eastward resultant sediment transport and the west-to-east tidal wave propagation.

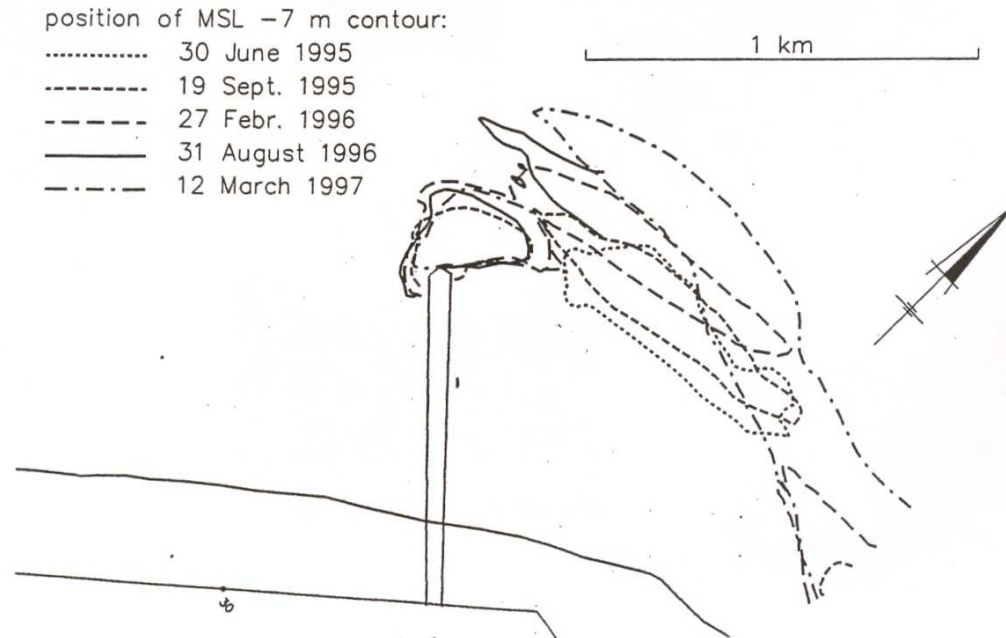


Figure 5 Movements of the MSL -7m depth contour

#### Coastal area north of the dam

Immediately after the dam construction, significant accretion rates were found in the area to the north of the dam. This area continued to accumulate sand (Figure 4), albeit at a steadily slower rate. In the period July - September 1995 a resultant sand accumulation of more than  $70,000 \text{ m}^3$  per month was found in an area of some  $0.4 \text{ km}^2$ . About one year later this accretion rate had reduced to some  $30,000 \text{ m}^3$  per month. Between the coastline of Texel, the dam and this accretion area, a small shortcut gully was present till early 1998, when it silted up.

#### Coastal area south of the dam

If we consider an area from the dunefoot to a shore-parallel line through the tip of the dam, and from the dam to a position  $2.5 \text{ km}$  south of the dam (Figure 4), then the total sand accumulation in this area in the period 1995 - 1997 is  $475,000 \text{ m}^3$  per year. This accretion can be attributed to the effect of the long dam; nourishments have not been carried out in that period.

If we disregard the upper part of the profiles, above MSL  $-1.5 \text{ m}$ , then the observations show that initially erosion took place ( $70,000 \text{ m}^3$  in the period July - September 1995). In volumetric sense not much changed in the foreshore area in the winter of 1995/1996. But after the winter of 1996/1997, when westerly storms had occurred, accretion of more than  $300,000 \text{ m}^3$  was observed. This demonstrates the importance of higher waves for the shoreward transport of sand from greater depths.



## Model predictions

A numerical model of the entire tidal inlet system including the long dam and dredging works (Figure 3) was set up. The model is based on the DELFT3D software package, which is described in more detail elsewhere in these proceedings (Roelvink, Boutmy and Stam, 1998). The model computes the tidal wave propagation, the tide-, wave- and wind generated flow conditions, the short wave conditions, sediment transport and seabed changes. The model is of the medium term morpho-dynamic type (MTM-model: De Vriend, e.a., 1993). A limited number of input conditions (waves, tides, wind) have been selected in such a way that they represent the annual sediment transports.

Figure 6 shows, as an example, the computed tide-averaged sediment transports in the vicinity of the dam for one of the selected wave conditions "West-High" (at deep water:  $H_s = 3.1$  m,  $T_p = 7.6$  s, from  $268^\circ$  N). These transports follow after one year of morphodynamic simulation, so when the deepest portions of the dredged borrow area have already largely silted up.

An interesting detail in the resultant sediment transport patterns was observed near the dredged borrow area. Here, the resultant sediment transport at the start of the morphodynamic simulation is directed from two sides towards the center of the borrow area, leading to a steady siltation of the center of the dredged hole. The flood-dominance on the west-side of the borrow area is due to relaxation effects: during flood the incoming concentration vertical is over-saturated while during ebb the incoming concentration vertical is under-saturated.

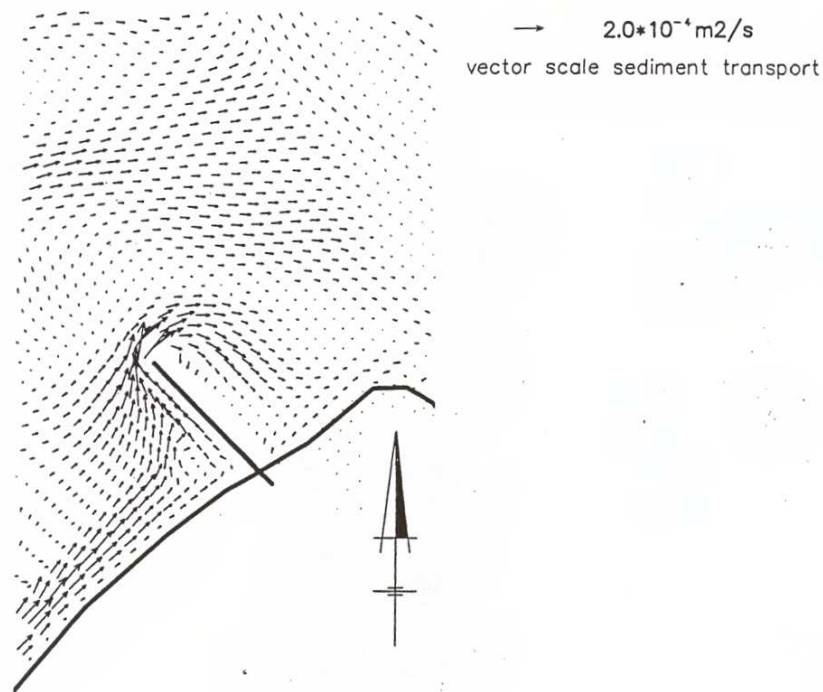


Figure 6 Tide-averaged sediment transport

A direct confrontation between the model predictions and the observations is given in Table 2 below. It gives the volumetric changes over a period of two years (1995 - 1997) for the five areas as indicated in Figure 3. It is noted that this table is not the only source for comparison: for that it lacks too much information on details of smaller scale phenomena.

Area	Surface	Reference computation			Observations (Rakhorst, 1997)		
		Sedimentation (m <sup>3</sup> )	Erosion (m <sup>3</sup> )	Volumetric changes (m <sup>3</sup> )	Sedimentation (m <sup>3</sup> )	Erosion (m <sup>3</sup> )	Volumetric changes (m <sup>3</sup> )
(Figure 3)							
South	510,000	169,000	-25,000	144,000	354,000	0	354,000
Scour hole	172,000	16,000	-115,000	-99,000	0	-466,000	-466,000
North	485,000	32,000	-323,000	-291,000	972,000	0	972,000
Southwest	1,278,000	260,000	-600,000	-340,000	987,000	-48,000	939,000
Northeast	785,000	156,000	-2,237,000	-2,081,000	15,000	-1,040,000	-1,025,000

Table 2: Computed and observed volumetric changes (1995 - 1997)

From the confrontation of the predictions with the observations it follows that:

- The predicted volume of the scour hole is much smaller than observed. Especially the maximum depth of the scour hole was not predicted. (MSL - 7 m in stead of MSL -18 m).
- The dredged borrow area north of the dam also stretched and aligned with the inlet's channel Robbengat in the computations. It even showed a tendency for a northward migration although not at the same rate as in the observations. A weak point is that the computed total volumetric changes in the large area NorthWest does not correspond with the observations.
- The accumulation of sand north of the dam was not predicted by the model. This could be related to the smaller scour hole (less sand available) or could be due to a too much restricted horizontal eddy exchange just behind the dam.
- The computed accretion south of the dam is almost half the observed accretion. Apparently, too much of the longshore sediment transport is directed in seaward direction along the darn, in stead of being stopped. This may also be one of the reasons why the computed scour near the tip of the dam remains so limited.

The conclusion that follows is that predictions with a state-of-the-art numerical morpho-dynamical model using "standard model settings", may still differ considerably from actual developments. This is even more true when looking at smaller-scale morphological developments.

### Sensitivity computations

The following series of sensitivity computations with the numerical model were carried out to get a better understanding of the behaviour of the model and to

improve our knowledge on how these type of models should be designed and operated for the current type of applications:

- Computation with a one-week storm-condition;
- Computation not with a full harmonic analysis of the tide, but by only applying the A0, M2 and M4 tidal constituents. The phases of these constituents were then varied to study the sensitivity of the tide-averaged sediment transport on the modelled phase difference between the M2 and M4 constituents;
- Computation with another tidal schematization;
- Computation with a different model boundary at the tidal flood basin;
- Computations with different values for the dispersion coefficient in the flow and sediment transport modules;
- Computation including a schematised reproduction of spiral flow;
- Computation with an adjusted bed roughness. The spatial differences in the bed roughness have been determined in such a way that it reflects the influence of larger-scale horizontal eddies on the bed shear stress. The applied method can only be regarded as a first attempt to schematise the complex influence of large-scale turbulence on the sediment transport capacities behind structures like the long dam;
- Computation with a different chronology in the wave and tidal conditions.

It goes beyond the scope of this paper to present the findings from the above set of model computations. Details can be found in Roelvink, van Holland and Steijn (1998). Yet, the following recommendations followed for improving the model:

- Take into account the actual chronology in the wave conditions for the simulated period. As stated before, the season 1995 / 1996 was completely different in terms of westerly heavy winds, than the 1996 / 1997 season. In the improved model hindcast (see below), it was therefore decided to run the model for its first year with no waves, and for its second year with a schematisation of the actually occurring wave conditions. This appeared to be especially important for the rapid development of the scour hole.
- Take into account the effect of spiral flow. This phenomenon appeared to be important for the curving of the new channel through the dredged borrow area. Spiral flow also appeared to be important for additional sand movement towards the inner bend of the curved channel, that is towards the accretion zone north of the dam.
- Use spatially varying bed roughnesses, in such a way that they represent the effect of increased turbulence behind the long dam.

### Results from the improved model hindcast

With the improved model a new hindcast was made of the morphological developments in the period 1995 - 1997. Table 3 summarises for the same areas as in Table 2, the computed and observed volumetric changes after one year (1996) and after two years (1997).

Area	Improved hindcast			Observations (Rakhorst, 1997)		
	Sedimentation (m <sup>3</sup> )	Erosion (m <sup>3</sup> )	Volumetric changes (m <sup>3</sup> )	Sedimentation (m <sup>3</sup> )	Erosion (m <sup>3</sup> )	Volumetric changes (m <sup>3</sup> )
South	11,000	-31,000	-20,000	12,000	-31,000	-19,000
Scour hole	22,000	-310,000	-288,000	0	-497,000	-497,000
North	147,000	-63,000	84,000	572,000	-96,000	476,000
Southwest	945,000	-46,000	899,000	641,000	-109,000	532,000
Northeast	232,000	-906,000	-675,000	127,000	-495,000	-368,000

a) After 1 year (1995-1996): no waves

Area	Improved hindcast			Observations (Rakhorst, 1997)		
	Sedimentation (m <sup>3</sup> )	Erosion (m <sup>3</sup> )	Volumetric changes (m <sup>3</sup> )	Sedimentation (m <sup>3</sup> )	Erosion (m <sup>3</sup> )	Volumetric changes (m <sup>3</sup> )
South	227,000	-281,000	-53,000	354,000	0	354,000
Scour hole	116,000	-271,000	-155,000	0	-446,000	-446,000
North	363,000	-121,000	241,000	972,000	0	972,000
Southwest	538,000	-882,000	-344,000	987,000	-48,000	939,000
Northeast	299,000	-2,515,000	-2,216,000	15,000	-1,040,000	-1,025,000

b) After 2 years (1995-1997)

Table 3: Comparison between predicted and observed volumetric changes

Figures 7 and 8 further show the computed sedimentation and erosion patterns in the vicinity of the long dam, respectively after one and two years of morphodynamic simulation. Figure 8 can be compared with Figure 4, which was based on the observations.

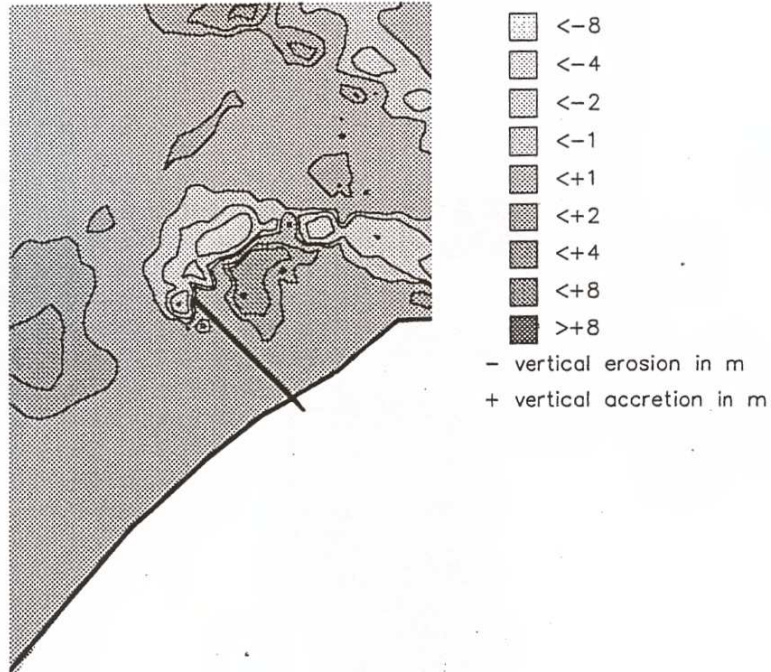


Figure 7 Computed sedimentation and erosion 1995 – 1996 (no waves)

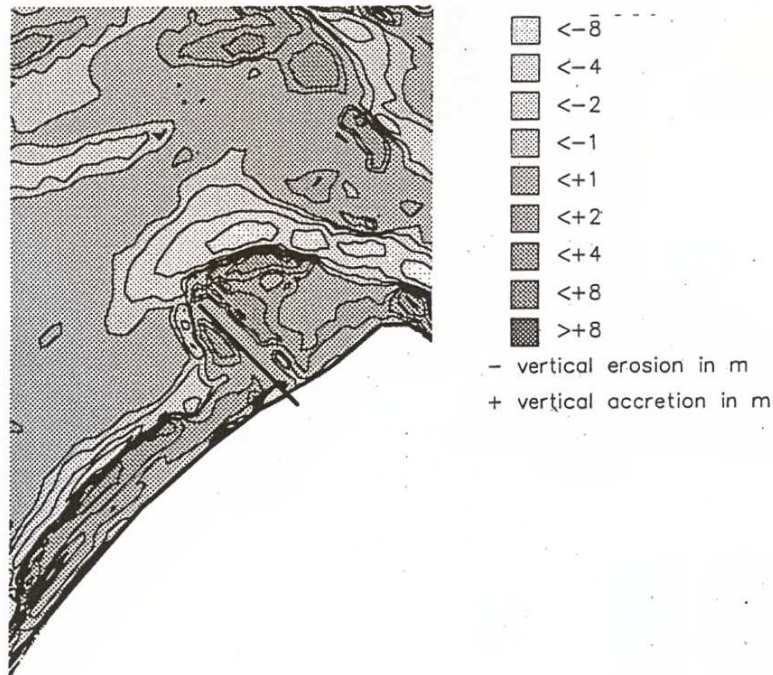


Figure 8 Computed sedimentation and erosion 1995 - 1997

## Conclusions

From a comparison of the results of the improved hindcast with the observations it follows that:

- The maximum depth in the scour hole now is computed at MSL -14 m after six months of simulated time, which is not far from the observed maximum depth of 18 m;
- In the first simulated year there is hardly any accretion south of the dam, which corresponds with the observations. In the next year, when waves are considered in the computations, there is significant accretion, which also fits with the observations.
- The coastal zone north of the dam now also accretes (contrary to the reference computation), which agrees with the observations. In absolute sense, however, there are still discrepancies between the computed accretion rates and the observed ones.
- The model shows that the dredged borrow area quickly develops into a tidal channel (in line with the Robbengat in the inlet throat), which starts to migrate in northward direction. This corresponds with the observations, albeit that the curvature of the channel as well as the migration speed differ.
- The coastal profiles in front of the north-coast of Texel (south of the dam) develop into unrealistic profiles, which would be corrected if cross-shore transport effects by waves were taken into account.

In summary, it can be concluded that the improved model simulates most of the observed morphological changes. The largest uncertainties are the modelling of the turbulence effects around the dam and the modelling of the effect of waves and turbulence on the sediment transport. For a correct representation of the morphological developments, the *behaviour* of the applied sediment transport formula as a function of the combined flow, turbulence and orbital velocities, is of special importance.

## Final remarks

The long dam has been effective in the protection of the north-coast of Texel. Contrary to the predictions it has not worsened the situation directly north of the dam. Possible negative consequences for the sand balance of the downdrift island Vlieland have not yet been recorded, but that is probably a matter of time. The morphological response have largely been restricted to the immediate surroundings of the works. But again, this may be a matter of time. After all, the new elongated tidal channel Robbengat has proven to play an important role in the filling and emptying of the flood basin.

Rijkswaterstaat will continue to monitor the situation in the tidal inlet and around the dam. We expect that after some time this data set will form a very valuable source for experimental testing of existing and new model concepts.

## Acknowledgements

The work is carried out as part of the Coast2000 programme of the Dutch Ministry of Transport and Public Works (Rijkswaterstaat). The authors further want to acknowledge the staff of the Regional Directorate North-Netherlands of Rijkswaterstaat for visualising the data sets of the Eijerlandse Gat.

## References

*De Vriend, H.J., J. Zyserman, J. Nicholson, J.A. Roelvink, P. Pechon and H.N. Southgate, 1993.* Medium-term 2DH coastal area modelling. Coastal Engineering, 21 (1993) pp. 193-224

*Hartsuiker, G., 1991.* Coastal Defence Eijerland- hydraulic morphologic effect-study; phase 1. Delft Hydraulics report number H1241, Delft, June 1991 (in Dutch)

*Negen, E.H., 1993* Morphologic investigations using 2DH numerical models at Eijerland (Texel). M.Sc. Thesis Delft University of Technology. Also: Delft Hydraulics report number H1887, Delft, The Netherlands (in Dutch).

*Rakhorst, D. 1997.* Morphological evaluation Dam at Eijerland (third report). Rijkswaterstaat, Regional Directorate North Holland, December 1997 (in Dutch).

*Rakhorst, D., D. De Wilde and C. Schot, 1997.* Seaward Coastal Defence Scheme Eijerland. Terra et Aqua - number 67 - June 1997, pp. 3-13.

*Ribberink, J.S. and J.H. De Vroeg, 1992.* Coastal Defence Eijerland - hydraulic morphologic effect-study phase II. Delft Hydraulics report number H1241, May 1992

*Ribberink, J.S., E.H. Negen and G. Hartsuiker, 1995.* Mathematical Modeling of coastal morphodynamics near a tidal inlet system. Coastal Dynamics '95, ASCE, Gdansk, Poland.

*Roelvink, J.A., A.E.G. Boutmy and J.M.T Stam, 1998.* A simple method to predict long-term morphological changes using complex model results. Thesis Proceedings.

*Roelvink, J.A., G. van Holland and R.C. Steijn, 1998.* Sensitivity computations Eijerland and SW- Texel - phase 1 Eijerland. Report jointly prepared by Alkyon (number A266) and Delft Hydraulics (number Z2430), May 1998, (in Dutch)

*Rijkswaterstaat, 1990.* A new coastal defence policy for the Netherlands. Ministry of Public Works, the Netherlands





# 9 Fundamentals of Mud

## 9.1 Introduction

In the previous chapters, the main emphasis has been on sandy coasts. But even in sand at the bottom of the sea some silt and clay particles occur. The fluid-sediment mixture of (salt) water, silt, clay and organic materials can be defined as *mud*. This chapter deals with some fundamentals of mud in coastal areas. Firstly, the relevance of mud will be discussed in Section 9.2, using examples of coastal systems where mud plays an important role. In Section 9.3, a definition of the term mud will be given and the characteristics of mud will be discussed. The focus will be on the different behaviour of mud compared to that of sand in the sediment transport processes. The effects of mud on the actual transport will be discussed in Section 9.4, followed by a reflection on the resulting bed level change in Section 9.5. Finally, in Section 9.6, some environmental issues and the consequences for the coastal engineer will be discussed, as mud is easily polluted by for example heavy metals.

## 9.2 Examples of coastal systems with mud

Based on the size and composition of the beach material, the world's coast can be classified as follows:

- muddy coasts;
- sandy coasts;
- gravel/shingle coasts;
- rock/cliff coasts.

The focus of this course is on the sandy coasts; approximately 10% to 15% of the world's coasts. About 5% to 10% of the world's coasts, however, consist of muddy coasts. The remaining 75% to 80% consists of rock, cliff and gravel-type coasts, which are beyond the scope of this course.

Muddy coasts are particularly found near the mouths of rivers. An example of a muddy coast is the Guyana coast in South America. This 1600 km long coast of Guyana, Surinam, French Guyana, parts of Brazil and Venezuela consists mainly of mud transported to the coast by the Orinoco and Amazon Rivers. Large parts of the coast consist of mangroves (see Fig.9.1; next page). Other examples of mud coasts can be found near the mouths of the Mississippi River (USA) and the Yellow River (China).

Mud also plays an important role in parts of the coastal system of The Netherlands. The low lying parts of The Netherlands are mainly formed by transported sediments by the rivers Rhine, Meuse and Scheldt. Especially the estuarine area in the south west (Zeeland) and the Wadden Sea are influenced by mud (see Fig.9.2; next page). In the following sections it will be made clear why mud is important for engineering practices.



**Figure 9.1 Mangroves**



**Figure 9.2 Satellite image of the Wadden Sea**

### 9.3 Characteristics of mud

The public perception of mud is that it is a dirty, sticky, dark-coloured and evil-smelling nuisance, whereas sand is generally seen as an asset, conjuring up pictures of golden or silver holiday beaches. But what is scientifically seen mud?

Sediments in a coastal system can be found in a large range of sizes. From large boulders with diameters exceeding 25 cm to very fine material like clay. The size of the sediment grains can be used to classify the sediment. An example of this classification is the Wentworth classification, which is often used by geologists (see Fig.9.3). According to this classification, sand is defined as grains with a size between 63  $\mu\text{m}$  (lower limit very fine sand) and 2 mm (upper limit very coarse sand). Material with a grain size smaller than 63  $\mu\text{m}$  can be defined as clay and silt.

Unified Soils Classification	ASTM Mesh	mm Size	Phi Value	Wentworth Classification
Cobble		256.0	-8.0	Boulder
Coarse Gravel		76.0	-6.25	Cobble
Fine Gravel		64.0	-6.0	Pebble
Coarse Sand	4	19.0	-4.25	
Medium Sand	5	4.76	-2.25	Gravel
Fine Sand	10	4.0	-2.0	
Silt	18	2.0	-1.0	Very Coarse Sand
	25	1.0	0.0	Coarse Sand
Clay	40	0.5	1.0	Medium Sand
	60	0.25	2.0	Fine Sand
Colloid	120	0.125	3.0	Very Fine Sand
	200	0.074	3.75	Silt
	230	0.063	4.0	Clay
		0.0039	8.0	Colloid
		0.0024	12.0	

**Figure 9.3** Wentworth classification

Mud is primarily a mixture of (a lot of) water, silt, clay and organic matter. In the stuff we normally call 'mud' also some very fine sand is often present.

Not only there is a difference in size between sand and silt/clay, but also the mineral constitution of silt/clay is different. Most of the sands in European waters consist of quartz minerals. These form chemically hard and stable crystals, with a spherical shape. Sand is a non-cohesive material; the individual grains do not stick together. Clay particles, on the other hand, consist of what chemists call 'metal silicates'. Their structure is plate-like (see Fig.9.4 next page). Clay particles have strong cohesive properties. These are largely attributable to chemical forces acting between

the grains on a small scale. The plate-like clay minerals are positively charged on the edges and negatively on the faces. When the distance between particles is small enough, they can become stuck in a ‘card-house’ structure. This process, called flocculation, is enhanced by the surrounding water environment and ionic constituents. Especially in a saline environment, free cat ions such as sodium  $\text{Na}^+$  and calcium  $\text{Ca}^{2+}$  form a layer around the negatively charged faces. These electrical double-layers around the clay particles enhance the bond between particles. Another factor enlarging the flocculation process is the presence of organic, sticky material, which is easily adsorbed on the flat clay particles.

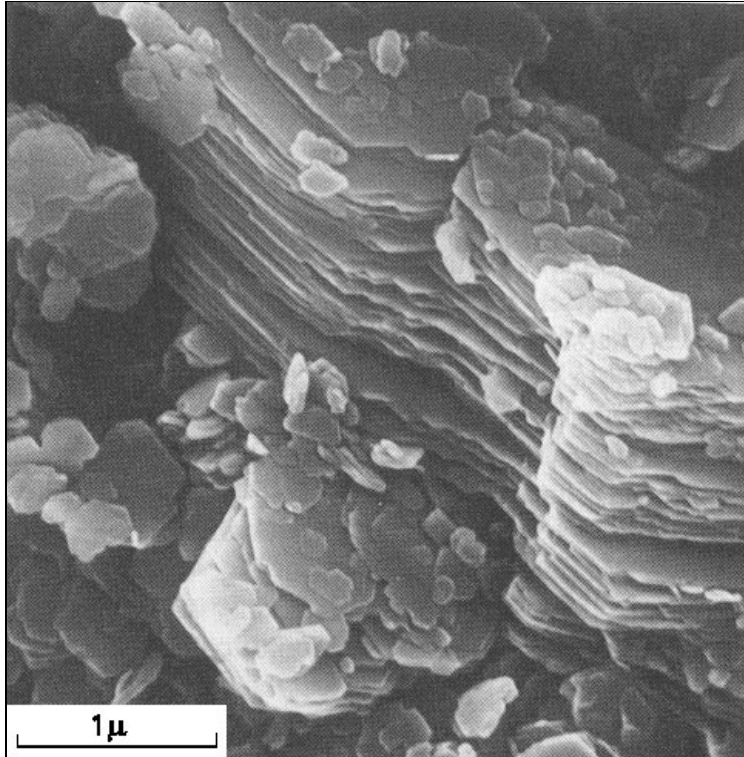


**Figure 9.4 Structure of clay particles**

Environmental factors that increase this flocculation process are:

- salinity: in salt water, more free cat ions are present;
- concentration: more particles in the water column increase the chance of collisions between the particles;
- water movements: especially in the turbulent motion caused by waves, the chance of collisions between particles is much larger than in still water.

The importance of the formation of flocks when sediment transport is considered, will be shown in the next section.

## 9.4 Sediment transport

Sand, silt and clay particles are continuously entrained, transported and deposited in the coastal system by currents and waves. Due to the difference in grain size and cohesiveness, the sediment transport characteristics of sand and mud are different.

In general, sand is transported as bed load, which occurs at the bed-water interface, and as suspended load, which occurs in the water column. For low sediment concentrations, silt and clay are only transported in suspension.

For high concentrations, silt and clay can also be transported as fluid mud in a layer near the bed. In that case, the fluid mud will act as a viscous layer on top of the bed, blocking exchange of sand between the bed and the water column.

A definition sketch of suspended load transport is given in Fig.9.5. Also the bed load transport is indicated.

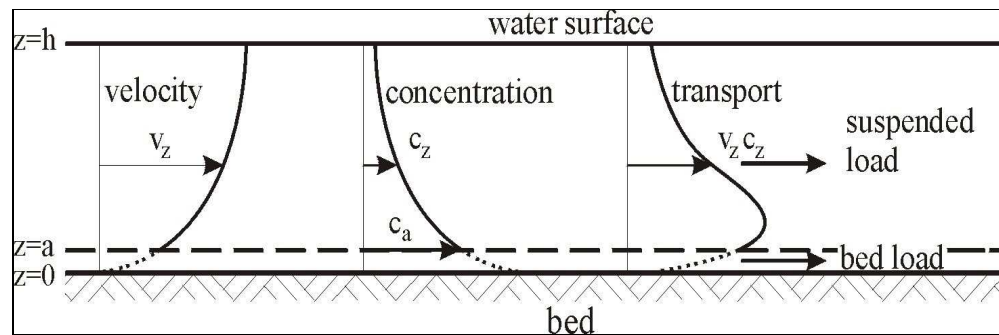


**Figure 9.5** Definition sketch of suspended sediment transport

In many cases the time-averaged convection-diffusion equation is used to compute the concentration distribution:

$$wc - \varepsilon_s \frac{dc}{dz} = 0 \quad (9.1)$$

where:

$w$	fall velocity of sediment	[m/s]
$c$	concentration	[m <sup>3</sup> /m <sup>3</sup> ]
$\varepsilon_s$	sediment mixing coefficient	[m <sup>2</sup> /s]
$z$	level above reference	[m]

An important parameter governing this equation is the fall velocity of the sediment particles. The fall velocity depends on the size, shape and specific density of the particles and of the water temperature and the sediment concentration. For sand, the particle properties are relatively independent of time (because the quartz crystals are chemically hard and stable, it takes years to change the size of a sand grain). But, as we have seen in the previous section, the size and shape of mud can change quite easily. As a result of flocculation, the size of individual mud particles increases. With this increase, particles become heavier, which will speed up the settling of the

particles. On the other hand, due to the increase in size, also the drag force, the resistance the particle ‘feels’ when settling, will increase. This will slow down the particle and can eventually cause deflocculation.

[An individual silt particle of 10  $\mu\text{m}$  has a fall velocity in still water of about 0.1 mm/s.]

Another factor influencing the sediment transport is the exchange between the bottom layer and the water column. The upward sediment flux from the bed into the water column strongly depends on the bed composition. From laboratory experiments it was concluded that two regimes can be distinguished: a non-cohesive and a cohesive regime [Van Ledden and Wang (2000)]. The clay content (the weight percentage of particles with a grain size smaller than 4  $\mu\text{m}$ ) of the bed material is the governing parameter for the transition between both regimes. For clay content of less than 5 - 10 % the bed behaves more or less non-cohesive. Sand and mud are eroded more or less independent, so the ‘normal’ formulations for the bed erosion can be used. For clay content exceeding 5 – 10 % the bed behaves cohesively. The sand and mud particles are eroded simultaneously.

This is supported by Fig.9.6 where critical velocities are given as a function of silt content in the bottom material.

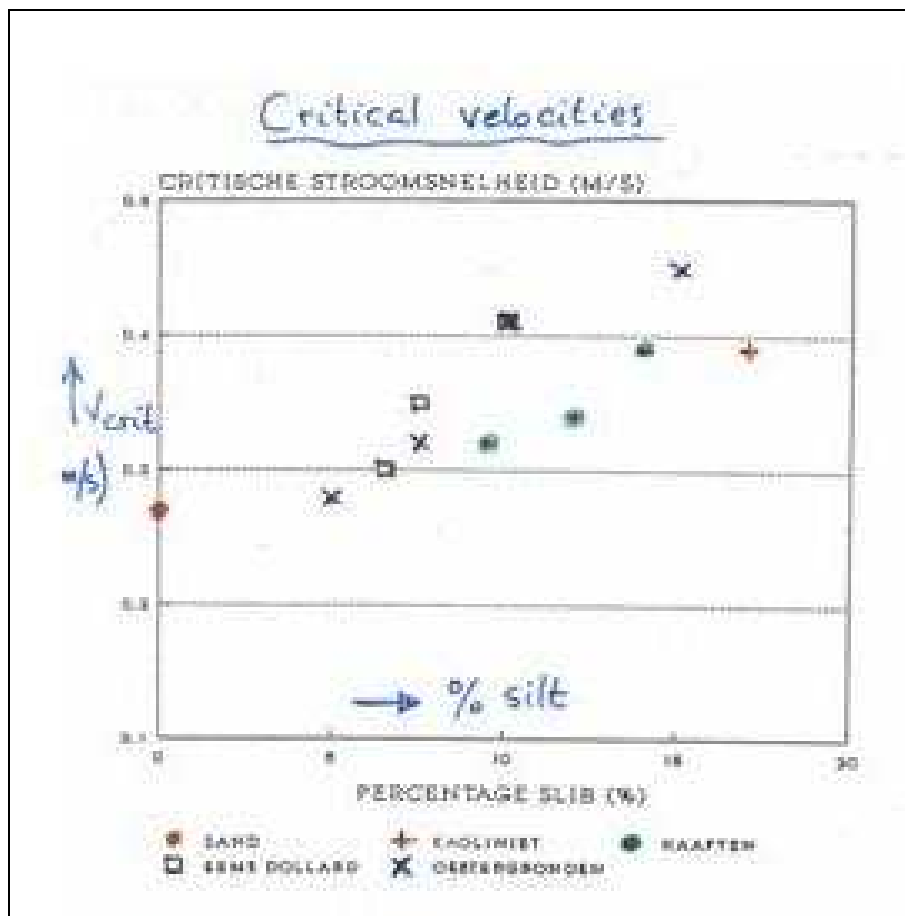


**Figure 9.6 Critical velocities as a function of silt content**



In sediment transport modelling, the exchange processes between water column and bottom layer are often assumed to be governed by the critical bed shear stress of the bottom material and the actual occurring bed shear stresses. For actual bed shear stresses larger than the critical bed shear stress of the bed material, the grains can be eroded, whereas for actual bed shear stresses smaller than the critical bed shear stress of the bed material, the grains can settle:

$$\begin{aligned}\tau_{b,actual} > \tau_{b,cr} &\rightarrow \text{erosion} \\ \tau_{b,actual} < \tau_{b,cr} &\rightarrow \text{sedimentation}\end{aligned}\quad (9.2)$$

For non-cohesive material the critical bed shear stress  $\tau_{b,cr}$  is for erosion equal to the critical bed shear stress for sedimentation. For cohesive material, where there is a strong binding force between the particles, this is not the case. The critical bed shear stress for erosion is *larger* than the critical bed shear stress for sedimentation. This implies that for a range of actual bed shear stresses, there is no exchange with the bottom layer in case of cohesive sediments:

$$\begin{aligned}\tau_{b,actual} > \tau_{b,cr,er} &\rightarrow \text{erosion} \\ \tau_{b,cr,sed} < \tau_{b,actual} < \tau_{b,cr,er} &\rightarrow \text{no exchange with bottom layer} \\ \tau_{b,actual} < \tau_{b,cr,sed} &\rightarrow \text{sedimentation}\end{aligned}\quad (9.3)$$

The exact formulations for sediment transport of mixtures of sand and mud are still subject of research.

## 9.5 Bed level change

As we have seen previously, bed level change, erosion or sedimentation, will take place in case of a horizontal variation in sediment transport:

$$(1-p)\frac{\partial z}{\partial t} = \frac{\partial S_x}{\partial x} + \frac{\partial S_y}{\partial y}\quad (9.4)$$

where:

$$\begin{array}{lll} S_x, S_y & \text{transport in respectively } x\text{- and } y\text{-direction} & [\text{m}^3/\text{s}/\text{m}] \\ p & \text{porosity } (\approx 0.4 \text{ for pure sand}) & [-] \end{array}$$

In Eq.(9.4), transports are expressed in  $\text{m}^3/\text{s}/\text{m}$  ('dry' volume of sediment). This means that the sediment transport is expressed in *volumes* of sediment. In many cases, use is made of transported *mass* in sediment transport computations. The conversion between volume and mass is given in the following equation:

$$M = \rho_s V\quad (9.5)$$

where:

$$\begin{array}{lll} M & \text{mass} & [\text{kg}] \\ \rho_s & \text{specific density} & [\text{kg}/\text{m}^3] \\ V & \text{volume} & [\text{m}^3] \end{array}$$

In the case of a real bottom, defined as a mixture of sand, silt and clay, the specific dry mass of the sediment varies between  $200 \text{ kg}/\text{m}^3$  [only silt and clay in fluid mud; density (including pore water)  $\rho_{soil} \approx 1125 \text{ kg}/\text{m}^3$ ] to  $1650 \text{ kg}/\text{m}^3$  (only sand;  $\rho_{soil} \approx$

2000 kg/m<sup>3</sup>). This means that an annual sedimentation of for instance 1000 kg per square meter bottom may result in a bed level change of 0.6 m (only sand) to 5 m (only silt and clay). Neglecting this notion could lead to large errors in bed level change computations!

(A mud bottom with a density of  $\rho_{soil} = 1300 \text{ kg/m}^3$  contains about 480 kg dry mass per m<sup>3</sup>.)

## 9.6 Environmental issues

Due to the chemical constitution of mud and especially clay, the particles have strong cohesive features, as we have seen in Section 9.3. Due to this characteristic, mud particles are easily bound together. But not only that, also other materials can easily be bound with mud particles.

Organic matter is also easily bound to mud particles. This is one of the main reasons why delta areas are so fertile and thus one of the main reasons why people settle in those low-lying, rather dangerous areas. The fertile coastal areas are also good habitats for flora and fauna.

But also contaminants are easily bound by the mud particles. At certain (low) concentrations, naturally occurring elements (i.e. copper and zinc) may have beneficial effects. But with increasing concentration, contaminants can become toxic and cause damage to the natural environment. An increase in concentration can occur due to fluvial inputs in the coastal system, but also as a result of a disturbance of a contaminated bed caused by, for example, dredging.

During dredging operations, extremely dangerous contaminants such as heavy metals and PCBs (PolyChlorinated Biphenyls) have to be accounted for. Highly contaminated mud has to be treated as chemical waste. This can have large consequences for the costs of a dredging project in a harbour. The dredged material has to be transported to special depots as for example the 'Slufter' near the Port of Rotterdam (see Fig.9.7) and to be isolated ('for ever') from the environment.

For the construction of large land reclamation projects, huge volumes of sand are required. These volumes are often dredged at the sea bottom as close as possible to the construction site; so in the most vulnerable area close to the coast. Let us assume that for a very large project 500 million m<sup>3</sup> of sand is required. The sand can be dredged at open sea, but the bottom contains 2% silt (a quite 'normal' content for natural sea beds).

During the dredging operation with hopper dredges, the bed material is pumped into the hopper. The sand remains in the hopper; the fines (silt) return to the sea with the overflow. Dredging 500 million m<sup>3</sup> in short notice in this case means that about 10 million m<sup>3</sup> of silt is mobilized in the same short notice. This might result in a heavy additional silt burden for the receiving sea system. Detrimental effects are likely.





**Figure 9.7 The Slufter (Rotterdam, The Netherlands)**



# 10 Channels and Trenches

## 10.1 Introduction

Now that we are familiar with the basic principles of sediment transport in coastal areas, we will take a closer look at the problems a coastal engineer has to deal with. One of these problems is sedimentation of channels and trenches. Channels are dredged to facilitate the entering of (large) ships in harbours. Trenches are similar features with smaller widths, used for e.g. pipelines.

When a channel is dredged it can be expected that this channel will silt up again from the simple but true statement that nature will try to restore the original situation. The necessary change in sediment transport rate is caused by a change in the current velocities and a change in the wave characteristics while crossing the channel. In this chapter the computation of this change in sediment transport rate will be elaborated.

First, in Section 10.2, a few examples of situations will be given where dredged channels are necessary. Next the computation of the sediment transport will be elaborated, starting in Section 10.3 with a discussion of the effect of the channel (or trench) on the current pattern in the area adjacent to the channel, followed by the discussion of the effects on the wave pattern in Section 10.4. Section 10.5 deals with the interaction between currents and waves in case of a dredged channel. After a description of the relevant transport processes in Section 10.6, the sedimentation rate of channels will be elaborated in Section 10.7.

## 10.2 Examples

Many harbours around the world are situated in shallow coastal systems. The waters directly in front of the harbour entrance are relatively shallow. To facilitate the entrance of (large) vessels, entrance channels have to be dredged. In a dynamic coastal system, such a channel could be prone to sedimentation. For the evaluation of the feasibility of the construction of an entrance channel, an estimation has to be made of the maintenance dredging quantities related to this sedimentation.

An example of a harbour in relatively shallow waters is the Port of Rotterdam. To facilitate the entrance of vessels with a draught of up to 75 foot (approximately 24 m), the Euro-Channel (Eurogeul in Dutch) has been constructed (see Fig.10.1; next page). To maintain the depth of the basins in the port and the entrance channel, every year a volume of approximately 20 million m<sup>3</sup> sediments have to be dredged. A large part of this dredged material is removed from the Euro-Channel itself.



**Figure 10.1 Dredging in the Euro-Channel, Rotterdam, The Netherlands**

Trenches are often used for laying pipelines used to transport e.g. oil or gas from offshore production sites to the mainland. It is necessary to know the rate of sedimentation of the trench during and after construction, as there will always be a time-lag between the construction of the trench and the laying operation of the pipe itself.

After the pipe has been laid, it is required to know the rate of sedimentation to estimate the time between construction of the pipe and the moment the pipe is covered by sediment. It is also desirable to know the constitution of the material. If the sedimented material contains a large fraction of mud, it might not be able to prevent the pipe from floating. In that case it is necessary to artificially fill the trench with sand after completion of the pipe (*backfill*).

### 10.3 Current pattern

In nearly all (undisturbed) coastal systems, currents are present (e.g. tidal currents, wave-induced currents, river discharges). A change in the magnitude of a current can have a strong influence on the sediment transport. The change in current velocity is elaborated in this section. The effects on the sediment transport can be found in Section 10.7.

When a current crosses a dredged channel the shortest way, which is *perpendicular* to the channel, its velocity will decrease due to the increased water depth. Once the current has passed the channel, its velocity will increase again. The direction of the current does not change in this case.

When the current direction and the channel are *parallel*, the current velocities in the channel might increase. The water surface slope remains approximately the same. This means that the driving force of the current remains the same. Assuming a

constant Chézy coefficient  $C$ , it can be shown with the well-known Chézy formula that the current speed will increase in the channel compared to the current speed above the banks. The formula reads:

$$v_n = C_n \sqrt{h_n i_n} \quad (n = 1 \text{ above the bank; } n = 2 \text{ inside the channel}) \quad (10.1)$$

with:  $C_1 = C_2$  and  $i_1 = i_2$ :

$$v_2 = \sqrt{\frac{h_2}{h_1}} v_1 \Rightarrow v_2 > v_1 \text{ for } h_2 > h_1 \quad (10.2)$$

If the current approaches the channel *obliquely*, the situation is more complicated. Fig.10.2 gives a definition sketch.

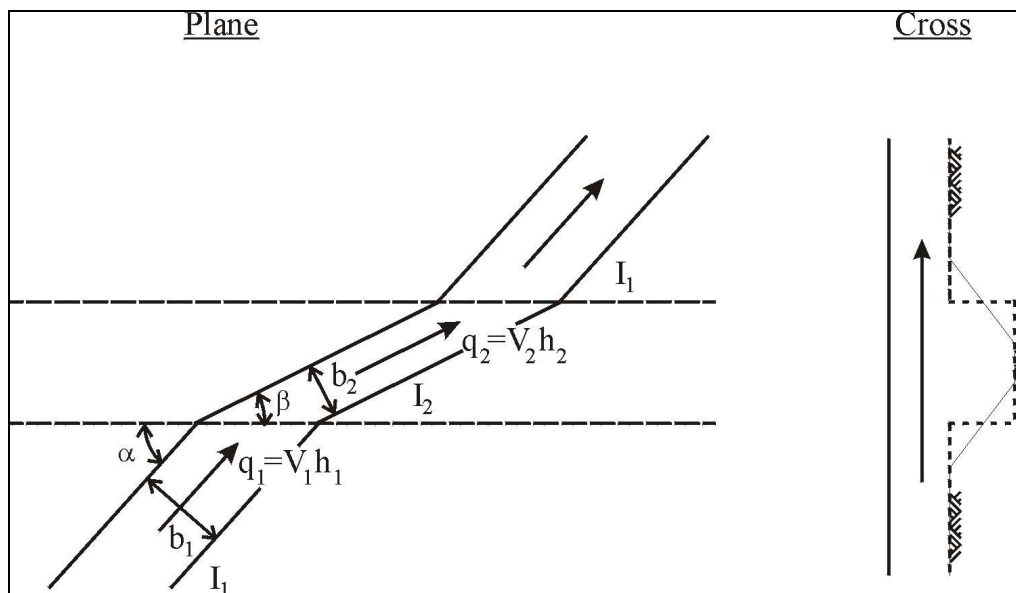


**Figure 10.2** Current pattern across a channel

There are (at least) two (analytical) methods available to compute the influence of trench on the current pattern. The first approach (denoted as *method a*) assumes that the component of the current velocity in the direction of the channel axis is the same inside the channel as on the shallower areas. This is based on the physical fact that

The second approach (*method b*) assumes equal water level slopes in the direction of the channel. This method is only valid for relatively small angles between the original current direction and the channel axis and stems from the approach in case of parallel channel axis and current direction.

### method a

The velocity component parallel to the channel axis on the bank is assumed to be equal to the velocity component parallel to the channel axis inside the channel; see Eq.(10.3):

$$v_{x1} = v_{x2}, \text{ with } v_{xm} = v_n \cos \varphi_n \quad (10.3)$$

where:

$v_n$	current velocity	[m/s]
$v_{xn}$	velocity component parallel to channel axis	[m/s]
$\varphi_n$	angle between current direction and channel axis	[°]
$n$	index ( $n = 1$ above the bank; $n = 2$ inside the channel)	[-]

Rewriting gives:

$$v_1 \cos \varphi_1 = v_2 \cos \varphi_2 \Rightarrow \cos \varphi_2 = \frac{v_1}{v_2} \cos \varphi_1$$

$$\text{using } \sin^2 \varphi + \cos^2 \varphi = 1 \text{ yields: } \sin^2 \varphi_2 = 1 - \left( \frac{v_1}{v_2} \right)^2 \cos^2 \varphi_1 \quad (10.4)$$

Assuming that there are no natural currents inside the channel, it follows from continuity that:

$$v_1 h_1 b_1 = v_2 h_2 b_2 \quad (10.5)$$

where:

$h_n$	water depth	[m]
$b_n$	mutual distance between two streamlines	[m]

From geometry it follows:

$$\frac{b_1}{b_2} = \frac{\sin \varphi_1}{\sin \varphi_2} \quad (10.6)$$

The combination of Eqs.(10.5) and (10.6) leads to:

$$\frac{v_2}{v_1} = \frac{h_1 \sin \varphi_1}{h_2 \sin \varphi_2} \quad (10.7)$$

Together with Eq.(10.4) this leads to:

$$\frac{v_2}{v_1} = \sqrt{\cos^2 \varphi_1 + \left( \frac{h_1}{h_2} \right)^2 \sin^2 \varphi_1} \quad (10.8)$$

This method implies that the current velocities inside the channel can never be higher than those on the shallower areas (in cases where there is no other current inside the channel).

### method b

The water level slope in the direction of the channel axis is assumed to be the same on the bank as inside the channel; see Eq.(10.9):

$$i_{x1} = i_{x2}, \text{ with } i_{xn} = \frac{v_{xn}^2}{C_n^2 h_n} \text{ and } v_{xn} = v_n \cos \varphi_n \quad (10.9)$$

where:

$i_{xn}$  water surface slope in parallel to channel axis  
 $C_n$  Chézy coefficient

Rewriting yields:

$$\begin{aligned} \frac{v_{x1}^2}{C_1^2 h_1} &= \frac{v_{x2}^2}{C_2^2 h_2} \\ \frac{v_1^2 \cos^2 \varphi_1}{C_1^2 h_1} &= \frac{v_2^2 \cos^2 \varphi_2}{C_2^2 h_2} \\ \left( \frac{v_2}{v_1} \right)^2 &= \left( \frac{C_2}{C_1} \right)^2 \left( \frac{h_2}{h_1} \right) \frac{\cos^2 \varphi_1}{\cos^2 \varphi_2} \end{aligned} \quad (10.10)$$

From continuity [Eq.(10.5)] and geometry [Eq.(10.6)] follows Eq.(10.7), which can be rewritten to:

$$\begin{aligned} \sin \varphi_2 &= \frac{v_1}{v_2} \frac{h_1}{h_2} \sin \varphi_1 \\ \sin^2 \varphi_2 &= \left( \frac{v_1}{v_2} \right)^2 \left( \frac{h_1}{h_2} \right)^2 \sin^2 \varphi_1 \\ \cos^2 \varphi_2 &= 1 - \sin^2 \varphi_2 = 1 - \left( \frac{v_1}{v_2} \right)^2 \left( \frac{h_1}{h_2} \right)^2 \sin^2 \varphi_1 \end{aligned} \quad (10.11)$$

Together with Eq.(10.10) this leads to:

$$\frac{v_2}{v_1} = \sqrt{\left( \frac{C_2}{C_1} \right)^2 \left( \frac{h_2}{h_1} \right) \cos^2 \varphi_1 + \left( \frac{h_1}{h_2} \right)^2 \sin^2 \varphi_1} \quad (10.12)$$

In this method, the current velocity inside the channel can become higher than the velocities outside the channel. This is consistent with measurements in nature, for example in the NEDECO study in 1983 for the dredging of an access channel to the Port of Bahía Blanca, Argentina. [NEDECO (1983).]

In Fig. 10.3 (next page) the relation  $v_2/v_1$  has been plotted for different approach angles; the ratio  $h_2/h_1$  is equal to 2 in this case. For simplicity, the Chézy coefficients  $C_1$  and  $C_2$  are taken equal. In the graphs, also the results of physical model tests by the Hydraulic Research Station Wallingford (1973) and WL | Delft Hydraulics (1983) have been plotted, together with the results of computations with three mathematical models by WL | Delft Hydraulics (1985). From Fig. 10.3 it can be concluded that *method a* underestimates the current velocities inside the channel (especially for small approach angles), whereas *method b* overestimates the velocities (especially for large approach angles).

For a first approach, both analytical methods can be used. However, when more detail is needed, the current velocities should be computed using sophisticated numerical models or be measured in a physical model.

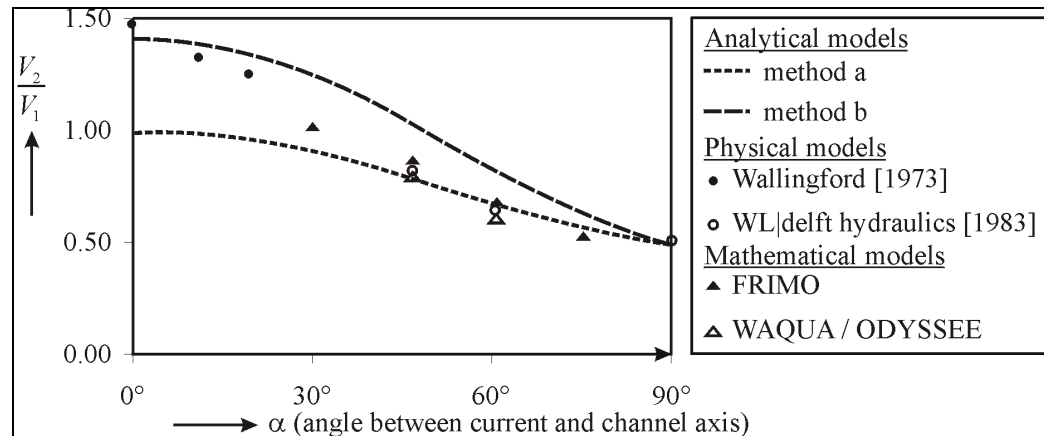


**Figure 10.3 Relationship  $v_2/v_1$**

## 10.4 Wave pattern

When a wave field crosses a (dredged) channel, a phenomenon occurs similar to a current crossing a channel. Again, the phenomenon depends strongly on the angle between the wave propagation and the channel axis.

When the waves are propagating *parallel* with the axis of a wide channel, the wave height above the channel will decrease somewhat due to the increased water depth. The wave propagation velocity in the middle of the channel will increase due to the increased water depth, since:

$$c = \sqrt{gh} \quad (\text{for shallow water}) \quad (10.13)$$

(For transitional water depths the propagation speed of the waves increases also for larger water depths.)

This increase in wave propagation velocity will yield curved wave crests.

When the waves are propagating *perpendicular* to the channel axis the primary effect is that the wave height above the channel will decrease due to the increased water depth. A secondary effect could be reflection of the waves on the edge of the side slopes of the channel.

As with the current, the most complicated situation occurs when the waves approach the channel *obliquely*. Not only the wave height changes, but also the direction of the waves. The change in direction of the waves is similar to the wave refraction mentioned in Chapter 2. In this case, however, the water depth increases instead of decreases. For a certain (critical) wave approach angle and channel depth the



incoming waves can become trapped inside the channel or even return in the direction of shallower depths.

## 10.5 Current-wave interaction

The situation becomes even more complicated in the case of interaction between waves and currents. This can be illustrated by a tidal channel (see Fig.10.4). The current direction changes with the tide. In this specific case, the waves are assumed to have a direction parallel to the channel axis. The refraction depends on the tidal phase:

- in case of an ebb current (current direction opposite to the direction of wave propagation), the waves are refracted into the channel;
- in case of a flood current (current direction and wave propagation direction the same), the waves are refracted into the shallower areas.

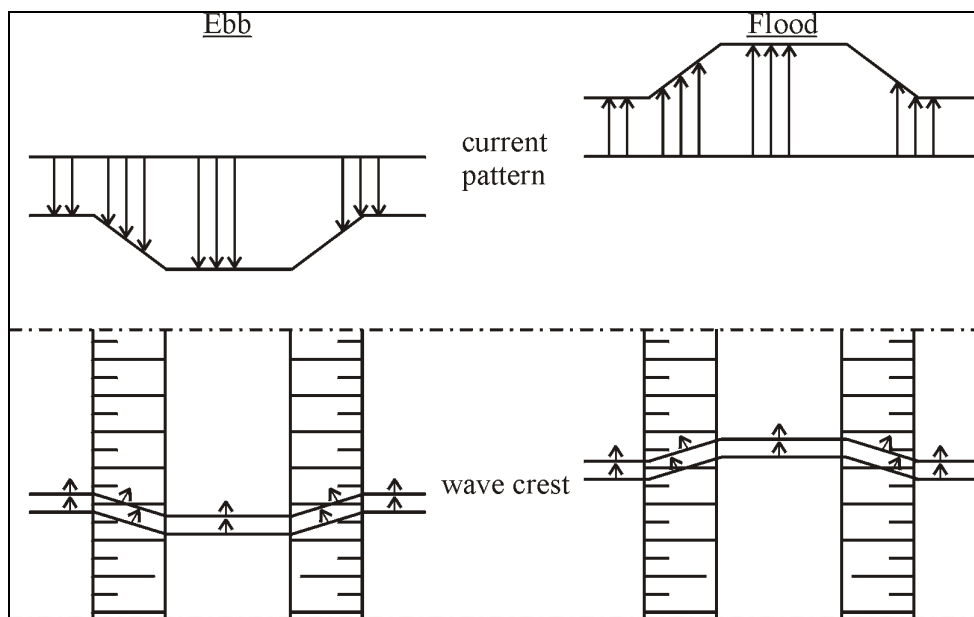


**Figure 10.4** Sketch of a tidal channel

As a result, there is more wave action inside the channel during the ebb phase and less wave action during the flood phase in comparison with areas next to the channel.

All these phenomena together imply a rapid change in radiation stress components near the channel. A new force balance should be formulated to determine the exact direction and magnitude of the resulting currents. As this new force balance is too complex for theoretical treatment here, the additional driving forces are neglected in this course. If needed for practical applications, the complex system of currents and waves can be determined using numerical or physical modelling.

## 10.6 Transport processes

Sedimentation (or erosion) in a (dredged) channel is determined by a change in the transport rate. The sediment transport can be divided in the transport of coarse material (sand,  $D_{50} > 63 \mu\text{m}$ ) and fine material (mud,  $D_{50} < 63 \mu\text{m}$ ). Coarse material is transported as bed load and suspended load, whereas fine material is transported as suspended load.

Bed load sediment transport can respond quite rapidly to changes in the physical conditions. The bed load transport is almost exclusively determined by the local velocity and bed shear stress conditions. This means that once the local current and wave conditions have been determined, it is possible to compute the local bed load transport.

With the bed load transport known as a function of position in the area of interest it is possible to compute the rate of erosion or sedimentation from the differences in bed load transport. Although this computation is rather simple, it would only be of practical importance for channel applications in the case of negligible or constant suspended load transport.

The suspended load transport is considerably more difficult to determine than the bed load transport. The material in suspension is distributed over the entire depth at any location. The local diffusion coefficient  $\varepsilon_s$  and the fall velocity of the material  $w$  are important, but also advection and diffusion processes. This implies gradual settling or re-suspension processes in case of changing conditions. This means that the local suspended sediment concentration at some point depends on the immediate local conditions of turbulence and bed load, as well as the past history of these phenomena; e.g. farther upstream.

Specifically, this means in the case of a current which meets a (wide) channel, where the depth suddenly increases, that initially the suspended sediment load will be redistributed over the entire water column (suspended particles remain in the stream tubes to a first approach). Only a few sediment particles will reach the bottom, while the current is passing the slope between bank and bottom of the channel. The suspended sediment concentration (just) inside the channel therefore depends strongly on the suspended sediment concentration just upstream of the channel and not, as is normally the case, on the concentration near the bed. The bed load transport adapts more or less instantaneously to the conditions belonging to the water depth inside the channel. With time, while the current is passing the channel, the suspended sediment concentrations in the water column tend to a new equilibrium based on the changed hydraulic conditions inside the channel. Because of the increased water depth, the concentrations will decrease. See also Fig.10.5.

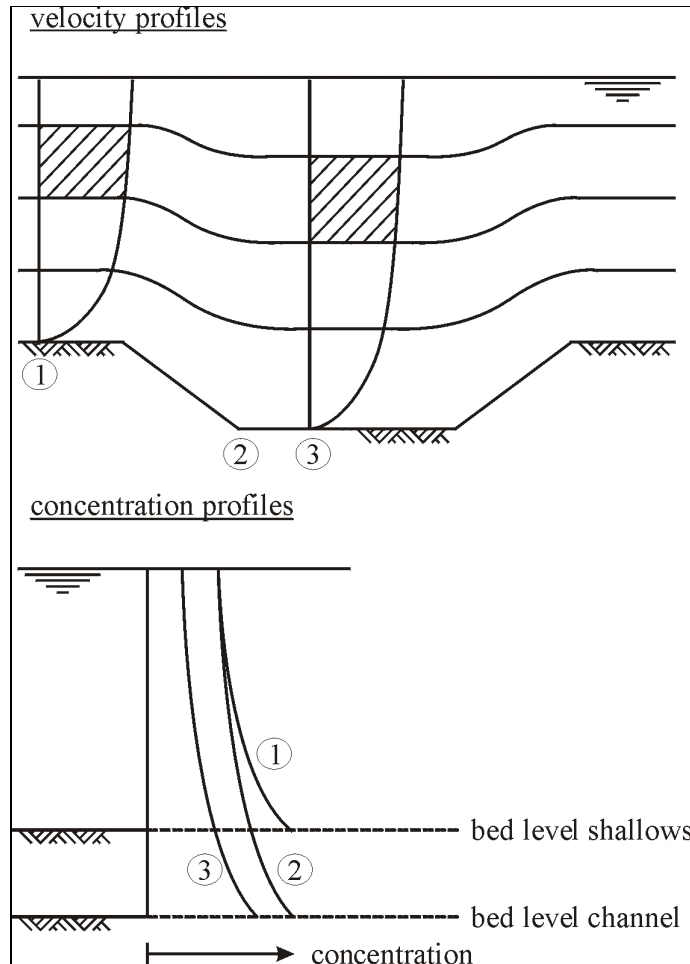


**Figure 10.5 Sedimentation mechanism**

For the determination of the suspended load transport of fine material, the situation is even more complicated due to the time- and concentration dependent fall velocities. As we have seen in Chapter 9, the fall velocity of mud changes as a result of flocculation. This flocculation depends on several parameters, amongst others the local concentration.

Finally, attention has to be paid to the possible effects of the sloping sides of the channel on the sediment transport. Due to gravity, sediment particles resting on the side slope are subject to a force which tries to move them down the slope into the channel. This mechanism is especially of importance for channels which are nearly parallel to the existing dominant current direction.

For the computation of the sedimentation (or erosion) in or near a channel, different methods are available. In the next section we will give:

- an approximation method to compute the extremes;
- a very rough approximation, which can be done by hand;
- the principles of a more sophisticated solution.

It should be noted that the two first approximation methods are determined for coarse sediments only. For situations where mud plays an important role, or generally more complicated situations, use should be made of numerical models based on physics, or of physical models.

## 10.7 Sedimentation computation

### 10.7.1 Extremes

To obtain a first, relatively easy solution to a channel siltation problem, it is suggested to determine the limits of the channel morphological changes. The basis for the determination of these extremes will be the (calculated) sediment transport rates holding for the steady state situations above the bank and inside the channel.

The first step is to evaluate the physical conditions at several places. Several points along the direction of the dominant current should be used, of course both inside the channel and in the shallower areas.

The second step is to evaluate the bed load transport and the suspended load transport separately at each chosen point. This is done under the (incorrect) assumption that the conditions are only slowly changing.

Finally, the sedimentation or erosion of an area can be found by examining the changes in transport rates between the chosen points.

For the bed load transport, this method yields fairly accurate sedimentation or erosion rates, as the bed load transport adapts quickly to new hydraulic conditions. This is not directly the case for the suspended sediment load transport.

The maximum values for deposition or erosion due to suspended material are found from the differences in the (calculated) suspended sediment transport rates in the chosen points. This yields indeed maximum values for deposition, as in the deposition area the actual suspended sediment transport rates will be larger than the equilibrium transport rates. In the erosion area the actual suspended transport rates will be generally smaller than the equilibrium transport rates.

Minimum values for sedimentation and erosion are found from the assumption that no change in suspended sediment concentration takes place in the considered area.

The values for the minimum and maximum rate of deposition or erosion can now be computed from the bed load transport effect plus the suspended transport effects. Hence, the minimum rate of deposition or erosion follows directly from the change in bed load transport rates, whereas the maximum deposition or erosion rate follows from the summation of the change in bed load transport rates and the maximum expected change in suspended transport rates.

The actual values of the deposition and/or erosion rates (in case of suspended transport) depend strongly on the sediment size in the area and the 'width' of the channel measured in the direction of the dominant current. For small grains (with low fall velocities) and/or channels with a small width, the actual rates of deposition and/or erosion are small, whereas for larger grains (with higher fall velocities) and/or wider channels, the deposition and/or erosion rates are relatively high.

## 10.7.2 Rough approximation

For a more accurate estimation of the deposition rate inside the channel use is made of the equilibrium sediment transport capacity on the shallow area and inside the channel. If the channel is wide enough (seen in the direction of the current), after a certain distance, the sediment transport rate becomes equal to the sediment transport capacity based on the local hydraulic conditions (see Fig.10.6).

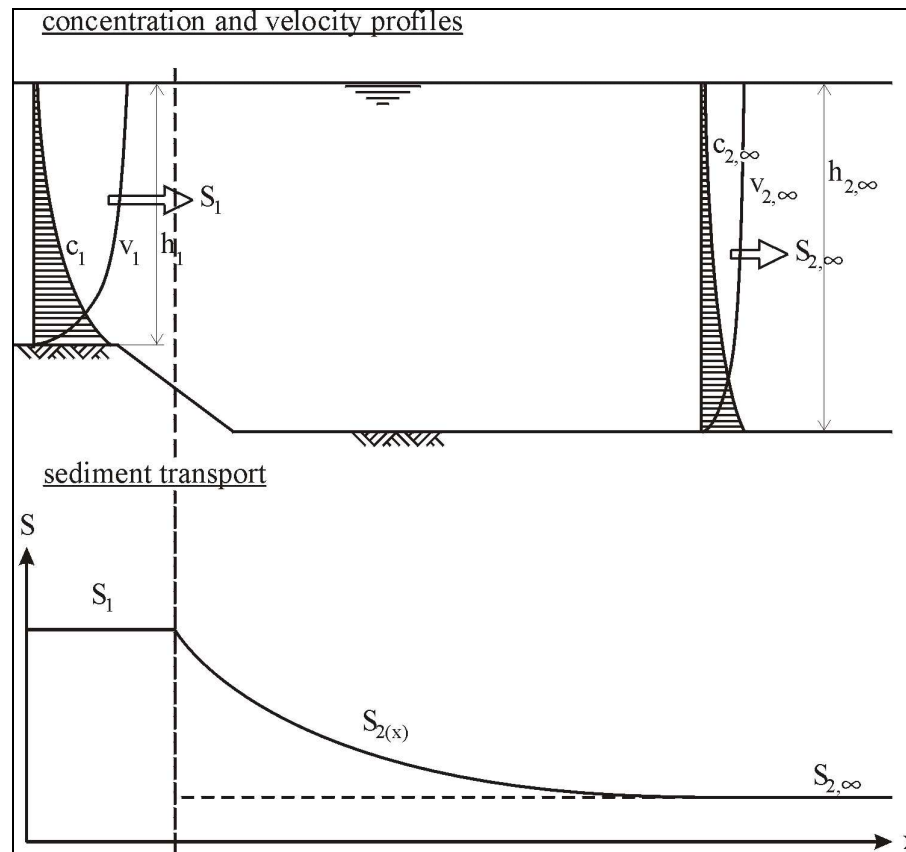


**Figure 10.6 Sedimentation rate in a wide channel**

For the transition between these two equilibrium conditions, often an exponential behaviour is assumed:

$$\frac{b_1 q_{s,1} - b_2 q_{s,x}}{b_1 q_{s,1} - b_2 q_{s,2}} = (1 - e^{-Ax}) \quad (10.14)$$

where:

- $b_1, b_2$  width of stream tube (resp. in the shallow area and in the channel) [m]
- $q_{s,1}, q_{s,2}$  suspended sediment transport per unit width (resp. in the shallow area and in the channel) [ $\text{m}^3/\text{s}/\text{m}$ ]
- $x$  distance from channel side slope in the direction of the current [m]

$A$  coefficient  $[m^{-1}]$

The coefficient  $A$  depends on the fall velocity of the sediment. Various authors give a solution for the computation of the exponential function, amongst others Mayor *et al.* (1976), Lean (1980), Bijker (1980) and Eysink and Vermaas (1983). More information can be found in Van Rijn (1993).

It should be noted that these solutions are only valid for the deposition of material at the upstream side of the channel; not for the possible erosion at the downstream side. Thus, the application of these formulae may lead to an overestimation of the total deposition in the channel.

### 10.7.3 Sophisticated solution

For a more detailed theoretical description of sedimentation (or erosion) under conditions of changing depth, more variables have to be included than those discussed in earlier sections. In order to make a better theoretical approach possible, three assumptions have to be made:

- No flow separation occurs on the side slopes of the channel; the current streamlines near the bed follow the slope; this will be true for channels with side slopes not steeper than  $\approx 1:7$ .
- Flow streamlines remain horizontal (except while passing the slope between bank and bottom of the channel). This implies that the suspended sediment is only moved along the streamline by the current which, in turn, can cause no direct sedimentation.
- The rate of turbulence, characterised by the diffusion coefficient  $\varepsilon$ , adapts instantaneously to each new situation.

A fourth assumption, of an instantly varying bottom concentration, is quite common in literature, but is in fact not so evident as it would appear, at least not in cases with deposition. In principle, the initial concentration vertical can contain more particles than the equilibrium vertical. The ‘extra’ particles have to settle (sedimentation), so, consequently, the particles have to pass through the bottom transport layer. Temporarily, this could mean a higher than equilibrium concentration than associated with the boundary conditions.

In the following, the equations of (sediment) continuity and motion are given, together with the boundary conditions necessary to resolve the equations.

#### Equation of (sediment) continuity

We consider a volume of water above the area where a sedimentation prediction is required. The block has a width perpendicular to the flow of one unit, a height  $dz$  and a length in the direction of the flow of  $dx$  (see Fig.10.7). The equation of continuity of this block is given by:

$$v \frac{\partial c}{\partial x} = w \frac{\partial c}{\partial z} + \frac{\partial}{\partial z} \left( \varepsilon_s \frac{\partial c}{\partial z} \right) \quad (10.15)$$

where:

$v$	current velocity	$[m/s]$
$c$	suspended sediment concentration	$[m^3/m^3]$
$\varepsilon_s$	diffusion coefficient	$[m^2/s]$

$w$  fall velocity [m/s]

Eq.(10.15) can be rewritten as:

$$\frac{\partial}{\partial x} S_s(x, z) dx dz + \frac{\partial}{\partial z} S_v(x, z) dx dz = 0 \tag{10.16}$$

where:

- $S_s(x, z)$  horizontal transport of suspended sediment
- $S_v(x, z)$  vertical transport of suspended sediment (positive downward)

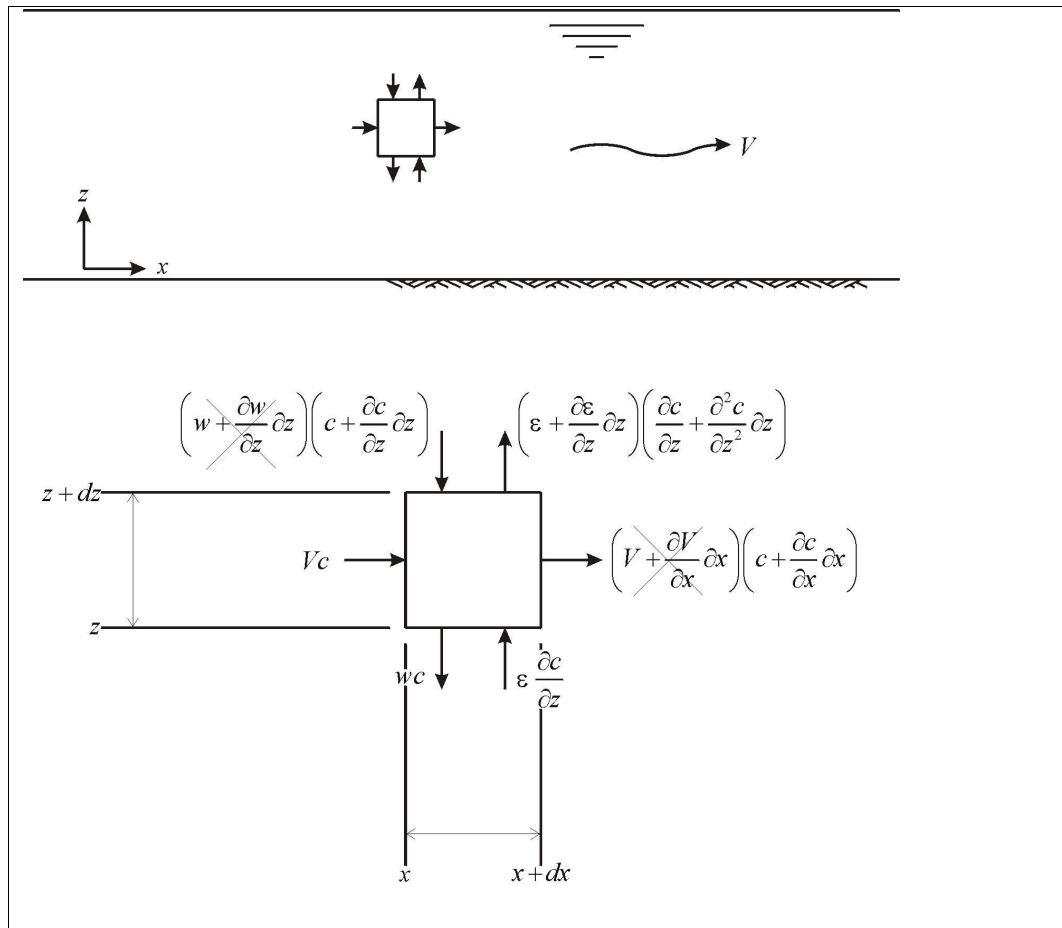


**Figure 10.7 Continuity equation**

**Equation of (sediment) motion in vertical direction**

For the vertical transport of sediment  $S_v$  we can find:

$$S_v(x, z) = w \cdot c(x, z) - \varepsilon_s \frac{\partial c(x, z)}{\partial z} \tag{10.17}$$

In a steady state situation the vertical transport is zero,  $S_v = 0$ . In that case, Eq.(10.17) results in (the already known equation, see e.g. Eq.(9.1)):

$$w \cdot c(x, z) - \varepsilon_s \frac{\partial c(x, z)}{\partial z} = 0 \quad (10.18)$$

### Equation of (sediment) motion in horizontal direction

The horizontal suspended sediment transport is determined by the resulting water velocity  $v$  and the concentration  $c$ :

$$S_s(x, z) = v(x, z)c(x, z) \quad (10.19)$$

### Boundary conditions

To resolve these equations, boundary conditions are needed at the free surface and at the bottom. At the free surface,  $z = h$ , no sediment is added or removed, so Eq.(10.17) reduces to Eq.(10.18):

$$w \cdot c(x, h) - \varepsilon_s \frac{\partial c(x, h)}{\partial z} = 0 \quad (10.20)$$

For the boundary condition at the bottom, the following possibilities are suggested:

- In the case of increasing water depth, the (unknown) actual bottom concentration is larger than the equilibrium bottom concentration as is found in steady state relations. Therefore, sedimentation takes place. The boundary condition in this situation is often given by:

$$\left[ \frac{\partial c}{\partial z} \right]_b = 0 \Rightarrow S_v(x, z) = w \cdot c(x, z) \quad (10.21)$$

- Sometimes, the bottom concentration is assumed to directly adapt to the new local conditions. In that case the boundary condition at the bottom is given by:

$$c = c_b, \text{ with } c_b \text{ computed from bottom transport formulae} \quad (10.22)$$

Several authors describe the numerical integration procedures needed to resolve this set of equations, amongst others Kerssens and Van Rijn (1977) and Van Rijn (1986).

Another option is to simplify the aforementioned formulae in order to find a solution using a simple calculator or even by hand. This is the approach Bijker (1980) used. He separated the effects of suspended load and bed load. The bed load was assumed to follow the physical changes directly. The suspended load was assumed to follow more slowly. So the reference concentration  $c_b$  used in the formula for suspended sediment transport can differ from the one used in the bed load transport formula. In effect, Bijker resolved the solution in a similar way as the rough approach described in Section 10.7.2, with an exponentially changing suspended sediment transport rate. This relatively simple methods yields result with an accuracy of approximately 10% in comparison with the WL | Delft Hydraulics' model SUTRENCH [WL | Delft Hydraulics (1977)].

With sophisticated computation models like Delft3D and MIKE 3 also sedimentation (and erosion) calculations can be made for channels. Tonnon (2005) shows rather fair agreements between results of calculations and actual measurements. [In Tonnon's simulations the morphological behaviour with time of sand dumps (instead of a channel) was compared with calculations.]



# 11 Coastal Protection

## 11.1 Introduction

The transition between sea and land (waterline / coastline) is never a fixed line along our (sandy) coasts.

Seen at a short time scale, e.g. scale of tidal variations, the waterline continuously shifts in landward and seaward direction. This is a well-known example of the natural behaviour of our coasts and is often considered as an intriguing feature of our coasts.

Seen over a longer time scale, many coasts all over the world show a structural, gradual and continuous accreting or eroding tendency (although also stable coasts do occur). Pure natural (autonomous) reasons, or man-induced reasons might cause this behaviour.

While accreting coasts are welcomed in most cases by coastal zone managers and by people living near the sea, eroding coasts bother the people. Valuable land with most likely various existing interests, will be lost.

How to deal with eroding coast problems is a main topic of this chapter. Selecting a proper approach for a protection scheme calls, however, for a detailed insight in the real causes of the actual erosion problem as it is felt. So also some reasons for erosion problems will be discussed.

Although important, eroding coasts form as a matter of course only a restricted class of coastal engineering problems. Also problems like coastline stabilization (e.g. near tidal inlets), widening of (recreation) beaches and reduction of erosion during a severe storm surge are typical examples of problems to be resolved with the help of coastal engineering knowledge and coastal engineering tools. Such problems are mainly discussed in Chapter 12.

Coastal systems are generally vulnerable systems. It is very easy to harm such a vulnerable system with thoughtless surgery. This calls for a skilled and powerful, and, that is very important, a legally backed system of Coastal Zone Management.

In Section 11.2 some examples of coastal erosion are dealt with. In Section 11.3 the fundamental approach of coastal protection is discussed. A few remarks on Coastal Zone Management are made in Section 11.4.

In the discussions in the present chapter and Chapter 12 also the various coastal engineering tools to achieve the aims are discussed. It will be argued that these aims must be well-defined. Without well-defined aims never adequate solutions to coastal engineering problems can be found.

It is good to realize that our earth exists for about 4.5 billion years. During most of this time pure natural developments shaped and reshaped our coasts. At some places new land was created; at other places erosion occurred. Nowadays coastal accretion

is often felt 'good' and erosion 'bad'. In the past these notions did not exist. Accretion was not better than erosion or vice versa.

Since say 45,000 years ( $\approx 0.001$  % of the age of the earth!) mankind living along coasts is faced with the caprices of the evolving systems (coastal behaviour). Since mankind has to do with this behaviour, value judgements play a role. Often e.g. coastal erosion is felt annoying and bad. Mankind, facing for instance a 'bad' structural eroding behaviour of the coast, shows an increasing assertive attitude with time. The next notions might be discerned in sequence of time since mankind got in trouble with eroding coasts:

- It is a pity; we must pull down our *humble hut* close to the sea and rebuild the hut just a little bit farther landward; that is nature.
- It is a pity, but we notice some trends; it is clever to take past developments into account while choosing a new place for our *hut*.
- We don't like to replace our *nice hut* every moment; it would be nice if we could do something; but we realize that it is still impossible.
- Rebuilding our *house* every time becomes very annoying; we must find some tools to protect us; let us try somewhat to do.
- *Houses, roads and infrastructure* are at stake; we can spend some money to protect us; various tools have been developed; with some kind of a trial-and-error method we will see which tool might serve our goals.
- *Large hotels and many tourist facilities* face the consequences of a 'bad' behaviour of the coast; an integrated protection scheme based on scientific research will do the job.
- The coast must behave according our wishes and rules!

We must be very careful with the last attitude. At present, applying the best of our knowledge and experience, we are able to deal effectively with coastal systems. However, some modesty remains highly recommended.

## 11.2 Coastal erosion

### 11.2.1 What is coastal erosion?

Considering a (still) more or less natural stretch of a sandy coast (so without any hard structures) a cross-shore profile, seen in seaward direction, consists out of the mainland or dunes at a level well above mean sea level (MSL), an often rather steep mainland or dune face, a beach and a shoreface; see Fig.11.1 for a schematic cross-shore profile. In Fig.11.1 also two vertical lines and a horizontal line have been indicatively sketched; these lines and the position of the actual cross-shore profile enclose a so-called control volume area. The developments of the volume  $V$  (in  $\text{m}^3/\text{m}$ ) with time of this control volume area, is further used to explain some typical features which might occur along a coast. (*Mainland or dunes* is further written in this chapter as *mainland* only.)

Let us look at the erosion of the mainland, so often the most valuable part of a cross-shore profile to mankind. The very seaward part of the mainland sometimes carries valuable properties like houses and hotels or infrastructure like roads and car park areas.

In fact two entirely different processes might cause loss of mainland, viz. dune erosion during a severe storm (surge) and structural erosion.

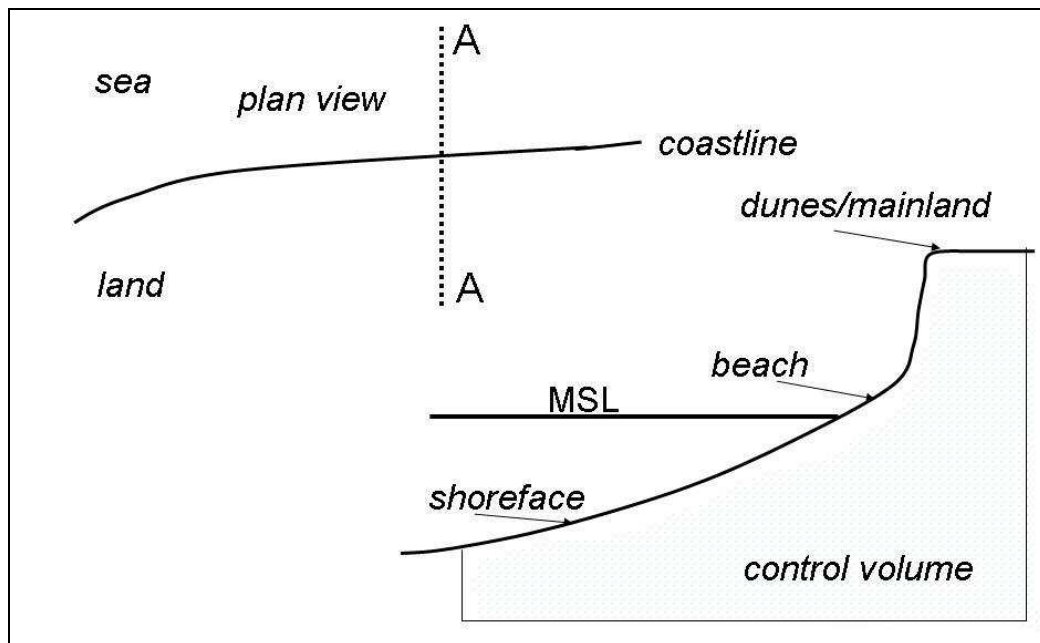


**Figure 11.1** Control volume

### 11.2.2 Dune erosion (see also Chapter 7)

During a severe storm sediments from the mainland and upper parts of the beach are eroded and settled at deeper water within a short time period; this is a typical cross-shore sediment transport process. Often a storm is accompanied with much higher water levels at sea than usual (storm surge) and also much higher waves do occur. While under ordinary conditions the shape of a cross-shore profile might be considered to be in accordance with these normal conditions ('dynamic equilibrium' shape), under storm (surge) conditions the initial shape before the storm can be considered to be far out of the equilibrium shape which belongs to the severe storm conditions. Profile re-shaping processes will occur, causing erosion of sediments from the mainland and the settlement of these sediments at deeper water again (see Fig.11.2 next page). Notice in Fig.11.2 that the control volume does not change by the storm surge processes. Although this phenomenon will cause loss of mainland, to a first approximation no loss of sediments out of the cross-section occurs; only a redistribution of sediments over the cross-shore profile takes place during the storm.

After the storm generally a recovery towards the original situation will occur due to the processes under normal conditions. Of course depending on the characteristics of the storm, erosion rates of several metres per event (say per day) have to be considered.

These episodic events do occur along all types of coasts (along structural eroding, stable and even along accreting coasts).

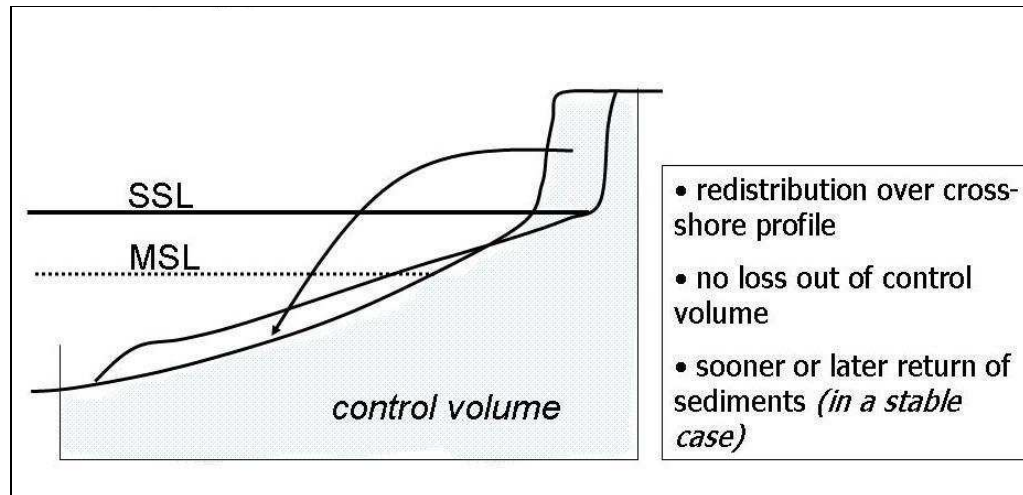


**Figure 11.2 Dune erosion due to storm**

### 11.2.3 Structural erosion

Structural, long-term erosion yields a gradual loss of sediments out of a cross-shore profile. Looking at the volume of sediments in the control volume area as a function of time, we will see a diminishing tendency with time. A gradient in the longshore sediment transport is often the reason of structural erosion. See Fig.11.3 for the development with time of an eroding cross-shore profile. Notice the change with time of the control volume. Notice also that the mainland is eroding as well, although the longshore sediment transports, and so the gradients in the longshore sediment transport, do not occur at the mainland level. Fig.11.4 shows the loss out of a control volume. (See Example 11.1 for an explanation of the relationship between the annual loss of volume out of a cross-section and the annual rate of recession of the coastline.)

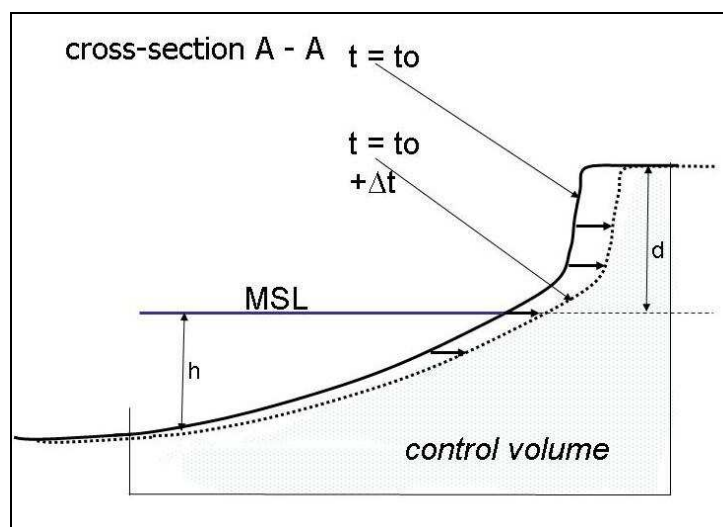


**Figure 11.3 Structural erosion**

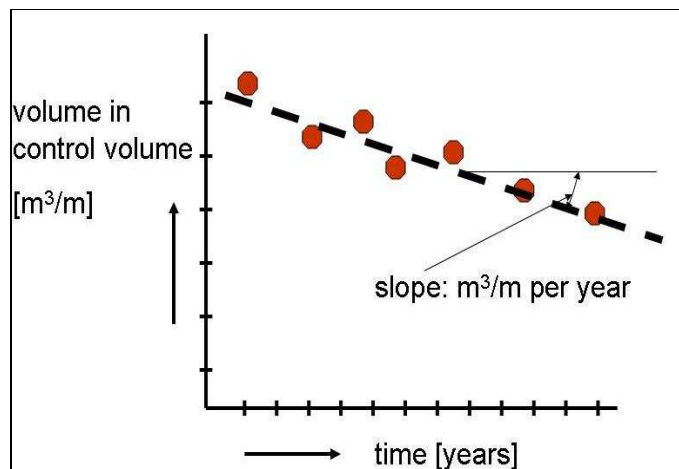


**Figure 11.4** Volume loss out of control volume due to structural erosion

### Example 11.1

In Fig.11.3 a typical structural erosion case has been sketched. Two cross-shore profiles have been indicated, representing the position of the profiles at two different moments. To a first approximation it can be assumed that the shape of the profiles are identical (the boundary conditions; e.g. wave climate and tides are the same indeed). The one profile can be found from the other by a horizontal shift. It is assumed that not only for example the waterline shifts in landward direction with a certain speed, but that this holds in fact for all depth contours.

If on an average the waterline shows a recession of  $r$  m/year, the annual loss of volume out of the control volume area  $\Delta V$  ( $m^3/m \cdot year$ ) is  $r$  times  $(h + d)$ ; see Fig.11.3 for the definition of  $h$  and  $d$ .

The dune height  $d$  with respect to MSL is easy to determine. The under water part of the cross-shore profile  $h$  which has to be taken into account is more difficult to determine. Often the depth of the so-called active part of the profile is taken as representative. The depth belonging to the active part of the profile is related to the annual wave climate. A first approximation for depth  $h$  can be found by multiplying the significant wave height which is exceeded for one day a year, with 2 - 3. With actual profile measurements often a more accurate estimate of  $h$  can be determined.

In Fig.11.4 the development of the volume  $V$  of the control volume area with time of cross-shore profile has been given. The slope  $m = dV/dt$  ( $m^3/m \cdot year$ ) is in this case a measure of the gravity of the erosion problem

A similar figure like Fig.11.4 can be made of the recession of the position of the waterline (in m with respect to a reference point) with time of an eroding profile in a structural eroding part of the coast. The slope  $r$  (m/year) is a measure for the erosion rate.

From a morphological point of view representing erosion rates according to volumes is preferred above a representation according to distances.

### Example 11.1 Rate of recession versus volume rate of erosion

While the associated longshore sediment transports take place in the 'wet' part of the cross-shore profile, at the end of the day, also the mainland will permanently lose sediments. This can be understood by taking the erosion processes during a(n even moderate) storm into account. In a (seen over a number of years) stable condition the erosion of mainland is in fact only a temporary loss. In a structural erosion case this is (partly) a permanent loss. Sediments eroded from the mainland during the storm and settled at deeper water are eroded (by the gradient in the longshore sediment transport), before they have the chance and time to be transported back to the mainland. Although it looks like that the storm is the reason of the (permanent) erosion problem of the mainland, in this case the actual reason is the gradient in the longshore sediment transport. The storm is only to be considered as a necessary link in a chain of processes.

Structural erosion rates are often in the order of magnitude of a few metres per year.

To overcome erosion problems related to either dune erosion or structural erosion, calls for quite different counter-measures. A coastal zone manager must be aware of this.

For people living along the coast the distinction between both causes for erosion is often not so clear. In both cases it looks like that the storm is the malefactor. During a storm actual damage at the mainland will occur. In the structural erosion problem the storm is, as said, only a link in the various processes.

#### 11.2.4 Possible causes of structural erosion

In order to select a proper scheme to protect a structural eroding stretch of coast, it is necessary to understand the cause of the erosion problem. Principally pure natural and man-induced causes are to be distinguished. A pure natural morphological development of a part of the coast is often called autonomous behaviour. What looks like an autonomous behaviour at present, is in some cases in fact (the tail of) a man-induced development started a long time ago. So the distinction between both is not very clear in many cases.

A convex stretch of coast under wave action is a typical example of a natural, structural eroding coast. (See Example 11.2.)

#### Classical examples

Three classical examples of man-induced structural erosion problems are mentioned here viz.:

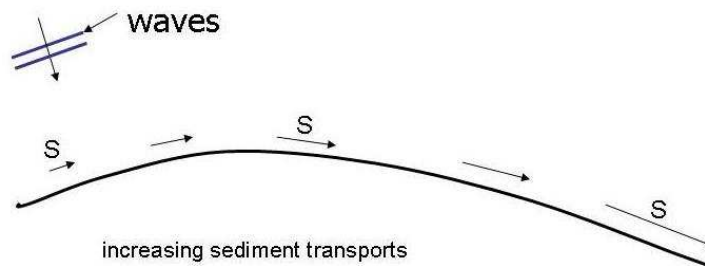
- building a new port along a sandy coast;
- stabilization of a river mouth / tidal inlet;
- coastal erosion due to changes in river characteristics.

#### New port

Building a port with two long breakwaters along a sandy coast with a net longshore sediment transport in a given direction (e.g. in  $\text{m}^3/\text{year}$ ), induces two typical morphological features at the updrift and the downdrift side of the port respectively. The downdrift side is relevant for the structural erosion discussion.

**Example 11.2**

Consider a part of a sandy coast; a few kilometres long. In plan view it refers to a convex coast (see sketch below). In the sketch only the waterline is indicated, but it is assumed that the depth contours are more or less parallel to the waterline. Waves approach the coast as indicated in the sketch. Along the part of the coast as has been plotted, the angle between the wave crests and the orientation of the coast is ever changing. Longshore currents and longshore sediment transports [ $S$ : e.g. in  $\text{m}^3/\text{year}$ ] are generated. In the sketch the magnitude and direction of the longshore sediment transport rates are schematically indicated. Gradients in the longshore sediment transport rates seem to occur [ $dS/dx \neq 0$  in  $\text{m}^3/\text{myear}$ ]. Due to the gradients loss of sediments out of the control volume area (see Fig.11.1) occur; volume  $V$  ( $\text{m}^3/\text{m}$ ) is diminishing [ $dV/dt = dS/dx$ ].

**Example 11.2 Convex coast**

A net longshore sediment transport is assumed to occur in this discussion. For understanding the morphological response of the coastal system to the construction of the breakwaters, it makes sense to make a distinction between cases without and with serious tidal currents.

*Without* tidal currents effects, the net longshore sediment transport is mainly confined to the surf zone (sediment transports because of wave driven longshore currents). With long breakwaters the sediment transport might be totally interrupted. *With* serious tidal current effects, the (net) longshore sediment transport is spread over a much wider part of a cross-shore profile than only the surf zone. Even rather long breakwaters will not totally interrupt the sediment transport.

In the next discussion a case without serious tidal effects is the starting point.

Updrift side

The updrift breakwater interrupts the longshore sediment transport; accreting of the beaches and mainland will occur at the updrift side of the new port. (See also Section 6.4.) In many cases this gain of land is welcomed; after some time after the construction of the port this new land can be used for example for an extension of the port. On a long run, however, also the accreting side of a port will create problems as well. As soon as the accretion of the position of the waterline approaches the end of the updrift breakwater, sedimentation of the approach channel to the port will occur. A safe entrance to the port will be hindered. See Fig.11.5 (next page) for a sketch of the developments of the coastline near a port.



Downdrift side

At least in the first years after the construction of the port, no (or hardly any) sediments will pass the breakwaters. Because at the downdrift side of the port the original (undisturbed) longshore sediment transport takes place again, while no sediment is passing the breakwaters, large gradients in longshore sediment transport do occur at the downdrift side of the port. Massive erosion occurs at this side; the so-called lee-side erosion. This downdrift erosion is a typical example of a structural erosion process. Year after year the volume of sediments in the control volume area in a cross-shore profile is decreasing. This diminishing tendency of the control volume, which is typical for structural erosion, is expressed in  $\text{m}^3/\text{m}$  per year. Sooner or later the lee-side erosion will harm interests located at the downdrift side of a port. Building a new port at the given location, undoubtedly will serve an important goal for the socio-economic development of a country. In the ultimate decision making process, the adverse effects of the port to the downdrift side have to be taken fully into account. If the unavoidable lee-side erosion is unwanted, adequate counter-measures (preferable for account of the port project) have to be taken. A proper system of artificially sand by-passing has to be considered as a serious option.

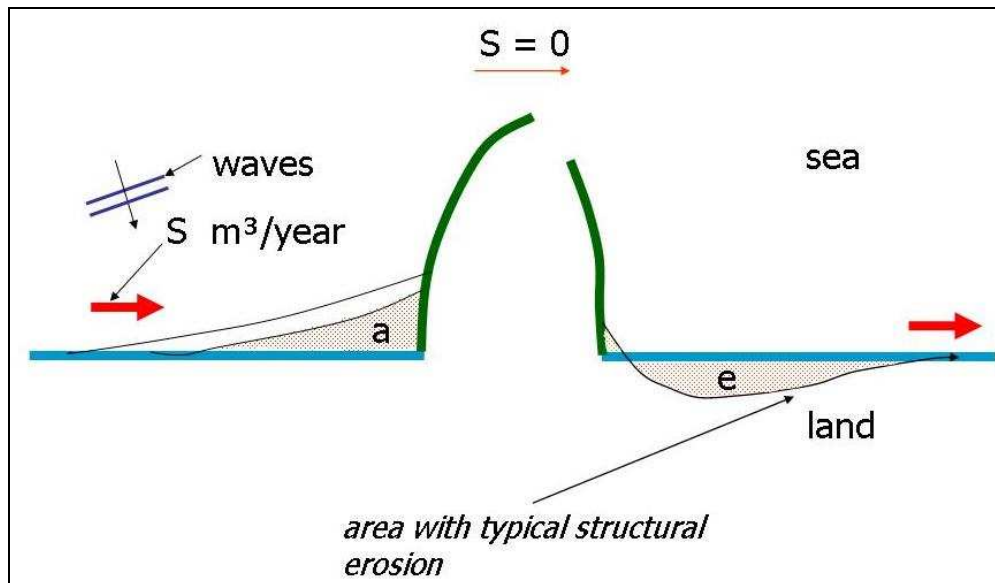


**Figure 11.5** Developments of coastlines near port

### Stabilization of a river mouth / tidal inlet

Similar accretion and erosion features like in the previous example, are to be expected if one likes to stabilize a natural river mouth with two jetties at both sides of the mouth. In the following description mainly river mouths are considered, but some similar processes occur and similar effects are to be expected if one likes to stabilize a tidal inlet.

Let us assume a modest river flowing out in open sea. The position of a fully natural river mouth is often unstable. Accumulation of sediments at one side of the mouth, while forming a growing spit with time, together with the discharges through the



mouth, cause erosion of the other side of the mouth. The position of the mouth shifts with time along the coast in the direction of the net longshore sediment transport along the coast. The river flows, landward of the spit, more or less parallel to the coast for some distance. By the growing spit, the length of the river becomes longer and longer with time (see Fig.11.6).

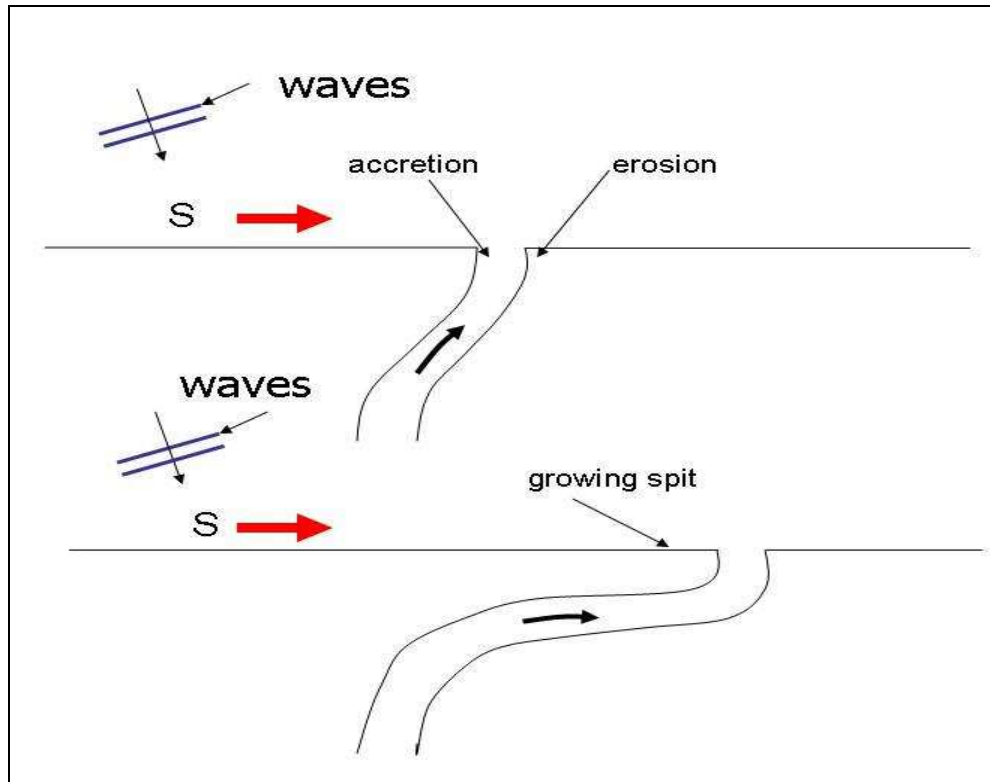


**Figure 11.6 Spit and river mouth**

When a rather long spit has been formed, often a new break-through occurs somewhere at the updrift side of the spit. Due to the increased length of the river, the water levels in the river behind the spit increase, and with a rather large discharge in the river (e.g. during a wet season), such a break-through of the slender spit is to be expected. This is a periodic process for a fully natural river mouth. Existing interests at the eroding side of the mouth (roads, buildings), and the desire to have a fixed entrance to the river for shipping (yachts; fishery vessels) call for stabilization. So two jetties at both sides of the inlet will serve that goal (see Fig.11.7 next page). We assume that the position of the river mouth at the moment of stabilization is at a 'pleasant' position out of the many possible positions of the river mouth during a full natural cycle. Without an adequate sand by-pass system, the induced erosion at the downdrift side of the jettied inlet is also a typical man-induced structural erosion problem.

At a first glance the (yearly) growth of the spit might be considered as useful measure for the annual net sediment transport. Be aware, however, that in natural systems often only a part of the annual net sediment transport is 'used' for the growth of the spit; the other part by-passes at a natural manner. If these features are not taken

properly into account, the rates of accretion and erosion after stabilization, might become surprisingly large.

Also in the case of stabilization of a river mouth or tidal inlet, a comprehensive decision making process has to be carried out, taking primary aims, but taking also the possible adverse consequences into account.

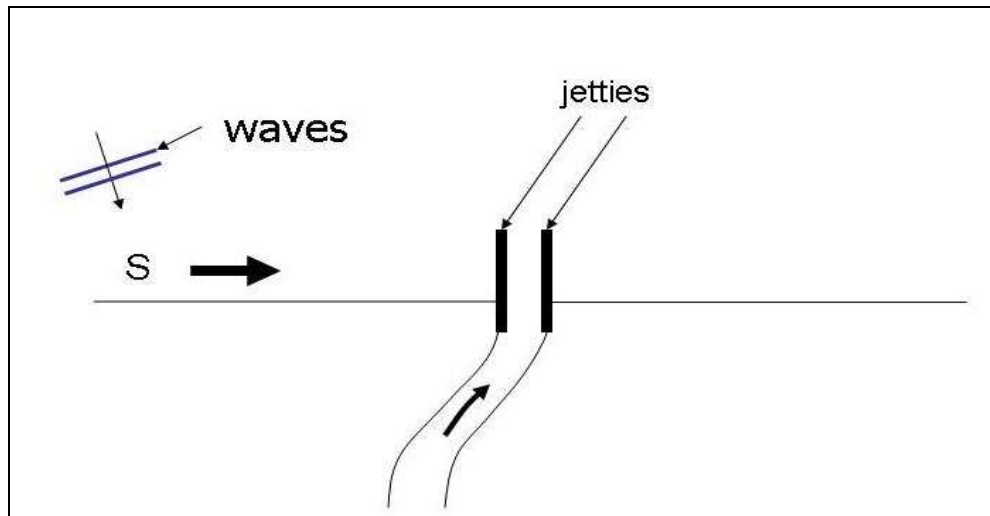


**Figure 11.7 Stabilized river mouth**

### Changes in river characteristics

In a still fully natural situation where a (small) river brings year after year sediments into the sea, the coast in the vicinity of the river outlet is ever growing in seaward direction. The sediments from the river are distributed by the longshore sediment transport processes along the coast, while the coast is ever growing. In plan view such a river-sea system is often to be noticed as a crack in the orientation of the coastlines at both sides of the river outlet. (See Fig.11.8 for a sketch of the development with time.)

Man-induced changes in the characteristics of the river (e.g. serious sand-mining in the river-bed, or damming of the river for irrigation or hydro-power purposes), might change the natural accreting tendency of the coast in an eroding tendency of the coast in the vicinity of the river outlet. When this occurs, it is also to be considered as a typical structural erosion problem for some stretches of the coast.

In all cases as were mentioned (natural and man-induced), the control volume in a cross-shore profile is reducing with time; sooner or later also the interests at the mainland will be endangered.

Coastal erosion due to a severe storm and/or structural erosion calls often for some counter-measures (coastal protection). The possibilities will be briefly discussed in the following section. Chapters 12 and 13 deal with more details.

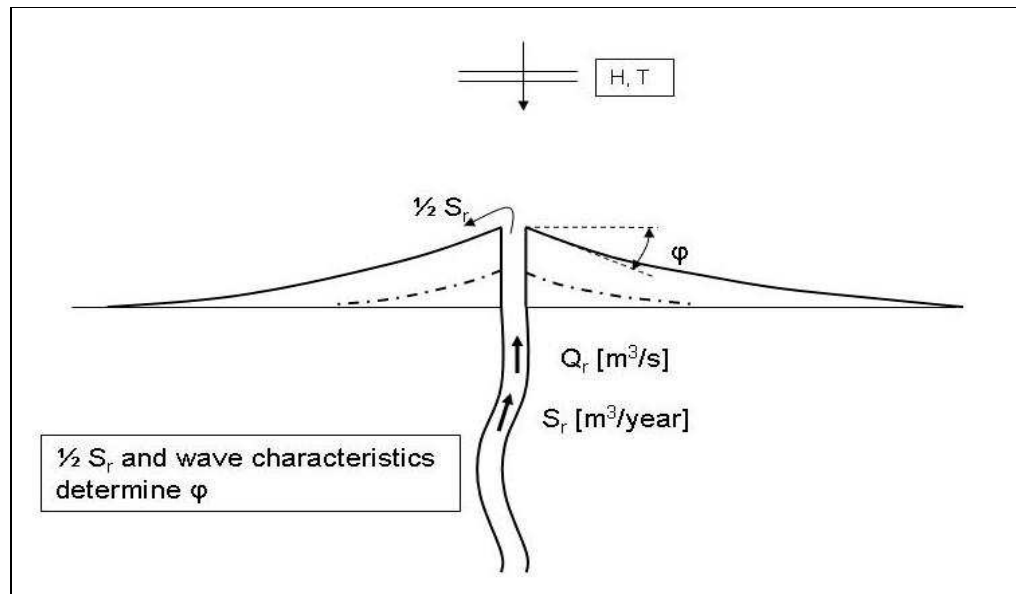


**Figure 11.8** Developments of coastline near river outflow

## 11.3 Protection measures

### 11.3.1 General

First of all it has to be stressed that with a proper system of Coastal Zone Management, some troublesome coastal protection issues can be avoided. If, for instance, it is not allowed (and the legal system is able to compel this!) to build too close to the brink of the mainland, a lot of (future) problems with respect to erosion due to severe storms and even due to structural erosion (for the time being), are avoided. With well-defined (and maintained) set-back lines, the risks of damage to, and losses of, properties are reduced.

Furthermore it is not excluded that as a result of a comprehensive, but most important: a honest decision making process, it is decided to renounce an intended project because of the too large adverse effects elsewhere along the coast.

### 11.3.2 Mitigation effects severe storm (surge)

#### 'Hard' solutions

If it is felt that e.g. an existing house or an existing hotel is situated too close to the sea, and one likes to reduce the chance of damage due to a severe storm surge (see Section 7.4 for a discussion of the dune erosion processes), in fact the only possibility to reduce the risks of an existing building is to protect the site by a revetment along the face of the mainland or by a seawall. (See Example 11.3 next page, for some remarks about chances and risks.)

**Example 11.3*****Chances, consequences and risks***

Some (coastal) events cause damage to properties; e.g. erosion of dunes during a severe storm surge if close to the brink of the dunes houses or hotels have been built. Given the position of e.g. a house on top of the dunes, there exists a certain *chance* [per year] that the house will be destroyed during a storm surge. This destruction might be called *consequence* [expressed in money and/or losses of life in some serious cases]. Chances as well as consequences might vary from case to case. Intuitively one might understand that an event with a rather large chance, but with small consequences could be more or less comparable with an event with a rather small chance, but with large consequences.

The notion *risk* takes that into account, viz.;

$$\mathbf{risk = chance \times consequence}$$

The unit of risk is in simplified form: [amount of money per year]. In management issues the notion risk is a far better parameter than e.g. chance.

The outcome of a risk calculation might serve as a first rough estimate of the money one has to save on a yearly basis (and put that money on a safe bank!), in order to be able to pay the costs of rebuilding of the property involved from time to time. (Average period between two rebuilding operations; return period: 1/chance [unit: year].)

Consider a house (value: EURO 500,000) on top of the dunes at a position that the chance of destruction is 1/500 per year (according to Fig.7.9 the distance between the house and the brink of the dunes is then  $\approx 20 - 30$  m). The risk for the owner of that house is then  $\approx$  EURO 1000 per year. The owner of the house has to make a quite personal choice whether a nice sea view is worth about EURO 3 per day!

If the same house, assuming having the same value (but that is quite questionable, since sea view houses are much more expensive than comparable non-sea view houses), is situated at a position with a chance of destruction of 1/5000 per year ( $\approx 25$  m more landward) the risk is only EURO 100 per year.

**Example 11.3 Chances, consequences and risks**

Revetments or seawalls, if well-designed to withstand the storm attack, are physically able to protect the properties built at the mainland. In the unprotected situation sediments from the mainland are transported towards deeper water during the storm. If by the revetment or seawall sediments from the mainland are denied to join the physical processes, erosion of the beaches just in front of the revetment or seawall will occur, causing deep scour holes. With the choice of the foundation depth of the revetment or seawall, one has to take this phenomenon into account (see Fig.11.9).

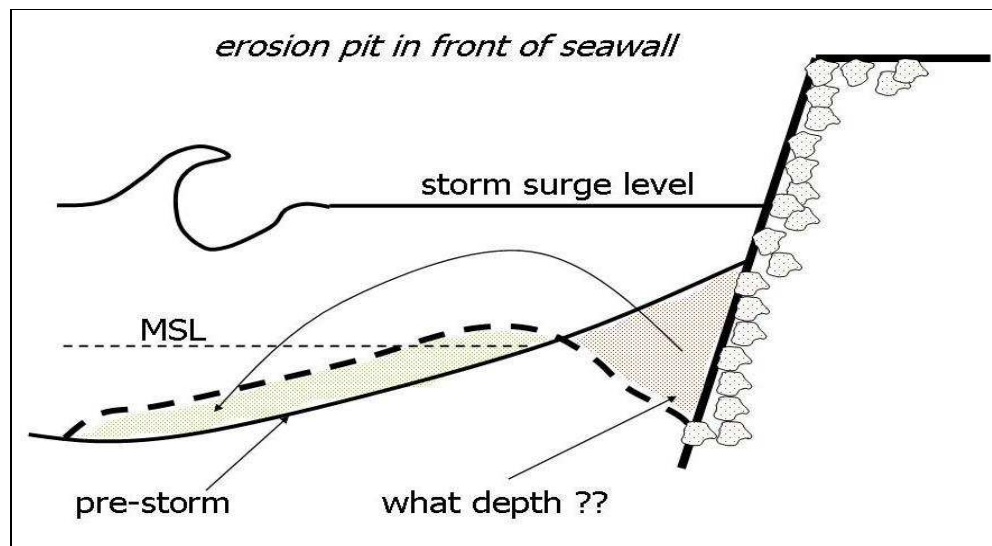


**Figure 11.9 Scour in front of seawall**

Revetments and seawalls are so-called 'hard' structures. They might be applied in this special case, provided that the storm (surge) protection problem is the only issue for this stretch of coast. So it refers in fact to a stable part of the coast (stable: seen over a number of years) or an accreting part of the coast. If (also) structural erosion occurs along the stretch of coast under consideration, revetments or seawalls can **in no way** be selected as the only protection measure. (See also Section 11.3.3.)

### 'Soft' solutions

Besides 'hard' solutions, also 'soft' solutions might in principle be selected as a possible solution in this case (reducing the chances at damage during a severe storm surge). By artificially widening the mainland in seaward direction, the risks might be relieved. However, this calls for rather large volumes of sediments, because not only the face of the mainland has to be shifted in seaward direction, but also at least the active part of the cross-shore profile. Furthermore a 'soft' solution must in this case be applied over a rather long distance alongshore. Applying a 'soft' solution only locally, calls for a large maintenance effort because of the redistribution processes in both alongshore directions of the artificial nourishments.

Widening (and perhaps heightening) of the mainland / dunes in seaward direction might cause loss of undisturbed sea views of the most seaward row of houses and hotels. Although the widening measure was primarily meant for the owners of these buildings, they might be unhappy with this solution.

### 11.3.3 Mitigation effects of structural erosion

#### 'Soft' solutions

Structural erosion means in fact the gradual loss of sediments with time out of the control volume (see Fig.11.3). Sooner or later not only the foreshore is losing volumes of sand, but also the beaches and mainland. At the end of the day also properties built at the mainland will be lost. Artificial nourishments, but certainly to be repeated at a regular time basis, and to be continued for ever, are nevertheless a perfect solution in many cases. The occurring losses are to be refilled from time to time. Seen over a number of years the average position of the coastline will be stable. Because artificial nourishments, to a first approximation, do not interfere in the occurring sediment transport processes, this method has to be applied for ever indeed.

The source of the fill material (borrow material), might be outside the nearshore coastal system, or inside the coastal system. In the latter case a perfect source of borrow material would be for example the accumulated sediments at the updrift side of a new port which interrupts the occurring longshore sediment transport. (Applying a sand bypass system.)

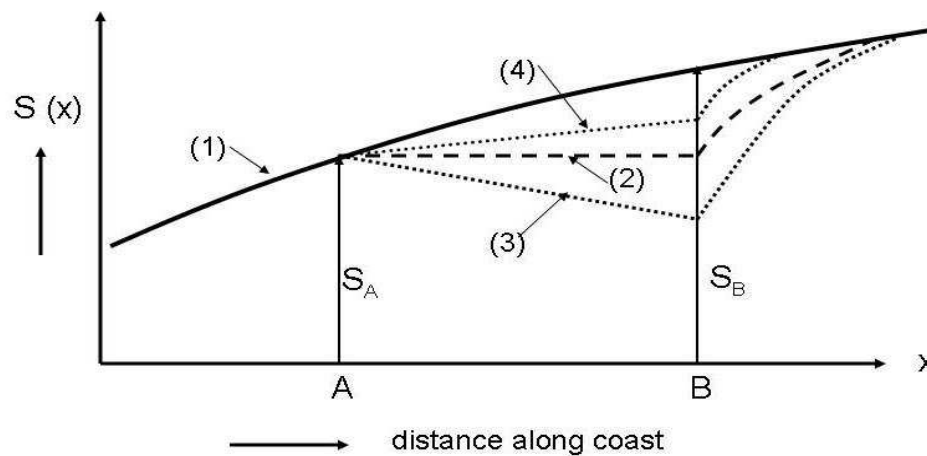
Sometimes it is felt that artificial nourishment schemes are too expensive for developing countries. Good alternatives (if any?) are at the long run in many cases, however, even more expensive. More details about the application of artificial nourishments can be found in the special issue on artificial nourishments of *Coastal Engineering* (1991).

The structural erosion of the upper parts of the cross-shore profiles (beach; mainland) is the most visible, and striking phenomenon. To replenish just the upper part of the profile seems consequently logical. However, also nourishing the deeper part of the cross-shore profile (shoreface nourishments) fulfils the requirements. By redistributing cross-shore sediment transport processes, also the upper part of the profile is fed at the end of the day. See for more details Chapter 13.

#### 'Hard' solutions

If the structural erosion problem is due to a gradient in the longshore sediment transport ( $dS/dx \neq 0$ ;  $S$ : annual sediment transport rate;  $x$ : alongshore coordinate), with the application of 'hard' solutions to the erosion problem, the coastal zone manager intends to interfere into the occurring sediment transport processes. If the protection measure is properly designed, the gradient in the longshore sediment transport along the part of the coast to be protected, just vanishes. ( $dS/dx = 0$ ). In Example 11.4 some basic notions regarding the application of 'hard' solutions in case of a structural erosion problem are outlined.

Series of groynes or series of shore parallel offshore breakwaters are able to interfere into the sediment transport processes. So in principle they might 'work' as a tool in a protection scheme. Application requires, however, a difficult process of fine-tuning of the design layout. An unavoidable consequence of a well-designed protection scheme in the stretch of coast to be protected, is the lee-side erosion.

**Example 11.4**

Consider a stretch of coast of several km including a part A - B . The coast shows structural erosion. Year after year the coastline retreats. Stretch A - B is considered as a very important part of the coast; e.g. houses, hotels and infrastructure are present there. Without counter-measures sooner or later these valuable properties will be destroyed because of the continuous erosion.

One likes to resolve the erosion problem in stretch A - B with the help of 'hard' structures. [Left from A and right from B it is not (yet) necessary to combat the erosion problem.]

In the sketch above the distribution of the (longshore) sediment transport along the coast has been given; distribution (1). Going from left to right the transport increases, yielding a positive gradient in the longshore transport. [ $dS(x)/dx = \text{positive}$ .] This gradient in the sediment transport distribution is the reason that gradual erosion occurs.

A 'better' sediment transport distribution (at least for part A - B) might be distribution (2). In part A - B the sediment transport is constant [ $dS(x)/dx = 0$ ]; with distribution (2) no erosion would occur in part A - B anymore.

In order to achieve the 'better' distribution; one has to interfere in the occurring transport processes. With the help of 'hard' protection tools (e.g. groynes; detached shore parallel offshore breakwaters) one is indeed able to interfere in the transport processes, but from the sketch it will become clear that tuning is quite difficult. If along part A - B indeed distribution (2) is achieved, from the sketch it is also clear that the 'solution' for A - B is at the spent of the part of the coast right from B; (increased) lee-side erosion.

Distribution (3) reflects a situation where the tuning (probably) failed; even accretion in part A - B occurs, but more lee-side erosion is expected.

Distribution (4) reflects a case where the interference of the 'hard' protection system was not large enough; the erosion rate has been reduced, but still some erosion will occur in stretch A - B.

**Example 11.4 Basic notions 'hard' solution of structural erosion**

Downdrift of the protection scheme (with reduced longshore sediment transports), the original sediment transport rates do occur. This leads to large gradients in the longshore sediment transport (much larger than the original gradients), causing the

lee-side erosion as was mentioned. While protecting the coast in the area of interest, in fact this is achieved at the spent of the coast just outside (at the lee-side of) the area of interest. While applying series of groynes or series of shore parallel offshore breakwaters, the coastal zone manager has to take these (adverse) consequences fully into account in the decision making process. Often these types of protection measures are too rashly applied.

From the notion that, when 'hard' structures are applied as a tool to resolve a structural erosion problem due to a gradient in the longshore sediment transport, one has actively to interfere into the occurring transport processes, it is easily understood that the application of revetments or seawalls along the face of the mainland, do not, and cannot 'work' properly. Under ordinary conditions the revetments or seawalls do not interfere into the transport processes. They are outside the reach of the waves and currents at sea which are causing the (gradient in the) longshore sediment transport. Under ordinary conditions the loss of sediments out of the control volume of a cross-shore profile continues. Only during storm conditions the parts of the cross-shore profiles which are 'protected' by revetments or seawalls, form an integrated part of the entire, then active, cross-shore profile.

While the mainland is physically protected from erosion, the erosion of the beaches continues. Due to cross-shore sediment transport processes the beach sediments are transported towards deeper water and next eroded by the gradient in the longshore sediment transport. After some time all the beaches have disappeared. The attack to the revetment or seawall occurs more frequently and is much heavier than just after the construction of these structures. (At the time of construction still a beach was present in front of the revetment or seawall.) Often the level of the foundation is not designed at these conditions after some years, and damage and collapse of the structures will take place.

While it is quite clear that the application of revetments or seawalls in a structural eroding coastal problem is an inherent 'bad' solution, it is a pity to observe that they are so often (wrongly) applied in practice. This can be considered as a blot on the reputation of our coastal engineering profession.

## 11.4 Coastal Zone Management

A skilled, powerful and legally backed system of Coastal Zone Management can avoid many coastal erosion related problems in future. An experienced coastal zone manager is able to overview most of the coastal engineering issues associated with the further developments of the coastal zone. In some countries (in most cases as a long lasting learning process) suitable systems of (Integrated) Coastal Zone Management (ICZM) are in operation at present.

Coastal Zone Management is a profession that has as yet not developed generally accepted methodologies and techniques. One of the possible ICZM frameworks is characterized by five key words (the so-called “5 I - Approach”):

- issues;
- information;
- infrastructure;
- ICZM process;
- interaction.



This division was first introduced by Chua (1993); a graphical representation was developed by the Coastal Zone Management Center in The Hague. It includes the above five components of ICZM and defines a series of phases, together with the tasks that should be performed for each phase. A simplified version is given in Fig.11.10.

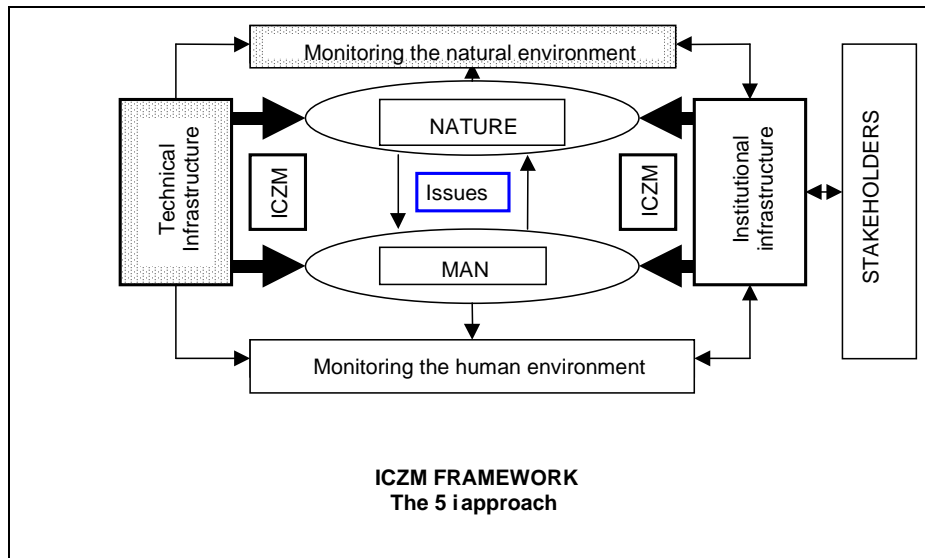


**Figure 11.10 Graphical representation of the '5 I-approach'**

The interaction between nature and man is the starting point of the framework. It defines the *issues* that will be addressed by ICZM. These are generally defined during an inception phase of a project. The importance of the issues is determined by *information* on the state of the natural and human environment. This information is collected by monitoring of the respective environments, under the guidance and control of the *institutional infrastructure*. Hereto, the monitoring system is used that is part of the *technical infrastructure*. Collected data flow back into the institutional infrastructure and is used as a basis for management actions. The resulting technical and administrative actions are indicated by the bold arrows in Fig.11.10. They are effectuated through the technical and institutional infrastructure respectively. Together they are the inputs for the *ICZM Process*. The right box in the figure shows the stakeholders. The arrow shows the *interaction* with these stakeholders through an open communication process.

At Delft University of Technology in the course CT5307 'Integrated Coastal Zone Management' much more details of ICZM are discussed.



# 12 Application of Structures

## 12.1 Introduction

In Section 11.3 some basic requirements of 'hard' structures have been given; also the 'tasks' have been mentioned these structures must fulfil in properly resolving erosion problems. If one likes for example to resolve a structural erosion problem with the help of a series of groynes, then the groynes should interfere in the occurring sediment transports. How the various hard structures 'work' in different possible applications, will be discussed in the present chapter. Coastal protection is a main issue, but we will see that structures are sometimes also applied in coastal engineering practice where the distinction between coastal 'protection' and coastal 'management' is somewhat vague.

In each following section a well-defined type of structure is discussed; viz.:

- seawalls;
- revetments;
- jetties / (port) breakwaters;
- (series) of groynes;
- detached shore parallel offshore breakwaters;
- piers / trestles;
- sea-dikes;
- miscellaneous.

In the further discussion the *functional* design aspects of the various structures are the starting points. Aspects like position, crest height, length, etc. will be discussed. No attention will be paid to real *constructive* design aspects like for example the required mass of stones of armour layers, thickness of various layers in the structures, etc. Special courses at DUT deal with these aspects. We assume that if we like to apply a given structure, the structure will be well-constructed in practice and will keep its integrity up to a well-chosen set of design conditions.

In the further discussions always a coastal engineering 'problem' (as it is felt by a coastal zone manager or by the people) is the focal point. Some typical 'problems' will be discussed. It was not the intention to cover all conceivable coastal engineering 'problems'. Slightly different issues might be discussed at a similar manner.

An alternative (as the starting point of a discussion) which could resolve the problem as was defined, might have serious (not meant) consequences for quite different other aspects of the coastal behaviour. If relevant some remarks will be made on these topics.

## 12.2 Seawalls

*A seawall is a shore parallel structure at the transition between the low-lying (sandy) beach and the (higher) mainland or dune. The height of a seawall fills the total height difference between beach and surface level of the mainland; often adjacent at the crest of a seawall a horizontal stone covered part is present (e.g. boulevard; road; or parking places). At the initial time of construction a seawall is situated close to the position of the dune foot. In the present discussion with a seawall an almost vertical structure is meant. The seaward side of the seawall is thought to be rather smooth. (See Fig.12.1.)*

[The main differences between a seawall and a revetment are that a revetment has a distinct slope (e.g. 1: 2 or 1: 4), that surface of a revetment might be either smooth or rough and that the height of a revetment does not necessarily fill the total height difference between beach and mainland.]



**Figure 12.1 Seawall** (Cascais, Portugal; high water, no beach in front of seawall)

### Problem: clear transition beach - mainland

Especially in coastal areas with a lot of human (recreational) activities, a clear and fixed distinction between beach and mainland is desirable. A seawall will serve that aim. At the sea side of the seawall a more or less normal beach is assumed to be present; at the land side a road or a boulevard (see Fig.12.2). Staircases facilitate the access to the beach. The coast is assumed to be stable, or in case of a structural eroding coast with e.g. regular artificial beach nourishments an essentially (time-averaged) stable situation has been achieved. So a normal beach is present in front of the seawall.

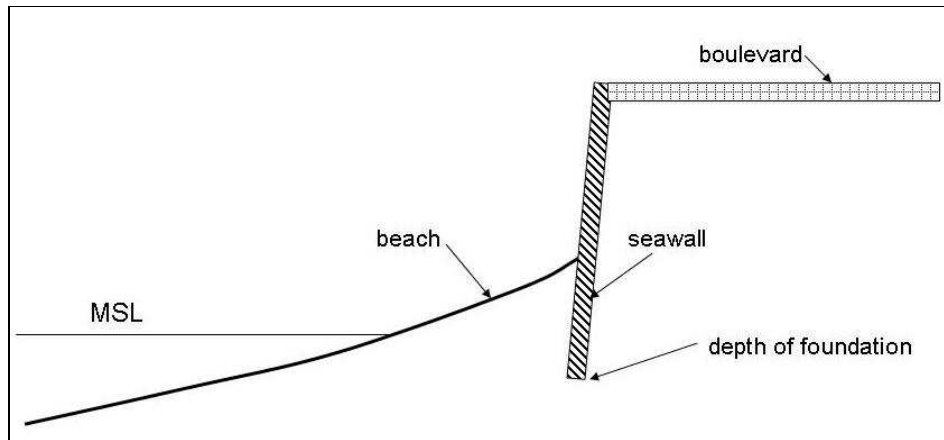


**Figure 12.2 Seawall and boulevard**

While in a situation without a seawall even a moderate storm (surge) will attack and erode the mainland, in the situation with a seawall this is prevented. Some scour in front of the seawall during a storm (surge) must be taken into account in the design. (A part of) the 'denied' erosion volume from the mainland, is now eroded just in front of the seawall. The scour hole might undermine the seawall. With the DUROSTA computation model an estimate of expected scour depths can be made [Steezel (1993)].

The design conditions for the seawall have to be properly chosen. The heavier the design conditions, the heavier the seawall must be and especially the 'safe' foundation depth will increase accordingly. To build a seawall which will be safe under 'all' conditions might be an unrealistic option.

Although achieving a clear transition between beach and mainland was the primary goal so far in the discussion, automatically some protection of the (infrastructure at the) mainland is achieved. The design conditions as selected, determine the rate of provided protection.

The crest height of a seawall determines (together with the boundary conditions at sea) to a great extent the rate of overtopping (water reaching the mainland by wave run-up and breaking waves and splash water transported by landward directed wind). With an additional wall and/or a slightly curved front, rates of overtopping might be reduced. (See Fig.12.3 next page.)

### **Problem: decrease risks of valuable infrastructure / buildings**

Infrastructure and buildings situated close to the edge of mainland or dunes have a chance to be destroyed during a severe storm surge. The risk (risk = chance x consequence; see Example 11.3) is felt to be too large. E.g. by extension and improvements of an existing hotel the 'consequence' has been increased and so the risk. By reducing the 'chance', the 'risk' will reduce as well.

With a robust seawall the required aim can be achieved. Aspects like proper design conditions and scour holes are in this case similar to the discussion in the previous case.

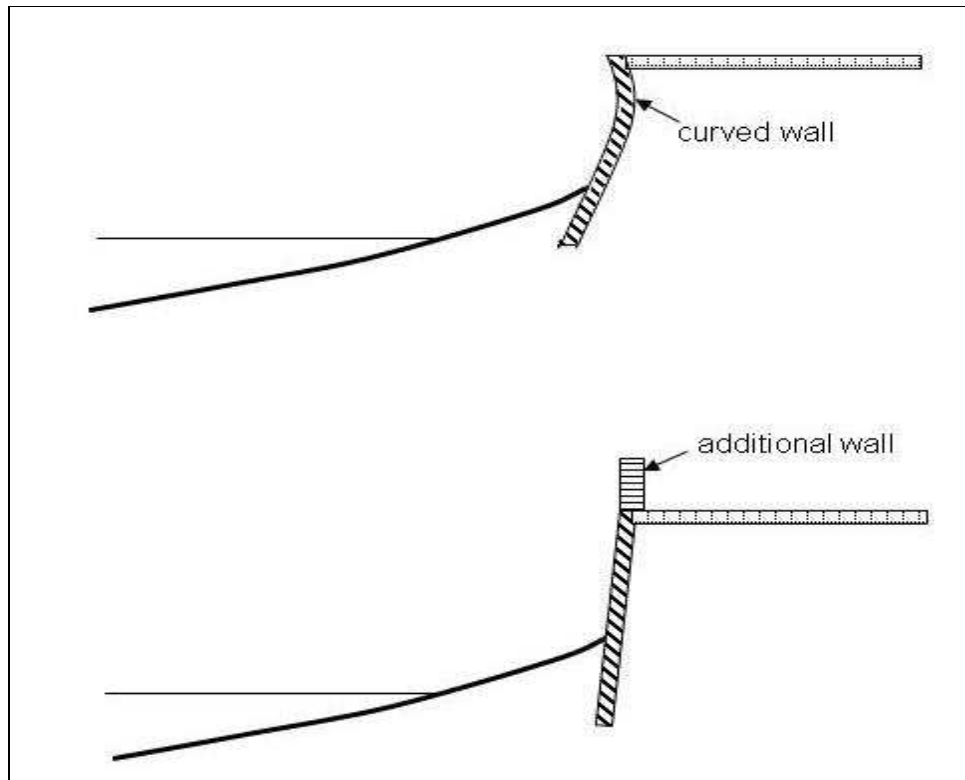


**Figure 12.3 Seawall with measures to reduce overtopping**

Let us consider a given a stretch of sandy coast. A very severe storm surge will cause a rate of mainland erosion of say 40 m in case the stretch of coast is unprotected. With a seawall which is able to withstand these conditions the erosion of the mainland will be zero. (In front of the seawall a deep scour hole will be formed.) When the entire seawall keeps its integrity; no further problems arise. (The scour hole will be re-filled again after some time with ordinary boundary conditions.) If, however, the seawall partly collapses and locally a gap in the seawall is formed during the severe storm surge, a rather dangerous situation will occur. Large volumes of sediment from the mainland are able to disappear through the gap and will flow along the sections of the seawall which are still in good condition in both longshore directions, filling the scour hole. It is expected that the ultimate rate of erosion of the mainland behind the gap will be larger than the 40 m as mentioned for the unprotected case.

Similar phenomena will occur at the two transitions between seawall and the adjacent, unprotected parts of the coast. Especially just adjacent to an abrupt end of a seawall, relatively much erosion is expected during a severe storm surge.

### Seawall is no solution for a structural erosion problem

In the present chapter we generally start our discussion with a type of structure and next some actual problems or a goals to be achieved are mentioned which might be resolved or achieved with the help that structure. It makes then no sense to mention various problems which cannot be resolved with that type of structure. An exception to this rule will be made for the 'solution' of a structural erosion problem with the

help of seawalls (or revetments). This is because in coastal engineering practice too often this principally 'wrong' combination is applied. Many bad examples can be found all over the world.

Structural erosion caused by a gradient in the longshore sediment transport, means that volumes of sediment are lost out of the control volume area. This loss process takes mainly place under ordinary conditions; the contribution of storm conditions to this loss process is often rather small. The initial losses of sediments out of a cross-shore profile take place where water and waves are; where actual longshore sediment transports do occur; so in the 'wet' part of a cross-shore profile. The 'dry' parts of a cross-shore profile are not involved in the longshore sediment transports; it looks like that the 'dry' parts do not form an integral part of the cross-shore profile. During high tides and/or modest storms all parts of a cross-shore profile participate in the coastal processes. By offshore directed cross-shore sediment transports, sediments from the higher parts of the profile ('dry' beach; even mainland under the more severe conditions) are transported to deeper water, filling the 'gap' that has been developed because of the gradient in the longshore sediment transport (see Fig.12.4 ). This sequence of processes causes a permanent loss of material out of the upper parts of a cross-shore profile.

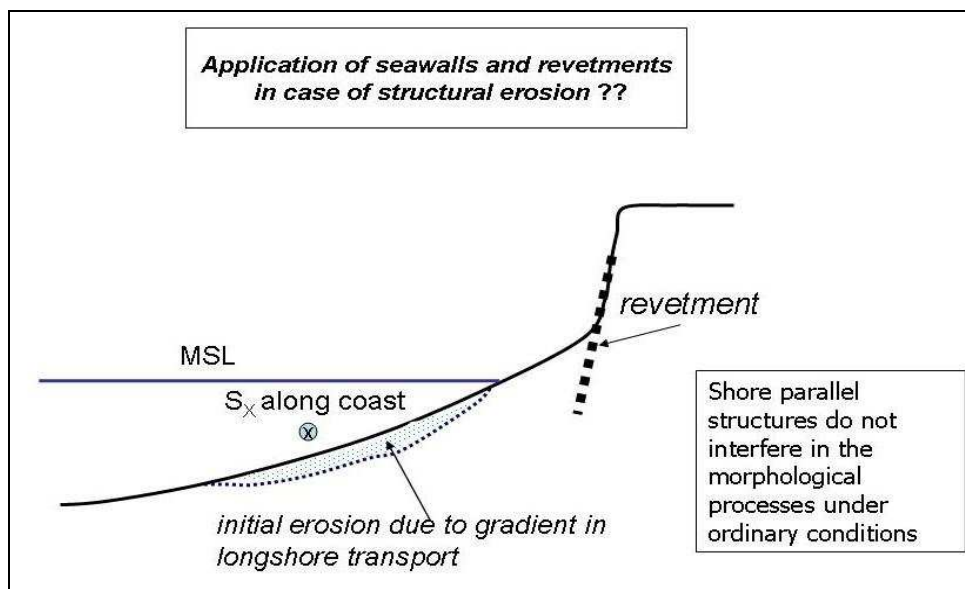


**Figure 12.4 Seawall and gradient in longshore sediment transport**

By 'protecting' the mainland in this case with a seawall, one indeed prevents that sediments from the mainland are transported in seaward direction (less filling of the 'gap'). The losses, however, continue; the 'dry' beach disappears; it becomes deeper and deeper in front of the seawall. Initially, right after the construction of the seawall, still a more or less normal beach was present. The beach did 'protect' the seawall to some extent; only moderate storms could reach the seawall. When the beach had disappeared, much more frequent wave attacks directly to the seawall will occur. (Most likely in the design of the seawall this was not taken into account.) Damage occurs; reinforcements have to take place.

A somewhat confusing element is the time-scale of the developments as have been



discussed so far. Local people (their houses are at stake) have noticed in the past that every storm surge has taken some square metres of their gardens. The edge of the mainland is coming closer and closer to their houses. Not seldom the responsible coastal zone manager is 'forced' by the local people 'to do something'. Building locally a seawall (e.g. in front of the properties which are situated closest to the sea) indeed seems to resolve the problem. During the next storm surge, the just 'protected' parts of the coast do not show any further erosion; in the un-protected parts the erosion of the mainland continued. Local people believe that this solution 'works' (own experience). The coastal zone manager is forced to build seawalls along the other parts of the coast. However, when time elapses, it will be quite clear that a quite wrong solution has been chosen. Only with huge costs the situation can be redressed.

### Problem: existing row of dunes does not meet safety requirements

Row of dunes is apparently too weak (too slender) to guarantee the safety requirements. Under design conditions a break-through is expected; the low-lying hinterland behind the slender row of dunes will be flooded.

A seawall might be chosen as a solution, provided that the seawall will keep its integrity during the design conditions. A risky alternative would be that the seawall is 'allowed' to collapse in a latter stage of the storm surge. The time left to the end of the storm surge (with lower water levels) is then too short to cause yet a break-through.

## 12.3 Revetments

*Similar to seawalls; often distinct slopes; smooth or rough; not necessarily filling total height between beach and surface level of mainland. (See Fig.12.5.)*



**Figure 12.5** Revetment



**Problem: decrease risks of valuable infrastructure / buildings**

**Problem: existing row of dunes does not meet safety requirements**

As a solution to both problems, a revetment could be an alternative. Similar remarks are to be made as in the preceding section on seawalls.

Two aspects call for some remarks, viz.:

- slope of revetment in relation to depth of scour hole;
- level of upper end of revetment.

At least for rather smooth revetments it has (also experimentally) been proven that the depth of the scour hole depends on the slope characteristics. During tests in the Delta Flume of Delft Hydraulics it turned out that with a slope of 1:3.6 a deeper scour hole was found than with a slope of 1:1.8 (other test conditions the same). The deepest point of a scour hole is not always found at the intersection point between revetment and cross-shore profile (see Fig.12.6 for a sketch).

It is conceivable that the depth of a scour hole is less for a rough slope than for a smooth slope.

The level of the upper end of a revetment (above that level the normal front slope of the dunes is assumed to be present up to the top of the dunes) determines the still occurring (remaining) dune erosion above that level, but also to some extent the depth of the scour hole. The higher that level the less remaining erosion, but also the deeper the scour hole. It is remarkable that if the level of the upper end of a revetment is equal to the storm surge level (or lower than that level), no reduction in dune erosion is found compared to a situation without any protection.

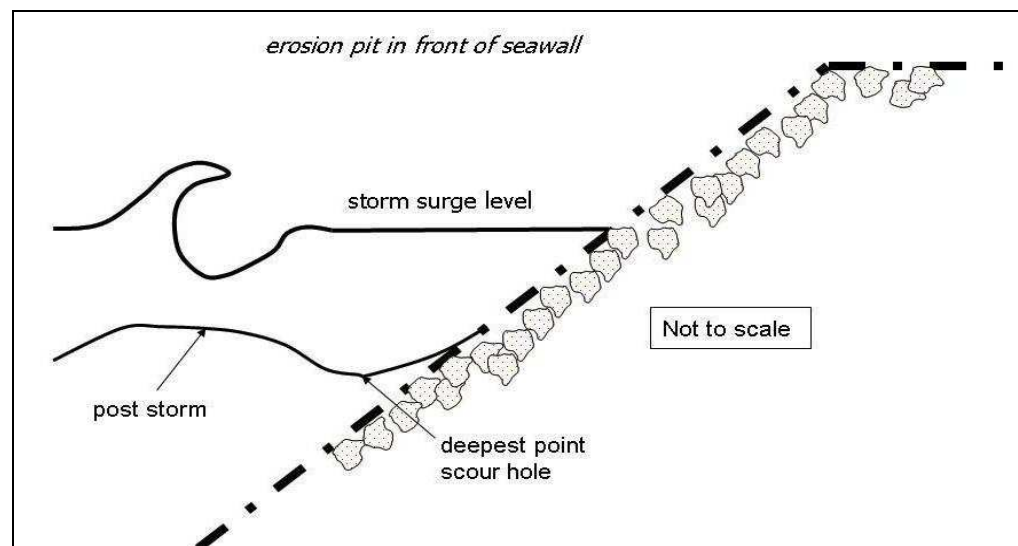


**Figure 12.6 Scour in front of revetment**

## 12.4 Jetties / (port) breakwaters

*Rather long structures extending more or less perpendicular to the coast. Jetties: guiding currents (e.g. river outflow or currents in tidal inlet). Jetties and (port) breakwaters: preventing sedimentation of entrance to river or port. Crest height often well above MSL. (See Fig.12.7.)*



**Figure 12.7 Port breakwaters** (Misawa, Japan and Scheveningen, The Netherlands)

**Problem: Stabilization of river mouth / tidal inlet**

**Problem: Construction of a port along a sandy coast**

Both problems call for long structures extending into open sea. Jetties and breakwaters might be used. (In The Netherlands the breakwaters of the port of IJmuiden extend for about 2.5 km into the sea.) The required length of the breakwaters is related to the depth which has to be guaranteed in the approach channel. (A main aim of breakwaters is to prevent too much sedimentation of the approach channel.) In many cases, however, seaward of the end of the breakwaters still an artificial dredged channel is present up to the required depth contour. A fair balance has to be found between the costs of longer breakwaters and probably less maintenance costs of the channel outside the breakwaters.

Long structures extending into the sea affect the (tidal) currents. The longer the structures the more impact. Contraction of the currents (high velocities) just near the entrance to the port hamper a safe sailing of vessels up and down the port and might

lead to local scour (important for the stability of the breakwaters). With a well-chosen layout currents might be guided as such that the nuisance for shipping operations will be acceptable and scour is reduced as much as possible.

Long structures extending into open sea might also affect the silt transport along the coast and even the transport of e.g. fish larvae. These impact effects might be felt to rather large distances from the structures. [Compare the discussion in The Netherlands of the possible impact of an extension of the Maasvlakte (Port of Rotterdam) on the processes in the Wadden Sea.] Also these aspects must be taken into account in a final decision making process.

The impact of these long structures on the morphodynamics of the adjacent coasts might be very large. Longshore sediment transports are interrupted; sedimentation and coastline progress at the updrift side is expected. At the downdrift side erosion and coastline retreat will occur. (See Section 6.4.)

Many morphodynamic problems are avoided with an adequate sand by-pass system. (See also Section 13.4.)

### Problem: stretch of sandy coast near tidal inlet suffers from structural erosion

The stretches of coasts near tidal inlets are often very dynamic. Not seldom at the one side of the inlet the coasts are eroding, while at the other side accretion occurs. Sediments from the one side disappear into the tidal basin, via a lot of complex processes within the tidal basin, at the end of the day sediments reach the other side of the inlet causing accretion.

By building a long pier (dam) near the inlet at the end of the eroding coast (crest level of the dam high enough to catch the sediments) one prevents that sediments disappear into the tidal basin. (The construction of an 800 m long dam at the northern part of the Dutch island of Texel in 1995 is such an example; see Fig.12.8 and see reprint in Chapter 8.)

For the time being this solution 'works' very well. The erosion has been stopped. However, because of this measure the tidal inlet and tidal basin is denied, compared to the past, an annual volume of sediments. Partly because of the rather large surface area of the tidal basin, it is not yet clear what the 'reaction' of the coastal system is on this surgery. Probably only at a long run the consequences will become clear.



**Figure 12.8 Long dam Texel**

## 12.5 (Series) of groynes

*Rather short structures extending essentially perpendicular to the coast. Should interfere in the coastal processes close to the shore (e.g. currents; sediment transport processes). Modest crest heights. Material 'closed' structures: stone, sheet piles (wood or steel). 'Open' structures: e.g. rows of vertical (wooden) piles (e.g. diameter piles  $\approx 0.3$  m; mutual distance between piles equal to diameter of piles). (See Figs.12.9 and 12.10.)*



**Figure 12.9 Groynes**



**Figure 12.10 Row of piles**



### Problem: stretch of sandy coast suffers from structural erosion

The structural erosion is thought to be caused by a gradient in the longshore sediment transports along the coast. (See also Example 11.4.) One likes to prevent this erosion for a well-defined stretch of coast. (E.g. over 5 km of a long sandy coast; over these 5 km it is assumed that infrastructure, houses and hotels are present rather close to the sea.)

Series of groyne might be applied to resolve the structural erosion problem along this stretch of coast. In order to 'work' properly the groyne must interfere in the occurring longshore sediment transports. Since a part of the sediment transport takes place in the zone close to the waterline, and the groyne cover just this part of the coastal profile, it is conceivable indeed that groyne will do the job. To stop further structural erosion it is necessary and sufficient that the gradient in the longshore transport is just cancelled. With a constant net longshore sediment transport along the part of the coast to be protected, no further erosion occurs. By selecting a proper length and a proper mutual distance between the groyne of a series, it must be possible to just achieve what the designer likes to achieve. This calls for a very difficult procedure of fine tuning.

To illustrate some difficulties in the process of fine tuning, the next two cases are considered:

- A: stretch of coast 5 km:  $S_{in} = 100,000 \text{ m}^3/\text{year}$ ;  $S_{out} = 200,000 \text{ m}^3/\text{year}$
- B: stretch of coast 5 km:  $S_{in} = 200,000 \text{ m}^3/\text{year}$ ;  $S_{out} = 300,000 \text{ m}^3/\text{year}$

In both cases the same annual loss ( $100,000 \text{ m}^3/\text{year}$ ) takes place along the stretch. Both cases suffer from the same rate of structural erosion; on an average of  $20 \text{ m}^3/\text{m}$  per year, i.e. a quite usual yearly loss in case of structural erosion.

It will, however, be quite clear that an adequate groyne system for case A should be different from an adequate groyne system for case B. In case A the net sediment transport near the downdrift side of the stretch of coast must be reduced by 50 % in order to achieve that  $S_{out}$  equals  $S_{in}$ . In case B the reduction should be only 33 %.

The required length of a groyne depends on the required rate of reduction of the occurring sediment transport. If one has determined the distribution of the longshore sediment transport over the near shore zone (e.g. in case of wave driven sediment transport only: a little bit more than the width of the surf zone), some very first reduction estimates are based on the idea that a groyne might interrupt that part of longshore transport which agrees with the length of the groyne (see Fig.12.11 for a sketch).

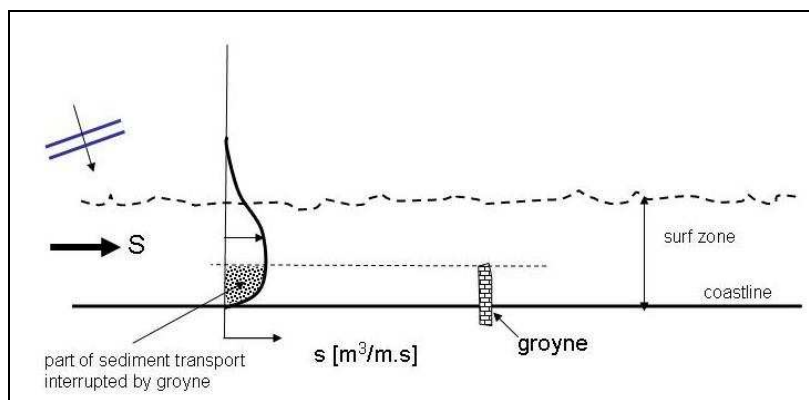


**Figure 12.11** Sketch of rate of interruption of sediment transport by a groyne

A different approach is based on the notion that the occurring sediment transport depends amongst others on the orientation of the coastline. With the help of a groyne (some accretion at the updrift side) a rotation of the coastline might be achieved. 'Playing' with the lengths and the spacing of the groynes of a groyne system, one might be able to reduce the occurring sediment transports to just the required transport. (All along the stretch of coast a constant sediment transport equal to  $S_{in}$ .) Tidal current effects and water level changes due to astronomical tide in combination with the crest height of the groynes complicate a clear view on the effectiveness of a groyne system. (E.g. crest of groyne above water level during LW and partly under water during HW.)

All these complications contribute to the observation that simple 'rules of thumb' cannot exist. (E.g. 'rules of thumb' in the sense of: the spacing - length ratio of a groyne system must be in the range 1 to 3.)

In summary: it is quite clear that series of groynes are able to interfere in the occurring sediment transports along a given stretch of coast, but it will also be clear that a lot of fine tuning should be necessary. Our knowledge of the coastal system and our tools to perform a proper fine tuning are for the time being not yet sufficient. When applying a groyne system in a specific structural erosion case, means in fact often that some kind of a trial and error method is chosen. Good, but also wrong examples of applied systems are found all along our coasts.

It has to be stressed that a properly working groyne system might stop the structural erosion in the protected part of the coast. But that automatically means that the part of the coast downdrift from the protected area, will suffer from much more erosion than before the protection was applied. ( $S_{out}$  of the protected area which is  $S_{in}$  of the downdrift area has seriously reduced!) The solution in the protected area is at the spent of the downdrift area. (If there is no downdrift part of a coast, things are of course different.)

Coastal engineering 'experts' who promise you to design a groyne system without downdrift erosion in a structural erosion case, must be characterised as charlatans.

Achieving a constant net sediment transport along the stretch of coast to be protected (equal to  $S_{in}$ ) was a main notion and requirement in the discussion. If in the area to be protected, the net sediment transport would be 'set' to zero ( $S = 0$  is chosen), the design problem for a series of groynes would be rather simple. With a series of rather long groynes the area to be protected is divided in a series of 'closed' cells (no sediment transport from the one cell to the other). Depending on the original magnitude of  $S_{in}$ , at the updrift side of the area accretion is expected; at the downdrift side of the area to be protected the lee-side erosion is then much larger than strictly necessary.

The discussion so far holds in fact for all types of groynes.

For traditional groynes of stone ('closed') we are able to understand with rather general, but also somewhat obscure, notions how they 'work' (how they could interfere in the occurring sediment transports). 'Open' structures (e.g. rows of piles) operate in fact much more clearly. Rows of piles cause more resistance to the occurring water motion in the near shore zone. The current velocities reduce and so do the sediment transports.

## 12.6 Detached shore parallel offshore breakwaters

Structures built essentially parallel to the coast at a certain distance from the position of the initial coastline (detached: in this respect 'free' from coastline). Often like ordinary (port) breakwaters built from stone. Often series of breakwater segments with gaps in between. Two distinct types (see Fig.12.12):

- emerging (crest above MSL);
- submerged (crest below MSL).

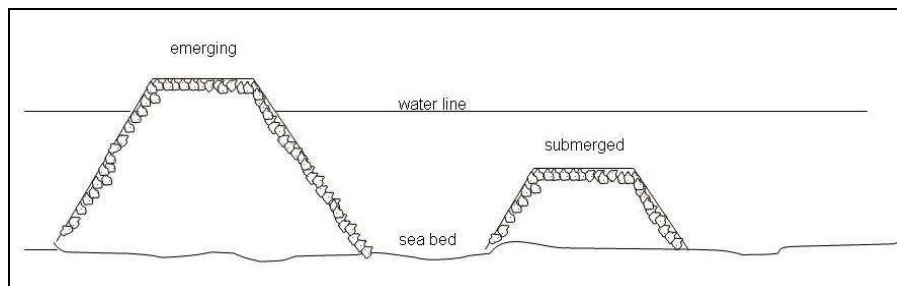


**Figure 12.12 Detached shore parallel breakwaters** (*slopes in figure are too steep*)

**Problem: risks of valuable buildings and infrastructure must be reduced; safety hinterland insufficient**

In principle the rate of erosion of the mainland because of a severe storm surge can be reduced with the help of detached shore parallel offshore breakwaters. The rate of erosion depends amongst others on the height of the waves which are able to reach the mainland. The shore parallel breakwaters might cause the incoming waves to break, so a reduction of the wave heights landward of the breakwaters is expected. [The ratio  $H_t/H_i$  is often used to indicate the rate of wave height reduction;  $H_t$ : transmitted wave height (i.e. wave height just landward of the breakwater);  $H_i$ : incoming wave height (i.e. wave height just seaward of the breakwater).

The higher the crest of the breakwater is above the occurring water level, the smaller the ratio  $H_t/H_i$ . If the crest level of the breakwater is equal to the occurring water level, the ratio  $H_t/H_i$  is already about 0.5.]

In this respect emerging breakwaters are much more effective than submerged breakwaters. However, accompanied with a severe storm often also a surge effect will occur. To be effective also under these conditions the crest height of the breakwaters should be very (unattractively) high.

So in practice detached shore parallel offshore breakwaters are no serious alternative for the present problem. Two additional effects make this alternative very unattractive in the present possible application.

1): If under severe storm surge conditions some wave overtopping of the breakwater segments occurs (discharge of water over the breakwater towards the coast), this volume of water is 'free' to select the easiest way to return to open sea

(continuity). The easiest way in this case is as a concentrated flow through the gaps in between the breakwater segments (and not over and through the breakwater segments). This might cause very high seaward directed current velocities within the gaps, transporting also sediments in seaward direction. (This process / effect is comparable with rip currents.) The ultimate effect might even yield an increase of the erosion of the mainland compared with the 'unprotected' situation.

2): The application of detached shore parallel offshore breakwaters as a possible solution for the problem as was defined (reduction of rate of erosion during a severe storm surge), means automatically that these structures are also present (and will have their effects) under ordinary conditions. These effects will be mentioned while discussing the next problem, but might be quite unwanted. One should always take these additional effects into account in the final decision making process.

### Problem: stretch of coast suffers from structural erosion

Before discussing the application of detached shore parallel offshore breakwaters as an alternative to resolve the problem as stated, it is useful to make some general remarks on the effect of this type of structures on the occurring coastal processes.

Consider a situation with waves continuously approaching a perfect straight coast (parallel depth contours) perpendicularly; ordinary wave conditions are assumed. *[Most likely this is a situation where there is no need to apply detached shore parallel offshore breakwaters; it refers to a stable situation.]*

The waves approach perpendicular to the straight coast; the shape of the cross-shore profile is assumed to be in equilibrium with the wave conditions. We will construct one single detached shore parallel offshore breakwater. This structure will disturb the stable situation. It makes in this case a great deal of difference whether an emerging or a submerged breakwater is applied.

*Emerging* (see Fig.12.13):

It is assumed that the crest level of the breakwater is well above MSL; no wave overtopping occurs; waves hitting the breakwater will break and partly reflect to deeper water again; landward of the breakwater a 'shadow' zone is present.



**Figure 12.13 Emerging breakwaters**



Adjacent to the ends of the breakwater, the waves will still approach the coast unhindered. At both ends of the breakwater diffraction processes take place, causing rather modest wave heights in the shadow zone behind the breakwater. Because of the diffraction process these waves approach the coastline under an angle. Starting at some distance from the 'protected' part of the coast, and going towards the middle of the 'protected' part, we notice some interesting features. At our starting point the wave conditions are still as without the breakwater. Rather wide surf zone and rather high wave set-up. Approaching the 'protected' zone, the wave heights reduce; the surf zone becomes smaller; the wave set-up decreases. (Because of the diffraction process the wave heights in the cross-shore profile just at the end of the breakwater are theoretically 50 % of the original incoming wave height; this holds in fact only if the water depth is constant; due to the sloping cross-shore profile also shoaling will occur; so 50 % is in reality just an order of magnitude.) Proceeding along the coast farther into the shadow zone, the wave heights will further reduce; smaller surf zones; further decrease of wave set-up. (If a rather long breakwater was chosen, and the distance of the breakwater from the initial shoreline position is rather modest, it is possible that in the middle of the shadow zone no wave action at all is present.)

Along the coast from our starting point to the middle of the 'protected' zone an ever decreasing wave set-up will be noticed. This means that a gradient in the water level is present in the near shore zone, causing shore parallel currents from outside the 'protected' area towards the shadow zone (from two sides). Because of continuity also a return flow will be present (at deeper water). A characteristic flow pattern is generated (see Fig.12.14).

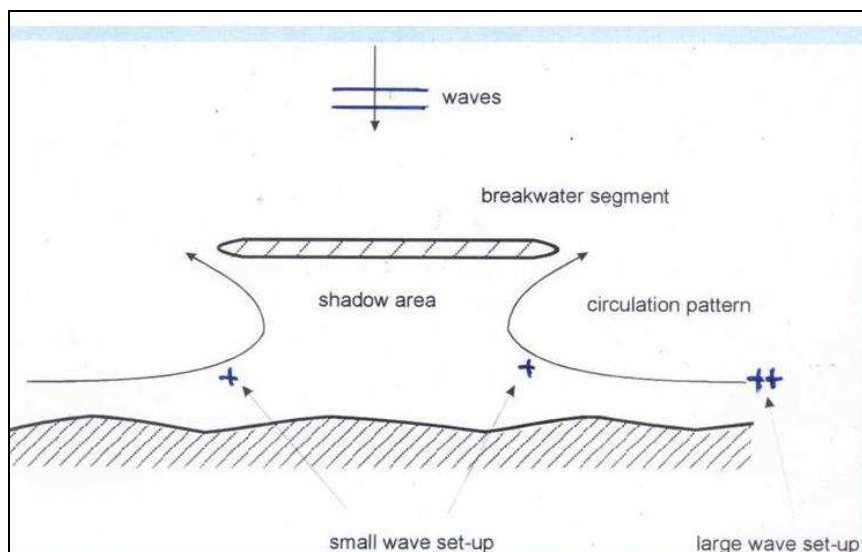


**Figure 12.14 Processes near emerging breakwater**

Current pattern together with wave action cause sediment transports towards the shadow zone. Depending on the boundary conditions (and the layout characteristics of the breakwater) at the end of the day a salient or a tombolo will be formed as a final equilibrium situation. In both cases locally accretion takes place (in the shadow

zone), but that automatically means that elsewhere erosion had to occur (see Fig.12.15).

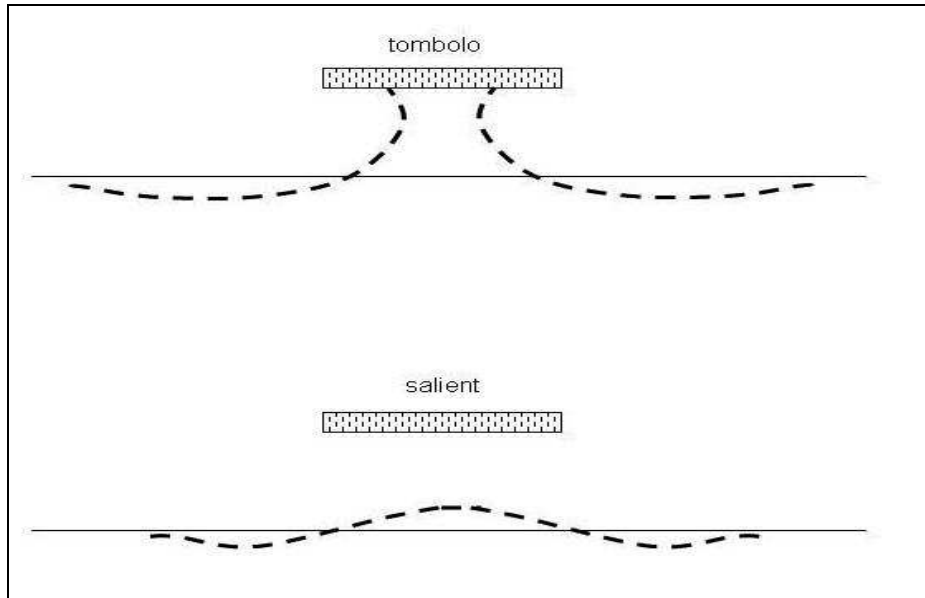


**Figure 12.15 Tombolo and salient**

The forming of tombolo's and salients can also be observed in nature as a quite natural process; e.g. if a small island is (in case of a salient) or was (in case of a tombolo) situated in front of a sandy coast. (See Fig.12.16).

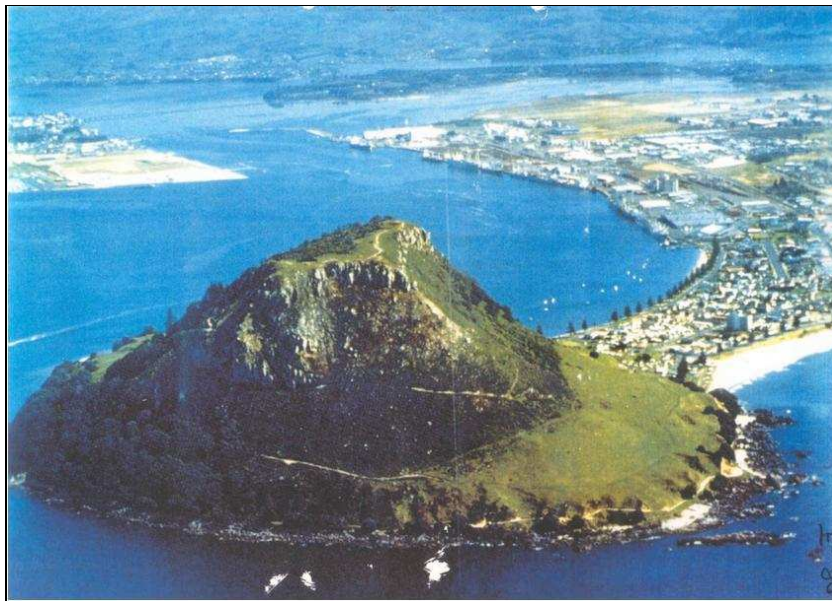


**Figure 12.16 Tombolo behind island**

*Submerged* (see Fig.12.17.)

Also in this case a single breakwater is thought to be constructed in front of a sandy coast (wave approach perpendicular to the coast); but the crest level of the breakwater is now below MSL. The remaining water depth above the crest of the breakwater is assumed to be rather small; the submerged breakwater initiates wave breaking.



**Figure 12.17 Submerged breakwater**

Compared with the emerging case the processes are quite different. First of all the waves are assumed to break at the breakwater, but landward of the breakwater still a lot of (slightly reduced compared to the situation without breakwater) wave action is present. With the breaking waves on the breakwater, volumes of water are transported towards the coast over the breakwater (mass transport). Because of continuity the same volume of water has to return to open sea again. The easiest way is in this case at the both ends of the breakwater. A for submerged breakwaters typically flow pattern results (see Fig.12.18 next page). In this case the currents (together with the wave action) yield sediment transports from the zone landward from the breakwater to deeper water; erosion might be expected. In Dean *et al.* (1997) a striking example is described where the application of offshore breakwaters yields more erosion than without this 'protection' measure.

In the preceding examples the processes initiated by a single detached shore parallel offshore breakwater under perpendicular wave attack were discussed. Oblique wave attack, series of breakwater segments including gaps, and tide effects (water level and currents) seriously complicate the occurring processes. Simulations with (steadily improving) complex morphological computer models yield ever improving results. Sound and reliable applications in quite arbitrary cases are, however, not yet known.

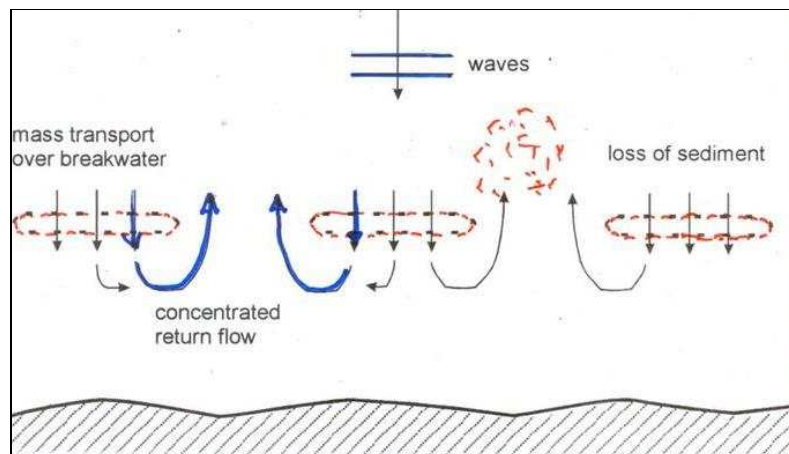


**Figure 12.18 Processes near submerged breakwater**

In the discussion so far a straight coast was assumed as starting point, so in fact no problems were to be expected with this coast. But the actual problem of this section was a structural eroding coast.

We have seen that detached shore parallel offshore breakwaters are able to interfere in the occurring sediment transport processes; so these structures might be an alternative for the solution of the erosion problem. (The application of submerged structures is questionable in this case.) To design an optimal system is, just like if groynes would be chosen, a difficult task. Also in this case remains that with a sufficient working system in the problem area, lee-side erosion is unavoidable.

### Problem: creation of new beaches

Existing beaches in booming recreation resorts are sometimes not wide enough to accommodate the large number of visitors. Or, sometimes the existing sea side consist out of stone instead of nice sandy beaches. Often it refers to projects with a limited dimension in the longshore direction. Just placing an artificial beach nourishment (see Chapter 13) will cause a lot of losses after the execution. Losses will occur in longshore direction and / or cross-shore direction to deeper water. With the help of (emerging) shore parallel offshore breakwaters the nourished volumes of sand can be confined between more or less arbitrarily chosen limits. (See Fig.12.19 for a sketch; Fig.12.20 shows a typical real life example.) With a solution according to Fig.12.19. it is conceivable that the limited widths of the gaps prevent offshore directed losses of sediment; the beaches are rather wide and the waterline is rather long. Fig.12.20 shows that even a playful layout can be achieved.

Artificially widening beaches over a rather large distance in seaward direction, calls for a large volume of sediment. Not only the upper part of a cross-shore profile has to be raised, but also the deeper parts of the cross-shore profile. In fact 'all' depth contours have to be shifted over a same distance in seaward direction. (An initial equilibrium profile remains by this operation then an equilibrium profile. See Fig.12.21.) By building a detached submerged breakwater, the upper part of the cross-shore profile can be 'supported' by the underwater dam. Large savings of sediment meant to fill the toe of the cross-shore profile might be achieved.

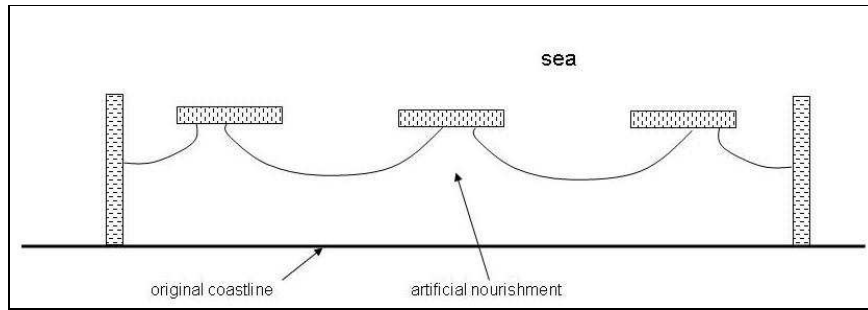


**Figure 12.19 Application of structures to confine sand**



**Figure 12.20 Real life example**

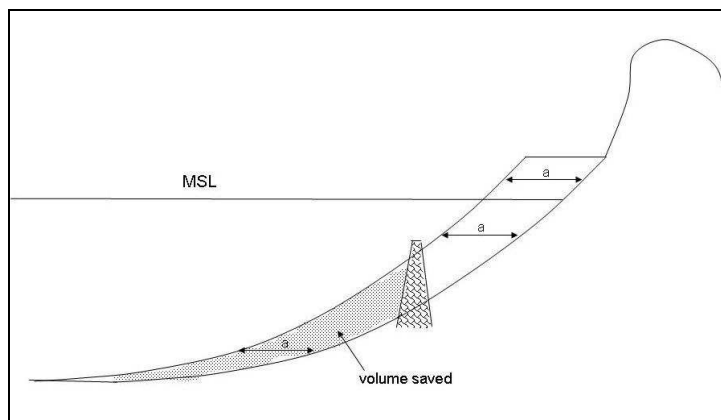


**Figure 12.21 Expected cross-shore profiles large scale land reclamation**



To an even larger extent similar considerations hold if a large land reclamation project is taken into account, because then often even larger depths have to be taken into account.

## 12.7 Piers and trestles

*Rather long structures with a horizontal deck on series of piles extending perpendicular to the coast into the sea. Serving as a landing place for vessels, as a recreation facility, as a measuring facility for coastal processes or as a part of sand by-pass facility. (See Fig.12.22.)*

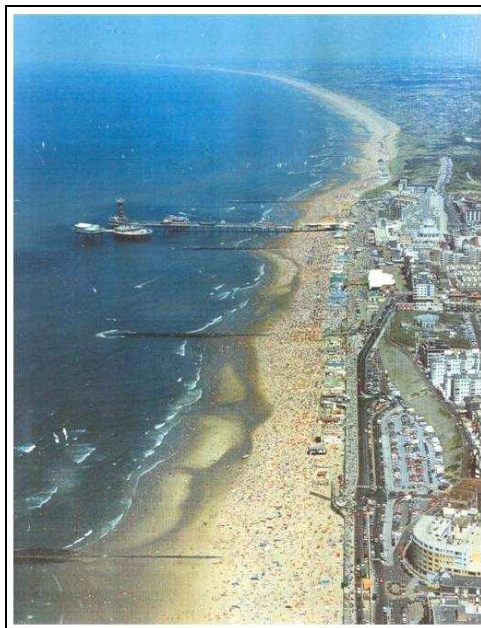


**Figure 12.22 Recreation pier**

The aims to construct piers and trestles are in fact sufficiently mentioned in the preceding definition of this type of structures. Only the possible impact of these structures on the coastal processes needs some discussion. The supporting piles might cause some impact. Especially if the number of piles is rather large and with large diameters of the piles, obliquely arriving waves will cause in the lee of the rows of piles an area with reduced wave heights. The sediment transports will be reduced as well; spots with some accretion might occur (in general at both sides since waves will approach from both sides). Especially for measuring piers this might yield atypical measuring conditions.

## 12.8 Sea-dikes

*Like revetments (see Section 12.3), but without, or hardly any, beach in front of the structure. Just like dikes along e.g. a river, sea-dikes are often meant to prevent flooding. (See Fig. 12.23.)*



**Figure 12.23** Sea-dike (Westkapelle, The Netherlands)

The design crest height of a sea-dike has to be carefully chosen in order to prevent too much overtopping. In The Netherlands the so-called Hondsbossche and Pettemer sea defence is a good example (see Fig. 12.24). Because of the flat slope the wave run-up under the Dutch design conditions reaches rather high levels (about 8 m above design storm surge level).



**Figure 12.24** Hondsbossche and Pettemer sea defence

New (preliminary) insights in possible wave characteristics during design conditions learned that the crest level of the existing sea defence was probably too low. As a 'no-regret' measure for the time being the sea defence is partly provided with an additional sheet piling (see Fig.12.25).

An additional point of concern is the position of the (sandy) bottom just in front of the sea defence. The ultimate wave run-up depends on the local wave height just at the toe of the sea defence. The wave height is usually depth limited. However, when during design conditions erosion of the sandy bottom just in front of the sea defence is expected, the characteristic wave height might be higher than expected.

If a sea-dike consists out of a (rather steep) rubble mound structure (like in case of an artificial island in open sea), fierce wave breaking on the structure will occur. Together with landward directed wind, this might lead to a lot of salt spray at the artificial island. Depending on the ultimate use of the island salt spray should be avoided as much as possible. (E.g. salt spray and aluminium aircrafts are a bad combination in case an artificial island is used to host an airport.)



**Figure 12.25** Additional sheet piling (Hardly visible at crest of dike.)

## 12.9 Miscellaneous

*In this section some remarks are made with respect to various proposed 'tools' in resolving actual coastal engineering problems.*

From time to time inventors come up with various ideas to resolve coastal engineering problems or other general societal problems. Not seldom the 'solution' comes first and the associated 'problem' has to be found afterwards. Without further discussion here, only a few recent developments are just mentioned.

- Beach dewatering; in order to achieve steeper and wider beaches than normally.
- Building a very long dam into the sea with electricity generators. Dam and tidal motion cause head differences.



- Bio-dune developments; specific bacteria with sufficient nutritious matter are able to stick loose sand particles together forming some kind of sandstone. To be applied for instance as an erosion reducing part of a dune.
- Floating breakwaters; large steel or concrete structures anchored at some distance from the shoreline. Structures cause wave damping.
- Eco-beach developments; some people believe that by just putting some vertical, perforated tubes into the beach, accretion takes place. Indeed a very cheap method to strengthen a coast (if it works!).
- Series of artificial islands in front of the coast. (E.g. a tulip shaped island in front of the Dutch coast.)
- Sand-engine; very large artificial nourishment (tens of million m<sup>3</sup> sand in a restricted area) meant to naturally feed large stretches of adjacent coasts.



# 13 Application of Nourishments

## 13.1 Introduction

Artificial nourishments are increasingly used to resolve various coastal engineering problems. In many cases ('soft') nourishments are a very good alternative compared to solutions with 'hard' measures.

Basically an artificial nourishment means that sediments (usually sand) from an external source are artificially (truck; dredge) brought into the coastal system. Of course such an action is driven by a well-defined aim.

In Section 13.2 a few typical coastal engineering problems and issues are mentioned, which can be resolved with artificial nourishments as tool. That will be a rather straightforward discussion. If an artificial nourishment scheme is selected as tool to resolve a coastal engineering problem, next many details and aspects are important to reach a proper design. Most of these details and aspects are relevant for all possible applications, so it is useful to discuss these in a separate section (Section 13.3). In that section the next items will be discussed:

- beach and shoreface nourishments;
- borrow and native sand;
- methods of execution;
- ecological impact;
- losses and effectiveness;
- monitoring and evaluation;
- sand bypass systems.

## 13.2 Problems to be resolved with artificial nourishments

Chapter 12 has revealed that with the help of 'hard' measures various coastal engineering problems could be resolved. If properly applied these 'hard' measures *must* interfere in the occurring coastal processes at the right place and the right moment. (E.g. a series of groynes interfering in the occurring longshore transports; a well-designed seawall which prevents that sediments from the dunes will participate in the cross-shore sediment transport processes during a severe storm surge.)

A basic nature of a 'soft' measure (like an artificial nourishment) is that this measure *has not* the intention to interfere in the occurring coastal processes. (This statement is not quite strict; in some cases interfering in coastal processes while applying an artificial nourishment, might be an inevitable consequence or an additional aim; see Section 13.3).

### Problem: stretch of coast suffers from structural erosion

If a stretch of coast suffers from structural erosion it means that volumes of sediments are lost out of that stretch. At the scale of an individual cross-shore profile it means that the control volume is losing sand at a regular basis ( $\Delta V \text{ m}^3/\text{m}$  per year). With an artificial nourishment the occurring losses are replenished. Because it is generally not useful to repeat the replenishment of the stretch every year (the initial costs of a nourishment operation are often rather high), the annual losses of several years (say 5 years) are usually taken together.

In Fig. 13.1 a very basic plot is given of the development with time of the volume of sediments in a cross-shore profile. Apparently erosion of the volume occurs; a minimum volume is given as a limit; if the limit is threatened to be surpassed, an artificial replenishment is executed.

The material present in the cross-shore profile is usually called the native material; the material to be supplied the borrow material.

If after the replenishment the same processes occur as before the replenishment, the development with time continues with the red line. If the same material is used for the nourishment as was originally present at the beach ( $D_{\text{borrow}} = D_{\text{native}}$ ), that behaviour might be expected. Given a required lifetime of the nourishment operation the required volume can be estimated.

If the borrow material deviates from the native material, different post nourishment developments are to be expected, yielding different lifetimes.

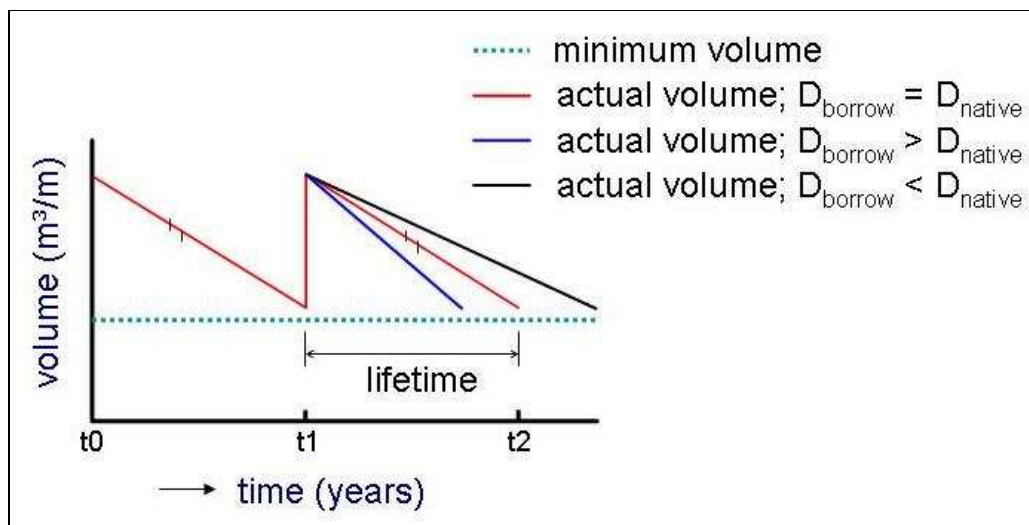


**Figure 13.1** Development with time of volume of cross-shore profile with nourishment

[With an average value for  $\Delta V$  of  $20 \text{ m}^3/\text{m}$  per year (annual retreat of coastline of about 1 m per year; see Example 11.1), a time period between nourishments of 5 year means that about  $100 \text{ m}^3/\text{m}$  every 5 year has to be replenished; that is quite normal value. If the relevant stretch of coast is 5 km, a total volume of  $500,000 \text{ m}^3$  has to be nourished every 5 year.

In practice one has to take some additional losses during execution into account.]

The position in a cross-shore profile where the replenishment is placed, is to some extent rather 'free'. Two general positions are usually applied:

- mainly at the beach;
- at the shoreface (under water).

In Section 13.3 the differences between both possibilities are discussed in more detail; Fig. 13.2 gives a schematic representation.

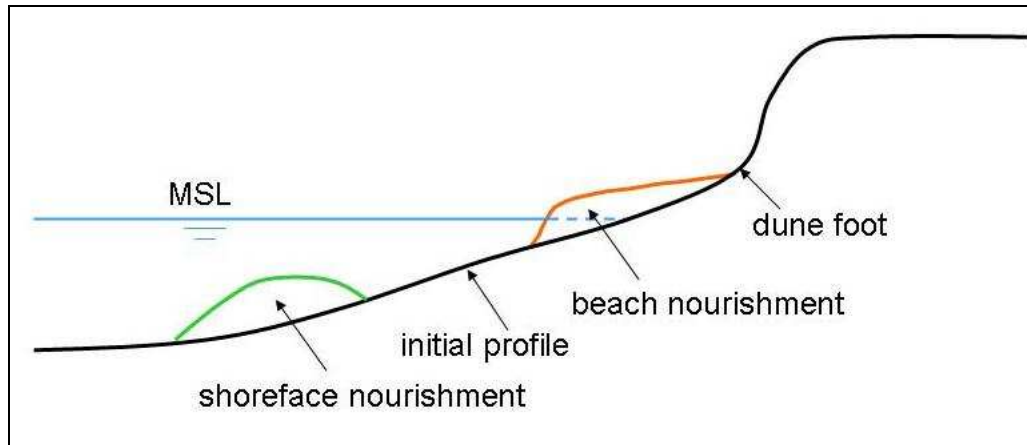


**Figure 13.2 Beach nourishment and shoreface nourishment**

Assuming that the particle diameter of the borrow material is equal to the particle diameter of the native material, the nourishment means in fact that the shape of the cross-shore profile is locally perturbed. Morphological processes tend to tackle the perturbations.

With the order of magnitude of the volumes of sand as were mentioned for the nourishment operation ( $500,000 \text{ m}^3$  over 5 km), the alignment of the coast in longshore direction is hardly changed. (The perturbation is in fact rather small.) To a first approach one could assume that the (longshore) processes which cause the losses out of the stretch of coast, do not seriously change by the nourishment operation. This 'soft' method does not interfere in the relevant sediment transports. The losses occurring before the replenishment operation, just continue after the operation. In the present example it means that after 5 years the pre-nourishment situation has reached again. And if one likes to achieve (on an average) a status quo situation, one has to repeat the nourishment operation, and again, and again. This 'eternal' repetition might be considered as a serious disadvantage of this method. However, in many cases where an honest comparison is made between various alternatives, it turns out to be the most cost effective method.

The largest positive aspect of the application of artificial nourishments is that no lee-side erosion occurs. (Lee-side erosion always occurs when one applies 'hard' structures to resolve this type of erosion problems; see Chapter 12.)

As previous said, the nourishment forms a perturbation on top of the shape of the cross-shore profile which was present just before the nourishment operation. To ease the further discussion we assume that this initial shape was (almost) an equilibrium shape. After the replenishment operation two processes are to be considered:

- steady losses of sand out of the cross-shore profile in longshore direction; not necessarily at the same place of the perturbation;
- flattening out of perturbation and redistribution of material over cross-shore profile.

The first process is just the very reason to carry out an artificial nourishment project. In Section 13.3 some additional remarks are made concerning the second process.

### Problem: dunes do not offer enough 'safety' to the low-lying hinterland

If it turns out that a (rather slender) row of dunes does not meet the requirements (design conditions) to properly protect the hinterland, the dunes are to be reinforced with additional sand. It is assumed that the coast is stable; no structural erosion. Fig.13.3 gives two possibilities to reinforce a row of dunes with sand. (Also heightening of the dunes might be a possibility in some cases.) While nourishments meant to overcome the effects of structural erosion must be regularly repeated, a reinforcement of the dunes for the present aim have to be carried out once.

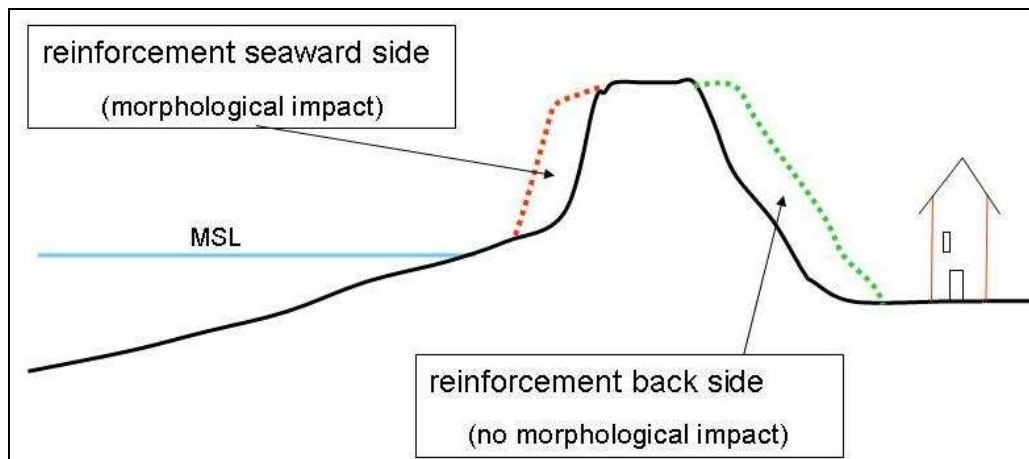


**Figure 13.3 Reinforcement of dunes**

Reinforcement at the back side of the dunes is the best solution; the sand as supplied does not affect the normal occurring morphological processes. However, if buildings or infrastructure are present just landward of the dunes, this alternative might be cumbersome.

Reinforcement at the sea side of the dunes seems attractive; a rather small volume of sand is required and no possible impediments at the landward side will occur. However, by widening the dunes in seaward direction the dune foot is shifted in seaward direction. In a dynamic equilibrium condition a certain distance between the dune foot and say the position of the MSL does exist. The 'system' likes to redress the unbalance; sand from the new dune is transported in seaward direction. At the end of the day the additional volume of sand is redistributed over a large part of the cross-shore profile (say up to the active part of the cross-shore profile). In the design of the reinforcement one has to take these 'losses' into account.

Reinforcement of the dunes might be necessary over an often restricted distance in longshore direction. In Fig.13.4 a situation has been sketched where the dunes have been reinforced in seaward direction (40 m; remaining after the redistribution processes just mentioned) over a longshore distance of 2 km. Also in this case one cannot 'unpunished' locally change the morphology of the coast. Losses in longshore direction are to be expected.

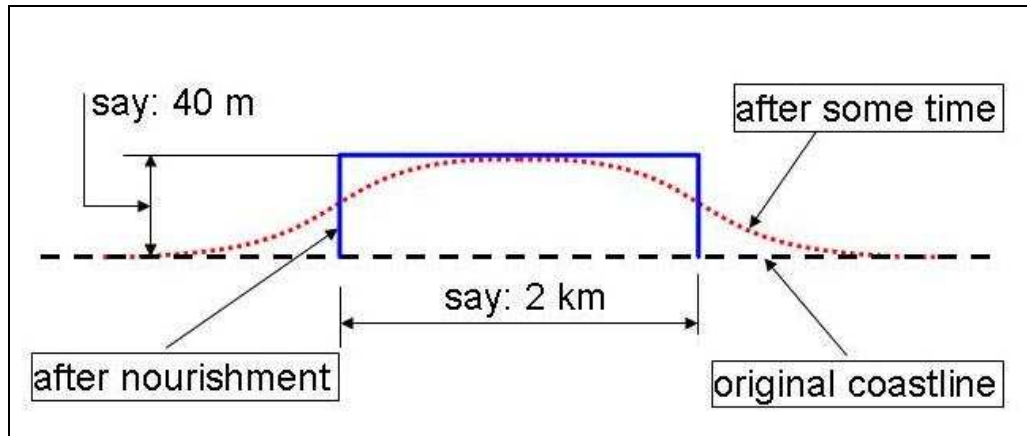


**Figure 13.4 Losses in longshore direction**

#### Problem: existing beaches not wide enough for prosperous recreation

In some cases it is felt that the width of the existing beaches is too small for a further prosperous recreational development. E.g. in a booming coastal resort with many new hotels and recreation developments. Over a part of the coast in longshore direction one likes to broaden the beaches. It is assumed that the existing coast is more or less stable seen over a number of years.

It is assumed that the borrow material is equal to the native material. Changing only the upper part of the cross-shore profile (beaches) of an intrinsic stable coastal system, will trigger a process of redistribution of the nourished volumes of sand over a much larger part of the cross-shore profile at the end of the day. Since the widening of the beaches takes place over a restricted distance in longshore direction, also losses in longshore direction are to be expected. (Similar processes as indicated in Fig.13.4.) So 'losses' seem to occur in cross-shore and longshore direction; at least sediments disappear from the area where we like to keep the sediments. In the design of the project one has to take these consequences into account.

#### Problem: no (sandy) beaches present; beaches are wanted

In many places the available stretch of coast is small and e.g. rocky. Hardly any 'normal' sandy beaches are present. For recreational purposes it is then often desired to create broad sandy beaches. This can be achieved by applying artificial nourishments. In principle the occurring processes are mainly the same as in the previous problem. There are, however, two differences. The first point is that since there was no (sandy) equilibrium profile before the nourishment, the entire profile has to be nourished. The second point is that the longshore spreading as described as

described in the previous problem, will erode the newly created beaches quite seriously. In this case the erosion will be much larger compared with the previous case, because in the original situation in this case hardly any 'normal' sandy beaches were present, and then, consequently, rather high waves might be expected rather close to the coast. Rather large sediment transport capacities occur; causing the large losses in longshore direction.

Some precautions might be taken to keep the sediments of the artificial beach at the desired position. To confine the artificial beach, groynes or breakwaters might be applied. If applying groynes they have to extend long enough in seaward direction so that the nourished sand cannot easily escape. Perhaps even an additional (submerged) breakwater built parallel to the shoreline might serve as an extra measure to keep the sand properly confined.

### Problem: land reclamation

For large scale land reclamation in open sea, large volumes of sand are necessary. (Reclamation: either connected to the present coast, or as a large island in open sea.)

In Fig. 13.5 an existing cross-shore profile is sketched; from the mainland down to a depth of say 20 m below MSL. In the figure also the same cross-shore profile is given which is horizontally shifted over a few kilometres in seaward direction. (A few kilometres: we are assuming a really large reclamation project.)

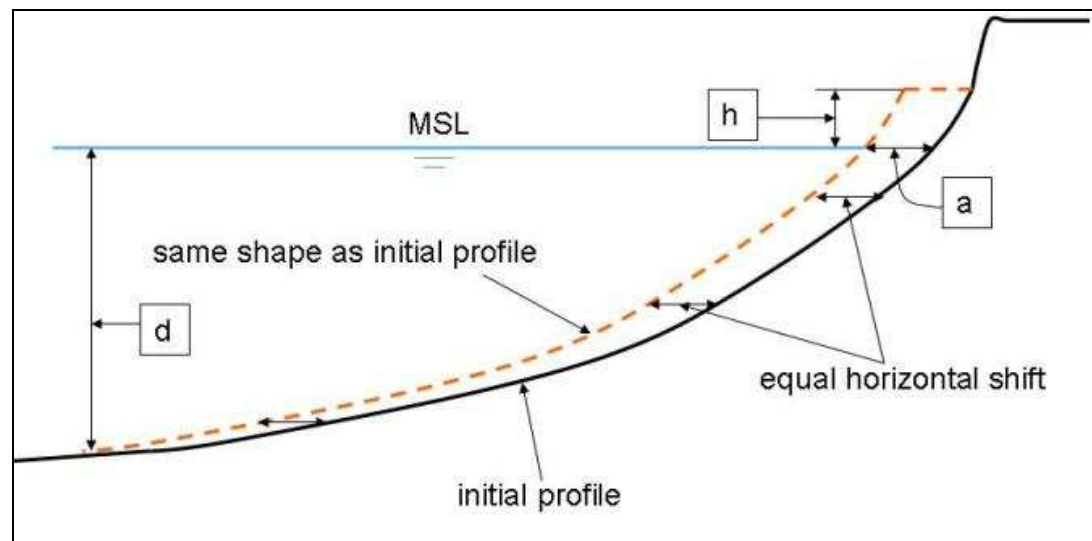


**Figure 13.5 Land reclamation: cross-shore profile entirely shifted**

With a shift of  $a$  m in seaward direction a volume  $V = a(d + h) \text{ m}^3$  per m in longshore direction is necessary. With  $a = 2 \text{ km}$ ,  $h = 5 \text{ m}$  and  $d = 20 \text{ m}$ ,  $V$  becomes  $50 \times 10^6 \text{ m}^3$  sand per km in longshore direction. (For  $1 \text{ m}^2$  of new land,  $25 \text{ m}^3$  of sand is required.) A relatively large part of the required volumes is meant to shift the cross-shore profile at the deeper parts of the cross-shore profile. Between MSL -10 m and MSL -20 m is 40% of the total volume present in our example!

To save construction costs two ideas have been raised: i) cut off the shifted profile at a reasonable depth with a steep slope towards the original profile (see Fig.13.6) and ii) build a submerged breakwater which supports the upper part of the cross-shore profile (see Fig.13.7).



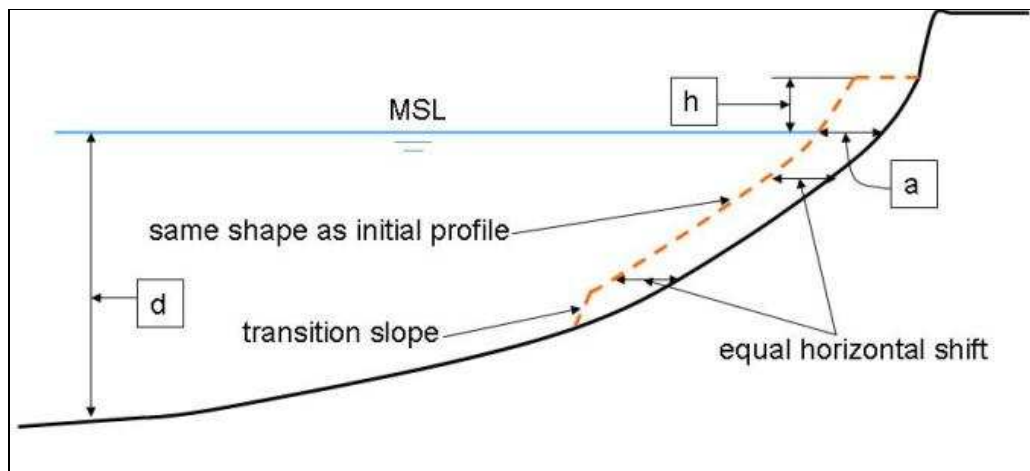


**Figure 13.6 Land reclamation: shifted profile with transition slope**

With the first idea the initial construction costs are far less, although the maintenance costs for the upper part of the cross-shore profile might be large. In fact it refers to some kind of postponed construction costs.

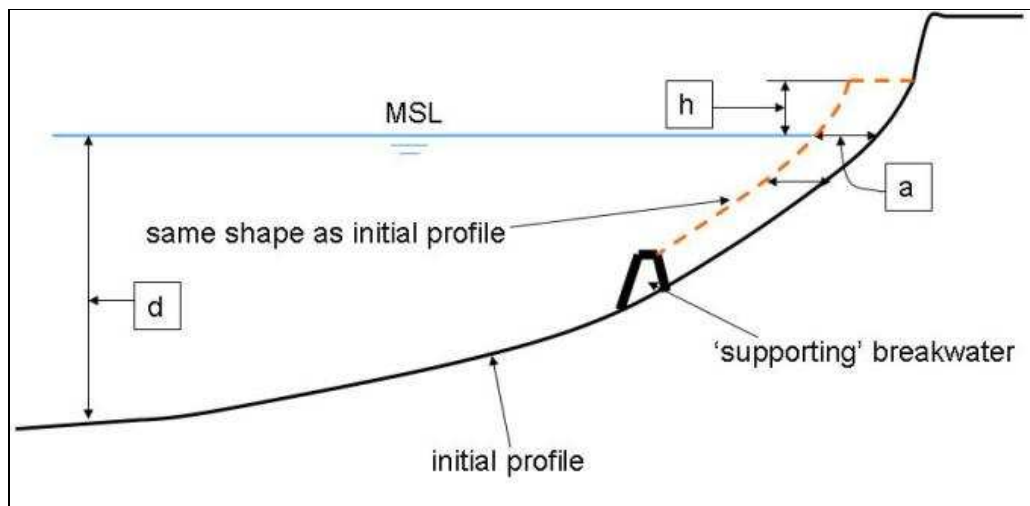


**Figure 13.7 Land reclamation: shifted profile with 'supporting' breakwater**

In both cases cost-benefit considerations might help to find an acceptable final solution.

### Problem: Global sea level rise and retreat of coast

With the notion of the existence of some kind of an equilibrium shape of a cross-shore profile (shape with respect to MSL 'fits' with the occurring tide and wave conditions) it is easy to understand what will happen when the mean sea level rises.

In the next discussion it is assumed that the tide and wave conditions have not been changed after some sea level rise.

Given (for the discussion: at once) a higher MSL the shape of the cross-shore does not fit anymore with the tide and wave conditions; the actual cross-shore profile

seems to be too steep (see Fig.13.8 profile [1] and explanation later on). Morphological processes will start to achieve again an equilibrium situation. In an entirely natural development that means that coastal retreat will occur.

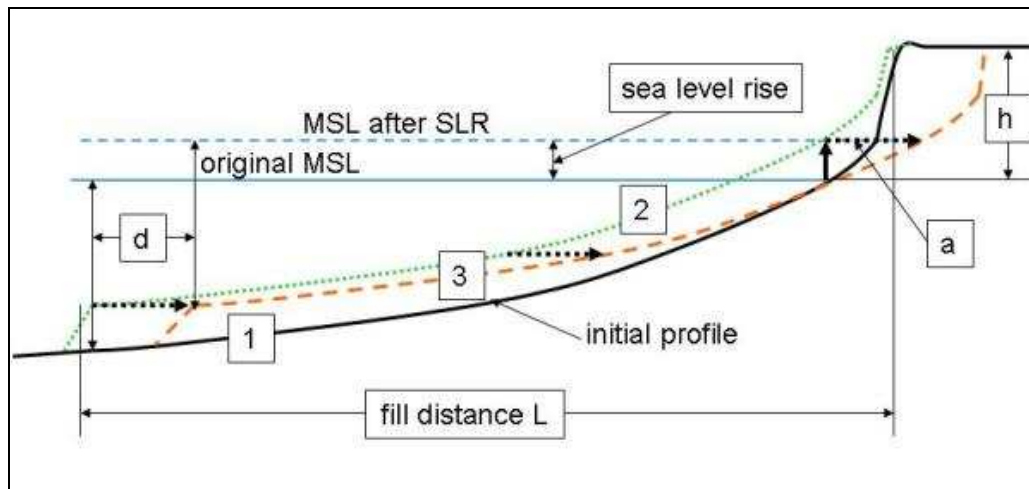


**Figure 13.8 Profile adaptations and sea level rise**

In the present situation profile [1] is assumed to be in equilibrium with the wave and tide conditions. If after sea level rise (SLR) profile [1] would be artificially (vertically) filled with a layer with thickness SLR over a sufficient long distance in sea ward direction (fill distance  $L$  in Fig.13.8), the position of the coastal profile in horizontal sense is still the same; profile [2]. The beach is for instance at the same position as before SLR, but at a higher level compared to the original MSL. If one likes to keep the position of the coast at the same position, irrespective of the rate of SLR, a volume of SLR times  $L$  is necessary. With e.g. SLR = 1.0 m per century and  $L = 1000$  m, a volume of  $1000 \text{ m}^3/\text{m}$  is required in 100 years. A volume of  $10 \text{ m}^3/\text{m}$  per year is a quite acceptable volume to artificially nourish in order to overcome the 'threats' of such a sea level rise.

If nature is allowed to do the adaptation job without human interference, a new equilibrium is achieved by a horizontal shift [a] of profile [2] towards profile [3] in Fig.13.8.

The horizontal shift [a] can be determined from:  $a = (\text{SLR} * L)/(d+h)$ .

With SLR = 1.0 m (e.g. per century),  $L = 1000$  m,  $d = 10$  m and  $h = 10$  m, a becomes 50 m. [C.f. Bruun (1962).]

In some situations such a gradual retreat of the coast might be acceptable (in the example 0.5 m per year), in other cases that is not felt as acceptable (e.g. a coastal zone with infrastructure and buildings close to the sea).

The policy in The Netherlands is to avoid any coastal retreat so the option with profile [2] in Fig.13.8 is strived after.

### 13.3 Various aspects

In this section some general aspects related to artificial nourishments are discussed. They are relevant for many applications as mentioned in Section 13.2.

#### Beach and shoreface nourishments

To overcome the effects of structural erosion (sediment losses out of coastal profile) artificial replenishments are carried out at a regular basis. In principle the supplied sediments are meant to disappear sooner or later again. For this aim it is not very important where in the cross-shore profile the nourishments are positioned. It is for sure that the actual gradual losses out of the cross-shore profile do not take place precisely at the position where the nourishment was positioned. In practice that is no serious problem because cross-shore sediment processes redistribute the sediments over the cross-shore profile. A shoreface nourishment should not be positioned at a too large water depth; the nourishment might then be out of the 'reach' of the waves.

Because the costs per m<sup>3</sup> of a shoreface nourishment project are far less than these costs of a beach nourishment project, often much higher quantities are involved for a shoreface nourishment project in comparison to a beach nourishment project. If large volumes are involved indeed with a shoreface nourishment project, the rather basic assumption that a replenishment does not drastically interfere in the occurring morphological processes, cannot be true anymore. Examples are known where the bar motion in seaward direction is disturbed by a large shoreface nourishment project; see e.g. Spanhoff and Van de Graaff (2006).

#### Borrow and native sand

The sediment present in the cross-shore profile is called the native material.

(This definition looks clear. In many cases, however, the sediment sizes are varying over a cross-shore profile. With the sediment size at the beach as starting point, the sediments become finer in seaward direction; also the sediments in the dunes are usually finer.)

The sediments to be nourished are called the borrow material.

Depending on the aim of the replenishment project and the (possible?) availability of various borrow materials, one might choose favourable characteristics of the borrow material. E.g. in a large land reclamation project the use of coarse material is favourable in order to diminish the losses. In a structural erosion case (regular nourishments) the use of borrow material which fits the native material to some extent is recommended. By doing so the existing coastal morphological system remains unchanged as much as possible.

A coastal system is at the one side often a vulnerable system, at the other side resilient elements are present. Volumes of artificial replenished sediments which differ from the native material will 'tackled' by the coastal system; at the end of the day the system has adapted itself to the changed situation.

If no strict requirements for the borrow material are posed, sometimes the sediments of the one project (e.g. deepening of an approach channel) can be used for another project (beach nourishment) yielding cost effective projects.

In selecting the source of the borrow material one has to take into account the possible impact of the deepening of bottom on the coastal system. In general the depth (or the distance from the coast) must be large enough in order to avoid unfavourable effects on the existing coast.

### Methods of execution

With sources for the borrow material at open sea (in some cases land based sources might be used for a replenishment project), dredges are used to carry the borrow material to the project side; e.g. using a trailing hopper dredge. The procedures at the borrow site are for all applications in principle the same (just dredging). The method how to bring the sediments to the required position, depends on the aim of the nourishment project. Also the size of the dredge as used is important. It is beyond the scope of these Lecture Notes to go into details, but using pipelines from the vessel to the project site, rain-bowing, and just using the doors in the bottom of the dredges are some methods to release the sediments of the dredges.

For a beach nourishment project often a final cross-shore profile is prescribed. At the end of the project the contractor has to demonstrate that the profile as prescribed is present indeed. (Losses during the execution of the project are at the costs of the contractor.) It is conceivable that the stricter the requirements are, the more expensive the project will be. For some projects (e.g. to overcome the effects of structural erosion) in fact mainly the volume of nourished material does count.

### Ecological impact

The borrow material as it is in the bottom of the source area, contains sometimes some (immobile) silt (2 % silt is a quite normal percentage). During the dredging operation this silt is released; with the overflow system of the dredge the silt is brought into the sea water. A negative impact at the marine environment might occur.

In Europe large areas have been allocated as Natura 2000 sites. Also dune and coastal areas are part of the Natura 2000 areas; protection and prosperous developments are policy aims of these areas. If a nourishment project is foreseen in the vicinity of Natura 2000 areas, an assessment has to be made whether negative effects are to be expected.

### Losses and effectiveness

The basis for the design of an artificial nourishment project should be a set of realistic requirements the project has to meet. After realizing a projects one is often interested in whether the project did come up to the expectations. Also in the definition of losses and effectiveness one has to be quite clear. If a beach nourishment is e.g. meant to improve the beach, different definitions might be applied compared to the case the beach nourishment is meant to overcome the effects of structural erosion.

### Monitoring and evaluation

The need to apply an artificial nourishment results of course from (regular) observations and measurements. After execution of the project these regular measurements will continue. Often it is felt that more measurements are desirable to

be able to better follow and evaluate the project. Because artificial nourishment projects are still in its infancy, with good monitoring and evaluation efforts many valuable aspects might be clarified.

### Sand bypass system

A special application of an artificial nourishment project is when a sand bypass system is used. Building a port along a sandy coast or building jetties to stabilize a mouth of a river flowing out into the sea, causes often updrift sedimentation and downdrift erosion of the coast. To avoid the erosion at the leeside a sand bypass system is a perfect tool. Sand is artificially transported from the one side to the other. In Australia various examples are known of adequate and cost effective systems. (E.g. Nerang River project and Tweed River project.)



# 14 Background Information

## 14.1 General handbooks

General background information on coastal engineering and coastal morphology is provided in a number of handbooks. Each of them is devoted to some, but mostly not all, topics relevant for coastal engineering. Some of them are listed hereafter in alphabetical order:

- Dean, R.G. (2002).** *Beach Nourishment: Theory and Practice*.  
World Scientific Publishing, Advanced Series on Ocean Engineering,  
Vol.xx.
- Fredsøe, J. and R. Deigaard (1992).** *Mechanics of Coastal Sediment  
Transport*. World Scientific Publishing, Advanced Series on Ocean  
Engineering, Vol.3.
- Horikawa, K. (1978).** *Coastal Engineering*.  
University of Tokyo Press.
- Kamphuis, J.W. (2000).** *Introduction to coastal engineering and  
management*. Advanced series on ocean engineering, Vol. 16.
- Nielsen, P. (1992).** *Coastal Bottom Boundary Layers and Sediment Transport*.  
University of Queensland, World Scientific Publishing Co., Singapore.
- Sleath, J.F.A. (1984).** *Sea Bed Mechanics*.  
Cambridge University, Wiley Interscience Publication, New York.
- Soulsby, R.L. (1997).** *Dynamics of marine sands*.  
Hydraulics Research Wallingford, Thomas Telford Publications, London.
- Van Rijn, L.C. (1999).** *Principles of coastal morphology*.  
Aqua Publications, Amsterdam, The Netherlands.
- Whitehouse, R.J.S., 1998.** *Scour at marine structures*.  
Hydraulics Research Wallingford, Thomas Telford Publications, London.
- The **Coastal Wiki** ([www.encora.eu](http://www.encora.eu)) is an ever growing source of topics also related to Coastal Morphology, Coastal Engineering and Coastal Zone management.

A very practical handbook, which covers nearly all the topics of coastal engineering, is the **Shore Protection Manual (1984)**.

(A new version is available as an electronic version: Coastal Engineering Manual; see for link: [www.waterbouw.tudelft.nl](http://www.waterbouw.tudelft.nl))

## 14.2 Interesting journals

Many coastal engineering topics are discussed in journals. Some examples of such international journals are mentioned.

**Coastal Engineering.** An international journal for coastal, harbour and offshore engineers, Elsevier Science.

**Journal of Waterway, Port, Coastal and Ocean Engineering.** American Society of Civil Engineers (ASCE) Publications

**Coastal Engineering Journal.** World Scientific Publishing Co.

**Journal of Geophysical Research - Oceans.** American Geophysical Union (AGU) Publications.

**Ocean & Coastal Management.** Elsevier Science.

**Journal of Coastal Research.** Coastal Education and Research Foundation.

## 14.3 Conference proceedings

In the field of coastal engineering many, more or less regular, conferences are organised. At these conferences many papers are presented. Often the papers are summarised in Proceedings. The proceedings related to major conferences provide valuable information on the topics discussed in these Lecture Notes. The contents tables form a good starting point for finding further and recent information on specific items. Four major conferences will be discussed, namely:

International Conference on Coastal Engineering (ICCE);

Coastal Sediments (CS);

Coastal Dynamics (CD);

International Conference on Coastal and Port Engineering in Developing Countries (COPEDEC).

### International Conference on Coastal Engineering

The International Conference on Coastal Engineering (ICCE) is the world's premier forum on coastal engineering and related sciences. The Institution of Civil Engineers and the Coastal Engineering Research Council (CERC) of the American Society of Civil Engineers (ASCE) organise the bi-annual conference. The conference includes papers on theory, measurement, analysis, modelling and practice. The invitation brochure of ICCE 2004 mentions the following topics:

**Coastal Processes and Climate Change.** Oceanography, meteorology, morphodynamics and sediment processes, macro and micro tidal regimes, extreme events, coastal waves, effects on coastal management.

**Flood & Coastal Defence Engineering and Management.** Beach management and nourishment, coastal and beach control structures, construction techniques and performance.

**Flood Risk Management.** Strategic planning, flood warning, forecasting and coastal change monitoring, data management and exchange, risk and uncertainty, decision making.



**Coastal Environment.** Recreation, industrial activity, water quality, wetlands and estuaries, sustainability, environmental economics.

**Ports and Harbours.** Siltation, dredging and dredged material re-use, navigation channels, optimization, wave-structure interactions, breakwater monitoring, coastal interactions.

**Coastal Legislation, Planning and Co-operation.** Government policy, funding, collaborative projects, integrated coastal zone management, international co-operation and conventions, law enforcement, effects of coastal hazards on land use planning.

## Coastal Sediments

Coastal Sediments is a multi-disciplinary international conference convened for researchers and practitioners to discuss science and engineering issues of coastal sediment processes. The conference is organised every fourth year by the Committee on Coastal Engineering of the Waterway, Port, Coastal and Ocean Division of the American Society of Civil Engineers. The conference provides a high level technical forum for exchange of information among the fields of coastal engineering, geology, oceanography, meteorology, physical oceanography, and biology.

## Coastal Dynamics

The Coastal Dynamics conferences (CD) are held under the auspices of the American Society of Civil Engineers (ASCE) every four years and are a sequence of technical speciality conferences bringing together field and laboratory experimentalists, theoreticians and modellers conducting research on coastal hydrodynamics and sediment transport. The proceedings of the multi-disciplinary conference are of interest to coastal engineers, coastal geologists, oceanographers, and related sciences.

## Conference on Coastal and Port Engineering in Developing Countries

The mission of the COPEDEC conferences was originally to provide an international forum where coastal and port engineers from developing countries can exchange know-how and experience amongst themselves and with their colleagues from industrialised countries. In 1999, this was expanded to the following mission: To enable the developing countries to have a sustainable human resources pool of highly skilled coastal and port development professionals. On the conference, that is held every four years, papers are presented on many subjects with special reference to needs in developing countries; viz.:

### **Port and Harbour Infrastructure Engineering in Developing Countries.**

Port infrastructure design: choice of structures, design methods and techniques. Port construction: choice of materials, dredging and construction techniques. Port renovation: renovation and demolition techniques.

### **Port Infrastructure Planning and Management in Developing Countries.**

Port planning: economic forecasts, site selection, layout and nautical aspects. Economic aspects: BOT, PPP, privatisation, containerisation. Operations and maintenance: performance, safety, management.

### **Coastal Sediments and Hydrodynamics.**

Coastal stability, beach erosion, control and nourishment. Sedimentation,

maintenance dredging of harbours basins and approach channels. Waves, currents and tides: field survey and measuring techniques.

**Coastal Zone Management in Developing Countries.**

Integrated coastal planning: development, implementation, evaluation.

Impacts of coastal use: fisheries, infrastructure, tourism, recreation. Policy, regulations and guidelines for coastal zone management.

**Coastal and Port Environmental Aspects.**

Environmental Impact Assessment: pollution control and treatment.

Sediment and dredging materials: characterisation, treatment, disposal.

Waste management: reception facilities, prevention, treatment.

## 14.4 Interesting internet sites

An overwhelming number of internet-sites exist with more or less relevant information concerning coastal engineering topics. Sites are changing very fast which means that references to any specific list of sites may be outdated after the appearance of these Lecture Notes.

# 15 References

*(NOT YET UP-DATED)*

- Airy, G.B. (1845):** On Tides and Waves: Encyclopedia Metropolitana.
- Al-Salem, A.A. (1993):** Sediment transport in oscillatory boundary layers under sheet flow conditions. Ph.D. Thesis Delft University of Technology.
- Bailard, J.A. (1981):** An energetics total load sediment transport model for a plane sloping beach: Journal of Geophysical Research, Volume 96, No. C11, pp 10938-10954.
- Bailard, J.A. (1982):** Modelling on-offshore sediment transport in the surf zone: Proceedings 18<sup>th</sup> International Conference on Coastal Engineering, Cape Town, Volume II, Chapter 87, pp 1419-1438.
- Bailard, J.A. and D.L. Inman (1981):** An energetics bedload model for a plane sloping bed: Journal of Geophysical Research, Volume 86, No. C3, pp 2035-2043.
- Battjes, J.A. (1974):** Surf similarity: Proceedings 14<sup>th</sup> International Conference on Coastal Engineering, Copenhagen, Volume I, Chapter 26, pp 467-479.
- Battjes, J.A. (1977):** Probabilistic aspects of ocean waves: Delft University of Technology, Department of Civil Engineering, Laboratory of Fluid Mechanics, Report No. 77-2.
- Bijker, E.W. (1967):** Some considerations about scales for coastal models with movable bed: Ph.D. Thesis Delft University of Technology. Also: Publication No.50, Delft Hydraulics, Delft, The Netherlands.
- Bijker, E.W. (1971):** Longshore transport computations: Journal of the Waterways, Harbors and Coastal Engineering Division, American Society of Civil Engineers, Volume 97, WW4, pp 687-701.
- Bogaard, T. and W.T. Bakker (1977):** Zandtransportberekeningen voor het Noordostelijk deel van het Oosterschelde bekken: Afstudeerverslag Delft University of Technology.
- Bosman, J.J. (1982):** Concentration measurements under oscillatory water motion: Delft Hydraulics Laboratory/TOW Report on model investigation M 1695, part II, Delft.
- Boussinesq, J. (1872):** Théorie des ondes et des remous qui se propagent le long d'un canal rectangulaire horizontal, en communiquant au liquide contenu dans ce canal des vitesses sensiblement parallèles de la surface au fond: Journal de Math. Pures et Appliqués, Vol. 17 Ser. 2, pp 55-108.

- Bruun, P. (1954):** Coast erosion and the development of beach profiles: Beach Erosion Board Technical Memorandum No. 44. U.S. Army Corps of Engineers.
- Bruun, P. (1962):** Sea-level rise as a cause of shore erosion: ASCE, Journal of Waterways and Harbours Division. Vol. 88, pp117-130.
- Coastal Engineering (1991):** Special Issue: Beach nourishments. Coastal Engineering Volume 16.
- Chen, Z. (1992):** Sediment concentration and sediment transport due to the action of waves and a current: Ph.D. Thesis Delft University of Technology.
- Cokelet, E.D. (1977):** Steep gravity waves in water of arbitrary uniform depth: Philos. Trans. Roy. Soc. Ser., A286, pp 183-230.
- Davis, A.G., L.C. van Rijn, J.S. Damgaard, J. van de Graaff and J.S. Ribberink (2002):** Intercomparison of research and practical sand transport models: Coastal Engineering: Volume 46, No. 1, pp 1 - 23.
- Dean, R.G. (1965):** Stream function representation of non-linear ocean waves: Jour. Geophys. Res. 70(18), pp 4561-4572.
- Dean, R.G. (1970):** Relative validities of water wave theories: Journal of the Waterways, Harbors and Coastal Engineering Division, American Society of Civil Engineers, Volume 96 (WWI), pp 105-119.
- Dean, R.G. (1977):** Equilibrium beach profiles, U.S. Atlantic and Gulf Coasts: Tech. Report No. 12. Univ. Delaware, Newark.
- Dean, R.G., R. Chen and A.E. Browder (1997):** Full scale monitoring study of a submerged breakwater, Palm Beach, Florida, USA: Coastal Engineering: Volume 29, NOS. 3-4, pp 291 - 315.
- Dohmen-Janssen, C.M. (1999):** Grain size influence on sediment transport in oscillatory sheet flow: Ph.D. thesis Delft University of Technology.
- Du Boys, M.P. (1879):** Le Rhone et les rivieres a lit affouillable: Mem. Doc. Ann. Ponts Chaussees, Ser.5.18, pp141-195.
- Eijsink, W. D. (1990):** Morphological response of tidal basins to changes: 22<sup>nd</sup> International Conference on Coastal Engineering: Vol. 2: Delft.
- Einstein, H.A. (1950):** The bed load function for sediment transportation in open channel flows: United States Department of Agriculture, Soil Conservation Service, Washington, D.C. Technical Bulletin No. 1026.
- Engelund, F. and E. Hansen (1967):** A monograph on sediment transport in alluvial streams: Teknisk Forlag, Copenhagen, Denmark.
- Engelund, F. and E. Hansen (1973):**
- Fredsøe, J. (1984):** Turbulent boundary layer in wave current motion: Journal of Hydraulic Engineering, Volume 110, Number 8.
- Frijlink, H.C. (1952):** Discussion des formules de débit solide de Kalinske, Einstein et Meyer-Peter et Mueller compte tenue des mesures récente de transport dans les rivières Néerlandaises: 2<sup>me</sup> Jorn. Hydraulique: Soc. Hydr. de France, pp 98 - 103.

- Gallapatti, G. and C.B. Vreugdenhil (1985):** A depth-integrated model for suspended sediment transport: *J. Hydr. Res.*, 23(4), pp 359 - 377.
- Gerstner, F. (1802):** *Theorie der Wellen: Abhandlungen der Königlichen Bömischen Gesellschaft der Wissenschaften*, Prague.
- Graaff, J. van de (1977):** Dune erosion during a storm surge: *Coastal Engineering: Volume 1*, pp 99 - 134.
- Graaff, J. van de (1986):** Probabilistic design of dunes; an example from The Netherlands: *Coastal Engineering: Volume 9*, pp 479 - 500.
- Hydraulic Research Station Wallingford (1973):**
- Iribarren, C.R. and C. Nogales (1949):** Protection des ports: XVII<sup>th</sup> Int. Nav. Congress, Section II, Comm.4, Lisbon, pp 31-80.
- Jonsson, I.G. (1966):** Wave boundary layers and friction factors: *Proceedings 10<sup>th</sup> International Conference on Coastal Engineering, Tokio, Volume I, Chapter 10*, pp 127-148.
- Kalinske, A.A. (1947):** Movement of sediment as bed load in rivers: *Tr. Am. Geoph. Union, Vol. 28*, pp 615 - 620.
- Karman, Th. von (1930):** Mechanical similarity and turbulence: *Proceedings 3<sup>rd</sup> International Congress of Applied Mechanics, Stochkhholm, Sweden, Volume I*, pp 85-92.
- Madsen, O.S. and W.D. Grant (1976):** Sediment transport in the coastal environment: Technical Report 209, MIT, USA.
- Le Mehaute, B. (1976):** An introduction to hydrodynamics and water waves: Springer Verlag, Dusseldorf.
- Nielsen, P. (1985):** A short manual of coastal bottom boundary layers and sediment transport: Technical Memorandum T.M.85/1, Public Works Department N.S.W., Australia.
- Oost (1995):** Dynamics and sedimentary development of the Dutch Wadden Sea with emphasis on the Frisian Inlet: Ph.D. Thesis Utrecht University.
- Prandtl, L. (1926):** On fully developed turbulence: *Proceedings 2<sup>nd</sup> International Congress of Applied Mechanics, Zurich*, pp 62-74. In German, original title: *Über die Ausgebildete Turbulenz*.
- Ribberink, J.S. and Z. Chen (1993):** Sediment transport of fine sand under asymmetric oscillatory flow: Report H840, part VII, Delft Hydraulics.
- Rijn, L.C. van (1984):** Sediment Transport:  
Part I: Bed load transport,  
Part II: Suspended load transport,  
Part III: Bed Forms and Alluvial Roughness:  
*Journal of Hydraulic Engineering*, volume 110, No 10, 11, 12.
- Rijn, L.C. van (1993):** Principles of sediment transport in rivers, estuaries and coastal seas: Aqua Publications Amsterdam.
- Rijn, L.C. van (2000):** General view on sand transport by currents and waves: Delft Hydraulics: Report Z2899.30: Delft.

- 
- Roelvink, J.A. and M.J.F. Stive (1989):** Bar generating cross-shore flow mechanisms on a beach: *J. Geophysical Res.* 94, C4, pp 4485 - 4800.
- Shields (1936):** Anwendung der Ahnlichkeitsmechanik und der Turbulenzforschung auf die Geschiebebewegung: *Mitt. Der Preuss. Versuchsanst. Fur Wasserbau und Schiffbau*, Heft 26, Berlin, Germany.
- Shore Protection Manual (1984):** Coastal Engineering Research Center.
- Sistermans, P.G.J. (2002):** Graded sediment transport by non-breaking waves and a current: Ph.D. thesis Delft University of Technology.
- Spanhoff, R and J. van de Graaff (2006):** Towards a better understanding and design of shoreface nourishments: *Proceedings 30<sup>th</sup> International Conference on Coastal Engineering*, San Diego, Volume 4, pp 4141 - 4153.
- Steetzel, H.J. (1993):** Cross-shore transport during storm surges: Ph.D. Thesis, Delft University of Technology.
- Swart, D.H. (1974):** Offshore sediment transport and equilibrium beach profiles: Ph.D. thesis Delft University of Technology.
- Swart, D.H. (1976):** Coastal sediment transport; Computation of longshore transport: Delft Hydraulics, The Netherlands, Report R968.
- Swart, D.H. and C.C. Loubser (1978):** Vocoidal theory for all non breaking waves: *Proceedings 16<sup>th</sup> International Conference on Coastal Engineering*, Hamburg, Volume I Chapter 26, pp 467-486.
- TAW (1984)/CUR(1989):** Guide to the assessment of the safety of dunes as a sea defence: Centre for Civil Engineering Research and Codes, Gouda / Technical Advisory Committee on Water Defences, The Hague.
- Vellinga, P. (1986):** Beach and dune erosion during storm surges: Ph.D. thesis Delft University of Technology.
- Vriend, H.J. de, T. Louters, F. Berben and R.C. Steijn (1989):** Hybrid prediction of a sandy shoal in a mesotidal estuary: In: Falconer, R.A. (Ed.) *Hydraulic and environmental modelling of coastal, estuarine and river waters*: Gower Technical: Aldershot.
- Wiegel, R.L. (1964):** *Oceanographical Engineering: Fluid Mechanics Series*, Prentice-Hall, Englewood Cliffs, New Jersey.